

**ELECTRONIC SPECTRA OF 2-SUBSTITUTED BENZIMIDAZOLES:
A STUDY OF SOLVATOCHROMISM AND PROTROPISM**

A Thesis Submitted
In Partial Fulfilment of the Requirements
for the Degree of

DOCTOR OF PHILOSOPHY

105801

by
HEMANTA KUMAR SINHA

to the
DEPARTMENT OF CHEMISTRY
INDIAN INSTITUTE OF TECHNOLOGY, KANPUR

MAY, 1987

in fond memory of
my parents

✓ CHM-1987-D-SIN-E

Th
541.22
Si 64e

- 8 NOV 1989

106261

CERTIFICATE-I

Certified that the work presented in this thesis entitled, ''ELECTRONIC SPECTRA OF 2-SUBSTITUTED BENZIMIDAZOLES: A STUDY OF SOLVATOCHROMISM AND PROTOTROPISM'' by Mr. Hemanta K. Sinha, has been carried out under my supervision and not submitted elsewhere for a degree.



Dr. S.K. Dogra
Department of Chemistry
I.I.T., Kanpur-208016

May, 1987

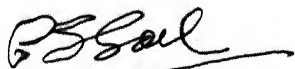
DEPARTMENT OF CHEMISTRY
INDIAN INSTITUTE OF TECHNOLOGY KANPUR, INDIA

CERTIFICATE OF COURSE WORK

This is to certify that Mr. H.K. Sinha has satisfactorily completed all the courses required for the Ph.D. degree programme. These courses include:

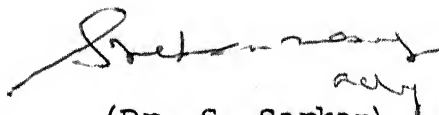
Chm 525 Principles of Physical Chemistry
Chm 505 Principles of Organic Chemistry
Chm 545 Principles of Inorganic Chemistry
Chm 524 Modern Physical Methods in Chemistry
Chm 521 Chemical Binding
Chm 622 Chemical Kinetics
Chm 534 Electronics for Chemists
Chm 800 General Seminar
Chm 801 Graduate Seminar
Chm 900 Post-Graduate Research

Mr. H.K. Sinha was admitted to the candidacy of the Ph.D. degree programme in January 1985, after he successfully completed the written and oral qualifying examinations.



(Prof. P.S. Goel)

Head,
Department of Chemistry,
Indian Institute of Technology,
Kanpur

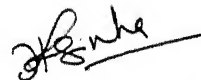


(Dr. S. Sarkar)
Convener
Departmental Post-
Graduate Committee,
Dept. of Chemistry,
IIT-Kanpur-208 016

STATEMENT

I hereby declare that the work embodied in this thesis entitled, ''ELECTRONIC SPECTRA OF 2-SUBSTITUTED BENZIMIDAZOLES: A STUDY OF SOLVATOCHROMISM AND PROTOTROPISM'' has been carried out by me under the supervision of Dr. S.K. Dogra.

In keeping with scientific tradition, wherever work done by others has been utilized, due acknowledgement has been made.



H.K. Sinha


ACKNOWLEDGEMENTS

It gives me a great pleasure to record my deep sense of gratitude and heartfelt thanks to Professor Sneh K. Dogra for his invaluable guidance, constant encouragement and stimulating discussions throughout the course of this work.

I offer my special thanks to Dr. Ashok K. Mishra (the then research fellow), Dr. M. Krishnamurthy (the then research associate), Mr. R. Manoharan, Mr. Ranjit S. Sarpal, Mr. Sanjay Srivastava and Mr. Joy K. Dey for their whole hearted co-operation and lively companionship in and outside the laboratory.

I thank my colleagues in the Chemistry Department for rendering their help whenever I approached them and for providing me a very friendly atmosphere, the names which need special mention are those of Dr. Sujit Roy, Mr. Manoj Kumar, Mr. R. Roy and Mr. Siddharth S. Ray.

I also thank the Authorities of the Indian Institute of Technology, Kanpur for giving me a fellowship and for providing all the necessary facilities. My thanks are also due to Mr. Anil Kumar Johri, for meticulous typing the manuscript and to Mr. Gowri Singh, for his nice drawings of the figures and schemes included in this thesis.


(H.K. SINHA)

SYNOPSIS

The absorption and fluorescence spectra of benzimidazole molecule [BI] is extensively studied because some of its derivatives form an integral part of the biological active molecule as well as the derivatives of BI are commercially and pharmaceutically important. But the detailed study on these derivatives of BI has received attention recently and that is too the work from this laboratory. Few groups are also working on the spectral characteristics of BI derivatives both as a function of solvents and hydrogen ion concentration. The present study has been extended to study the electronic spectra of some 2-substituted benzimidazoles. The effect of solvents and proton concentration on the spectral characteristics have been carried out to study the effects of interaction of the chromophores on BI moiety, geometry of the chromophores with respect to BI and the various prototropic species formed in the ground and excited states. The thesis has been divided into five chapters.

First chapter gives a brief introduction of some of the phenomena occurring in the ground and excited states. This chapter also gives a brief description of the status-quo report of the benzimidazole [BI] and its homologues as well as the justification for carrying out the present study.

Second chapter describes briefly the instrumentation and methods of preparation of model compounds used in the present study. It also describes the procedure for correcting the fluorescence spectrum and the determination of quantum yield.

Chapter three and four deal with the effect of solvents and hydrogen ion concentration on the absorption and fluorescence spectral characteristics of 2-substituted benzimidazoles. The latter also includes the identification of various prototropic species formed in the ground and excited singlet states. The dissociation constants of various prototropic species have been determined both in the ground and excited singlet states. About twenty compounds have been designed for the study. The results obtained can be summarised as follows:

- (i) Introduction of a methylene group in between the two chromophores reduces their direct interactions. The absorption and fluorescence spectra, therefore resemble that of the parent molecule (BI in the present case).
- (ii) Effects of substituents at 2-position have indicated that the nature of the emitting state depends on the nature of substituent. For example, in case of strongly electron withdrawing substituents (e.g. $-\text{CF}_3$ and $-\text{CCl}_3$ groups), the lowest energy emitting state is of charge-transfer (CT) character, whereas with other substituents it is of $\pi\pi^*$ character.

- (iii) Monocations, formed by protonating the tertiary nitrogen atom, also have the CT state as the lowest energy emitting state and the driving force for this charge-transfer from the carbocyclic ring to heterocyclic ring is the presence of positive charge on the tertiary nitrogen atom, on the other hand, the lowest energy transition in case of monoanion, formed by the deprotonation of the imino group, is always of $\pi\pi^*$ character irrespective of the nature of the substituent. These observations indicate that the negative charge, present on the imino nitrogen atom prevents the charge migration from the carbocyclic to the heterocyclic ring.
- (iv) Presence of electron withdrawing substituents (e.g. $-\text{CF}_3$, $-\text{CCl}_3$, $-\text{COOCH}_3$ and $-\text{COOH}$ groups) at 2-position reduces the charge density at the basic and acidic centers of the parent BI. Due to this the pK_a values for the protonation and deprotonation reactions of BI are affected considerably. The removal of the imino proton can be prevented if intramolecular hydrogen bond is formed between the imino proton and the negative centres present on the substituent of 2-position. This conclusion has been made from the observation that for the deprotonation, the pK_a value is either increased or the deprotonation does not occur even at highly basic condition (H_{16}). For example, deprotonat

of imino group of BI is not observed in case of benzimidazole-2-acetic acid both in the S_0 and S_1 states, whereas the same is observed for 2-(2'-hydroxyphenyl)benzimidazole in the S_0 state only.

- (v) pH study carried out on 2-(hydroxymethyl)benzimidazole and its N-methyl derivative has clearly demonstrated that the first deprotonation occurs from the imino group rather than from OH group. This removes the anomaly present in the literatures for a long time.
- (vi) Monoprotonic phototautomerism is observed in case of 2-(2'-hydroxyphenyl)benzimidazole. Solvent dependence study has clearly indicated that this phototautomer is exclusively formed in the non-polar solvents, whereas the normal neutral compound is also observed in polar solvents. Depending upon the concentration of H^+ , the zwitterion is formed only in the S_1 state.
- (vii) Biprotonic phototautomerism is absent in 2-(3'-hydroxyphenyl)- and 2-(4'-hydroxyphenyl)benzimidazoles, indicating that the rate of deprotonation of aromatic hydroxyl group and the rate of protonation of tertiary nitrogen atom are not comparable with the rate of radiative decay of these two compounds.

- (viii) The effects of solvents on the spectral characteristics of benzimidazole-2-carboxylic acid (BIA) and 5-chlorobenzimidazole-2-carboxylic acid (CBIA) have indicated that the molecules are planar and held in a rigid frame by the intramolecular hydrogen bond. Whereas in case of the ester derivative of the above acids, the intramolecular hydrogen bonding is absent and the structure is not rigid and both absorption and fluorescence spectra are sensitive to the nature of solvents.
- (ix) A study on benzimidazole-2-acetic acid (BIAA) has shown that the carboxyl group affects the spectral characteristics of the BI moiety, even though these are separated by insulating methylene group. A similar study on its ester derivative has confirmed that the interaction in BIAA is through a intramolecular hydrogen bond. The spectral study shows that the structure of BIAA is not as rigid as in BIA and CBIA. On the other hand, the ester derivative of BIAA Since intramolecular hydrogen bonding is absent, behaves like BI. This is further confirmed from the study of benzimidazole-2-propionic acid (BIPA), which contains two methylene groups in between the BI moiety and the carboxylic group.

The conclusions drawn and the possible extension of the work are given at the end of the thesis.

CONTENTS

			<u>page no.</u>
CERTIFICATE-I	i
CERTIFICATE OF COURSE WORK	ii
STATEMENT	iii
ACKNOWLEDGEMENTS	iv
SYNOPSIS	v
CHAPTER-I : INTRODUCTION			
1.1 Introduction	1
1.2 Solvatochromism	3
1.3 Proton transfer reactions	12
1.4 Phototautomerism	21
1.5 Applications	24
Scope of the present work	27
CHAPTER-II : INSTRUMENTATION AND METHODS			
2.1 Spectrofluorimeter	36
2.2 Experimental procedure	41
2.3 Other instruments	48
2.4 Materials	48
2.5 Adjustment of $H_0/pH/H_-$ values	56
2.6 Ground state equilibrium constant	57
2.7 Quantum yield calculation	59
2.8 Preparation of solutions	60
2.9 Other details	60

..contd.

CHAPTER-III: ABSORPTION AND FLUORESCENCE SPECTRA
EFFECT OF SOLVENTS

3.1	2-(Aminomethyl)benzimidazole	62
	2-(Hydroxymethyl)benzimidazole	66
	2-(Chloromethyl)benzimidazole	68
	2-(Dichloromethyl)benzimidazole	70
	5-Chloro-2-(trichloromethyl)benzimidazole	70
	2-(Trifluoromethyl)benzimidazole	73
	2-(Cyanomethyl)benzimidazole	75
	2-Chlorobenzimidazole	75
3.2	2-(Hydroxyphenyl)- and 2-(methoxyphenyl)- benzimidazoles	91
	2'-Hydroxyphenyl- and 2'-methoxyphenyl substituted compounds	92
	3'-Hydroxyphenyl- and 4'-hydroxyphenyl substituted compounds	102
3.3	Benzimidazole-2-carboxylic acids	110
	Benzimidazole-2-carboxylic acid and its methyl ester	110
	Benzimidazole-2-acetic acid and its ethyl ester	125
	Benzimidazole-2-propionic acid	133

CHAPTER-IV : ABSORPTION AND FLUORESCENCE SPECTRA
STUDY OF PROTOTROPISM

4.1	2-(Aminomethyl)benzimidazole	138
4.2	2-(Hydroxymethyl)- and N-methyl-2-(hydroxymethyl)benzimidazoles	149
4.3	2-Halo substituted benzimidazoles	161

..contd.

4.4	2-(2'-Hydroxyphenyl)- and 2-(2'-methoxyphenyl)benzimidazoles	175
4.5	2-(4'-Hydroxyphenyl)- and 2-(4'-methoxyphenyl)benzimidazoles	192
4.6	2-(3'-Hydroxyphenyl)- and 2-(3'-methoxyphenyl)benzimidazoles	201
4.7	Benzimidazole-2-carboxylic acid and its methyl ester	211
4.8	Benzimidazole-2-acetic acid and its ethyl ester	225
4.9	Benzimidazole-2-propionic acid	238
CONCLUSIONS		244
SCOPE OF FURTHER WORK		247
REFERENCES		248
VITAE		x
LIST OF PUBLICATIONS		xi

....

CHAPTER-I

1.1 INTRODUCTION

Whenever a molecule is excited electronically, the charge density at each atom changes and this is quite different from that in the ground state. Due to this, the characteristics of the molecule in the excited state are different from those in the ground state, i.e. geometry of a molecule, dipole moment and acid-base properties etc. A molecule in its excited state can also be called as an isomer of the species in its ground state.

The behaviour of an electronically excited molecule (i.e. how it loses energy and returns to its ground state) can be very nicely illustrated by the Jablonski diagram, as shown in Fig. 1.1. There are many pathways by which the electronically excited molecule can come to its ground state, as indicated in the diagram. An attempt will be made in the following sections to briefly describe the phenomena in which we are interested, for detailed studies books on photochemistry can be consulted. These phenomena are: (i) effect of solvent:

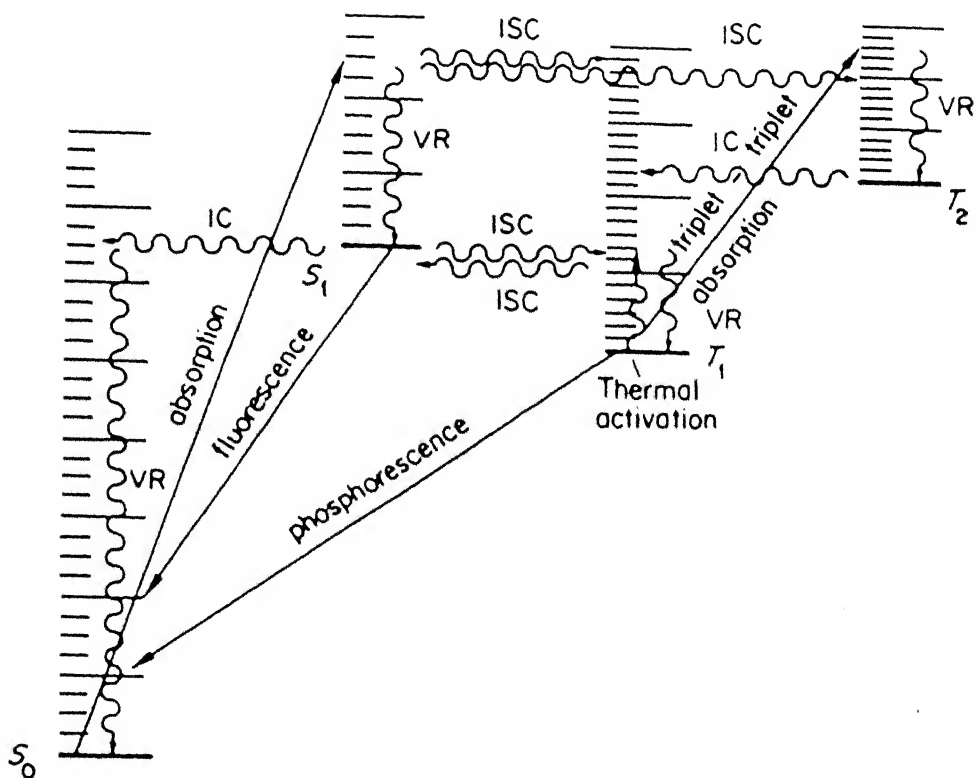


Fig.1.1 Jablonski diagram showing some of the radiative and non-radiative processes available to molecules (VR = vibrational relaxation; IC = internal conversion; ISC = intersystem crossing).

on the spectral characteristics and how these data can be used to get useful information about the nature of transition and proton transfer reaction, (ii) phototautomerism, (iii) proton transfer reactions and determination of pK_a values for both the ground and excited states and (iv) change of geometry of the substituent upon excitation and its effect on the spectral characteristics of the parent molecule.

1.2 SOLVATOCHROMISM

All the theoretical treatments regarding the calculation of energy levels are based on an isolated molecule. These studies do not consider the interactions due to the presence of other molecules, which may be of similar or of different species. Thus the spectral transitions observed in molecules can be either closely correlated to the theoretical studies, when the experimental studies are carried out in a low pressure gas phase or nearly represented when the spectrum is recorded in dilute solutions, using saturated hydrocarbon as solvents. In these solvents, the solute-solvent interactions are minimum. Since all the studies in this thesis deal with the spectral characteristics of the molecules in solution phase, these interactions will be discussed briefly with particular emphasis on some important results. The

books and review articles, mentioned in the references can be consulted¹⁻²⁰ for a complete understanding.

It is clear from Fig. 1.1 that the molecule ends up invariably in the higher vibrational levels of the first excited singlet state after absorption of appropriate amount of energy. This is in accordance with the Franck-Condon principle and the process is completed within 10^{-15} sec. Excitation of the molecules to the S_2 , S_3 states etc. are not considered here as our emphasis is only on the lowest excited singlet state. In the solution phase, the loss of vibrational energy, other than zero point energy, is very fast and hence molecules are present in the lowest vibrational level of the first excited singlet state, prior to the occurrence of fluorescence. This is known as vibrational relaxation. In the vibrationally relaxed excited state, the orientation of the solvent molecules is still the same as that of the ground state. Due to the change in charge densities, the solvent molecules tend to reorient in order to adjust themselves in the new environment. Since this process is similar to bond breaking and bond formation, this act will be completed within the period of vibrational frequency i.e. 10^{-12} sec. and of course, this will vary from solvent to solvent. The energy of the state in the new

environment will be either less or more than that of the vibrationally relaxed state, depending upon the nature of transition. Figures 1.2(a) and 1.2(b) represent the behaviour of $\pi \rightarrow \pi^*$ and $n \rightarrow \pi^*$ transitions respectively. Since this study deals only with $\pi \rightarrow \pi^*$ transition, therefore the case represented in Fig.1.2(a) will be considered. The molecule in the new environment is called solvent relaxed state. The combined effect of vibrational relaxation and solvent relaxation can be termed as the thermal relaxation of the excited state and this is at lower energy than that of the Frank-Condon state. After emission (fluorescence) the molecule will end up in the Frank-Condon groundstate and will reach the thermally relaxed ground state after vibrational and solvent relaxation. It is clear from Fig.1.2(a) that the frequency of fluorescence will be less than that of absorption. The red shift [also called Stokes shift, defined as $\bar{\nu}_{\max}(\text{abs}) - \bar{\nu}_{\max}(\text{flu})$] observed in the fluorescence spectrum depends upon the solvent relaxation and thus on the nature of the solvents, besides the vibrational relaxation. Stokes shift also depends on the change in the geometry of the molecule upon excitation.

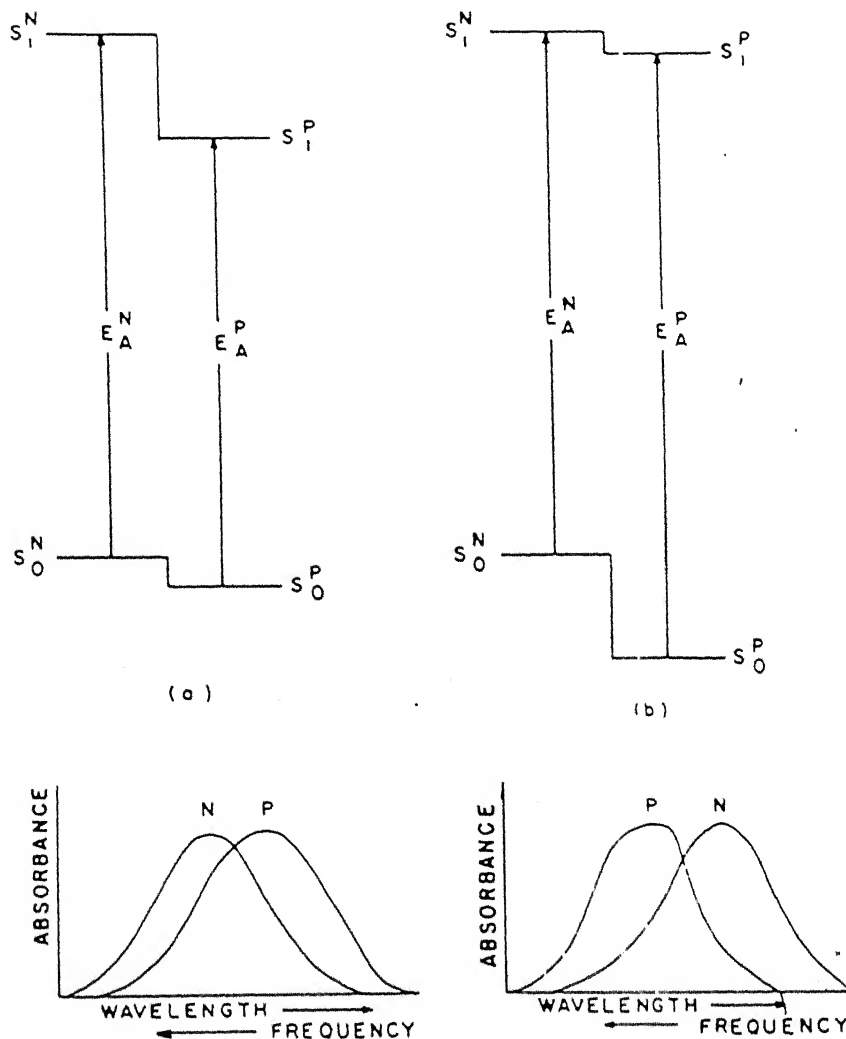


Fig.1.2 The effect of going from a nonpolar solvent (denoted by N) to a polar solvent (denoted by P), upon the energy (E_A) of an absorptive transition (a) when the excited singlet state to which absorption occurs (S_1) is more polar than the ground state (S_0) [$\pi \rightarrow \pi^*$], (b) when the excited singlet state to which the absorption occurs is less polar than the ground state [$n \rightarrow \pi^*$].

Solute-solvent interactions can be broadly discussed under the following two headings.

- (i) Dispersive interactions: These are basically electrostatic interactions and include dipole-dipole, dipole-induced dipole and induced dipole-induced dipole interactions. In $\pi \rightarrow \pi^*$ transitions the dipole moment of the molecule increases and thus a red shift in the absorption and fluorescence spectrum is observed with the increase in the polarity of the solvents.
- (ii) Specific interactions: These refer to specific chemical interactions between the chromophore and the solvent molecule, such as hydrogen bonding and complexation. Both these interactions can lead to drastic changes in the spectral characteristics of the molecules. In hydrogen bonding type interactions two cases can arise:
 - (a) Hydrogen donor interactions: In the hydrogen donor interaction, lowering of energy is produced by the electrostatic interaction of positively polarised hydrogen atom of the solvent with the lone pair of electrons on a basic atom of a solute in the ground or excited state. If during excitation, the electron density migrates away from the basic atom, (e.g. $n \rightarrow \pi^*$ transition), formation of hydrogen bond opposes this migration. As a result,

the energy separation between FC excited and ground states increases and a blue shift is observed with increase of hydrogen donor capacity of the solvent. On the other hand if the charge migration occurs towards the basic atom upon excitation, (e.g. $\pi \rightarrow \pi^*$ transition), energy of the FC excited state is lowered and a red shift as noticed with increasing hydrogen capacity of the solvent.

- (b) Hydrogen acceptor interactions: In hydrogen acceptor interaction, chemical energy is produced by the electrostatic interaction between the lone pair of the solvent with the positively charged hydrogen atom of the solute molecule. The effects would be opposite to what have been discussed for the hydrogen atom donor interaction. Hydrogen atom acceptor solvents causes red shift when solvating solutes at atomic centres which lose electron density in the FC excited state, and cause blue shift when solvating solutes at atomic sites which gain electron density in the FC excited state. If only hydrogen bonding interactions are present, shifts in the λ_{max} with change from non-polar to a hydrogen bonding solvent are related to the strength of the hydrogen bond in the ground state.

In general all these effects are present simultaneously and one observes the combined effect of solvent interactions on the spectral characteristics. Though it is not easy to identify the interactions separately, one can at least point out qualitatively by the judicious selection of solvents.

When the solute-solvent interactions are predominantly electrostatic in nature, the Stokes shift can be related to the change in dipole moment of the molecule upon excitation. Lippert⁴, McRae⁵, Suppan⁶, Mataga and Co-worker⁷ have successfully derived equations relating Stokes shift with the change in the dipole moment of the molecule, the refractive index and the dielectric constant of the solvents. Jaffe and Orchin⁸, Suzuki⁹. Mataga and Kutoba¹⁰ and Lakowicz¹¹ have given very nice description of the solvent relaxation processes. Costa et al.²⁰ from their study on absorption and fluorescence spectra in different solvents have attempted to calculate the dipole moments and found the geometries of some aromatic esters. Recently a method of determining dipole moment of the excited state from absorption/fluorescence solvatochromic ratios has been discussed by Suppan.^{21,22}

In 1949 Pringsheim¹² and later Förster¹³ in 1951, made the first systematic study of the environmental effects on the fluorescence spectra of aromatic compounds. The review

by Van Durren¹⁴ gives a detailed account of the environmental effects on the fluorescence spectra of aromatic compounds in solution.

Pimental¹⁵, Brearly and Kasha¹, and Mataga and Tsuno¹⁶ have stressed upon the significance of hydrogen bonding in the solvent effect in their works. Depending on the site and the nature of hydrogen bonding, the spectral shift can be explained in terms of hydrogen bond acceptor and hydrogen bond donor type interactions,^{17,18} as mentioned earlier. Weller¹⁹ found that the fluorescence intensity decreases on hydrogen bond formation. From the reduction of fluorescence intensity, he calculated the rate constants for hydrogen bond formation in the excited state. He explained the spectral shift on the basis that hydrogen bond formation can be considered as a preliminary stage of acid dissociation (in which proton is transferred completely to the base) for which the shift in the spectral bands are considerably greater.

Recent investigations by various groups²⁴⁻²⁶ have established that the main cause of decrease of fluorescence quantum yield on hydrogen bond formation is the enhancement of $S_1 \rightarrow S_0$ internal conversion. Various mechanisms have been proposed for the enhancement of internal conversion rate because of hydrogen bonding.²⁷⁻³⁰

Fluorescence is generally observed if $\pi \leftarrow \pi^*$ is the lowest energy transition and phosphorescence if $n \leftarrow \pi^*$ is the lowest energy transition. Bredereck, Förster and Oesterlin³⁰ have summarized in their work that separation of $n\pi^*$ and $\pi\pi^*$ singlet states determines the ability of the compound to fluoresce. They have suggested that the nature of emitting state depends on the solvent polarity because the reversal of states can take place in different solvents and hence one can determine the nature of the emitting state from the effect of the solvents. For example, chlorophyll a and b are nonfluorescent in pure and dry hydrocarbon solvents but fluoresce on addition of a small amount of water.³² Similar behaviour is also observed in case of quinoline and acridine³³ in different solvents.

Absorption and fluorescence spectra suffers a drastic change if a complex is formed by the interaction of solvents with the solute. If the complex formation takes place only in the excited state it is termed as exciplex. The quenching of fluorescence by solvents like carbon tetrachloride or chloroform has been explained in terms of an exciplex mechanism.^{34,35} Similarly a 1:1 complex formation between alcohols and 7-azaindole³⁶ or 1-azacarbazole³⁷ have been reported to be responsible for the dual fluorescence.

1.3 PROTON TRANSFER REACTIONS

The acidity and basicity of a molecule is determined by the electronic charge densities at various atomic centres. In general, the charge densities undergo large changes from those of ground state values by absorption of electronic energies i.e. the acidity and basicity of a molecule changes upon excitation. It has generally been observed that aromatic alcohols and amines become stronger acids, where as the carboxylic acids and tertiary nitrogen atom are stronger bases in the excited singlet state.³⁸

The pK_a value for the prototropic reactions in the excited state (pK_a^*) can be determined by:

- (i) Förster cycle method
 - (ii) Fluorimetric titration
 - (iii) Time dependent fluorescence technique
-
- (i) Förster cycle method^{39,40}: This method is based on the thermodynamic cycle involving (a) the acid (BH), excited to electronic excited state (BH^*), (b) dissociation of excited BH (BH^*) into excited base (B^{*-}), (c) emission of B^{*-} to ground state (B) and finally (d) formation of

acid (BH) in the ground state. The complete cycle is shown in Fig.1.3. Balancing the energies involved in the above cycle, equation (1.1) can be obtained.

$$\Delta E_{BH} + \Delta H_{BH}^* = \Delta E_{B^-} + \Delta H_{BH} \quad \dots (1.1)$$

where ΔE_{BH} and ΔE_{B^-} are the energies corresponding to the O-O transitions of acid BH and base B^- , ΔH_{BH} and ΔH_{BH}^* are the dissociation energies of the acid BH in the ground and excited singlet states respectively.

Using the relation $\Delta H = \Delta G + T\Delta S$

equation (1.1) can be written as

$$\Delta E_{BH} + \Delta G_{BH}^* + T\Delta S_{BH}^* = \Delta E_{B^-} + \Delta G_{BH} + T\Delta S_{BH} \quad \dots (1.2)$$

Rearranging the equation (1.2) and using

$$\Delta G^0 = -RT \ln K_a = 2.303 RT pK_a$$

$$\text{and } \Delta E = h\nu$$

where K_a is the dissociation constant and $\bar{\nu}$ corresponds to the O-O electronic transition, expressed in wavenumbers

$$2.303RT(pK_a^* - pK_a) = hc(\bar{\nu}_{B^-} - \bar{\nu}_{BH}) + T(\Delta S_{BH} - \Delta S_{BH}^*) \quad \dots (1.3)$$

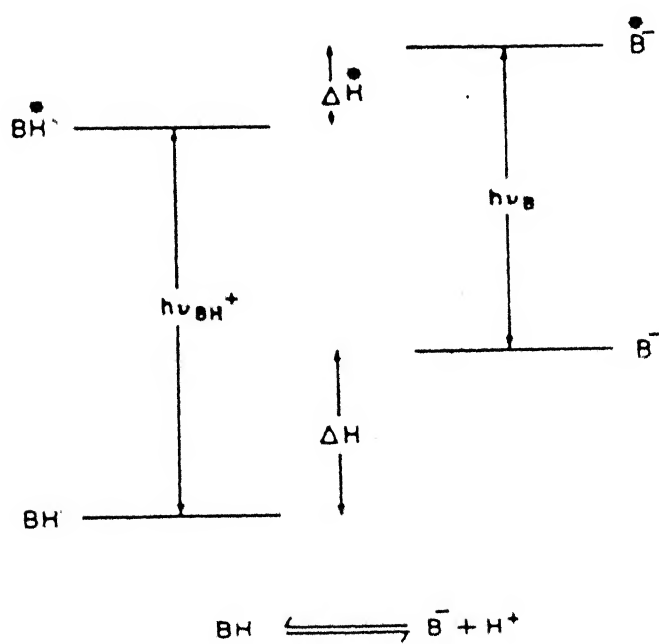


Fig.1.3 Förster's relationship of enthalpy changes to electronic transitions.

$$\text{or } pK_a^* - pK_a = \frac{hc}{2.303RT} (\bar{v}_B - \bar{v}_{BH}) + \frac{1}{2.303R} (\Delta S_{BH} - \Delta S_{BH}^*) \quad \dots (1.4)$$

Assuming $\Delta S_{BH}^* = \Delta S_{BH}$ i.e. there is no change in the entropy of dissociation in the ground and excited states, equation (1.4) becomes

$$pK_a^* - pK_a = 2.10 \times 10^{-3} (\bar{v}_B - \bar{v}_{BH}) \quad \dots (1.5)$$

The factor 2.10×10^{-3} is obtained by substituting the values of Planck's constant (h), velocity of light (c), gas constant (R) and temperature equal to 298°K. So knowing the ground state pK_a value, one can calculate the excited state pK_a value (pK_a^*) from the above relation.

Förster cycle method has been subjected to many critical discussions after its formulation. The assumptions made in the above derivation are the followings:

- (a) The entropy changes of the protropic reactions in the ground and excited states are same. Many authors have critically examined this assumption, both experimentally (by measuring the pK_a values at different temperatures) and theoretically. Maximum uncertainty observed due to this assumption is not more than 1-2 pK_a units.⁴¹⁻⁴⁴

- (b) The electronic states involved in BH and B should be the same.
- (c) The prototropic equilibrium should be same, both in the ground and excited states.
- (d) The vibrational spacing for the ground and excited states of the given acid as well as that of the base should be the same. In general it has been found that this assumption holds good.
- (e) The solvent relaxation of the given species should be same both in the ground and excited states. Since the molecules become more polar on excitation, this assumption is not satisfied for majority of the cases and leads to an error in the calculation of pK_a^* .

Further, sometimes the O-O transition is very difficult to locate in acid-base pair and thus O-O transition frequency is replaced by the band maxima in equation (1.5). Bartok et al.⁴⁵ have suggested that the O-O frequency can be calculated by taking the average of absorption and fluorescence band maxima. Schulman et al.⁴⁶ have clearly indicated that Bartok et al.'s procedure to calculate O-O frequency is valid only when the solvent relaxation for species in the ground and excited states are same and thus erroneous results can be obtained. Schulman and Capomacchia⁴⁷ have proposed a modified

Förster cycle which includes vibrational, solvent and geometrical relaxations in both the states and have derived an equation similar to that of Förster cycle.

- (ii) Fluorimetric titration method:⁴⁸ This method was developed by Weller. In this method the relative fluorescence intensities of the conjugate acid-base pair are plotted as a function of proton concentration. If both the species are fluorescent and it is established that only acid-base pair is involved in the prototropic reaction the intersection of the two curves will be at $I/I_0 = I'/I'_0 = 0.5$, where I_0 is the fluorescence intensity of the acidic species when present exclusively and I the fluorescence intensity when the conjugate base is also present in the solution. Prime refers to the similar terms for the conjugate base. This gives the pK_a value in the excited singlet state. The pK_a^* value can still be calculated from the fluorescence intensities vs $[H^+]$ plot of only one species, when $I/I_0 = 0.5$ provided the prototropic reaction is the only path available. This method is better than that of Förster cycle method as the fluorescence is always observed from the thermally relaxed state. Schulman has discussed the various kinds of fluorimetric titration curves observed in the experimental results:

- (a) If the rate of protonation or deprotonation of a base and acid is much less than that for radiative decay of the conjugate base-acid pair, the ground state pK_a values are obtained from these curves. This generally happens if the pK_a falls in the mid pH region (i.e. pH 3-11).
- (b) If the rate of deprotonation or protonation of conjugate acid-base pair is much larger than that of the radiative decay of the respective species, the pK_a values thus obtained from fluorimetric curves correspond to the excited state pK_a values. The following relations should hold for the fluorimetric titrations to give pK_a^* .i.e.

$$\frac{k_a}{k_{FM}(BH)} \ll 10 \quad \text{or} \quad \frac{k_{-a}[H^+]}{k_{FM}(B)} \ll 10, \text{ where } k_a \text{ and } k_{-a} \text{ are the}$$

psuedo first order dissociation constant for the acid and second order constant for the protonation reaction of base respectively, $k_{FM}(BH)$ and $k_{FM}(B)$ are the radiative decay rate for acid-base pair .

- (c) If the rates of deprotonation or protonation are comparable to the radiative decay of the acid-base pair, a stretch fluorimetric titration curve is observed over the complete pH range. These kinds of curves give both the ground and excited state pK_a values.

In general, the discrepancy observed between the pK_a values obtained by fluorimetric titrations and Förster cycle

method using fluorescence data is due to the difficulty in locating the O-O transition as well as unequal entropy changes in ground and excited states dissociation processes.⁴⁹ Sometimes the results obtained from the fluorimetric titrations agree well with those obtained by Förster cycle method, using average of absorption and fluorescence maxima but do not agree with the pK_a^* values calculated using either absorption data or fluorescence data. This is due to the cancellation of errors in the absorption or fluorescence results, occurring in the opposite directions. Such results therefore, should be dealt with care.

It had been observed earlier, especially in aromatic amines that the formation curve of one species does not correspond to the decrease in the fluorescence intensity of the other species, involved in the acid-base equilibrium.⁵⁰⁻⁶⁰ Many theories^{61,62} have been put forward to explain this discrepancy, but the most acceptable one is that of Shizuka et al.^{59,63,64} By carrying out carefully designed experiments and from the isotope exchange results, they have concluded that the above mentioned discrepancy is due to the proton induced fluorescence quenching of the basic species i.e. neutral aromatic amines. This arises due to the interaction of the proton with a particular site of a

molecule, where the charge density has accumulated. The proton induced fluorescence quenching is small if the charge is distributed over the complete molecule. Due to this the results of fluorimetric titrations should be looked carefully.

(iii) Time dependent fluorescence technique: With the commercialisation of nano-second and pico-second time dependent spectrofluorimeters, more insight in to the mechanism of proton transfer reactions has been achieved. By this method, one can directly calculate the rate constants for the forward and backward proton transfer reactions and thus the equilibrium constant. This has been extensively reviewed by many workers.^{50,57,64-66}

The use of photopotentiometric method has been tried to calculate the pK_a^* values by Rosenbrook and Brandt⁶⁷, but this method has not gained much importance, may be because of insufficient generation of photopotential in many organic molecules, as well as the reproducibility of the results because the electrodes are very sensitive to chemical or physical changes occurring during the process.

In the last two decades a huge amount of work has been done on the acid-base properties of aromatic molecules by workers like Mason⁴¹, Jaffe and Jones⁴², Jaffe et al.⁴⁴, Wehry and Rogers⁴³, Schulman et al.⁶⁸ and Shizuka et al.⁶⁹ Vander Donk⁷⁰ reviewed the acid-base properties of the excited state, wherein he discussed the effect of geometrical relaxation on Förster cycle calculations. Subsequently similar work has been reviewed by several authors.^{38,71-73} The review by Ireland and Wyatt³⁸ contains extensive references of experimental results available in the literature till 1974. Schulman and his co-workers⁷⁴⁻⁸² have done extensive work on pK_a^* of many classes of organic compounds including compounds of biological interest.

Despite the errors that can arise in the Forster cycle method and the fluorimetric titration method, these are still widely used, may be because the timedependent fluorimeters are expensive and difficult to maintain.

1.4 PHOTOTAUTOMERISM

Prototropic tautomerism of heteroaromatic compounds has its own place in chemistry. The importance of tautomerism in elucidation of reaction mechanism and biochemical processes

is well understood. The review by A.R. Katritzky and A.Z. Boutton⁸³ gives a detailed discussion about the prototropic tautomerism. This review also deals with the methods of investigation of tautomerism.

Electronic charge redistribution, as said earlier, in excited singlet state causes a change in the acid-base properties of various groups attached to a molecule. If a molecule contains both electron withdrawing and electron-donating groups, sometimes change in the charge densities are so large on excitation that the acid-base properties of the functional groups are very much different in the excited state from those in the ground state. Due to this, though no change is observed in the number of protons in a given species, a proton migration takes place from one functional group to another within the same molecule. This phenomenon is called phototautomerism. If a proton migration takes place across the intramolecular hydrogen bond, i.e. between the adjacent groups it is called monoprotonic phototautomerism and it does not depend on the nature of the solvents. On the other hand, if it takes place between two functional groups which are separated by large distance, it is called biprotonic phototautomerism and this depends on the nature of the solvent

Since the original work of Weller⁸⁴ on the excited state intramolecular proton transfer reactions of methyl salicylate, a great deal of studies have been made on excited state intramolecular proton transfer (ESIPT) of *o*-hydroxybenzophenone,^{85,86} 2-(*o*-hydroxyphenyl)benzotriazole,⁸⁷ 2-(*o*-aminophenyl)benzimidazole,⁸⁸ 2-(*o*-hydroxyphenyl)benzoxazole,^{89,90} 2-(*o*-hydroxyphenyl)-benzothiazole,⁹¹ phenyl salicylate⁹² etc. For this kind of proton transfer to occur, one of the groups should undergo a positive pK_a change, while the other should realize a negative pK_a change, following the absorption of a photon. Interesting results have been mentioned in case of 7-azaindole^{93,94} and 7-azacarbazole.⁹⁵ In these cases, one of the nitrogen atoms that is protonated in the ground state becomes more acidic in the excited state where as the second nitrogen atom becomes more basic. As a result of this, a double proton transfer reaction results either within a symmetric dimer or a complex between the fluorophore and a solvent molecule (alcohol).

The examples of the second kind, i.e. biprotonic phototautomerism, are β -methylumbliferrone,⁹⁶ 5-amino- and 6-amino indazole.⁹⁷ In these cases, the phototautomerism does depend on the nature of the environments.

Anomalous emission with large Stokes shift of these compounds have been ascribed to the phototautomerism in the molecule. This is due to the accumulative red shift observed from the deprotonation reaction of one functional group and protonation of the second group. The kinetics and mechanisms of the excited state proton transfer reactions have been investigated recently by various workers using picosecond laser spectroscopy.⁷³

1.5 APPLICATIONS

The excited state prototropism has been helping chemists in many ways to interpret the mechanism of organic photochemistry. Gutsche et al.^{98,99} have shown that the nature (whether it is electron-withdrawing or electron-donating type) and the position of the substituent can affect the reaction rate as well as can alter the photochemical product. Godfrey et al.¹⁰⁰ have mentioned that the acid-base equilibrium in the lowest excited singlet and triplet states is of prime importance in determining the course and the yield of photochemical reaction of aromatic ketones by hydrogen abstraction from the solvents.

The yield of different products from photoisomerisations have been shown to be dependent on acid-base equilibria in ground and excited singlet states.^{101,102} For example, the reactions of 3-styryl pyridines in the pH range are related to the acid-base equilibria in the ground and excited singlet states.¹⁰¹ The photoisomerisation processes are also dependent on the nature of the substituents.¹⁰³

Several molecules which can undergo intramolecular proton transfer in the excited singlet state are found to be usually photostable. The works of Heller,¹⁰⁴ Blattman^{105,106} and others¹⁰⁷⁻¹⁰⁹ have established that the stabilizing efficiency of molecule like 2-(2'-hydroxy-5'-methylphenyl)benzotriazole (widely used as UV stabiliser to diminish the photodegradation of polymers) is related to intramolecular hydrogen bond. Other example is that of 2-hydroxybenzophenone, which is used as photostabilizer in polymers while benzophenone itself is photoactive.¹¹⁰

In analytical chemistry the fluorimetric technique is considered to be very powerful tool because of its high sensitivity. The excited state acid-base behaviour of a molecule has a direct application in the field of analytical fluorimetry and phosphorimetry. The fluorimetric titration curves or the effect of pH on the intensity of emission, help in determining the optimal pH region corresponding to the maximum sensitivity of the fluorimetry. Thus the sensitivity and selectivity of analytical procedure can

be increased,¹¹¹⁻¹¹² if the prototropic reactions are well understood. For example, the limit of detection of 4-nitrophenol is much lower in solution containing anions.¹¹³ Other example is that of tryptophan, which is often present as a fluorescent contaminant in biophysical samples. However, intense fluorescence of tryptophan is quenched in solution at pH 1 and consequently in this region, the determination of other biophysical samples can be done in presence of tryptophan.¹¹⁴

In biochemistry, the excited state protolytic behaviour is largely used to interpret results.¹¹⁵ Loken et al.¹¹⁶ have suggested that the rate of excited state proton transfer should give a quantitative measure of the environment of a probe molecule. This is because the rate constants for the prototropic reactions depend on the solvent and the character of any possible proton donor and acceptor.

In fact, recently the principle of intramolecular proton transfer reactions has been shown to be capable of generating a large population inversion, like well known excimer and exciplex lasers. Mayer and coworkers¹¹⁷ in their survey of UV lasers have reported that stimulated emission is probably produced by excited state proton transfer reaction. They reported that an ethanolic solution of sodium salicylate produced tunable laser light from 395 nm to 418 nm. According to Acuna et al.,¹¹⁸ sodium salicylate

has an absorption maximum at 300 nm. It is very likely that the red shifted emission originated from the proton transfer product of salicylate anion. Chou et al.^{119,120} have also reported recently the efficient generation of amplified spontaneous emission (ASE) based on excited state proton transfer tautomerisation of 3-hydroxyflavone in solution, either alone or mixed with laser dye.

SCOPE OF THE PRESENT WORK

In the early 1950s, it was discovered that 5,6-dimethyl-1-(α -D-ribofuranosyl)benzimidazole is an integral part of the structure of vitamin B₁₂.¹²¹ These findings stimulated great interest in the chemistry of imidazoles and related compounds. Since then a lot of synthetic work has been done on imidazole, benzimidazole and their related compounds. These compounds are also found to be commercially important. Though the detailed study of absorption and fluorescence characteristics of benzimidazole molecule is available,¹²² similar study on derivatives of benzimidazole (BI) has received attention only recently. Most of the work on the derivatives of benzimidazole has been done in our laboratory, whereas some results have also been reported from couple of other laboratories. The important results of these studies are summerized below.

- (i) The long wavelength absorption band (ca. 278 nm) of BI is localized on the benzene ring and the short wavelength band (ca. 245 nm) is localized on the imidazole ring. It has also been shown experimentally as well as theoretically that these transitions are of $\pi \rightarrow \pi^*$ character. On Platt notation, the former is assigned to 1L_b (long axis polarized) and the latter 1L_a (short axis polarized).
- (ii) Solvents of different polarity and hydrogen bond formation tendency have little influence on the absorption and fluorescence characteristics of BI, but the substitution by different chromophoric groups manifests different types of solvent dependency and can cause spectral shift in the absorption and fluorescence spectra.
- (iii) Fluorescence quantum yield of BI has been found to be nearly independent of the nature of solvents, whereas those of substituted BIs' depend on the nature of solvents and substituents.
- (iv) The effect of pH on benzimidazole shows that absorption maximum of the monocation, formed by protonating the tertiary nitrogen atom, is slightly blue shifted, whereas the fluorescence maximum is largely red shifted, as compared to the absorption and fluorescence spectrum of neutral molecule, respectively. Barrensen¹²³ explained this large red shift in the fluorescence spectrum, because of the formation of 1:1

stoichiometric complex with the solvent molecule in the excited state. Later on Kondo and Kuwano¹²⁴ suggested that this large red shift is due to the reversal of two electronic states i.e. in neutral molecule the fluorescence originates from the less polar 1L_b state and in monocation the more polar electronic state 1L_a is responsible for the red shifted fluorescence. This conclusion is based on the facts that, the 1L_a band maximum is largely red shifted and gets mixed with 1L_b band, since 1L_a state is more polar than 1L_b and this is stabilised more in the excited state, leading to the formation of 1L_a as the low lying electronic state. This leads to large red shifted fluorescence band. A small blue shifted fluorescence band is noted if the energy gap between the 1L_a and 1L_b band maxima remains constant on protonation. Lastly both the fluorescence bands are recorded if the two states are nearly degenerate.

Recent studies in our laboratory have indicated that the above description of reversal of two electronic states can not be generalized to all the substituted derivatives of benzimidazole. It has been identified that multiple electronic states ($\pi \rightarrow \pi^*$ and CT) of nearly similar energy exist in case of methyl substituted benzimidazoles.¹²⁵ Simultaneous emission from CT as well as π^* state has also been observed depending upon the energy gap between the two states. These studies have also violated Kondo and

Kuwano's results,¹²⁴ in the sense that both the fluorescence bands are observed even if the two bands are largely separated or are lying close to each other. There is no correlation in the energy gap between the two states and the fluorescence spectra. The studies on substituted benzimidazoles in our laboratory have shown that the nature as well as position of the substituents determine the nature of the lowest lying emitting state. For example, electron-withdrawing group on imidazole ring or electron-donating group on benzene ring favours the charge transfer state to be the low lying emitting state. As the charge transfer takes place from benzene ring to imidazole ring, the driving force for the CT state to be the low lying state in the monocations of BI, is the presence of positive charge on the tertiary nitrogen atom. If the phenyl or aromatic ring is present at 2-position of BI, fluorescence is observed from the $\pi\pi^*$ state. This is because the positive charge is not localized on the tertiary nitrogen atom alone but is completely delocalized over the imidazole and the phenyl ring

- (v) The absorption and emission maxima of monoanions, formed by the deprotonation of imino group ($>NH$), are red shifted as compared to the neutral species and emitting state is of $\pi\pi^*$ character. This is because of the presence of negative charge which inhibits the charge migration from benzene to imidazole ring.

From the above results, it is clear that BI molecule contains two functional groups i.e. the basic tertiary nitrogen atom and the acidic imino group. Presence of further acidic or basic groups can create challenging features in the spectral characteristics of BI. Change of proton concentration can give rise to many prototropic species, the identification of which needs carefully designed experiments. The compounds chosen for the present study are the 2-substituted benzimidazoles. The 2-position is given importance because the tertiary nitrogen atom and the imino group are immediate neighbour to this and hence can bring about changes in the acidic and basic characteristics of the BI moiety. The compounds selected in this thesis can be divided into three categories.

- (i) It is well known that the spectral characteristics of an aromatic molecule is affected by the presence of substituents and thus depends on the extent of interaction of the substituent attached to aromatic ring. For example, in case of 2-aminobenzimidazole,¹²⁶ the amino group directly affects the characteristics of benzimidazole moiety and vice versa. Similar observation has also been made in case of 2-hydroxybenzimidazole.¹²⁷ So it is

interesting to see whether the same degree of interaction exists if two functional groups are separated by the presence of methylene groups, which is supposed to be acting as a kind of insulator. The inductive effect as well as the resonance effect have been seen to play a major role in determining the acid-base properties of a molecule. As the substituents chosen are the nearest neighbour to the acid-base sites of the parent molecule, the increase in the inductive power of the substituents is expected to make marked changes in the acid-base properties. Further, the introduction of methylene group is expected to decrease the inductive effect on the acid-base sites of the BI moiety, which could be reflected from pK_a values. So for this investigation the following compounds have been selected to carry out this study.

(1) 2-(aminomethyl)-, (2) 2-(hydroxymethyl)-, (3) 2-(chloromethyl)-, (4) 2-(cyanomethyl)-, (5) 2-(dichloromethyl)-, (6) 5-chloro-2-(trichloromethyl)-, (7) 2-(trifluoromethyl)- and (8) 2-chlorobenzimidazoles.

(ii) All three isomers in the series of 2-substituted (hydroxyl-phenyl)benzimidazoles have been studied. All of them are expected to show entirely different spectral characteristics in the following fashion.

- (a) In 2-(2'-hydroxyphenyl)benzimidazole, due to the proximity of acidic (-OH) and basic ($\gg N$) sites, hydrogen bonding in the ground state as well as intramolecular proton transfer in the excited singlet state is expected. Moreover the phenyl ring may have different orientations at different hydrogen ion concentrations, depending on the particular prototropic species. This could be reflected by a careful analysis of the absorption and fluorescence spectra in different environment.
- (b) In 2-(3'-hydroxyphenyl)benzimidazole both the chromophores are more or less expected to behave independently as there is no direct resonance conjugation between them i.e. its behaviour should resemble 2-phenylbenzimidazole¹²⁸ or substituted phenol. Intramolecular proton transfer is not anticipated here because the acidic (-OH) and basic ($\gg N$) sites are well separated as compared to its ortho-isomer. Biprotonic phototautomerism could be possible since the molecule contains both electron-donating and electron-withdrawing groups.
- (c) The hydroxy group of 2-(4'-hydroxyphenyl)benzimidazole can very nicely interact with the whole system and an extensive reorganisation of charges may occur in the excited singlet state. The compound is expected to show more planarity as compared to its meta-isomer.

Further the study on the methoxy derivatives of the above three isomers can provide further confirmation regarding the nature of proton transfer of the hydroxy group.

(iii) Benzimidazole-2-carboxylic, -2-acetic and -2-propionic acids have been considered for this study with the following points in mind. Specific interactions of the carboxyl group with the nearest acidic and basic sites of benzimidazole may bring about drastic changes in the spectral characteristics of benzimidazole. Zwitterion formation in the ground and excited singlet states is also a possibility. Further, by correlating the spectral shifts of the absorption and fluorescence bands, it may be possible to identify different molecular conformation, which may arise due to the rotation of carboxyl group around the single bond. The compounds are nicely designed to reveal the extent of these interactions when both the chromophores are directly attached or separated by saturated linkage.

Solvent study of all the 2-substituted benzimidazoles mentioned above have been carried out to comment on the nature of spectral transition and solute-solvent interactions. The pH dependence study have been performed to identify the different prototropic species and to calculate the ground and excited state dissociation constants.

The study of fluorescence in rigid matrix at low temperature (77K) can give valuable informations. Freezing 'locks' the fluorescing molecule in the ground state equilibrium solvent cage and molecular conformation, thereby prevents solvent cage relaxation and functional group reorganisation subsequent to excitation. Thus the comparison of absorption and fluorescence spectra, taken in frozen solutions with those taken in fluid media, permits distinction between solvent and conformational effects, arising from ground state circumstances of the molecule and those arising from electronically excited circumstances of the thermally equilibrated excited molecule. Therefore low temperature fluorescence studies, wherever necessary to supplement our ideas, have also been carried out.

CHAPTER-II

INSTRUMENTATION AND MATERIALS

2.1 SPECTROFLUORIMETER

Fluorescence spectra were recorded on a scanning spectrofluorimeter, fabricated in our laboratory. The block diagrams of the spectrofluorimeter and the arrangement to take spectra at low temperatures are shown in Figures 2.1 and 2.2 respectively. A brief description of various parts is given below.

A stabilized power supply (PS) for the lamp (LPS 251 HR) and the lamp housing (LH 150) were procured from Schoeffel Instruments. The lamp housing can accommodate 150 w Xe lamp, 200 w Xe-Hg lamp and 200w Hg lamp. The total energy output from the lamp could be monitored and kept constant by the power supply.

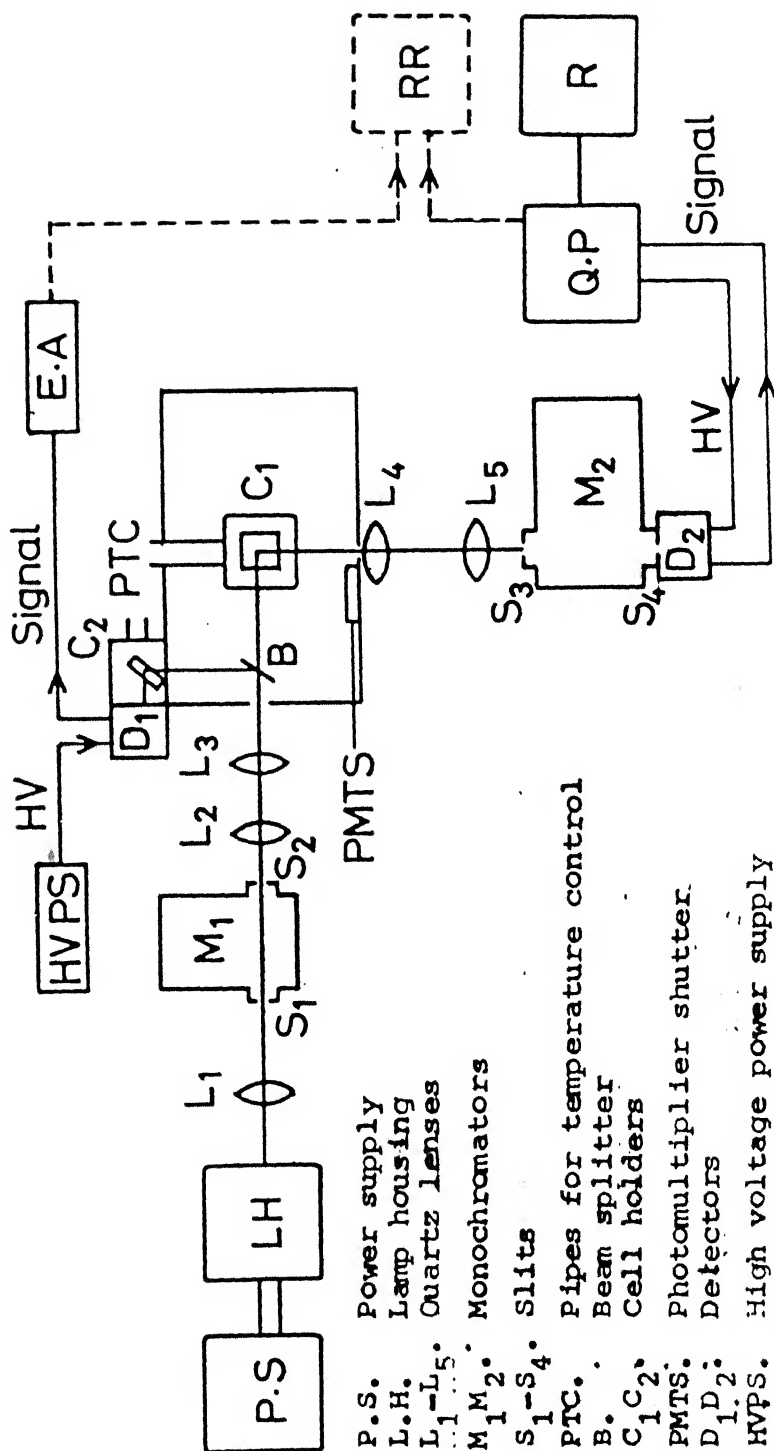


Fig. 2.1 Block diagram of the Spectrofluorimeter

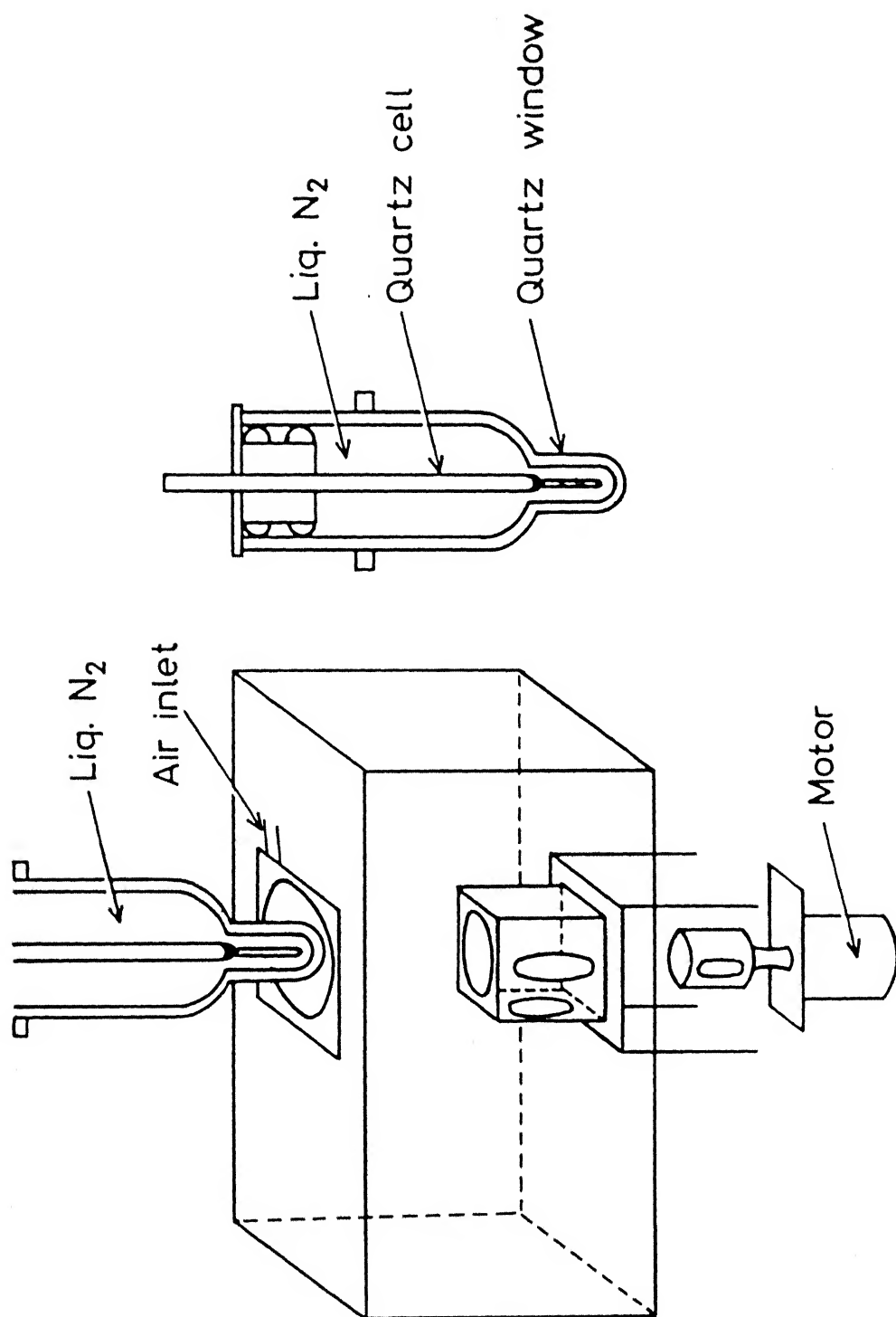


Fig. 2.2 Diagram of low temperature set up for fluorescence and phosphorescence.

Two Jarrel-Ash (0.25 m and $f/3.5$) Ebert grating monochromators (82-410 and 82-415) were used. The monochromator (M_1) with a grating, blazed at 300 nm (1160 grooves/mm with a reciprocal linear dispersion of 3.3 nm/mm) was used for selecting the excitation wave length. The monochromator (M_2) with two gratings, one blazed at 300 nm (2360 grooves/mm) with reciprocal linear dispersion of 1.65 nm/mm and other blazed at 500 nm (1180 grooves/mm) with reciprocal linear dispersion of 3.3 nm/mm were used for the resolution of the emission spectra. The focal length of quartz lenses (L_1 - L_5) were chosen to suit the aperture to focal length ratios of monochromators and to have maximum collection of the exciting as well as emitting light.

The cell compartment is designed in such a manner, so that both the room temperature and low temperature measurements can be done. The cell compartment is an anodized black to minimize scattering. The cell holder (C_1) is double walled with thermostating arrangement to maintain a constant temperature. For low temperature measurements (77K), Aminco-Bowman's low temperature fluorescence and phosphorescence accessory could be fitted in the cell compartment by replacing the normal cell holder C_1 (Fig.2.1)

Provision is there to pass dry air to remove the condensed moisture from the walls of the Dewar flask, used for the low temperature measurements. If necessary a beam splitter B could be fitted in the cell compartment. This is a 1 mm thick quartz plate, placed at an angle 45° in the path of the exciting light to reflect 5% of it to another cell holder C_2 . This is used to calibrate the light source from time to time and to determine the relative intensities of the excitation light emerging from M_1 at all wavelengths as described in this chapter.

Princeton Applied Research Quantum Photometer Console (model 1140A) was used for detection and amplification of emission. It consists of a detector assembly, an amplifier/discriminator (1140B) an electrometer, a highly stabilised voltage supply to give voltage to photomultiplier tube and two rate meters, one with log and the other with linear scale. The detector assembly with a 1P28 photomultiplier tube (Hamamatsu, Japan) was fixed at exit slit of M_2 . Very weak signals could be detected on the photon counting mode of the quantum photometer. The detected and amplified signal was read from the rate meter on the front panel. A multirange and multispeed digital

recorder (Fisher Recorder Series 5000) was used to record the signal out put from the quantum photometer. The emission monochromator M_2 was scanned by a digital drive system, specifically made for Jarrel-Ash monochromators (Jarrel-Ash omnidrive 82.462) which is coupled to the recorder. From time to time both the monochromators were calibrated with low pressure mercury lamp.

2.2.1 EXPERIMENTAL PROCEDURE

The quartz cell containing the sample is placed in the cell holder. The light of excitation wavelength selected by monochromator (M_1) is allowed to fall on the sample and the emission from the sample at right angle is directed to the other monochromator (M_2).

The emission intensities at wavelengths selected by M_2 are measured from quantum photometer reading. The complete emission spectrum is recorded by scanning M_2 . The total energy out put of the lamp is always kept constant by the suitable combination of current and voltage in the lamp power supply.

For the low temperature fluorescence spectra, the cell compartment is fitted with low temperature accessory.

The sample in the proper cell is placed in liquid nitrogen, kept in a quartz Dewar flask, for some time till the bubbling of nitrogen gets reduced. After removing the condensed moisture, the Dewar flask with the sample is placed in the cell compartment. During scanning, dry air is passed through the compartment to remove any moisture condensed.

The fluorescence excitation spectrum at room temperature or at low temperature can be obtained by setting M_2 at the fluorescence maximum and scanning M_1 .

The excitation and emission spectra thus obtained are uncorrected. The corrected fluorescence spectra have been obtained by determining the correction factors and by dividing the observed emission intensities by these factors at any specified wavelength. Automatic recording of the corrected excitation spectra is possible in this instrument if the signal from the sample cell and signal from the reference cell are fed into recorder which can record the ratio of the two signals. This part is indicated by dotted lines in the block diagram (Fig.2.1).

2.2.2 CORRECTION FACTOR DETERMINATION

In a spectrofluorimeter, the intensity of the lamp, efficiency of the monochromator and the response of the

photomultiplier tube are wavelength dependent. So all spectrofluorimeters record only an 'apparent emission spectrum' or an 'apparent excitation spectrum' in the absence of an automatic correction accessory.

Such spectra in some regions are grossly distorted version of the true spectra. Even though the uncorrected emission spectrum can be used for some experiments like fluorimetric titrations (where the relative fluorescence intensity measured at a particular wavelength), the apparent fluorescence spectra are not useful in calculating quantum yields and for reporting the fluorescence spectra of new compounds. Several methods have been described and are used for the determination of correction factor.¹²⁹⁻¹³⁴ The principles of Melhuish's¹³² method for the calculation of correction factor $Q(\lambda)$ for the light source (150 w Xe lamp) - Excitation monochromator combination have been followed in this study. The correction factor for emission monochromator-1P28 photomultiplier tube combination have been determined by following the procedure of Chen.¹³³ All calibrations are done with 150w xenon lamp.

2.2.3. CORRECTION FACTORS FOR THE LIGHT SOURCE (150.w Xe lamp)- EXCITATION MONOCHROMATOR COMBINATION

A concentrated solution of Rhodamine-B (3 gm/litre in ethyleneglycol) was taken in a quartz cell of size 1 cm x 0.5 cm and was placed in C_2 at an angle of 45° . The emission was viewed from the back of the cell (Fig. 2.1). The advantage of this arrangement is that if the incident radiation contains a small portion of 'impure wavelengths' not absorbed by the quantum counter (Rhodamine-B solution), they are not registered by the detector (D_2). The emission from this solution was passed through a narrow band metal interference filter placed before D_2 . It has a maximum transmission at 620 nm with a band width of 10 nm. The intensity of the fluorescence signal at 620 nm is proportional to the intensity of the excitation light. This signal amplified by the electrometer amplifier, was recorded by scanning the M_1 from 320 to 600 nm, during which the slits of M_1 were kept at 1 nm (11 nm band width). The spectrum recorded is called the excitation system calibration curve and it is shown in Fig. 2.3. This curve gives the relative intensities of the excitation light emerging from M_1 at all wavelengths. These are the correction factors at different wavelengths i.e. $Q(\lambda)$. This $Q(\lambda)$ was used for the calibration of emission system.

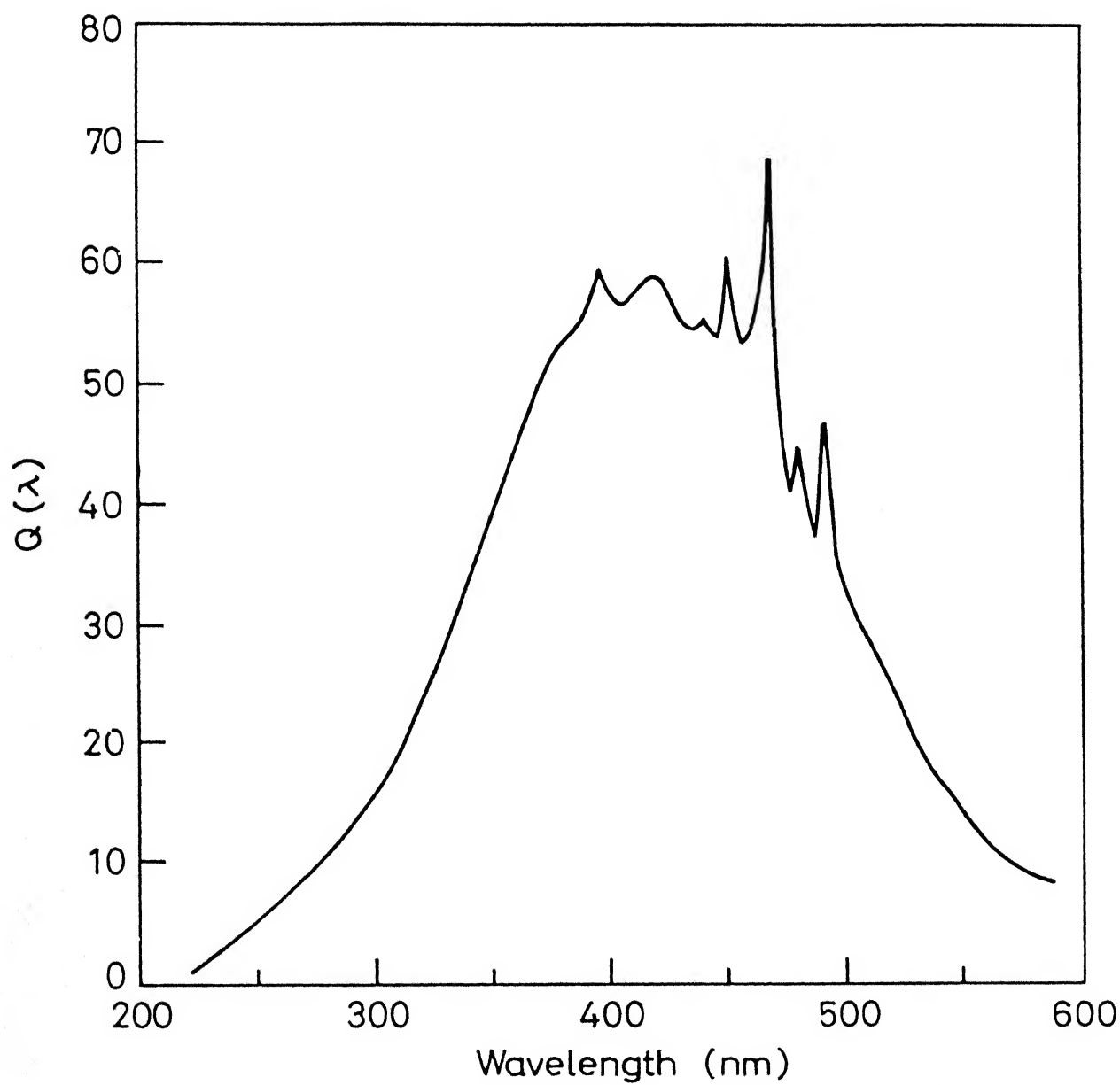


Fig. 2.3 Relative intensity distribution of excitation source.

2.2.4 CORRECTION FACTORS FOR THE EMISSION MONOCHROMATOR-1P28 PHOTOMULTIPLIER TUBE COMBINATION

The calibration factors for M_2 were calculated from 230 to 450 nm for the low blaze grating (300 nm) and 450 to 550 nm for the high blaze grating (500 nm).

A quartz plate at 45° to the incident light was placed in C_1 . The intensity of the incident light was reduced by adjusting the slit of M_1 . The slit of M_2 was set at 1 mm.

One selected wavelength was set at M_1 , the output of which was reflected by the quartz plate to M_2 . M_2 was adjusted manually to give the maximum reading at the wavelength set in M_1 . This maximum reading at this wavelength is the relative response of the emission monochromator-photomultiplier combination and is denoted by $R(\lambda)$. The maximum readings were obtained for each wavelength set at M_1 . This $R(\lambda)$ when divided by $Q(\lambda)$ determined earlier, gave $S(\lambda)$, the emission correction factor at λ . A plot of $S(\lambda)$ vs λ gives the emission spectral sensitivity curve or the correction curve, as shown in Fig. 2.4, for the low blaze and the high blaze gratings.

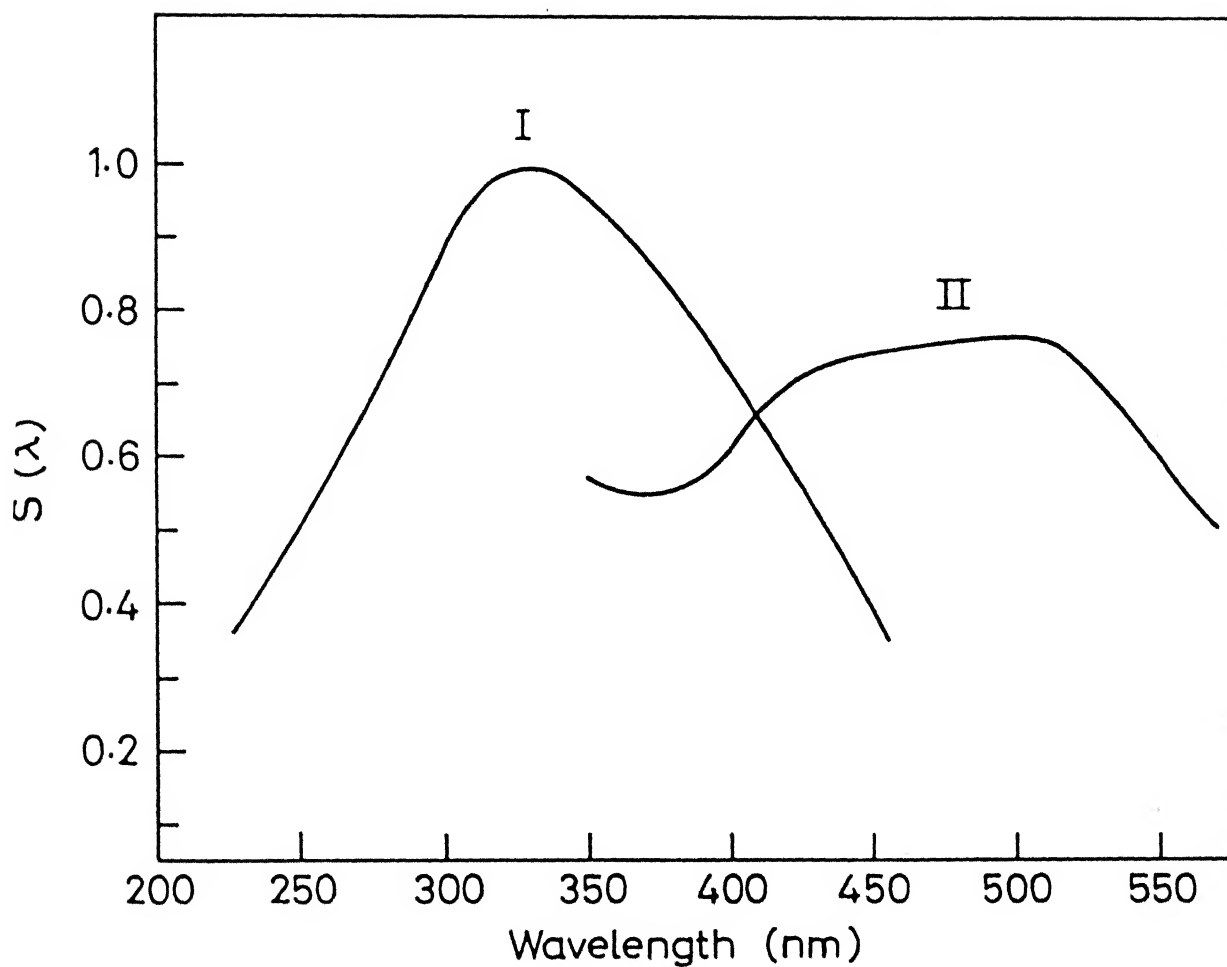


Fig. 2.4 Emission calibration curves : I 300 nm blaze grating
II 500 nm blaze grating.

These correction factors were used to correct the fluorescence spectrum of anthracene ($1 \times 10^{-5} \text{M}$ in ethanol), recorded using the low blaze grating and quinine sulphate ($1 \times 10^{-5} \text{M}$ in $0.1 \text{N H}_2\text{SO}_4$) recorded using high blaze grating. The corrected spectra thus obtained are shown in Figs. 2.5 and 2.6. They match exactly with the spectra reported in the literature.¹³²

2.3 OTHER INSTRUMENTS

All absorption spectra were recorded in a double beam Shimadzu 190 spectrophotometer, equipped with model U-135 recorder. pH of various solutions were measured by Toshniwal pH meter model CL44A. Standard buffer solutions were used for calibration of the pH meter.

3.4 MATERIALS

2-(aminomethyl)benzimidazole dihydrochloride and 5-chloro-2-(trichloromethyl)benzimidazole were obtained from Aldrich Chemical Company. These compounds were further purified by repeated crystallization from aqueous ethanol. 2-(Hydroxymethyl)-¹³⁵, 2-(cyanomethyl)-¹³⁵, 2-(chloromethyl)-¹³⁶, 2-(trifluoromethyl)-¹³⁷ and 2-(dichloromethyl)-¹³⁸ benzimidazoles were prepared by taking 1:1 molar ratio of o-phenylenediamine and the

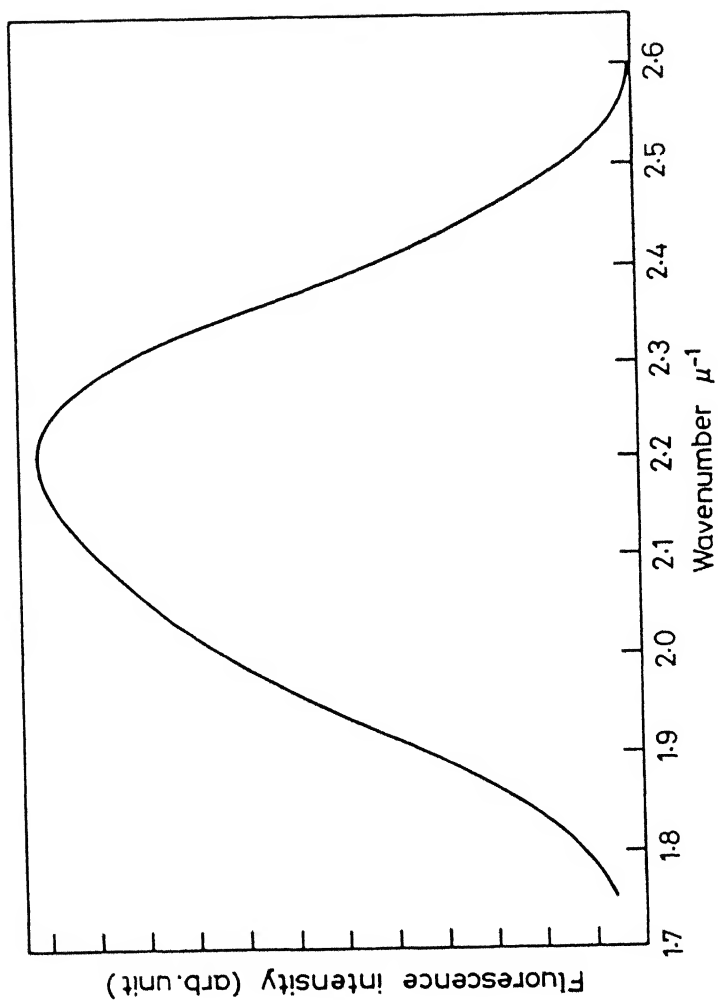


Fig.2.6 Corrected Fluorescence spectrum of Quinine Sulphate
(1×10^{-5} M in $0.1N H_2SO_4$)

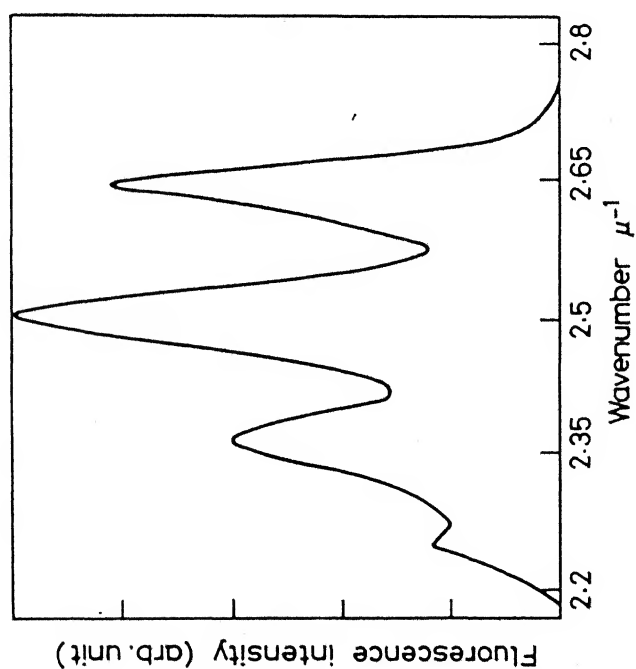


Fig.2.5 Corrected Fluorescence spectrum of
Anthracene (1×10^{-5} M in ethanol)

corresponding substituted acetic acid in 4N hydrochloric acid and refluxing the mixture for 30 to 40 minutes. On neutralization of the filtered solution with aqueous ammonia, the corresponding substituted benzimidazole was separated. These were recrystallized for further purification from aqueous ethanol.

2-(2'-hydroxyphenyl)benzimidazole and 2-(2'-methoxyphenyl)benzimidazole were prepared and purified in the following manner. o-Methoxybenzoic acid (0.02 mol), o-phenylenediamine (0.02 mol) and 60 gms of polyphosphoric acid were refluxed at 130°C for 15 hours and for an additional 48 hours at 185-190°C. The reaction mixture was cooled, poured into 300 ml of water and neutralized with 50% aqueous sodium hydroxide solution. The precipitates were removed by filtration, washed with water and dried under vacuum. Vacuum sublimation of the crude product gave pure 2-(2'-hydroxyphenyl)benzimidazole.¹³⁹ In a similar manner, 2-(2'-methoxyphenyl)benzimidazole was prepared by the condensation of o-methoxybenzoic acid and o-phenylenediamine in polyphosphoric acid at 135°C.¹³⁹

2-(3'-hydroxyphenyl)benzimidazole¹⁴⁰ was prepared by heating o-phenylenediamine and m-hydroxybenzoic acid for 3 hours under CO₂ atmosphere at 220°C. The resultant

melt was dissolved in minimum amount of methanol and poured in to 10% sodium bicarbonate solution. Precipitate was filtered off and recrystallised from methanol.

For the preparation of 2-(4'-hydroxyphenyl)benzimidazole¹⁴⁰ o-phenylenediamine in 20 ml of methanol was added portion wise at 0°C with stirring to p-hydroxybenzaldehyde in methanol and then with 30 ml of nitrophenol. This methanol was distilled out and the residue was refluxed for one minute. Its treatment with benzene gave the desired product. It was recrystallised from acetone.

2-(3'-methoxyphenyl)- and 2-(4'-methoxyphenyl)benzimidazole were prepared by usual methylation procedure using methyl sulphate¹⁴¹ in the following manner. Equimolar quantities of compound and sodium hydroxide were taken and the mixture was cooled to 10°C. Dimethyl sulphate was added slowly with stirring. The mixture was poured into cold water. The resultant solution was required compound was extracted with ether. Distillation of ether gave the desired compound which was again recrystallised from acetone.

Following method was under taken for the preparation of 2-chlorobenzimidazole.¹⁴² Benzimidazoline-2-one (15g) was boiled under reflux for 3.5 hours with phosphoryl chloride (150 ml). Hydrogen chloride was passed during the last 3 hours only. 2-Chlorobenzimidazole was obtained after recrystallisation

from aqueous ethanol.

N-Methylation of 2-(hydroxymethyl)benzimidazole to give N-methyl-2-(hydroxymethyl)benzimidazole was carried out in the following manner. Equimolar quantities of corresponding benzimidazole and methyl iodide was taken in 50% sodium hydroxide. The reaction mixture was kept on the ice bath and it was stirred for 3 minutes. Then the mixture was slowly heated and the temperature was maintained at 30-40°C for 10 minutes. The organic layer was extracted with chloroform, washed with water and dried over anhydrous sodium sulphate. The evaporation of the solvent in vacuo gave N-methyl-2-(hydroxymethyl)benzimidazole.¹⁴³

5-Chlorobenzimidazole-2-carboxylic acid¹⁴⁴ was prepared by hydrolysing 5-chloro-2-(trichloromethyl)benzimidazole in basic solution. 5-Chloro-2-(trichloromethyl)benzimidazole was treated with 2N sodium hydroxide till the vigorous exothermic reaction subsided. The resultant solution was neutralised with dilute hydrochloric acid and the precipitates were extracted with dioxane. The insoluble material was 5-chlorobenzimidazole-2-carboxylic acid. The corresponding ester of the acid was prepared by heating 2-(trichloromethyl)benzimidazole under reflux in methanol for 20 hours. On dilution and neutralisation with sodium carbonate gave methyl ester of benzimidazole-2-carboxylic acid.¹⁴⁴ It was recrystallised from ethyl acetate.

Methyltrichloroacetimidate was obtained from Aldrich to prepare 2-(trichloromethyl)benzimidazole.¹⁴⁵ To a cooled solution of o-phenylenediamine (0.1 mol) in acetic acid, methyltrichloroacetimidate (0.1 mol) was added slowly. When the resultant exothermic reaction subsided, the reaction mixture was kept at room temperature for several hours. According to literature report aqueous quenching of the solvent should give 2-(trichloromethyl)benzimidazole. But experiment in our laboratory showed that this method has always resulted in a mixture of 2-(trichloromethyl)benzimidazole and 2,2'-bisbenzimidazole as the products. Attempt to isolate only 2-(trichloromethyl)benzimidazole was a failure. Later these two compounds were separated by preparative thick layer chromatography using Merck Silica-gel G for thin layer chromatography. The eluting solvent was a mixture of ethylacetate and benzene in 1:1 (v/v) ratio. Benzimidazole-2-carboxylic acid was prepared from 2-(trichloromethyl)benzimidazole in the same manner as described earlier.¹⁴⁴

Benzimidazole-2-acetic acid¹³⁵ was prepared by hydrolysing 2-(cyanomethyl)benzimidazole in the following manner. 2-(cyanomethyl)benzimidazole (0.01 mol) was added to 20 cc of water solution containing 1.2 gm of NaOH and 3 cc of ethyl alcohol. The resulting mixture was refluxed for two hours until no more

ammonia gas was evolved. The precipitate came out when the solution was acidified with hydrochloric acid and it was recrystallised from aqueous ethanol.

Benzimidazole-2-propionic acid¹⁴⁶ was synthesized in two steps as described below. Succinic anhydride (5g) was suspended in 35 cc of hot dry benzene and to this o-phenylenediamine (5.4g) dissolved in 50 cc of benzene was added. The reaction was completed in few minutes by shaking well. A white mass (o-aminophenylamido succinic acid) was deposited, which was recrystallised from ethanol as colourless silky needles.

In the second step o-aminophenylamido succinic acid was boiled under reflux for three hours with absolute alcohol. The volume of the alcohol was reduced to one-third and allowed to stand overnight. Colourless crystals separated out which were recrystallised from ethanol.

2.4.1 PURIFICATION OF SOLVENTS

Spectroscopic grade methanol, analytical grade sulphuric acid, phosphoric acid and sodium hydroxide (BDH) were used without further purification. Acetonitrile (E. Merck), cyclohexane, ether (all BDH) and ethanol were purified as described in the literature.¹⁴⁷ Trifluoroacetic acid and piperidine from Fluka

were used as such. A brief description about the purification of solvents is given.

Cyclohexane was passed twice through a 11 mm diameter, 50 ml long column filled with 40g silica gel (60-120 mesh) to remove benzene, paraffinic hydrocarbons and carbonyl compounds. This was fractionally distilled over sodium at 80°C.

Ether was kept for one night over calcium chloride, refluxed and distilled. Again it was refluxed over sodium and fractionally distilled. Finally this was preserved over sodium.

Acetonitrile was further purified by fractional distillation over P_2O_5 at 81.5°C.

Ethanol was refluxed over calcium oxide for 36 hours and then fractionally distilled.

Triply distilled water was used for the preparation of all aqueous solutions.

2.4.2 PURITY OF THE MATERIALS

The purity of all the compounds prepared was checked by thin layer chromatography and by taking U.V and I.R. spectra, in addition to their sharp melting points, which one in agreement with the reported values. The purity was also checked by fluorescence techniques i.e. by getting same fluorescence maxima

when excited with different wavelengths. The purity and transparency of the solvents were checked by their U.V. spectra taken using triple distilled water as reference.

2.5 ADJUSTMENT OF H_o /pH/ H_- VALUES

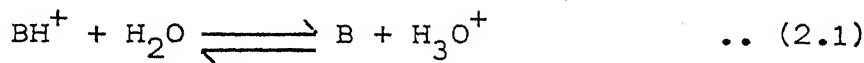
pH of the solution within the range 1-13 was adjusted by the addition of small concentrations of phosphate buffer ($10^{-3}M$), as it was found that these buffers do not quench the fluorescence of the compounds and also do not alter the prototropic equilibrium under study.¹⁴⁸ Acetate buffers are found to quench the fluorescence. The total analytical concentration of buffers i.e. ($[H_2PO_4^-] + [HPO_4^{2-}]$) was maintained constant for each pH solution.

Hammett's acidity scale (H_o)¹⁴⁹ was used for the solutions with pH below 1. The Hammett's acidity and basicity scales represent the actual (or free) amount of protons or hydroxyl ions present which is found by their reaction with a weak base or a weak acid (indicator) respectively. Hammett's acidity scale modified by Jorgenson and Hartter¹⁵⁰ was used in this study. Sulphuric acid was used to obtain these H_o values.

A similar scale known as ' H_- ' scale for aqueous basic solutions constructed by Yagil¹⁵¹ was used for measuring above pH 13.

2.6 GROUND STATE EQUILIBRIUM CONSTANTS

The dissociation reaction of any acid can be represented as



and the equilibrium constant by the relation

$$\text{pH} = \text{pK}_a + \log \frac{[\text{B}]}{[\text{BH}^+]} \quad \dots (2.2)$$

where $[\text{B}]$ and $[\text{BH}^+]$ are the concentrations of the base and its conjugate acid respectively. pH represents the hydrogen ion concentration at the above concentration of the species and pK_a , the equilibrium constant of the above reaction. Thus pK_a can be calculated if one knows the concentration of each species at the specific pH and these can be calculated spectrophotometrically as follows:

- (i) If the absorption spectra of acid and its conjugate base do not overlap, one can choose the two wavelengths, which only represent the respective species, and measure the absorbances (A) as a function of pH. The concentration of each species can be calculated from the Beer-Lambert's law i.e.

$$A = \epsilon Cl \quad \dots (2.3)$$

where ϵ , is the extinction coefficient at the respective

chosen wavelength, l , the pathlength and c , the concentration. ϵ can be calculated from the solution of known concentration which contains only the one specific form.

(ii) If the absorption spectra of both the species overlap each other, absorbances are measured at two chosen wavelengths λ_1 and λ_2 i.e.

$$A_{\lambda_1} = \epsilon_{\lambda_1}(\text{BH}^+) C_{\text{BH}^+} l + \epsilon_{\lambda_1}(\text{B}) C_{\text{B}} l \quad \dots (2.4)$$

$$A_{\lambda_2} = \epsilon_{\lambda_2}(\text{BH}^+) C_{\text{BH}^+} l + \epsilon_{\lambda_2}(\text{B}) C_{\text{B}} l \quad \dots (2.5)$$

The values of ϵ_{λ_i} 's of each form, at each analytical wavelength can be calculated as mentioned in (i) and the concentration of each species as

$$C_{\text{BH}^+} = \frac{A_{\lambda_1} \epsilon_{\lambda_2}(\text{B}) - A_{\lambda_2} \epsilon_{\lambda_1}(\text{B})}{\epsilon_{\lambda_1}(\text{BH}^+) \epsilon_{\lambda_2}(\text{B}) - \epsilon_{\lambda_2}(\text{BH}^+) \epsilon_{\lambda_1}(\text{B})} \quad \dots (2.6)$$

$$C_{\text{B}} = \frac{A_{\lambda_1} \epsilon_{\lambda_2}(\text{BH}^+) - A_{\lambda_2} \epsilon_{\lambda_1}(\text{BH}^+)}{\epsilon_{\lambda_1}(\text{B}) \epsilon_{\lambda_2}(\text{BH}^+) - \epsilon_{\lambda_2}(\text{B}) \epsilon_{\lambda_1}(\text{BH}^+)} \quad \dots (2.7)$$

if pathlength is 1 cm.

2.7 QUANTUM YIELD CALCULATION

The quantum yield of fluorescence (ϕ_f) of the compounds in different solvents were calculated relative to the commonly used fluorescence standards. Here quinine sulphate¹⁵² ($\phi_f = 0.55$) in 0.1N H₂SO₄ having fluorescence maximum of 440 nm and absorbance 0.1 was used as standard. The excitation wavelength used for this compound was 313 nm.

To avoid the effects like concentration quenching, self absorption, attenuation of absorbance through the path length of light inside solution, dilute solutions (absorbance 0.1) were used for quantum yield measurements. The longest wavelength absorption band was used for excitation of the molecule. The optical densities of the reference and test samples were always adjusted to the same or comparable values.

The formula used for the relative fluorescence quantum yield measurement¹⁵³ is

$$\phi_{\text{unknown}} = \phi_{\text{standard}} \times \frac{F_{\text{unknown}}}{F_{\text{standard}}} \times \frac{q_{\text{standard}}}{q_{\text{unknown}}} \times \frac{A_{\text{standard}}}{A_{\text{unknown}}}$$

where ϕ = fluorescence quantum yield.

F = Area under the fluorescence curve.

q = Excitation light intensity at the excitation wavelength taken from the curve (Fig. 2.3).

A = Absorbance at the excitation wavelength.

2.8 PREPARATION OF SOLUTIONS FOR ABSORPTIOMETRIC AND FLUORIMETRIC TITRATIONS

To maintain the constancy in the concentration of the compounds in all the $H_2O/pH/H_2O$ solutions, an accurately measured amount (.1 ml) of stock solution of the respective compounds was added to a constant volume (10 ml) of $H_2O/pH/H_2O$ solutions. OXFORD P-7000 micropipette system was used for pipetting 0.1 ml of stock solution. For fluorimetric titration the compounds were excited at respective isosbestic wavelength. The final concentration was in the order of $10^{-5} M$. The absorption and fluorescence spectra were taken immediately after the solutions were prepared, to avoid any chance of decomposition of the compounds.

2.9 OTHER DETAILS

The molar extinction coefficient (ϵ) values are given in $dm^3 mol^{-1} cm^{-1}$. The pK_a values listed in chapter 4 are in 1% (v/v) methanolic aqueous solutions.

CHAPTER-III

ABSORPTION AND FLUORESCENCE SPECTRA

EFFECT OF SOLVENTS

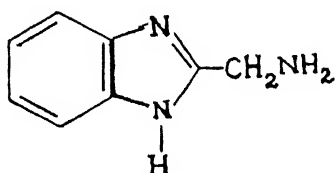
The absorption and fluorescence spectra of all the compounds studied have been divided into three sections.

- (i) 2-Methylbenzimidazole: Where one or more than one hydrogen atoms of the methyl group have been replaced by various functional groups or atoms. These compounds are 2-(aminomethyl)-, 2-(hydroxymethyl)-, 2-(chloromethyl)-, 2-(dichloromethyl)-, 5-chloro-2-(trichloromethyl)-, 2-(trifluoromethyl)- and 2-(cyanomethyl)benzimidazoles. 2-chlorobenzimidazole has also been included in this section.
- (ii) 2-(Hydroxyphenyl)- and 2-(Methoxyphenyl)benzimidazoles: This series includes 2-(2'-hydroxyphenyl)-, 2-(2'-methoxyphenyl)-, 2-(3'-hydroxyphenyl)-, 2-(3'-methoxyphenyl)-, 2-(4'-hydroxyphenyl)- and 2-(4'-methoxyphenyl)benzimidazoles.

(iii) 2-Substituted carboxylic acids of benzimidazoles: In this group, the compounds are; benzimidazole-2-carboxylic acid, 5-chlorobenzimidazole-2-carboxylic acid, 5-chlorobenzimidazole-2-methylcarboxylate, benzimidazole-2-acetic acid, benzimidazole-2-ethylacetate and benzimidazole-2-propionic acid.

In this chapter the results of the compounds described in each set will be given separately, and this will be followed by discussion.

3.1 2-(Aminomethyl)benzimidazole) (BINH₂)^{*}



Figures 3.1 and 3.2 depict the absorption and fluorescence spectra of BINH₂ in solvents of different polarity and hydrogen bond forming tendency at 300K. Tables 3.1 and 3.2 compile the relevant data i.e. absorption maxima, $\log(\epsilon_{\max})$, fluorescence maxima and the fluorescence quantum yield. Both the absorption and fluorescence spectra of BINH₂ resemble those of benzimidazole (BI) and 2-methylbenzimidazole¹²² (BIM) i.e. both the absorption band systems of parent BI molecule remain structured in all the solvents

^{*}H.K. Sinha and S.K. Dogra, Spectrochim Acta, 41A, 961 (1985).

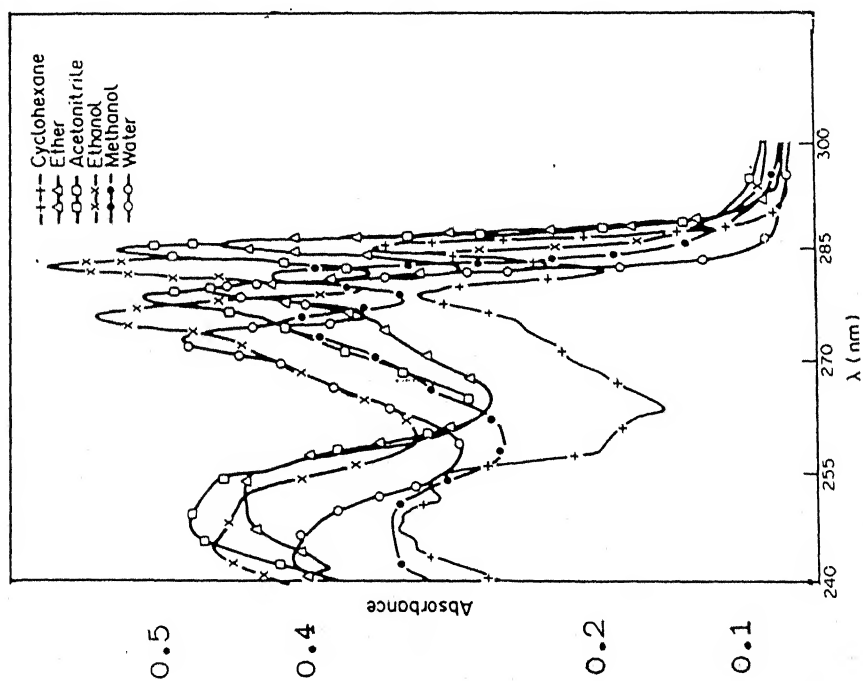


Fig.3.1 Absorption spectra of 2-(amino-methyl)benzimidazole (BINH₂) in different solvents at 298°K.

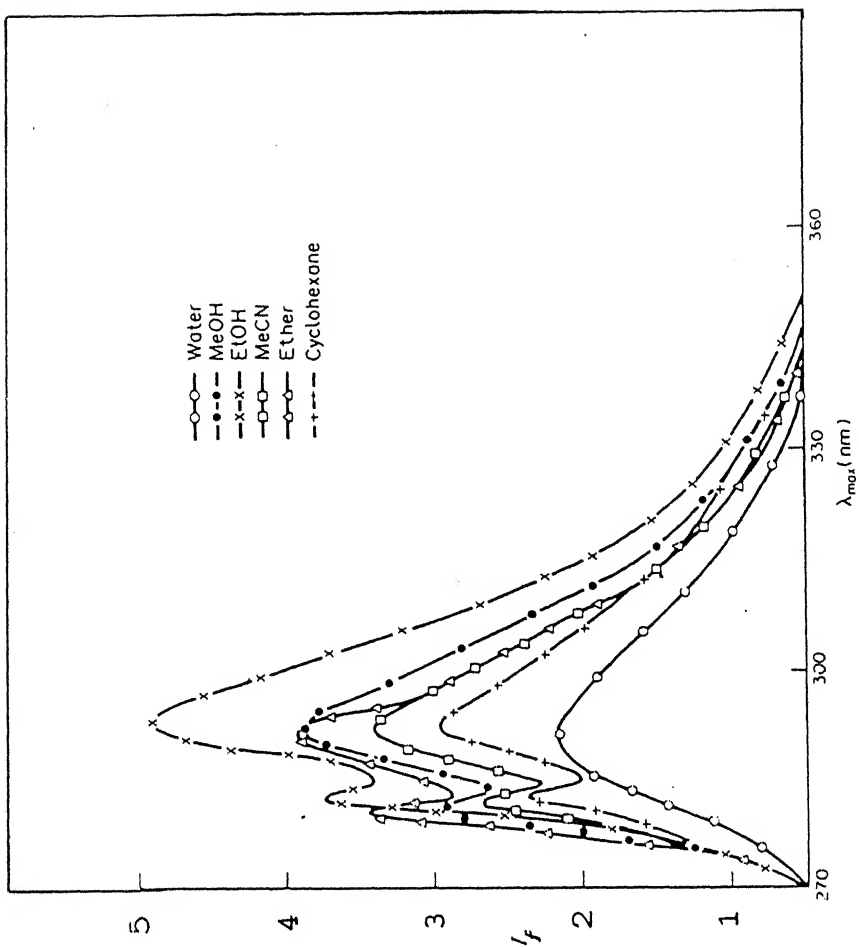


Fig.3.2 Fluorescence spectra of 2-(amino-methyl)benzimidazole (BINH₂) in different solvents at 298°K.

Table 3.1. Absorption maxima [λ_a (nm)] and $\log(\epsilon_{\max})$ of 2-(aminomethyl)benzimidazole (BINH₂) and 2-(hydroxymethyl)benzimidazole (BIOH) in different solvents at 298°K.

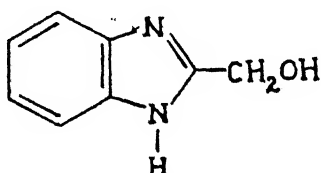
Compound	λ_a (nm) $\log(\epsilon_{\max})$					
	Cyclohexane	Ether	Acetonitrile	Methanol	Ethanol	Water(pH 7)
BINH ₂	283.5	284.5	283.5(3.80)	280(3.70)	281(3.84)	277.5(3.74)
	277.5	277.5	277.5(3.78)	—	—	—
	273	273	273(3.66)	273(3.68)	274(3.80)	271.5(3.76)
	252	250.5	250.5(3.74)	249(3.71)	249(3.71)	244.5(3.66)
	246	246	247.5(3.75)	246(3.58)	244(3.73)	243(3.66)
BIOH	—	284(3.60)	283(3.61)	283(3.75)	283(3.74)	278(3.63)
	—	277(3.62)	277(3.62)	276(3.77)	276(3.77)	271(3.68)
	—	271(3.49)	271(3.49)	270(3.63)	270(3.63)	265(3.58)
	—	249(3.63)	249(3.60)	247(3.69)	247(3.69)	243(3.59)

Table 3.2. Fluorescence maxima [λ_f (nm)] and quantum yield (ϕ_f) of 2-(aminomethyl)-benzimidazole (BINH₂) and 2-(hydroxymethyl)benzimidazole (BIOH) in different solvents at 298°K.

Compound	λ_f (nm) (ϕ_f)					
	Cyclohexane	Ether	Acetonitrile	Methanol	Ethanol	Water (pH 7)
BINH ₂	291	291	291	291	292	291
	(0.17)	(0.26)	(0.34)	(0.23)	(0.17)	(0.14)
	282.5	280	281.5	280.5	282	-
BIOH	-	294	294	293	294	292
		(0.22)	(0.20)	(0.26)	(0.22)	(0.17)
		285	285	285	284	284

but are slightly red shifted in any given solvent. The fluorescence spectrum of BINH_2 is also structured in all the solvents except water and is slightly red shifted as compared to BI and BIM in any one given solvent. The absorption spectrum gets slightly blue shifted with increasing hydrogen bond formation tendency of the solvent but the fluorescence maxima are hardly affected under similar environments. The fluorescence quantum yield of BINH_2 is less than that of BI¹²³ (0.7 ethanol) in any one particular solvent and decreases with increase in hydrogen bond forming tendency of solvents.

2-(Hydroxymethyl)benzimidazole (BIOH)* :



Figures 3.3 and 3.4 give the absorption and fluorescence spectra of BIOH in different solvents. The relevant data are compiled in Tables 3.1 and 3.2 respectively. BIOH does not dissolve in cyclohexane to give any measurable absorption or fluorescence spectra. The data of Tables 3.3 and 3.4 clearly indicate that the results observed for BIOH

* H.K. Sinha and S.K. Dogra, Indian J. Chem., 25A, 1092 (1986).

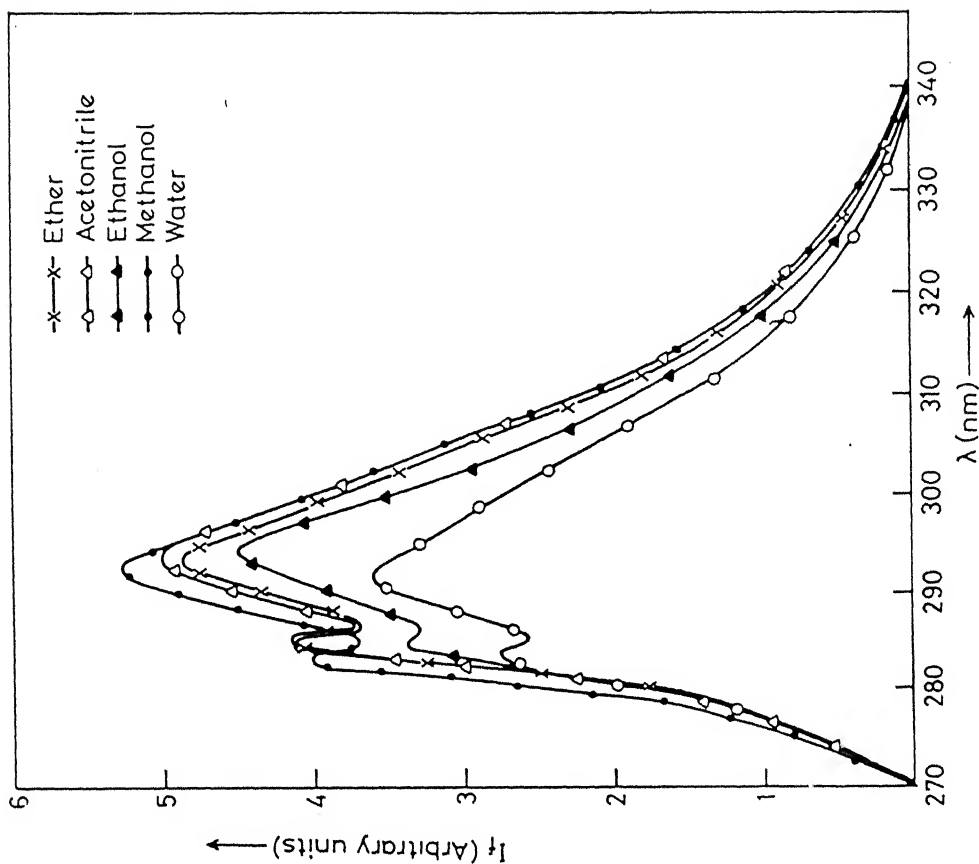


Fig.3.4 Fluorescence spectra of 2-(hydroxymethyl)benzimidazole (BIOH) in different solvents at 298°K.

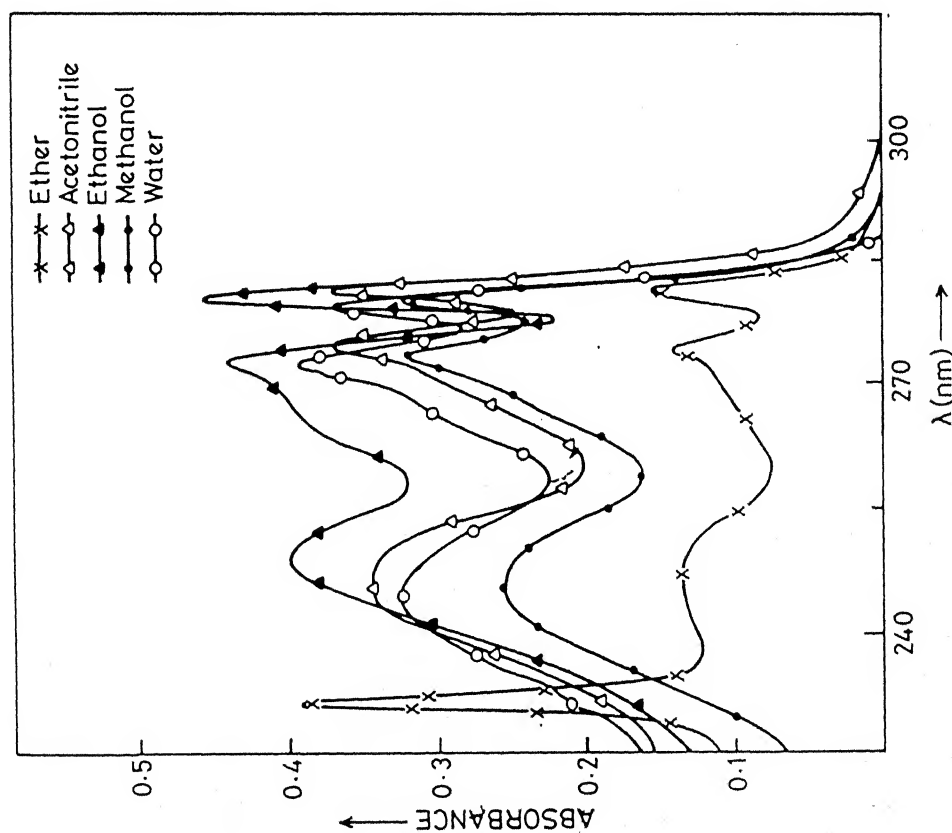
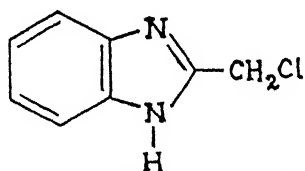


Fig.3.3 Absorption spectra of 2-(hydroxymethyl)benzimidazole (BIOH) in different solvents at 298°K.

are exactly similar to those of BINH_2 and inturn to those of BI and BIM. Like BI, the fluorescence quantum yield of BIOH is nearly independent of the nature of the solvents.

2-(Chloromethyl)benzimidazole (CMBI)*



Figures 3.5 and 3.6 depict the absorption and fluorescence spectra of CMBI in solvents of different polarity and hydrogen bond formation tendency. The relevant data have been compiled in Tables 3.3 and 3.4 respectively. Only the absorption band maxima of CMBI are given in cyclohexane and ether because the data have been recorded with saturated solutions due to its poor solubility in these solvents. The absorption spectrum of CMBI in any particular solvent resemble closely to BI and BIM and is slightly blue shifted as compared to BINH_2 or BIOH. On the otherhand fluorescence band maxima are slightly red shifted under the similar environment. Fluorescence quantum yield of CMBI is less than that of BINH_2 and BIOH. Unlike BINH_2

* H.K. Sinha and S.K. Dogra, J. Chem. Soc. Perkin Trans. 2, in press.

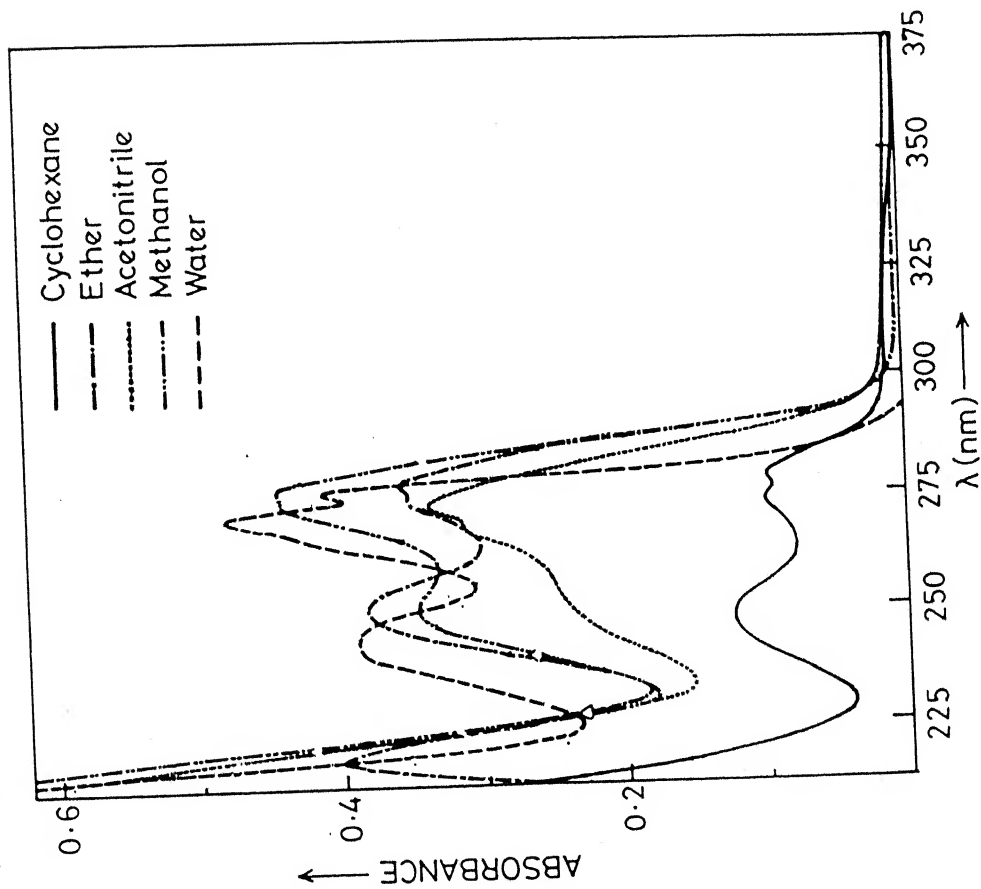


Fig.3.5 Absorption spectra of 2-(chloromethyl)benzimidazole (CMBI) in different solvents at 298°K.

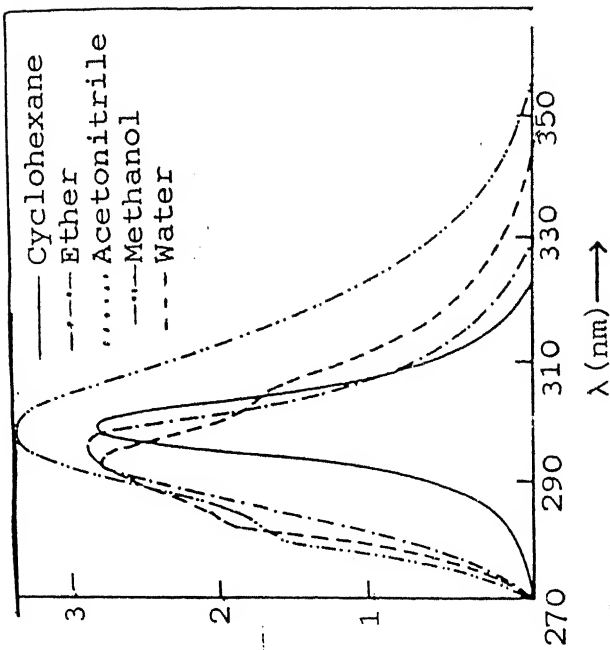
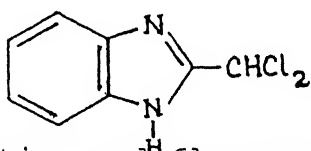


Fig.3.6 Fluorescence spectra of 2-(chloromethyl)benzimidazole (CMBI) in different solvents at 298°K

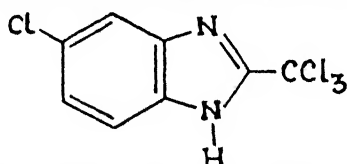
or BIOH it increases in going from non-polar (cyclohexane) to polar solvents (water). In acetonitrile the fluorescence is completely quenched.

2-(Dichloromethyl)benzimidazole (DMBI) *



The absorption and fluorescence spectra of DMBI in different solvents are shown in Figures 3.7 and 3.8 respectively. The relevant data are summarized in Tables 3.3 and 3.4. When compared with CMBI, absorption maxima of DMBI are slightly red shifted whereas the fluorescence maxima are nearly in the same region but the spectra are more structured. The behaviour of DMBI in different solvents are similar to those of BI, BIM and CMBI. The fluorescence quantum yield follow the same trend as observed in CMBI. But the fluorescence quantum yield is very small in acetonitrile, showing that this solvent acts as a quencher of fluorescence.

5-Chloro-2-(trichloromethyl)benzimidazole (TMBI) *



Figures 3.9 and 3.10 depict the absorption and fluorescence

* H.K. Sinha and S.K. Dogra, J.Chem.Soc.Perkin Trans. 2, in press.

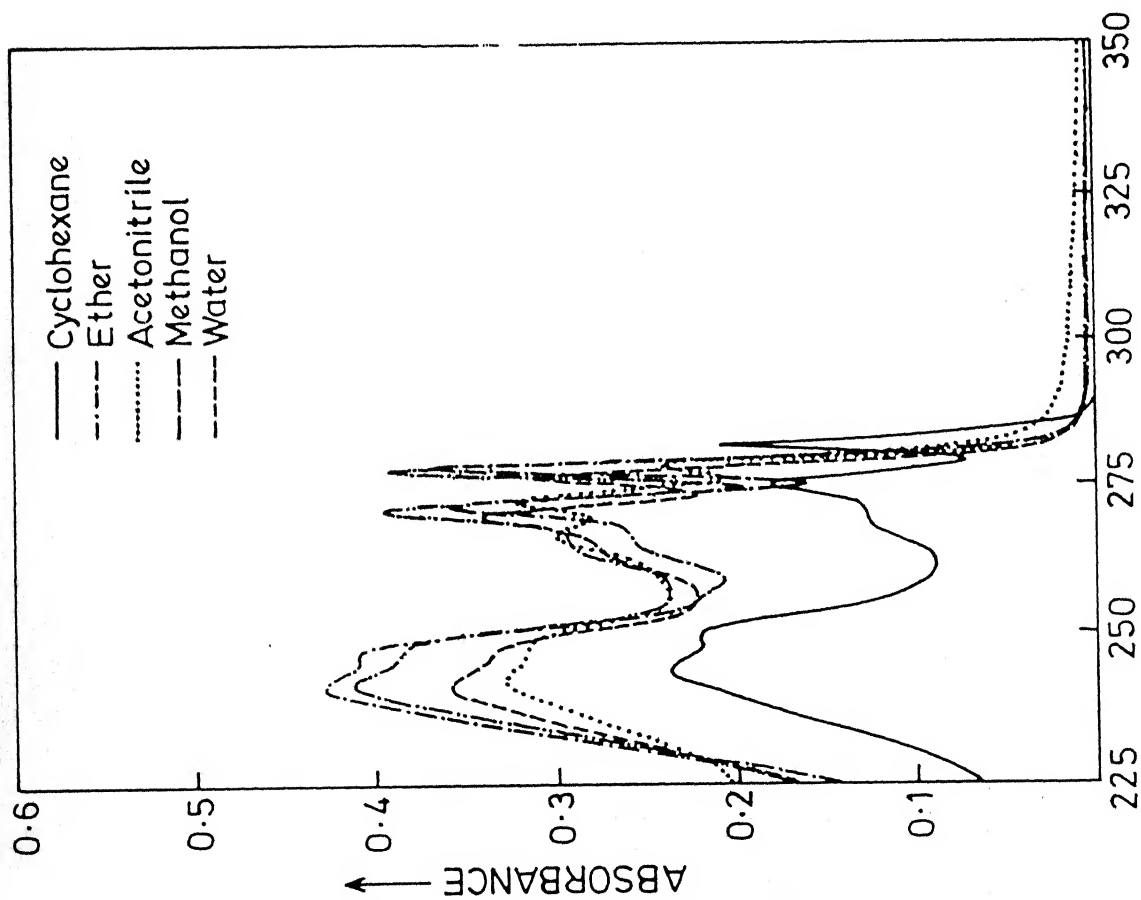


Fig.3.7 Absorption spectra of 2-(dichloromethyl)benzimidazole (DMBI) in different solvents at 298°K.

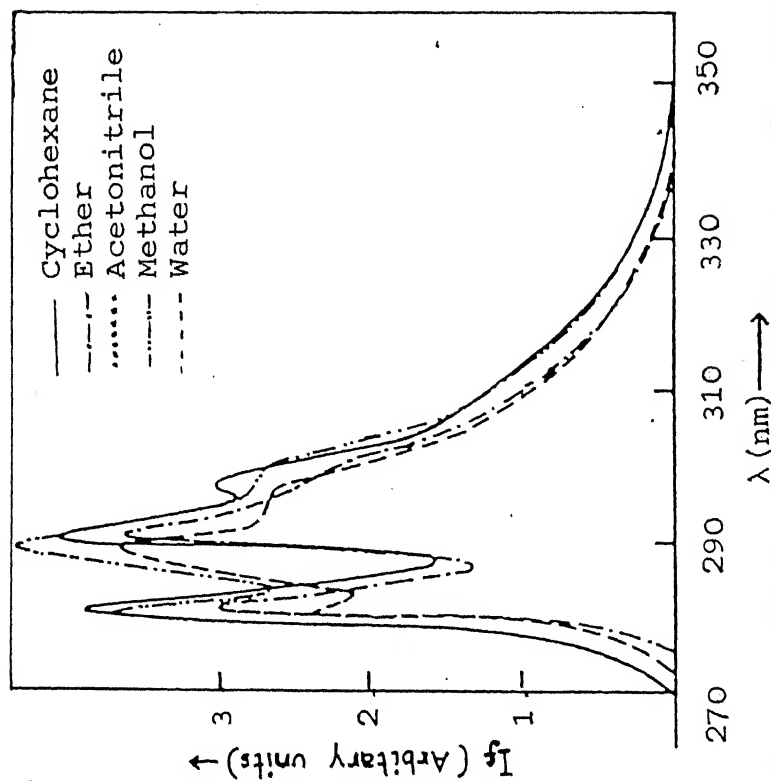


Fig.3.8 Fluorescence spectra of 2-(dichloromethyl)benzimidazole (DMBI) in different solvents at 298°K.

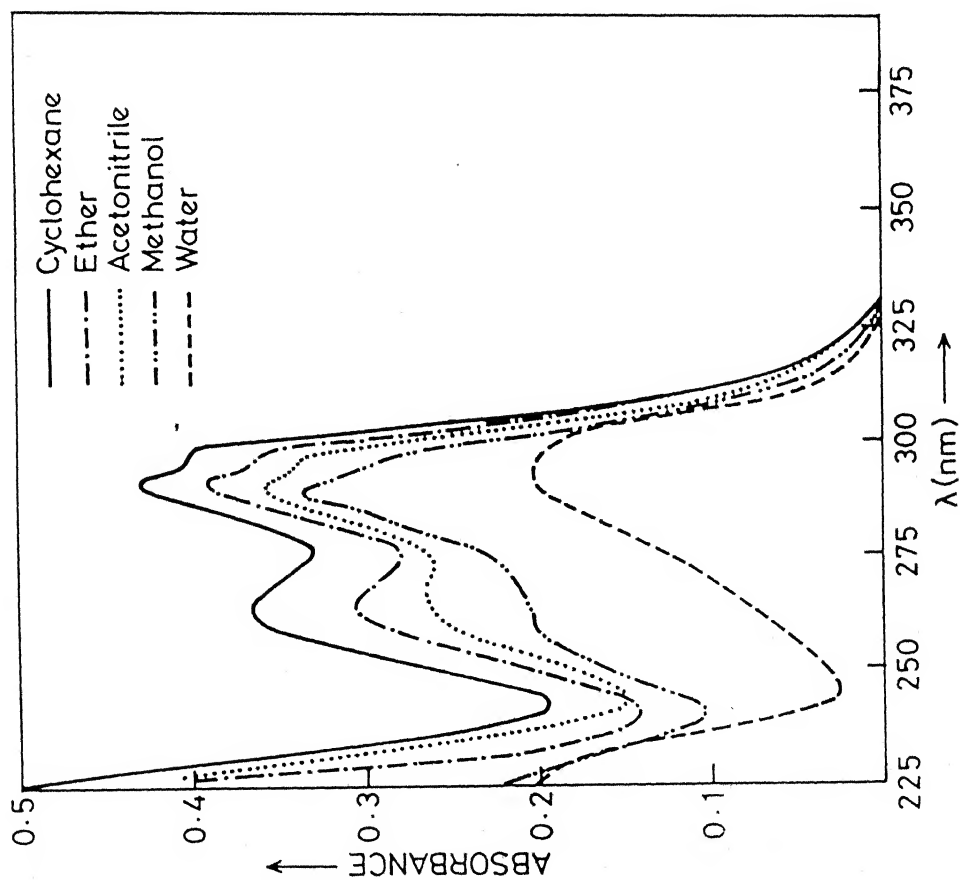


Fig.3.9 Absorption spectra of 5-chloro-2-(trichloromethyl)benzimidazole (TMBI) in different solvents at 298°K.

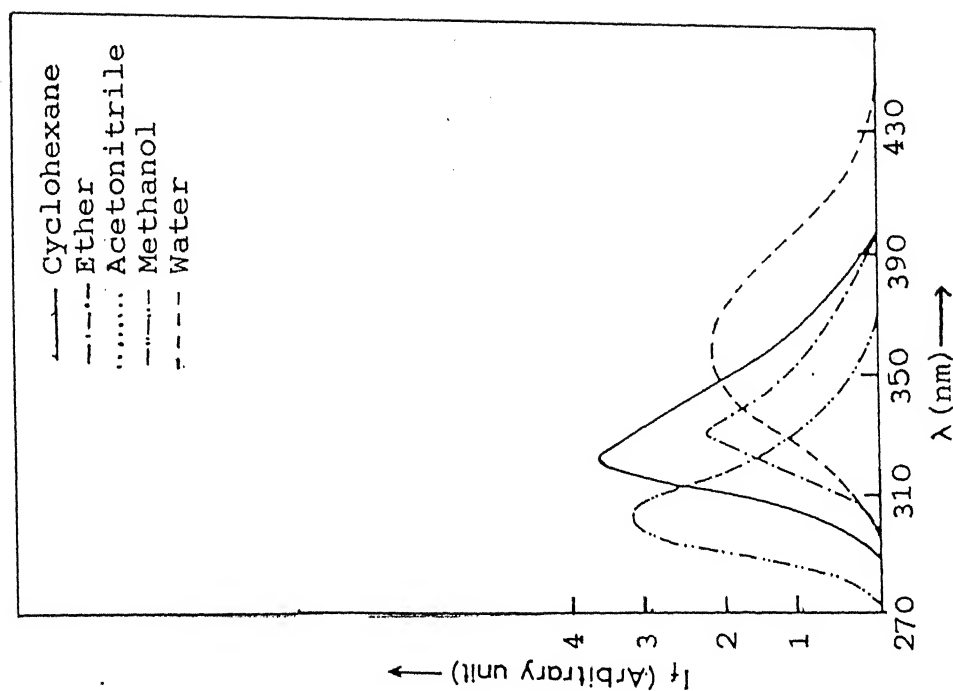
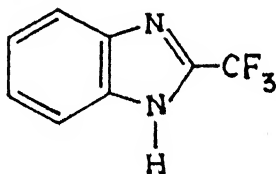


Fig.3.10 Fluorescence spectra of 5-chloro-2-(trichloromethyl)benzimidazole (TMBI) in different solvents at 298°K.

spectra in different solvents and the respective data are summarized in Tables 3.3 and 3.4. In TMBI, the red shift observed in absorption and fluorescence spectra in any one particular solvent is much greater than that noticed in case of BIM or CMBI or DMBI. The absorption maxima get slightly blue shifted on increasing the polarity and hydrogen bond formation ability of the solvents, whereas under the similar conditions, fluorescence maxima are red shifted. The fluorescence spectra show greater sensitivity towards the solvents than the absorption spectra. The fluorescence quantum yield is very low in any one particular solvent when compared with BI or CMBI or DMBI. Appreciable fluorescence is observed only in methanol as a solvent. Fluorescence is completely quenched in acetonitrile.

2-(Trifluoromethyl)benzimidazole (FMBI)*



The absorption and fluorescence spectra in different solvents are shown in Figures 3.11 and 3.12 respectively. Tables 3.3 and 3.4 summarize the respective data. The absorption and fluorescence characteristics of FMBI in different solvents are quite similar to those of TMBI except the fluorescence

* H.K. Sinha and S.K. Dogra, J. Chem. Soc. Perkin. Trans. 2, in press.

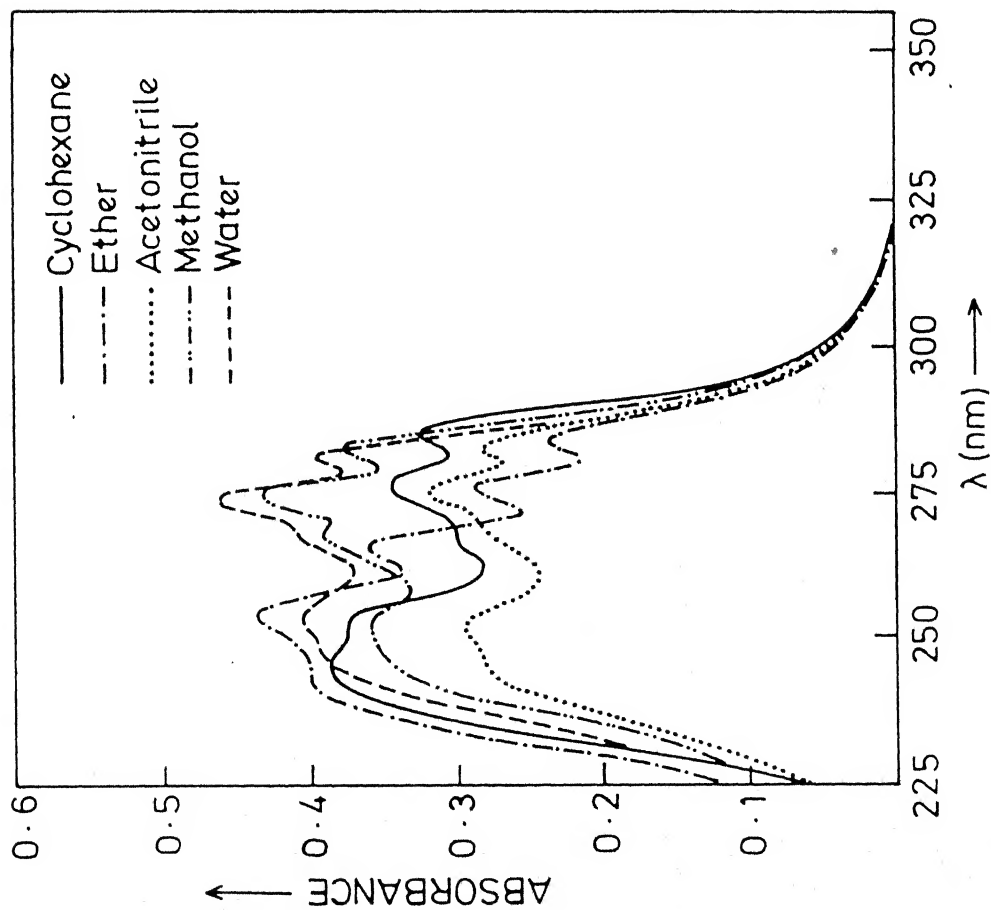


Fig.3.11 Absorption spectra of 2-(trifluoromethyl)benzimidazole (FMBI) in different solvents at 298°K.

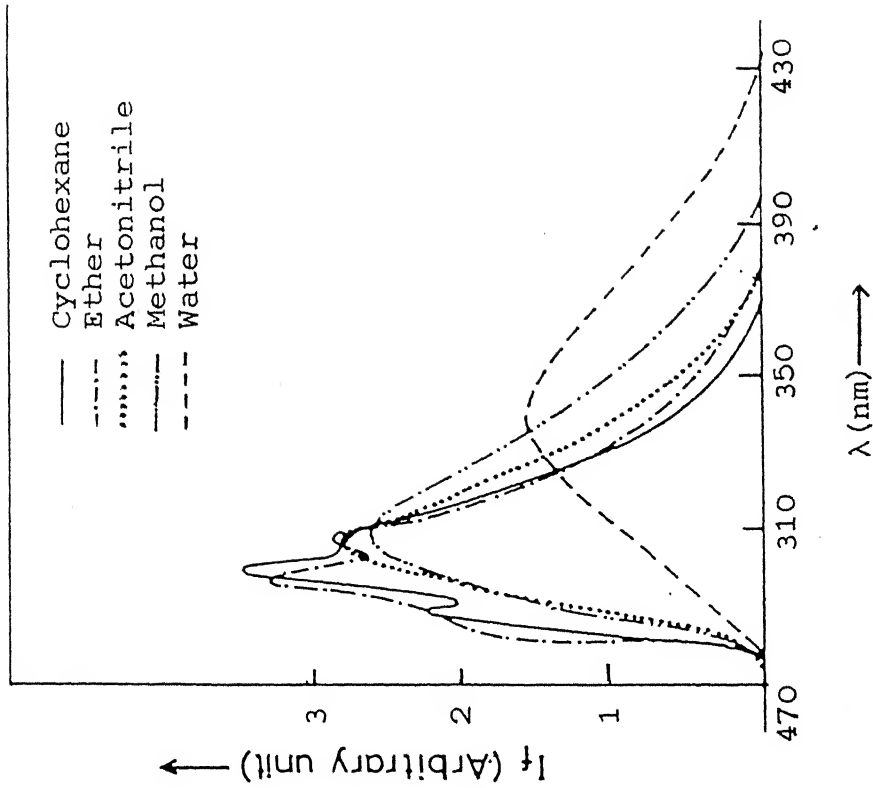
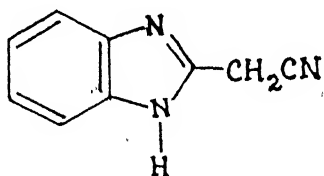


Fig.3.12 Fluorescence spectra of 2-(trifluoromethyl)benzimidazole (FMBI) in different solvents at 298°K.

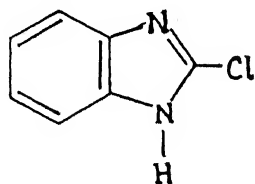
quantum yield. The fluorescence quantum yield of the former is greater than the latter in any one given solvent but it is less than that of BI or BIM. The structure of the absorption and fluorescence spectrum is lost on increasing the polarity or hydrogen bonding capacity of the solvents.

2-(Cyanomethyl)benzimidazole (CNBI)*



The behaviour of CNBI in different solvents resembles that of CMBI and inturn with BI or BIM. Figures 3.13 and 3.14 give the absorption and fluorecence spectral profiles, whereas the Tables 3.3 and 3.4 compile the respective data.

2-Chlorobenzimidazole (2CBI)*



Figures 3.15 and 3.16 give the absorption and fluorescence spectra in different solvents respectively. Tables 3.3 and 3.4 summarize the respective data. From the data of Table 3.3 it is clear that the absorption spectrum in different solvents nearly

* H.K. Sinha and S.K. Dogra, J. Chem. Soc. Perkin Trans. 2, in press.

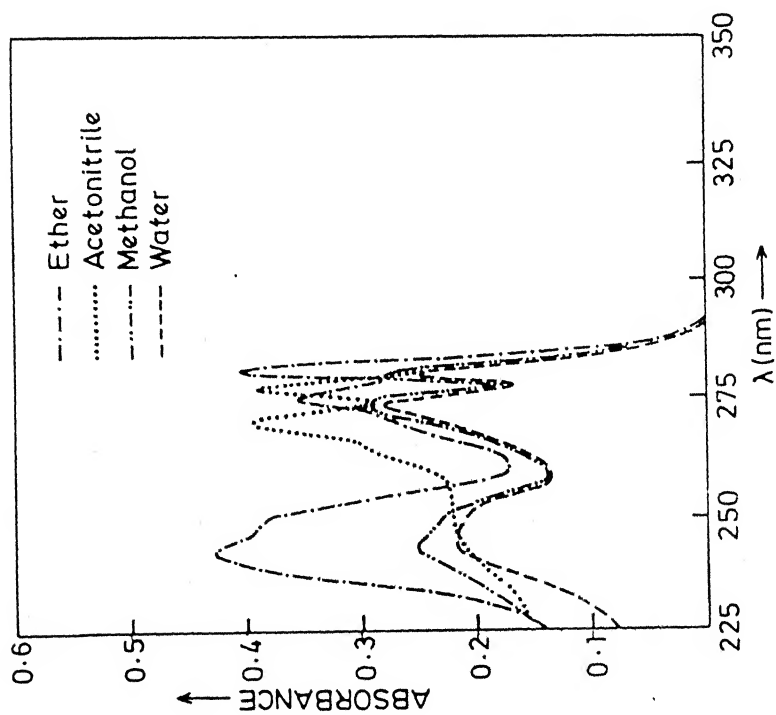


Fig.3.13 Absorption spectra of 2-(cyano-methyl)benzimidazole (CNBI) in different solvents at 298°K.

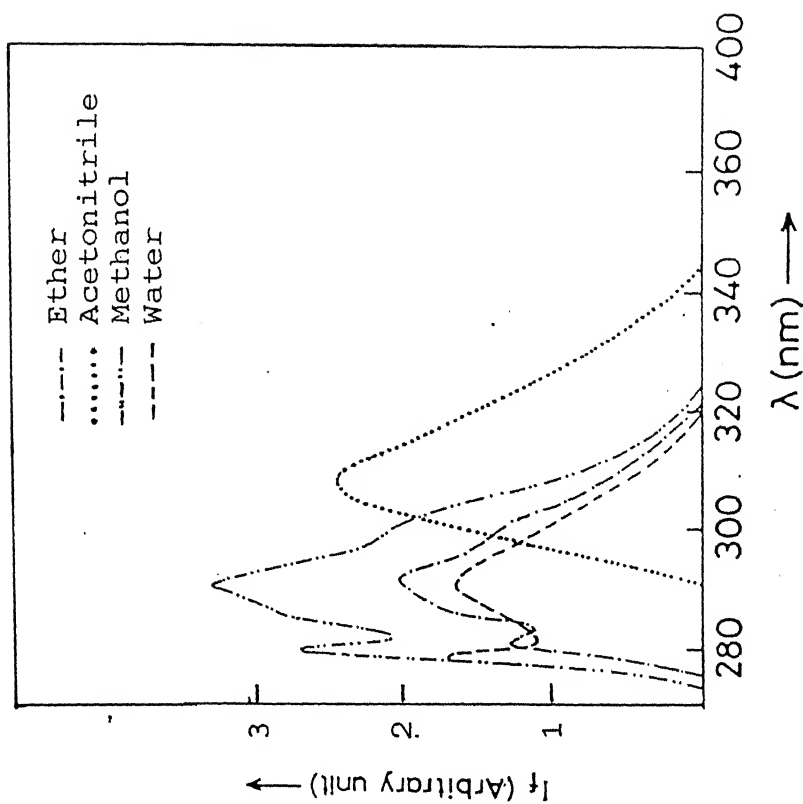


Fig.3.14 Fluorescence spectra of 2-(cyano-methyl)benzimidazole (CNBI) in different solvents at 298°K.

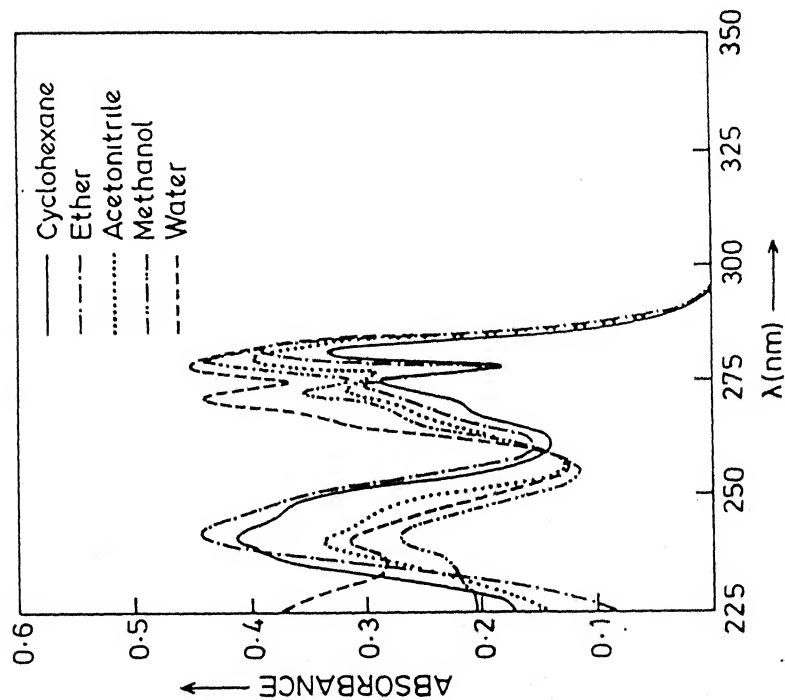


Fig.3.15 Absorption spectra of 2-chloro-benzimidazole (2CBI) in different solvents at 298°K.

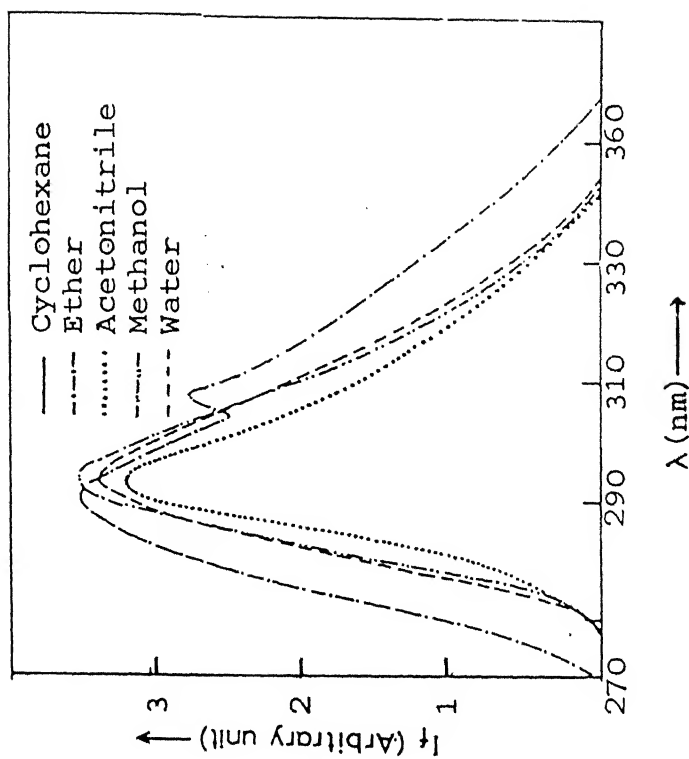


Fig.3.16 Fluorescence spectra of 2-chloro-benzimidazole (2CBI) in different solvents at 298°K.

Table 3.3. Absorption maxima [λ_a (nm)] and $\log(\epsilon_{\max})$ of 2-(chloromethyl)-[CMBI], 2-(dichloromethyl)-[DMBI], 5-chloro-2-(trichloromethyl)-[TMBI], 2-(trifluoromethyl)-[FMBI], 2-(cyanomethyl)-[CNBI] and 2-chloro-benzimidazoles [2CBI] in different solvents at 298°K.

Solvent	λ_a (nm) $\log(\epsilon_{\max})$						
	CMBI	DMBI	TMBI	FMBI	CNBI	2CBI	
1	2	3	4	5	6	7	
Cyclohexane	279	282	289	285		281	
	278	275	261	276		275	
	248	269	213	266	-	268	
	209	250		254		241	
		244		246		211	
		209		210			
Ether	279	281 (3.88)	298	285 (3.85)	281 (3.95)	281 (3.82)	
	274	275 (3.85)	290	276 (3.92)	275 (3.92)	274 (3.77)	
	250	269 (3.70)	265	266 (4.03)	268 (4.00)	243 (3.59)	
	219	250 (3.90)	227	254 (4.07)	242 (3.90)	219 (3.80)	
		245 (3.95)		248 (4.03)			
		215 (3.50)		224 (3.67)			

...contd...

1	2	3	4	5	6	7
Acetonitrile	278(4.05) 274(4.02) 250(3.90) 215(4.29)	279(3.86) 273(3.81) 268(3.78) 249(3.80) 244(3.81) 212(3.86)	297(3.61) 289(3.64) 266(3.51) 217(3.88)	284(3.76) 275(3.81) 269(3.72) 253(3.76) 204(4.45)	275(3.95) 269(4.00) 243(3.74) 203(4.35)	280(3.77) 273(3.75) 266(3.60) 241(3.73) 211(3.86)
Methanol	278(4.17) 274(4.12) 250(4.06) 209(4.49)	279(3.91) 272(3.90) 265(3.77) 249(3.89) 244(3.92) 208(3.96)	297(3.55) 288(3.61) 259(3.40) 217(3.67)	283(3.93) 275(4.03) 268(3.98) 254(4.00) 206(4.49)	279(3.86) 273(3.84) 243(3.79) 207(4.39)	280(3.78) 273(3.76) 266(3.60) 241(3.66) 213(3.84)
Water (pH 7)	277 271 244 203	278(3.81) 271(3.84) 265(3.74) 249(3.83) 244(3.86) 205(4.21)	292 230 198	281(3.50) 274(3.62) 268(3.58) 255(3.54)	278(3.86) 271(3.86) 243(3.78) 200(4.56)	279(3.81) 272(3.79) 263(3.71) 245(3.65) 200(

Table 3.4. Fluorescence maxima [λ_f (nm)] and quantum yield (ϕ_f) of 2-(chloromethyl)-[CMBI], 2-(dichloromethyl)-[DMBI], 5-chloro-2-(trichloromethyl)-[TMBI], 2-(trifluoromethyl)-[FMBI], 2-(cyanomethyl)-[CNBI] and 2-chloro-benzimidazoles [2CBI] in different solvents at 298°K.

Solvent	λ_f (nm) (ϕ_f)					
	CMBI	DMBI	TMBI	FMBI	CNBI	2CBI
Cyclohexane	299 (0.002)	298 290 (0.20) 280	322 (0.01)	307 298 (0.30) 288	-	-
	297 (0.007)	300 290 (0.15) 281	330 (0.01)	307 296 (0.23) 287	292 (0.16) 281	318 (0.08) 300
Acetonitrile	-	300 290 (0.01)	-	308 (0.24)	308 (0.25)	304 (0.04)
	297 (0.025)	297 289 (0.37) 280	303 (0.14)	310 (0.24)	290 (0.10) 280	304 (0.06)
Methanol	304	297				
	293	289				
	283	280				
Water (pH 7)			354 (0.03)	340 (0.18)	290 (0.01) 278	304 (0.07)

resemble to that of CMBI except that it is slightly red shifted in any one given solvent. But the fluorescence spectral data shown in Table 3.4, clearly indicate the larger red shift in case of 2CBI in comparison to CMBI in all the solvents. The characteristics of absorption and fluorescence spectral shifts in different solvents follow the same trend as that observed in case of CMBI or BIM. The fluorescence quantum yield is very low when compared with either BI or BIM in any one particular solvent.

As mentioned in chapter I, it has been well established from theoretical and experimental studies that the $\pi \rightarrow \pi^*$ is the lowest energy transition in BI.^{122,124-128,154-157} It has also been shown that in substituted BI, the lowest energy transition can be either $\pi \rightarrow \pi^*$ or charge transfer (CT) in nature.^{125,157} Which state is of lower energy, depends on the nature as well as position of the substituent, for example, the electron-donating groups on the benzene ring and the electron-withdrawing groups on the imidazole ring favour the CT state to be of lower energy. Moreover, in excited state in general the charge migration takes place from carbocyclic ring to heterocyclic ring. The extent of charge migration can be enhanced by the substitution of electron-donating group in the carbocyclic ring or by the presence of electron-withdrawing group in the heterocyclic ring or both. This will result in the stabilization of the excited

state. On the other hand, if the electron-donating group is present on the heterocyclic ring, the energy of the excited state may be lowered slightly, remain unchanged or increase slightly, depending on the interaction of the two charge cloudes. Again, it is also known that the effect of substituents (electron-donating or electron-withdrawing) on the spectral characteristics of the aromatic moiety is maximum if these groups are directly attached to the aromatic ring. The effect of these interactions keeps on decreasing if these chromophores are separated by the presence of methylene group, which acts as an insulator. Moreover, if the number of methylene groups, which separate the two chromophores is two or more, the two functional groups behave independently.

It is also established from our results that the lowest energy transition present in the compounds ' mentioned in Tables 3.1 to 3.4 are of $\pi \rightarrow \pi^*$ nature. High molecular extinction coefficients of the absorption band and reasonable fluorescence quantum yield, favour the above assignment. The only notable exceptions are TMBI and FMBI, where it appears that the lowest energy transition is of charge transfer (CT) character (see later). This assignment is based on the following observation. It is little difficult to distinguish between the $\pi \rightarrow \pi^*$ and CT transition because both these transitions lead to a gradual red shift with increasing the polarity of the solvents. But in case of latter, the red shift is more prominent than that observed in the former case.

With the exception of TMBI, FMBI and 2CBI, the fluorescence spectra of all the other compounds resemble to that of BI or BIM. Like BI or BIM, the fluorescence spectra are nearly insensitive or small blue shift is noticed on increasing the polarity or hydrogen-bond formation tendency of the solvents. This behaviour can be explained on the same lines as has been done for BI's.¹²⁵ Since the long wavelength band is localised on the benzene ring, the lone pair on the tertiary nitrogen atom can perturb this transition in the same manner as an amino group. But unlike amino group, the lone pair on the tertiary nitrogen atom is perpendicular to the π cloud of the benzene moiety and hence perturbation due to resonance effect will be negligible. The only way it can perturb this transition is through inductive effect and this effect is quite small. Hydrogen bonding to this nitrogen atom will reduce this effect and will lead to a very small blue shift, both in the absorption and fluorescence spectra. In case of BINH_2 and BIOH , the blue shift in the spectral characteristics can also be due to the hydrogen bonding with the lone pair of amino and hydroxy groups. This behaviour is consistent with those observed in case of aromatic amines or alcohols.¹⁵⁸⁻¹⁶¹ Similar behaviour has also been observed in case of phenanthro-[9,10]imidazole.⁶⁰

A small red shift is observed in the absorption maxima of all these compounds in comparison to those of BI or BIM in a

given solvent. The red shift observed in case of BINH_2 or BIOH is larger than that observed in case of CMBI , DMBI , 2CBI and CNBI . In the former compounds (BINH_2 and BIOH) the hydrogen atom of the methyl group, has been replaced by electron-donating groups like $-\text{NH}_2$ or $-\text{OH}$, whereas in latter cases it has been replaced by electron-withdrawing groups like halogen atoms or cyano group. The small changes observed in the absorption maxima of BI when these groups are substituted at 2-position, are consistent with the results that the methylene group in between the two functional groups prevents their direct interaction and thus the spectral characteristics of each chromophore become independent of each other. For example: (i) The absorption and fluorescence spectral behaviour of 2-aminobenzimidazole¹²⁶ (2BNH_2) differ remarkably from that of BINH_2 . In the former case, the amino group is directly attached to the BI moiety and hence affects the spectral characteristics drastically, i.e. the absorption and fluorescence spectra of the former are very broad. Moreover, the absorption spectrum gets blue shifted and the fluorescence spectrum gets red shifted with increase in the hydrogen bond formation tendency of the solvents. This clearly indicates that the amino group is acting as a proton acceptor in the ground state (S_0) and proton donor in the excited singlet (S_1) state, agreeing nicely to the fact that the charge migration takes place from the amino group to the BI ring in S_1 state, thereby

the release of proton is facilitated. On the other hand, in case of BINH_2 , the absorption spectrum does follow the trend similar to that of 2BNH_2 in different solvents but the fluorescence spectra are hardly affected. Further the structured absorption and fluorescence spectra confirm that the presence of methylene group drastically cuts down the direct interaction between the BI moiety and $-\text{NH}_2$ group. (ii) In 2-hydroxybenzimidazole (2BOH),¹²⁷ $-\text{OH}$ group is directly attached to the BI moiety at position-2. This provides a labile proton at ortho position to the basic nitrogen centre, giving rise to a keto-enol tautomerism. It has been observed that 2BOH behaves as a keto compounds, in all the solvents, both in the ground and excited singlet states. Introduction of a methylene group between $-\text{OH}$ group and BI moiety stops the intramolecular proton transfer. Thus BIOH behaves like a substituted methyl alcohol on one hand and 2-methylbenzimidazole with one hydrogen atom replaced by $-\text{OH}$ group on the other hand. (iii) The absorption spectrum of 2CBI is red shifted to a very little extent as compared to that of CMBI, on the other hand the fluorescence spectrum of the former is red shifted to a greater extent and more sensitive to the nature of the solvents as compared to CMBI. In 2CBI, the chlorine atom is directly attached to BI at position 2, whereas in CMBI, the chlorine atom and BI moiety are separated by a methylene group.

In case of CMBI, the absorption spectrum, fluorescence spectrum and charge densities at the basic and acidic centres, which are reflected from pK_a values (see chapter 4, page 172), are nearly resembling with those of BIM or BI. But the data in Tables 3.3 and 3.4 clearly indicate that 2CBI behaves differently from BI or BIM. The effect of solvents on the fluorescence spectrum of 2CBI is not that prominent as observed in case of TMBI or FMBI (see later) i.e. unlike other BI's studied, the fluorescence spectrum of 2CBI is red shifted, but not to a similar extent as noticed in case of TMBI and FMBI. It may not be possible to assign definitely CT state as the lowest energy emitting state for 2CBI but it outweighs the $\pi - \pi^*$ transition. This could further happen because chloro group can have both inductive effect as well as resonance effect, operating simultaneously. The former effect is of electron withdrawing in nature, whereas the latter will perturb the π cloud by donating electrons to the ring. Since both these effects act in opposite direction, the net effect will be quite small. These results clearly demonstrate that introduction of methylene group in between the two chromophores reduces their direct interactions drastically. The results of DMBI and CNBI are also consistent with the above explanation.

In TMBI and FMBI, a large red shift in the fluorescence spectra is observed in going from cyclohexane to water and thus

CT state is the low lying emitting state in the neutral species of TMBI and FMBI. The driving force behind this charge migration from homocyclic ring to heterocyclic ring, thus making CT state to be the low lying emitting state in these cases, is the presence of strong electron withdrawing group ($-\text{CCl}_3$ or $-\text{CF}_3$) at the position-2 of imidazole ring. Although in case of CNBI, the $-\text{CN}$ group is electron withdrawing in nature, however, the presence of a methylene group in between the BI moiety and $-\text{CN}$ group stops the direct interaction between them and two groups behave independently.

A close look at the Tables of absorption and fluorescence spectral data of BI's in different solvents, except TMBI and FMBI, shows that there is not much increase in the dipole moment upon excitation. But TMBI and FMBI and to a small extent, 2CBI become more polar in the excited singlet state because of greater degree of charge migration.

The decrease in the quantum yield of all the BI's studied here, as compared to that of BI in any one particular solvent could be due to the interactions of vibrational motions of the extra substituent groups, thereby increasing the rates of radiationless processes.

Fluorescence intensities of the neutral species of CMBI, DMBI and TMBI were quenched in case of acetonitrile as a solvent.

Systematic fluorescence quenching of these compounds by acetonitrile was studied. Fluorescence intensity follow the simple Stern-Volmer plot,

$$\frac{\phi_o}{\phi} = 1 + K_q \tau [Q]$$

where ϕ and ϕ_o are the fluorescence intensities with and without the presence of quencher, K_q is the quenching constant and τ is the lifetime of the respective compound. Fig. 3.17 shows the Stern-Volmer plot, and the values of $K_q \tau$, obtained from the slopes are given in Table 3.5. Natural lifetime, τ_{FM} was calculated from the corrected fluorescence spectra, using Strickler and Berg's equation. τ is determined from the relation $\tau = \tau_{FM} \phi$. These values alongwith K_q are also listed in Table 3.5. The values of K_q obtained are much less than the diffusion controlled limit ($1.1 \times 10^{10} \text{ dm}^3 \text{ mol}^{-1} \text{ s}^{-1}$). In these cases, the energy transfer from the excited species to acetonitrile can not be the direct energy transfer, since the singlet state energy of acetonitrile is much greater than that of the respective species. Although the substitution reactions of these compounds by nucleophilic reagents are reported in the literature,¹²² these reactions will not take place under these conditions or these reactions will be really slow to have any reasonable effect. We can not say much about the mechanism of this quenching but

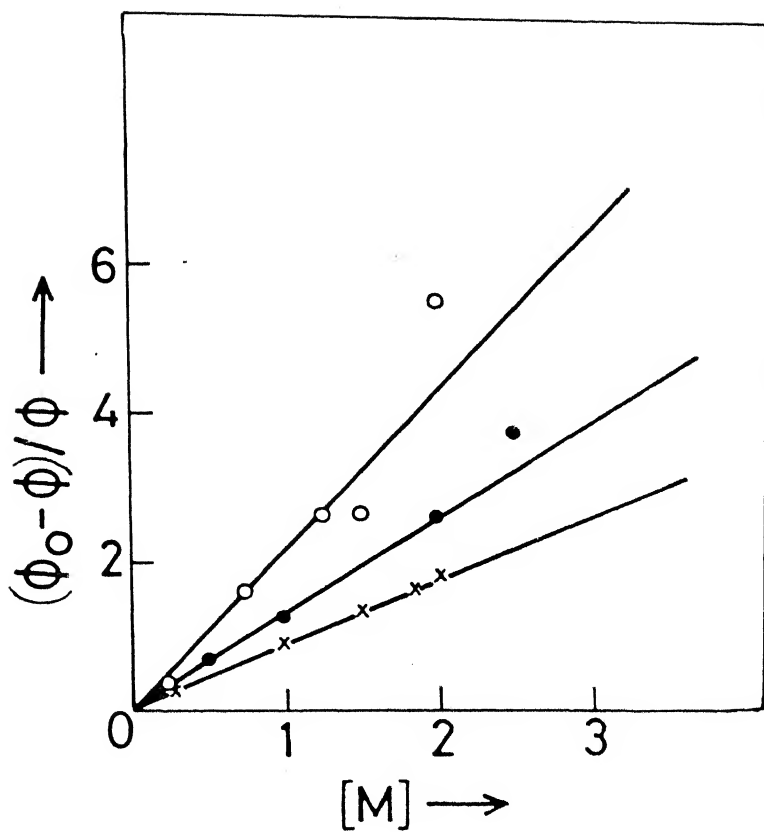


Fig.3.17 Stern Volmer plot ($I_0 - I / I_0$ vs $[M]$) for quenching of fluorescence by acetonitrile, (-o-o-, $[M] \times 0.4$) CMBI; (-●-●-, $\phi_0 - \phi / \phi \times 0.1$) DMBI; (-x-x-) TMBI.

Table 3.5. Values of the slope ($k_q\tau$), radiative lifetime (τ) and quenching constant (k_q) obtained from Stern-volmer plot.

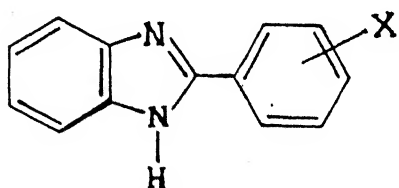
Compound	$k_q\tau$	$\tau \times 10^9$	$10^{-9}k_q^\phi$
CMBI	5.5	0.1	0.55
DMBI	0.12	0.9	13
TMBI	0.9	0.3	3.33

$^\phi \text{ dm}^3 \text{ mol}^{-1} \text{ sec}^{-1}$

the quenching by forming a collisional complex can not be the rate determining step as K_q observed is much smaller than K_{diff} . Other speculations could be either charge transfer or electron transfer and thus needs further investigation.

In conclusion, it can be said that $\pi \rightarrow \pi^*$ is the lowest energy transition in case of BINH₂, BIOH, CMBI, DMBI and CNBI, CT in case of TMBI and FMBI, whereas nothing conclusive can be mentioned for the lowest energy transition in case of 2CBI, though the latter transition outweighs the former.

3.2 2-(Hydroxyphenyl)- and 2-(Methoxyphenyl)benzimidazoles*



where X = 2'-OH(OHBI), 2'-OCH₃(OMBI),
3'-OH(MHBI), 3'-OCH₃(MMBI),
4'-OH(PHBI), 4'-OCH₃(PMBI).

The absorption and fluorescence spectra of all these compounds were studied in solvents of different polarity and hydrogen bond formation tendency. As these three sets of isomers show spectral characteristics which are quite different from each other, the result of each set of these isomers will

* H.K. Sinha and S.K. Dogra, Chem. Phys., 102, 337-347 (1986) ; J. Photochem., 36, 149-161 (1987).

therefore be discussed separately.

- (a) OHBI and OMBI : The absorption maxima and $\log (\epsilon_{\max})$ have been compiled in Table 3.6, whereas the fluorescence maxima and fluorescence quantum yield have been summarized in Table 3.7. Figures 3.18, 3.19, 3.20 and 3.21 depict the absorption and fluorescence spectral profiles.

A close look at the data of Table 3.6 shows that the absorption spectra of OHBI and OMBI can be divided into four distinct band systems: one around 330 nm, second around 280 nm, a third one at 240 nm and the fourth one below 210 nm. The structure of all the band systems is lost with increasing the polarity and hydrogen bond formation tendency of the solvents. Under similar conditions, the long wavelength band system gets largely blue shifted whereas the other three band systems are slightly blue shifted in case of OHBI. On the other hand absorption band maxima of OMBI are hardly affected under the above conditions but the absorption spectra of OHBI and OMBI in water exactly resemble each other. A comparison of the absorption maxima of OHBI and OMBI with that of parent BI molecule clearly shows that a large red shifted band is observed in the former set in any one particular solvent and the absorption spectra are structured in nearly all the solvents. The spectral shifts observed in the absorption spectrum of OMBI is small as compared to that noticed in OHBI.

Table 3.6. Absorption maxima [λ_a (nm)] and $\log(\epsilon_{\max})$ of 2-(2'-hydroxyphenyl)benzimidazole (OHBI) and 2-(2'-methoxyphenyl)benzimidazole (OMBI) in different solvents at 298°K.

Compound	λ_a (nm) $\log(\epsilon_{\max})$				
	Cyclohexane	Ether	Acetonitrile	Methanol	Water (pH 7)
OHBI	335	332.5 (4.14)	329 (4.04)	329 (4.04)	325
	321	317.5 (4.16)	316 (4.07)	316 (4.08)	312
	292	291 (3.94)	291 (3.91)	291 (3.92)	290
	286	285 (3.91)	285 (3.85)	285 (3.85)	-
	272	272.5 (3.83)	274 (3.56)	274 (3.66)	-
	262	262.5 (3.71)	262 (3.70)	262.5 (3.60)	-
	247.5	247.5 (3.67)	246.5 (3.67)	246.5 (3.67)	248
	235	235 (3.91)	231.5 (3.96)	231.5 (3.86)	241.5
OMBI	327.5	327 (4.14)	326.5 (4.20)	326.5 (4.20)	326.5 (3.99)
	319	-	-	-	-
	312.5	313.5 (4.35)	312.5 (4.39)	312.5 (4.39)	312.5 (4.19)
	305	-	-	-	-
	291.5	291.5 (4.18)	291.5 (4.22)	291.5 (4.28)	291.5 (4.09)
	239	239 (4.04)	237.5 (4.41)	237.5 (4.11)	248 (3.89)
	212.5	212.5 (4.58)	206.5 (4.70)	206.5 (4.73)	206.5 (4.56)

Table 3.7. Fluorescence maxima [λ_f (nm)] and quantum yield (ϕ_f) of 2-(2'-hydroxyphenyl)-benzimidazole (OHBI) and 2-(2'-methoxyphenyl)benzimidazole (OMBI) in different solvents at 298°K.

Compound	λ_f (nm) (ϕ_f)				
	Cyclohexane	Ether	Acetonitrile	Methanol	Water
OHBI	470(0.50)	456(0.51)	454(0.66)	438(0.82)	430(0.41)
	-	-	-	360	350(0.02)
				344(0.11)	
OMBI				328	
	376	380	380	386	-
	356(0.25)	364(0.29)	364(0.26)	366(0.34)	368(0.41)
	340	346	347	350	350

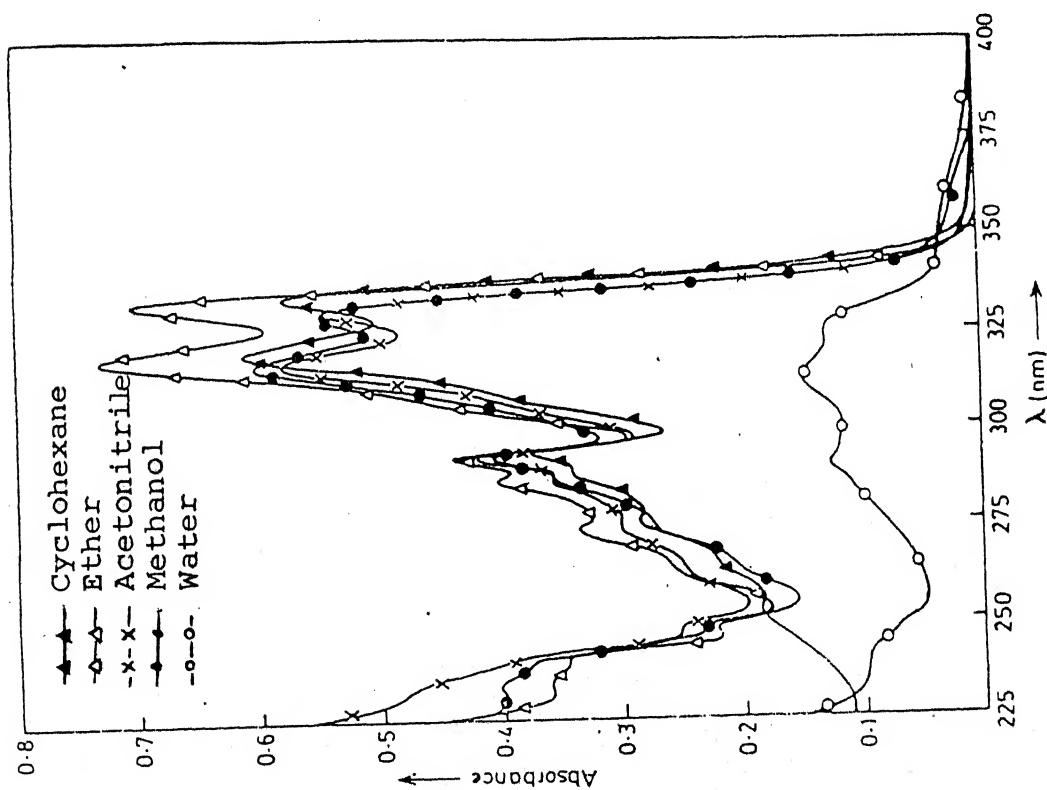


Fig.3.18 Absorption spectra of 2-(2'-hydroxyphenyl)benzimidazole (OHBI) in different solvents at 298°K.

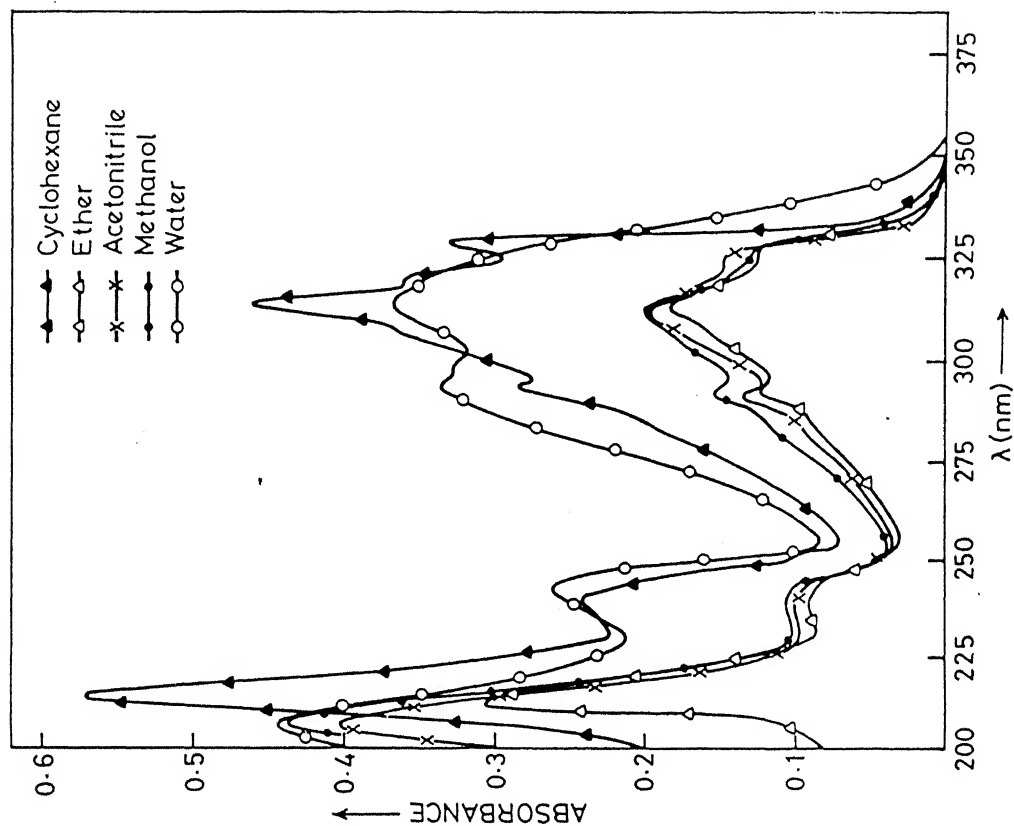


Fig.3.19 Absorption spectra of 2-(2'-methoxyphenyl)benzimidazole (OMBI) in different solvents at 298°K.

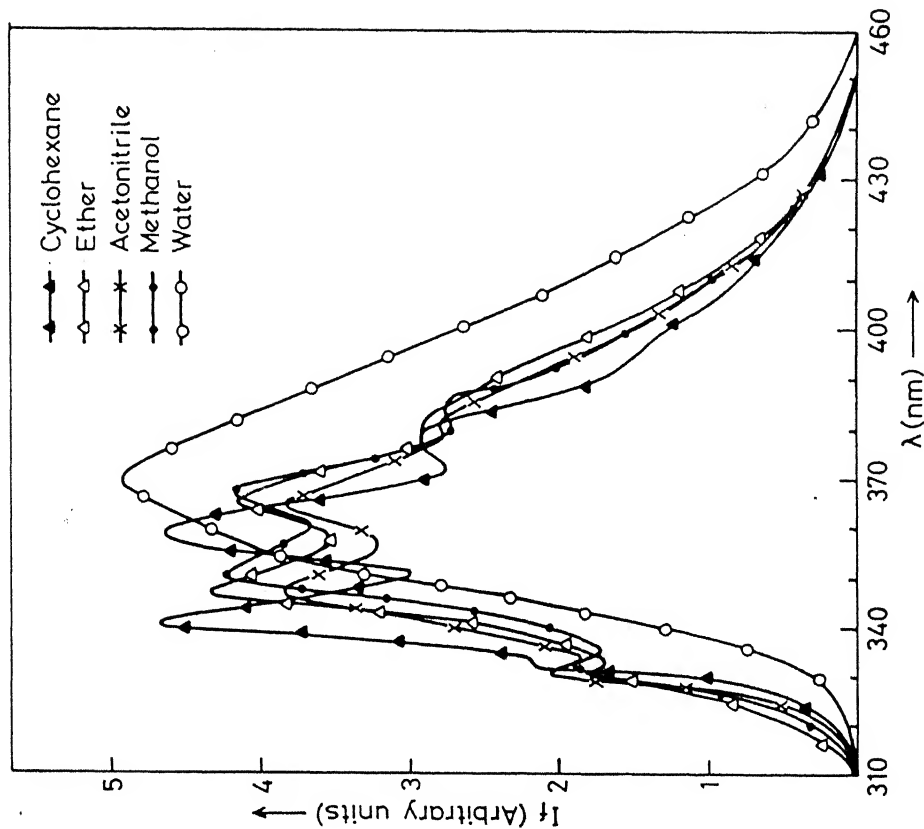


Fig.3.21 Fluorescence spectra of 2-(2'-methoxyphenyl)benzimidazole (OMBI) in different solvents at 298°K.

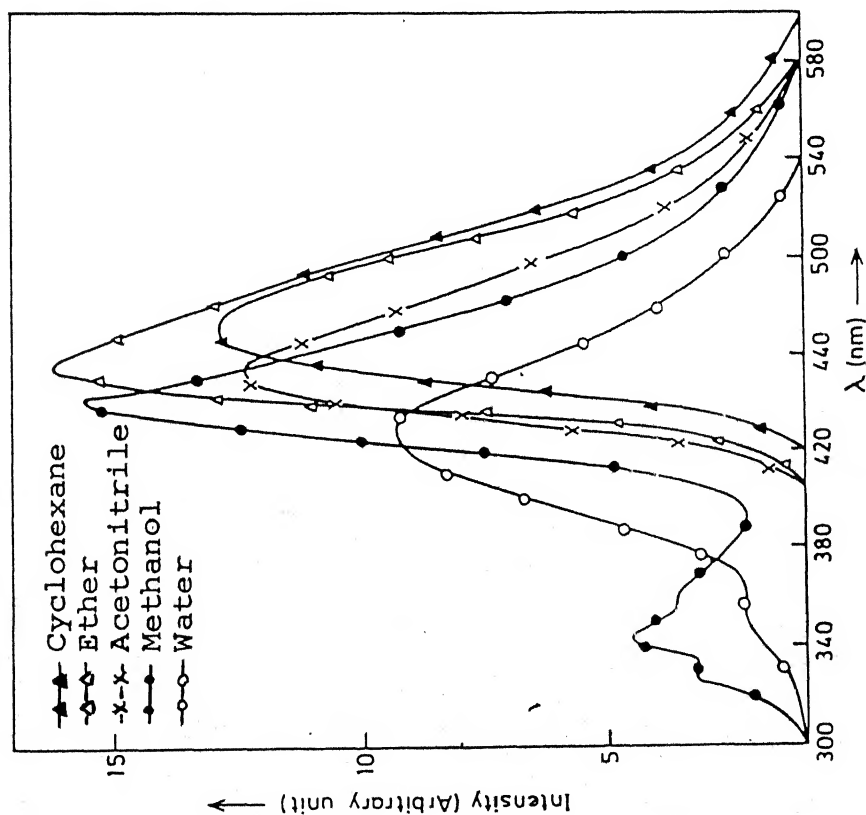


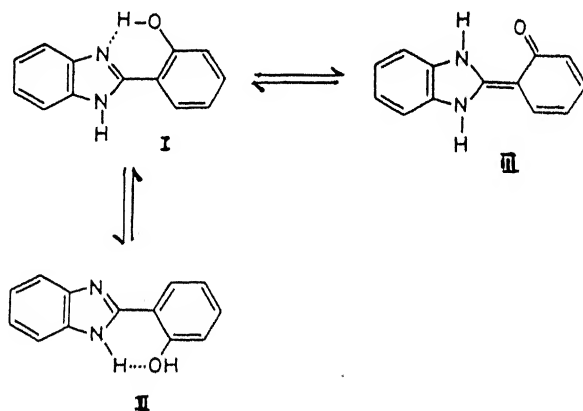
Fig.3.20 Fluorescence spectra of 2-(2'-hydroxyphenyl)benzimidazole (OHBI) in different solvents at 298°K.

On examining the fluorescence spectrum of OHBI in different solvents it can be seen that in non-polar solvents, like cyclohexane, a large Stokes shifted band is observed, whereas in polar or hydrogen bonding solvents like methanol or water, besides large Stokes shifted band, a normal Stokes shifted band is also observed. The former band system gets blue shifted whereas the latter gets red shifted with the increase in polarity and hydrogen bond formation tendency of the solvents. The intensity of the short wavelength band is much less as compared to the long wavelength band. In contrast to OHBI, only one fluorescence band system, resembling the normal Stokes shifted one, is observed in case of OMBI. Except in water, the structure of this band system is retained in all the solvents and can be explained by a vibrational frequency of $\text{ca. } 1470 \text{ cm}^{-1}$. This vibrational frequency nearly resembles to that observed in the fluorescence spectrum of 2-phenylbenzimidazole.¹²⁸

In OHBI and OMBI, based on higher values of extinction coefficients, greater red shift in the absorption spectrum as compared to BI in any one particular solvent, higher fluorescence quantum yield and mirror image symmetry of absorption and fluorescence spectra (normal Stokes shifted band of OHBI) the following conclusions can be drawn:

- (i) The lowest energy transition is of $\pi \rightarrow \pi^*$ character both in absorption and emission.
- (ii) The hydroxyphenyl ring is coplanar and extensively conjugated with benzimidazole moiety in S_0 and S_1 states.

The long wavelength absorption band in OHBI is further red shifted as compared to OMBI in any one given solvent, except in water, where it resembles with that of OMBI. This could be due to the existence of intramolecular hydrogen bonding between the phenolic proton and the tertiary nitrogen atom (structure I, scheme 3.1). Since this kind of intramolecular hydrogen bonding



is absent in OMBI, the structure I will be absent, thereby leading to the non-rigid structure of OMBI. Due to this absorption and fluorescence spectra of OMBI are more susceptible to the nature of solvent. Further, due to the competition between

the intra and intermolecular hydrogen bonding in water as solvent, the amount of structure I in OHBI will decrease and thus the absorption spectrum of OHBI in water will resemble that of OMBI. Though the existence of structure II is also possible in both OHBI and OMBI but it is rejected on considering the following points: (i) Absorption maxima of long wavelength band in OHBI and OMBI in water are in the same region as those observed in the case of 2-(3'-hydroxyphenyl)benzimidazole (MHBI), 2-(3'-aminophenyl)benzimidazole¹⁵⁵ and 2-(p-aminophenyl)benzimidazole.¹⁵⁶ In the latter set of molecules, intramolecular hydrogen bonding (structure II) is absent. This is further substantiated from the results that the vibrational frequency observed in case of fluorescence spectra of OHBI and OMBI resemble that of 2-phenylbenzimidazole.¹²⁸ (ii) If the structure II is possible for OHBI, it should also be possible for OMBI. Due to this the pK_a value for the deprotonation of imino group in OMBI should be greater than that observed for the similar reaction of benzimidazole. This is because the imino proton will be tightly bound to the lone pair of the oxygen atom of the methoxy group. The pK_a value calculated for this reaction in OMBI (see chapter 4, page 190) is nearly same as that observed for benzimidazole, thus rejecting the existence of structure II. (iii) A conformation similar to structure II has been predicted in 2-(o-aminophenyl)benzimidazole¹⁵⁴ in the S_0 state along with

the structure I. In the latter case, the presence of the structure II was confirmed from the excitation fluorescence spectrum, recorded at two fluorescence band systems. Since both the structures are present in the non-polar solvents, it gives rise to normal Stokes shifted as well as large Stokes shifted bands in the non-polar solvent (cyclohexane). But for OHBI only the large Stokes shifted band is observed in non-polar solvent indicating, therefore, the absence of structure II in OHBI.

By following the above mentioned arguments and comparing the data of OHBI and OMBI, the observed large Stokes shifted band in the fluorescence spectrum of OHBI in all the solvents is attributed to the isomeric species III (scheme 3.1) which is formed by the transfer of the labile proton across the hydrogen bond in the excited singlet state. The creation of a pK_a gradient upon excitation of the molecule is the driving force for this intramolecular proton transfer.

To decide about the precursors of the two fluorescence band systems, the excitation spectra have been recorded at the two fluorescence maxima. The excitation spectra (Fig. 3.22), observed for both the fluorescence bands are exactly similar and resemble the absorption spectra. This suggests that the precursor for these two fluorescence bands is merely the ground state intramolecular hydrogen bonded structure I (scheme 3.1). The large Stokes shifted fluorescence band is observed from species III and

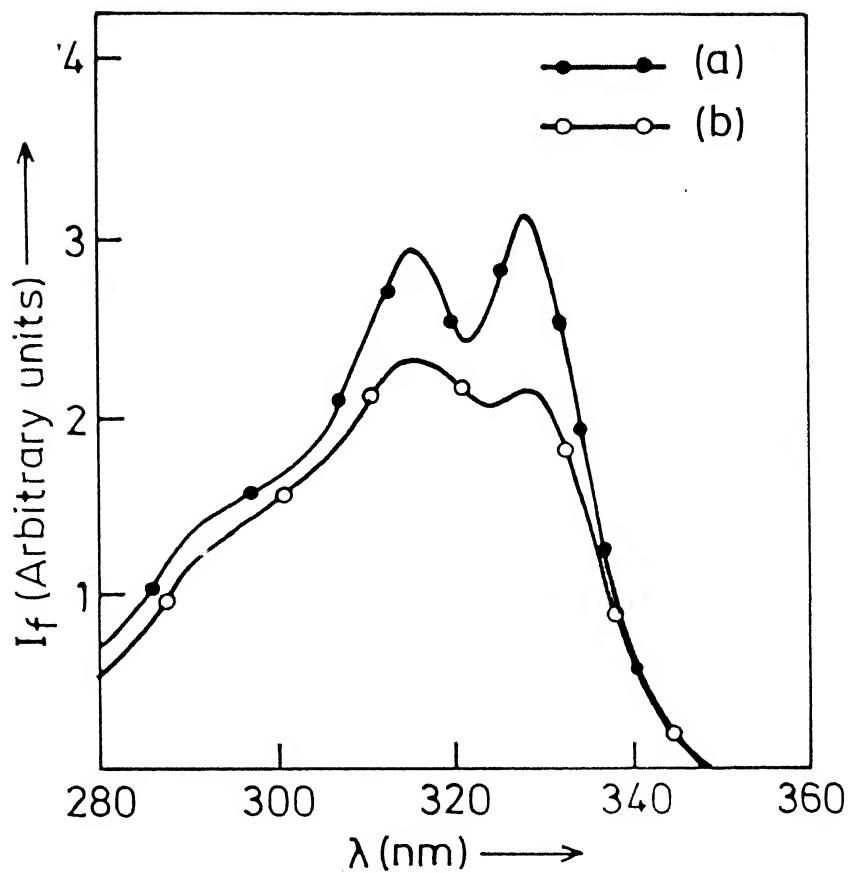


Fig.3.22 Excitation spectra of 2-(2'-hydroxyphenyl)benzimidazole (OHBI) monitored at two wavelengths, (a) 440 nm (b) 350 nm.

as said earlier, it is formed in the excited singlet state during the lifetime of the species I. This process of intramolecular proton transfer is known to be very fast. The normal Stokes shifted fluorescence band arises in the hydrogen bonding solvents because of the competition of intra and intermolecular hydrogen bonding. Thus it could be assigned to the open structure as suggested in case of OMBI where the molecule is engaged in intermolecular hydrogen bonding with solvents or to structure I in case of OHBI.

The decrease in the fluorescence quantum yield for both the fluorescence bands in water is more than that in methanol, especially for the normal Stokes shifted band. The decrease in the quantum yield of latter band system could be: (i) due to a larger fluorescence quenching rate of the latter as compared to that for the former one, (ii) the amount of species III formed in the excited singlet state and in water as solvent would be less than that in methanol, because of the stronger hydrogen bonding characteristics of water. The preferential rate of quenching for different fluorescence band systems has been observed in other similar systems.⁸⁹

(b) MHBI and PHBI

Tables 3.8 and 3.9 summarize the absorption and fluorescence spectral data respectively. The absorption spectra

Table 3.8. Absorption maxima [λ_a (nm)] and $\log(\epsilon_{\max})$ of 2-(3'-hydroxyphenyl)-benzimidazole (MHBI) and 2-(4'-hydroxyphenyl)benzimidazole (PHBI) in different solvents at 298°K.

Compound	λ_a (nm) $\log(\epsilon_{\max})$			
	Ether	Acetonitrile	Methanol	Water (pH 7)
MHBI	319(4.39)	318(4.22)	317(4.18)	317(4.16)
	304(4.48)	304(4.35)	300(4.36)	300(4.31)
	292(4.44)	291(4.21)	—	—
	242(4.16)	241(4.15)	240(4.02)	240(4.04)
	215(4.72)	210(4.62)	212(4.64)	212(4.64)
PHBI	319	—	—	—
	305	294(3.71)	292(3.82)	289(4.10)
	299	286(3.69)	—	—
	245	245(3.63)	246(3.71)	245(3.79)
	214	210(4.03)	209(4.11)	—

Table 3.9. Fluorescence maxima [λ_f (nm)] and quantum yield (ϕ_f) of 2-(3'-hydroxyphenyl)-benzimidazole (MHBI) and 2-(4'-hydroxyphenyl)benzimidazole (PHBI) in different solvents at 298°K.

Compound	λ_f (nm) (ϕ_f)			
	Ether	Acetonitrile	Methanol	Water (pH 7)
MHBI	354	354	358	-
	337 (0.40)	340 (0.38)	341 (0.20)	353 (0.16) 440
	322	326	326	330
PHBI	352	356	361	357
	338 (0.50)	342 (0.44)	345 (0.42)	344 (0.19)
	322	328	330	326

of MHBI and PHBI are given figures 3.23 and 3.24 respectively and the corresponding fluorescence spectra are shown in figures 3.25 and 3.26.

The absorption band maxima are red shifted as compared to BI in any one particular solvent. Both absorption and fluorescence spectra of MHBI and PHBI are structured nearly in all the solvents. This can be explained by the ground state vibrational frequency of ca. 1390 cm^{-1} in MHBI and ca. 1400 in PHBI. This vibrational frequency also matches with that observed in 2-phenylbenzimidazole,¹²⁸ 2-(3'-aminophenyl)benzimidazole¹⁵⁵ and 2-(4'-aminophenyl)benzimidazole.¹⁵⁶ The fluorescence quantum yield of MHBI and PHBI are less than that of BI in any one particular solvent and decreases with increase in the polarity and hydrogen bond formation tendency of the solvents.

Based on the same arguments as given in case of OHBI and OMBI, the following conclusions can be drawn:

- (i) The lowest energy transition in these compounds are of $\pi \rightarrow \pi^*$ character.
- (ii) The hydroxyphenyl ring in all these cases are coplanar and conjugated with the benzimidazole moiety, both in the S_0 and S_1 states.

The effect of solvents on the absorption spectra of these compounds are similar to that observed for BI, i.e. either

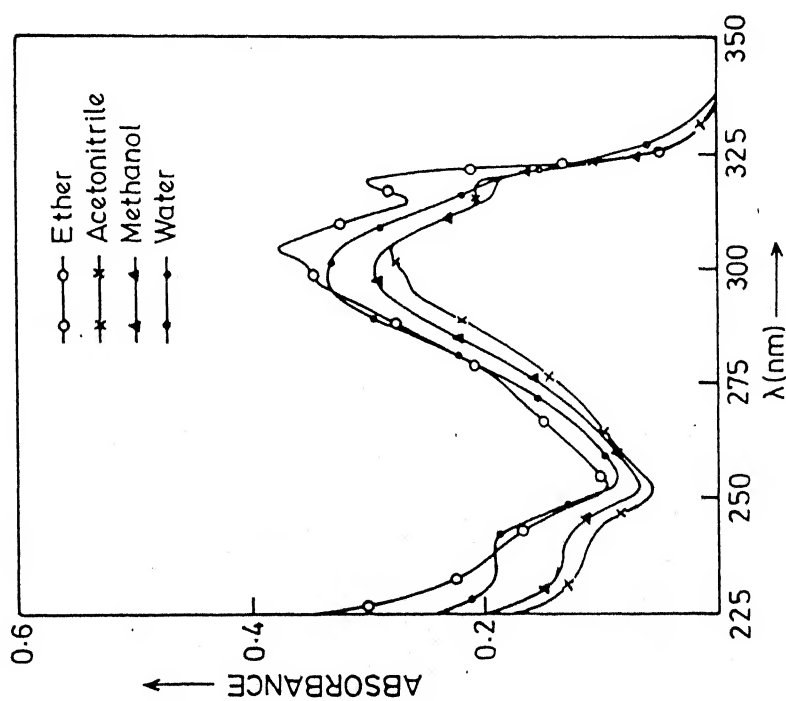


Fig.3.23 Absorption spectra of 2-(3'-hydroxyphenyl)benzimidazole (MHBI) in different solvents at 298°K.

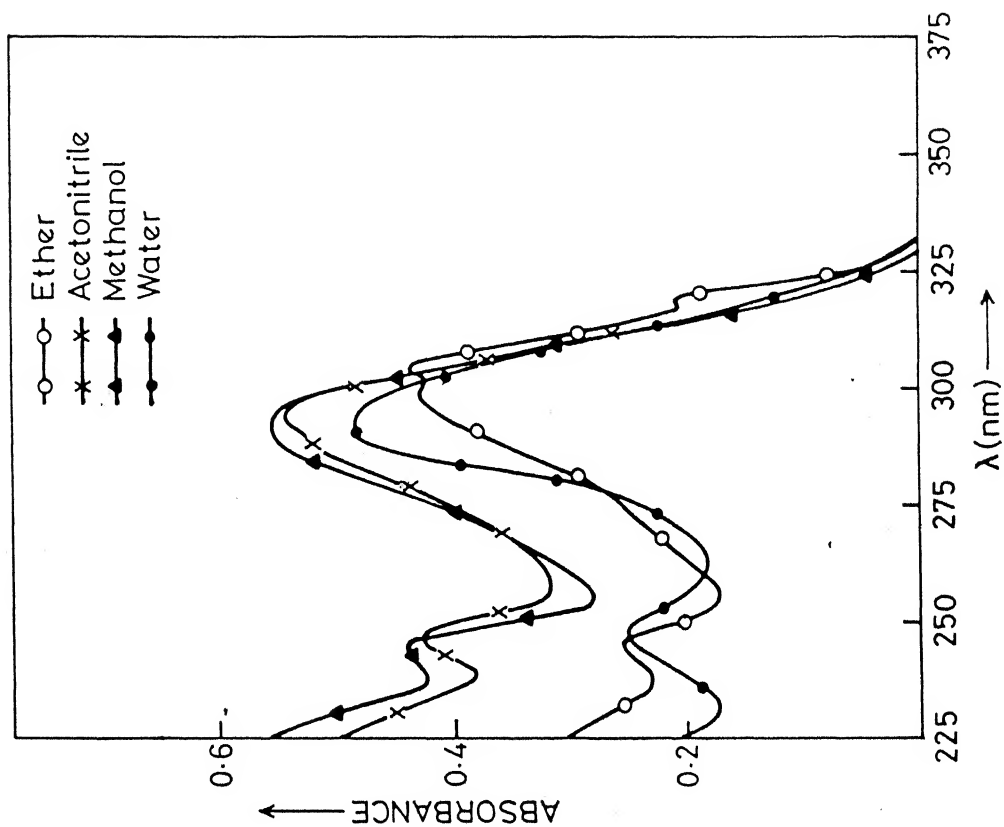


Fig.3.24 Absorption spectra of 2-(4'-hydroxyphenyl)benzimidazole (PHBI) in different solvents at 298°K.

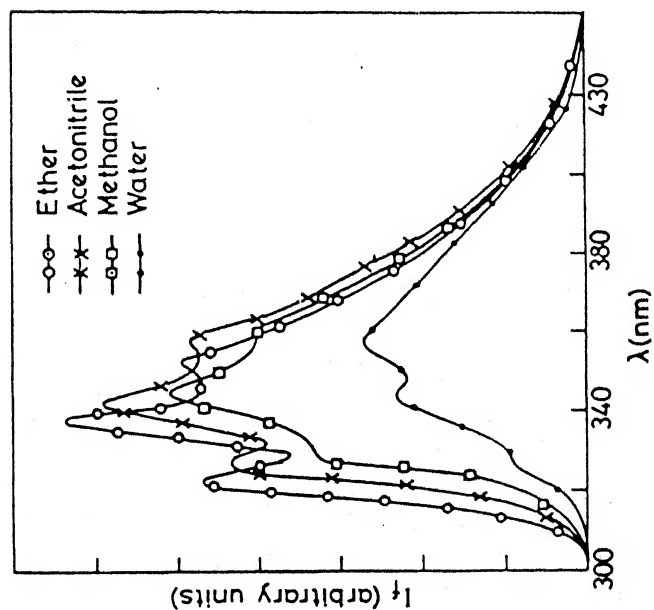


Fig.3.25 Fluorescence spectra of 2-(3'-hydroxyphenyl)benzimidazole (MHBI) in different solvents at 298°K.

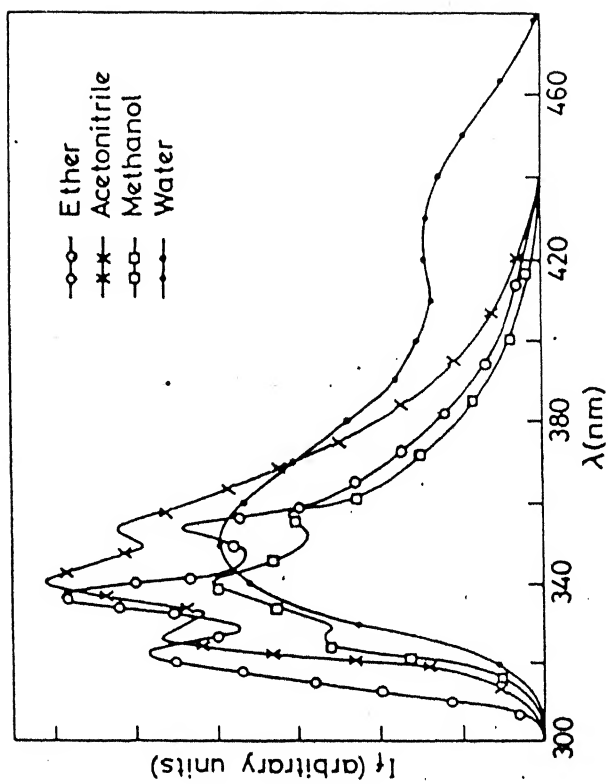
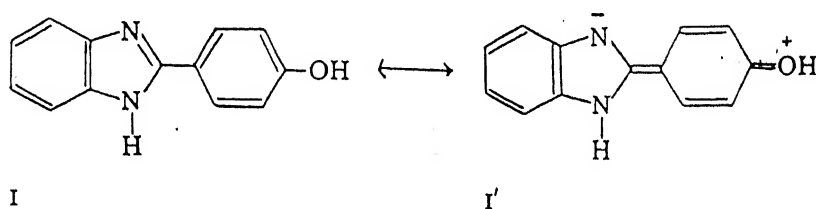


Fig.3.26 Fluorescence spectra of 2-(4'-hydroxyphenyl)benzimidazole (PHBI) in different solvents at 298°K.

insensitive or a small blue shift is observed on increasing the polarity and hydrogen bond formation tendency of the solvents. The spectral shifts in case of MHBI is very small as compared to that of PHBI in the above environment. The blue shift observed in the absorption spectrum of PHBI, but not much in that of MHBI, on increasing the hydrogen bond formation tendency of the solvents, could be due to the proton accepting nature of the hydroxyl group and thereby restricting the lone pair to have complete conjugation with the parent moiety. In case of MHBI, due to the meta position of hydroxyl group, the perturbation due to the lone pair of hydroxyl group may not have much effect on the spectral characteristics because of the lack of complete conjugation with the parent molecule. This could further be evident from the spectral changes observed due to the protonation and deprotonation reactions as described in chapter 4, page 209.

The fluorescence spectral shifts observed in case of MHBI are more than those observed in its absorption spectra, under the similar environment. Further, in comparison to the fluorescence spectral shifts observed for PHBI, those observed for MHBI is higher. This reveals that the change in dipole moment of MHBI upon excitation ($\Delta\mu$) is more than that of PHBI. This could be due to the fact that in PHBI the following canonical structure can be present and the structure I' is more favourable in the

excited state. Thus the charge transfer from carbocyclic to heterocyclic ring will leave some positive charge on the carbocyclic ring, whereas the similar structures are not possible in

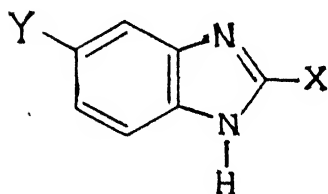


MHBI. The presence of structure I' in PHBI is also reflected from its structured fluorescence spectrum observed even in water. This structure also accounts for the red shift observed in the fluorescence spectrum on increasing the hydrogen bonding capacity of the solvents which is due to better proton donor nature of structure I' in comparison to structure I.

Besides the 353 nm fluorescence band observed in case of MHBI, another long wavelength fluorescence band (440 nm) is observed only in water as a solvent. Under the similar environment the long wavelength band is absent in case of its methoxy derivative. Fluorescence excitation spectra recorded at 353 nm and 440 nm have indicated that the ground state species is the same for both the fluorescence bands. The ratio of intensities of 440 nm band to 353 nm band (I_{440}/I_{353}) remains same in the concentration range 10^{-5} to 10^{-3} M, pH range 1 to 8 and at 77°K.

The above studies discard the possibility of formation of exciplex, excimer and/or the zwitterion. However, it is difficult at present, to comment anything about the identity of this fluorescence band.

3.3 Benzimidazole-2-carboxylic acids



- i) $X = \text{COOH}$, $Y = \text{H}$ (BIA)
- ii) $X = \text{COOH}$, $Y = \text{Cl}$ (CBIA)
- iii) $X = \text{COOCH}_3$, $Y = \text{Cl}$ (CBIM)
- iv) $X = \text{CH}_2\text{COOH}$, $Y = \text{H}$ (BIAA)
- v) $X = \text{CH}_2\text{COOC}_2\text{H}_5$, $Y = \text{H}$ (BIAE)
- vi) $X = \text{CH}_2\text{CH}_2\text{COOH}$, $Y = \text{H}$ (BIPA)

The absorption and fluorescence spectra of all these compounds have been studied in solvents of different polarity and hydrogen bond formation tendency. The results will be summarized under three sub-headings.

(a) BIA, CBIA and CBIM

Figures 3.27, 3.28 and 3.29 give the absorption spectra of BIA, CBIA and CBIM in different solvents respectively. The

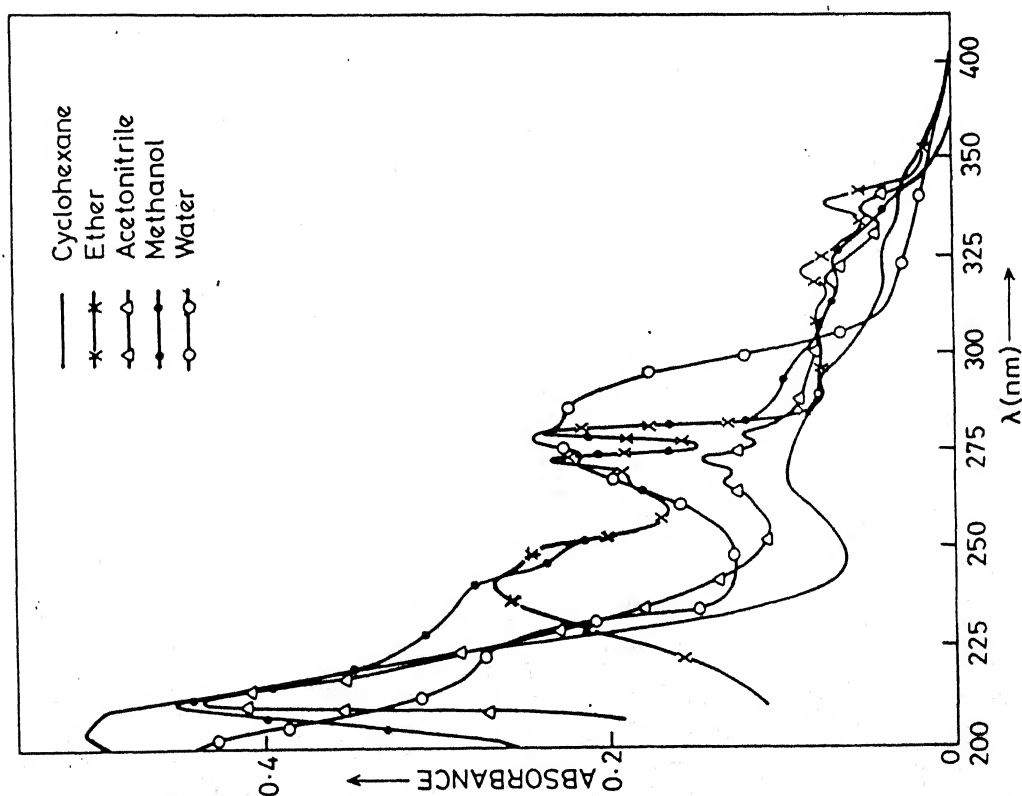


Fig.3.27 Absorption spectra of benzimidazole-2-carboxylic acid (BIA) in different solvents at 298°K.

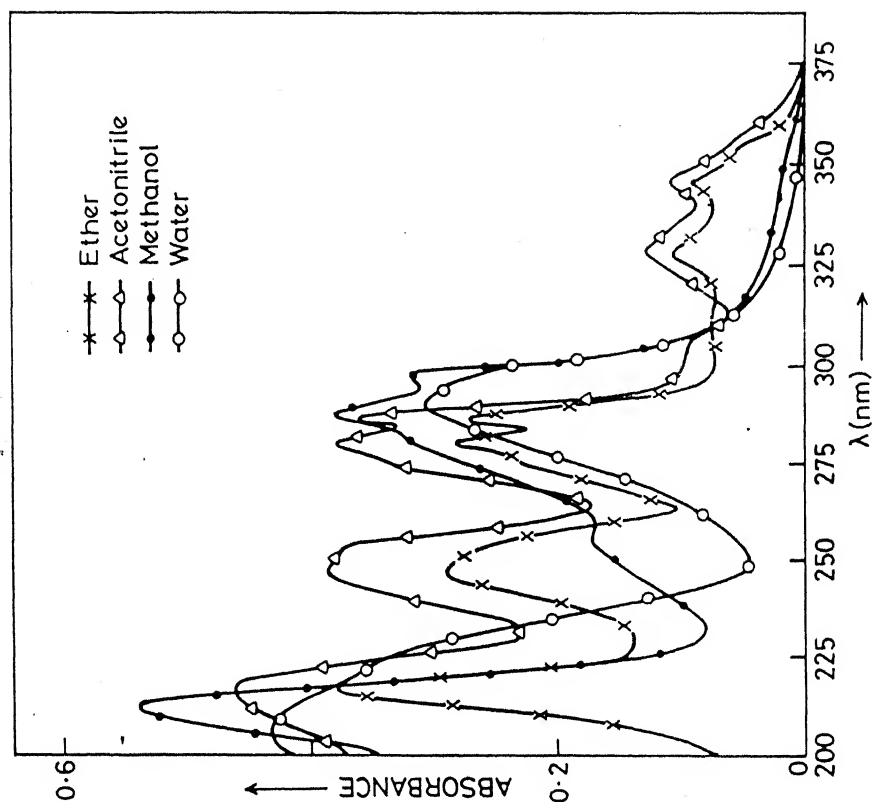


Fig.3.28 Absorption spectra of 5-chloro-benzimidazole-2-carboxylic acid (CBIA) in different solvents at 298°K.

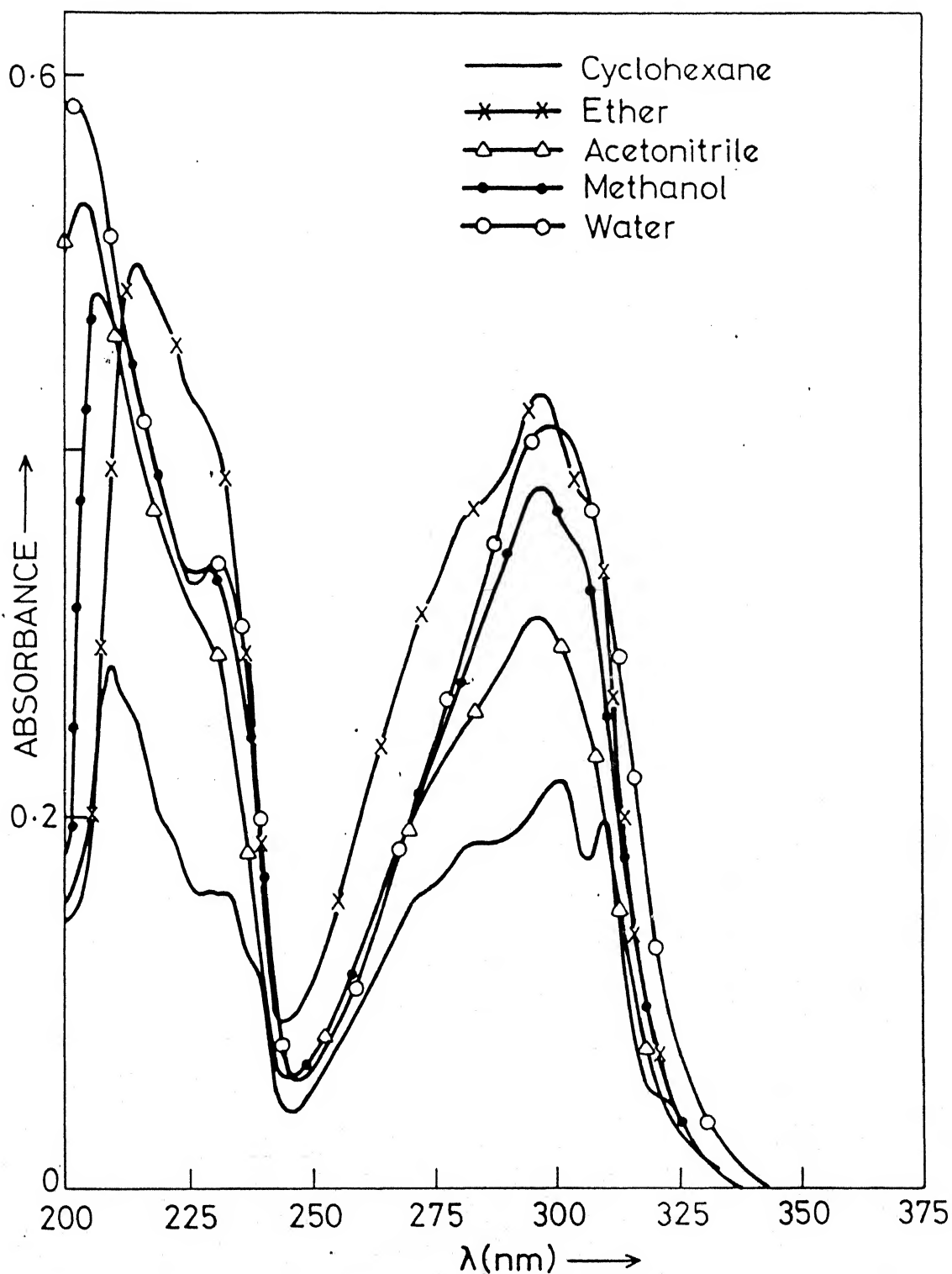


Fig.3.29 Absorption spectra of 5-chlorobenzimidazole-2-methylcarboxylate (CBIM) in different solvents at 298°K.

spectral data are compiled in Table 3.10, $\log(\epsilon_{\max})$ values have been reported only for methanol solution, because of the low solubility of these compounds in other solvents. Spectral characteristics of these compounds were determined with their saturated solutions.

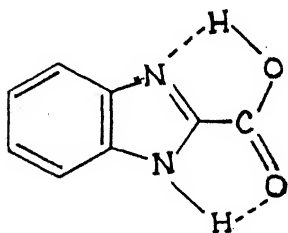
The absorption band maxima of all these compounds, in any one particular solvent, are very largely red shifted in comparison to that of BI moiety.¹²² Similar to the absorption spectrum of OHBI, the absorption spectra of BIA, CBIA and CBIM can also be divided into four band systems i.e. one above 300 nm, the second at ~ 280 nm, the third one at ~ 240 nm and the fourth one at ~ 210 nm. Above 300 nm, the absorption band system of BIA and CBIA are nicely structured and is very weak with respect to other three band systems, present below 300 nm, whereas in CBIM the long wavelength band is broad and is close to 300 nm. In BIA and CBIA the intensity of the long wavelength band system ($\lambda_{\max} > 300$ nm) further decreases on increasing the polarity or hydrogen bond formation tendency of the solvents. The structure of this band system is also lost under the above environment. Moreover, this band system is either insensitive to or a small red shift is noticed with increasing the polarity or proton donor capacity of these solvents.

Table 3.10. Absorption maxima [λ_a (nm)] and $\log(\epsilon_{\max})$ of 5-chlorobenzimidazole-2-carboxylic acid (CBIA), benzimidazole-2-carboxylic acid (BIA) and 5-chlorobenzimidazole-2-methylcarboxylate (CBIM) in different solvents at 298°K.

Solvent	λ_a (nm) $\log(\epsilon_{\max})$					
	CBIA		BIA		CBIM	
Cyclohexane					322	284
					310	271
					300	
Ether	357	286	254	216	338	279
	344	280	247		321	274
	327	275				266
	305					
Acetonitrile	357	286	254	-	337	279
	344	280	247		320	274
	327	275				266
	305					
Methanol	362	287	254	211	340	279
	(2.00)	(3.88)	(3.55)	(4.15)	(2.21)	(3.90)
	345	280			322	273
	(2.36)	(3.81)			(2.35)	(3.83)
	-	-				266
Water (pH 7)	296					(3.51)
	(3.82)					
	362	290	-	226	342	285
	345	-			325	277
	-					271

The other three band systems, present below 300 nm, are nearly similar to that of BI. The spectral behaviour of these band systems, under the influence of different solvents, are similar to that of BI, in the sense that either a small blue shift or insensitiveness is noticed in the absorption bands.

The data of Table 3.10 clearly indicate that the carboxyl group in these compounds are coplanar to the BI ring and hence extensive conjugation is observed. This behaviour is similar to that observed in case of 4¹⁶³ and 5-indolecarboxylic¹⁶⁴ acids and different to many other aromatic carboxylic acids,¹⁶⁴⁻¹⁶⁶ where -COOH group is not in the plane of the aromatic ring. We suggest that the long wavelength structured band of both the carboxylic acids (CBIA and BIA) is due to the presence of intramolecular hydrogen bonded structure as shown below.



This suggestion is based on the following reasons,

- (i) The model structures have clearly shown that the lone pair, on the tertiary nitrogen atom is at the same distance from the hydroxylproton as that of the lone pair of carboxyl group

from the imino proton. Although only five membered ring structure is formed which is not as stable as the six membered one, it gives rigidity to the molecule. The same argument does not hold for CBIM, because the hydroxyl proton has been replaced by the methyl group and hence the intramolecular hydrogen bonding interaction with the tertiary nitrogen atom is removed. Due to the above fact, though the long wavelength absorption band in CBIM is red shifted with respect to BI but the vibrational structure is completely absent in CBIM, reflecting the loss of rigidity. This is further manifested from the effect of solvents on the absorption spectrum of CBIM, where the long wavelength band (~ 300 nm) is largely blue shifted with increase in the polarity and hydrogen bond forming tendency of the solvents. Due to the intermolecular hydrogen bonding at the tertiary nitrogen atom, the $-\text{COOMe}$ group may be becoming non-planar with the BI moiety and hence causes a blue shift.

- (ii) The presence of long wavelength band due to the dimer formation (as it is formed in case of benzoic acid)¹⁶⁷ was rejected on the ground that the structured spectrum is observed even in polar solvents like methanol and acetonitrile. Secondly, the observation of vibrational structure in such a loosely formed dimer, especially in polar solvents, is difficult to explain.

- (iii) The decrease in the absorbance of the long wavelength band (~ 300 nm) in BIA and CBIA, with increase in polarity or proton donor capacity of the solvents is due to the competition between the intra and intermolecular hydrogen bonding. This reflects the loss of rigidity and inturn planarity due to the intermolecular hydrogen bonding with the solvents.
- (iv) Similar band system is also observed in the absorption spectrum of 2-(2'-aminophenyl)benzimidazole.¹⁵⁴ It was broad and the ring formed due to the intramolecular hydrogen bonding is a six membered one.

The fluorescence spectra of BIA, CBIA and CBIM in different solvents were recorded and are given in figures 3.30, 3.31 and 3.32 respectively. The relevent data are compiled in Table 3.11. As compared to BI, the fluorescence spectra of all the compounds are very large red shifted in any one particular solvent. The vibrational structure is observed in polar and non-polar solvents with the exception of CBIM, where the vibrational structure is noticed only in non-polar solvents and it is lost with the increase in polarity and hydrogen bond formation tendency of the solvents. The vibrational frequency ($1100 \pm 50 \text{ cm}^{-1}$) observed in the S_1 state of CBIM is similar to that

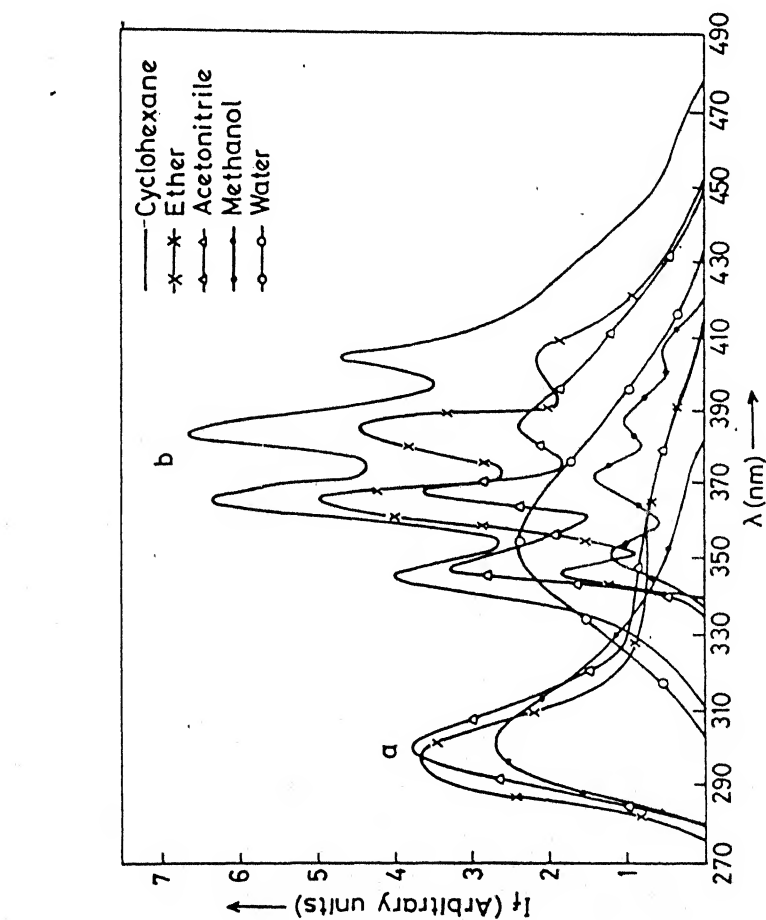


Fig.3.30 Fluorescence spectra of 5-chlorobenzimidazole-2-carboxylic acid (CBIA) in different solvents at 298°K, (a) $\lambda_{\text{excitation}}$ 280 nm, (b) $\lambda_{\text{excitation}}$ 350 nm.

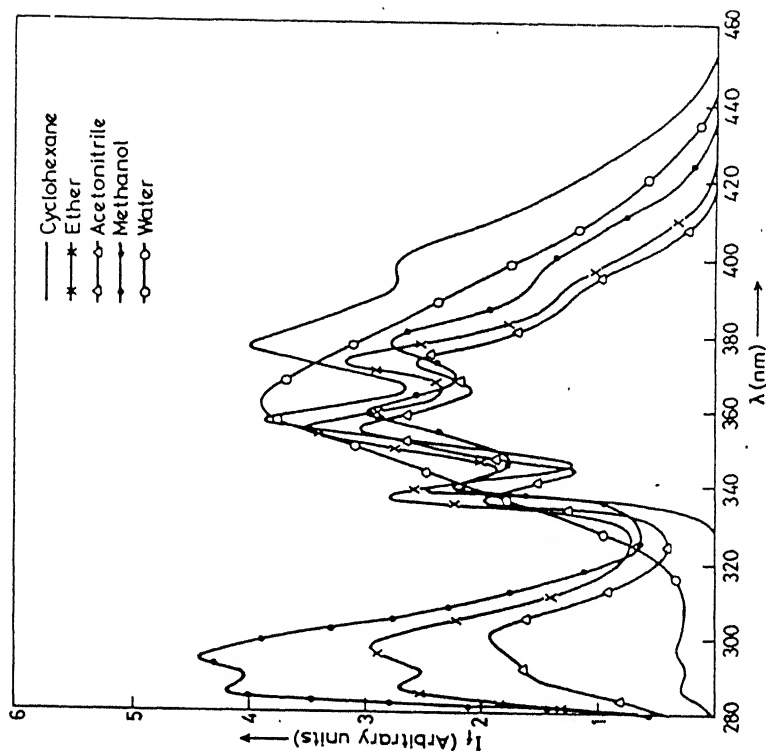


Fig.3.31 Fluorescence spectra of benzimidazole-2-carboxylic acid (BIA) in different solvents at 298°K, $\lambda_{\text{excitation}}$ 280 nm.

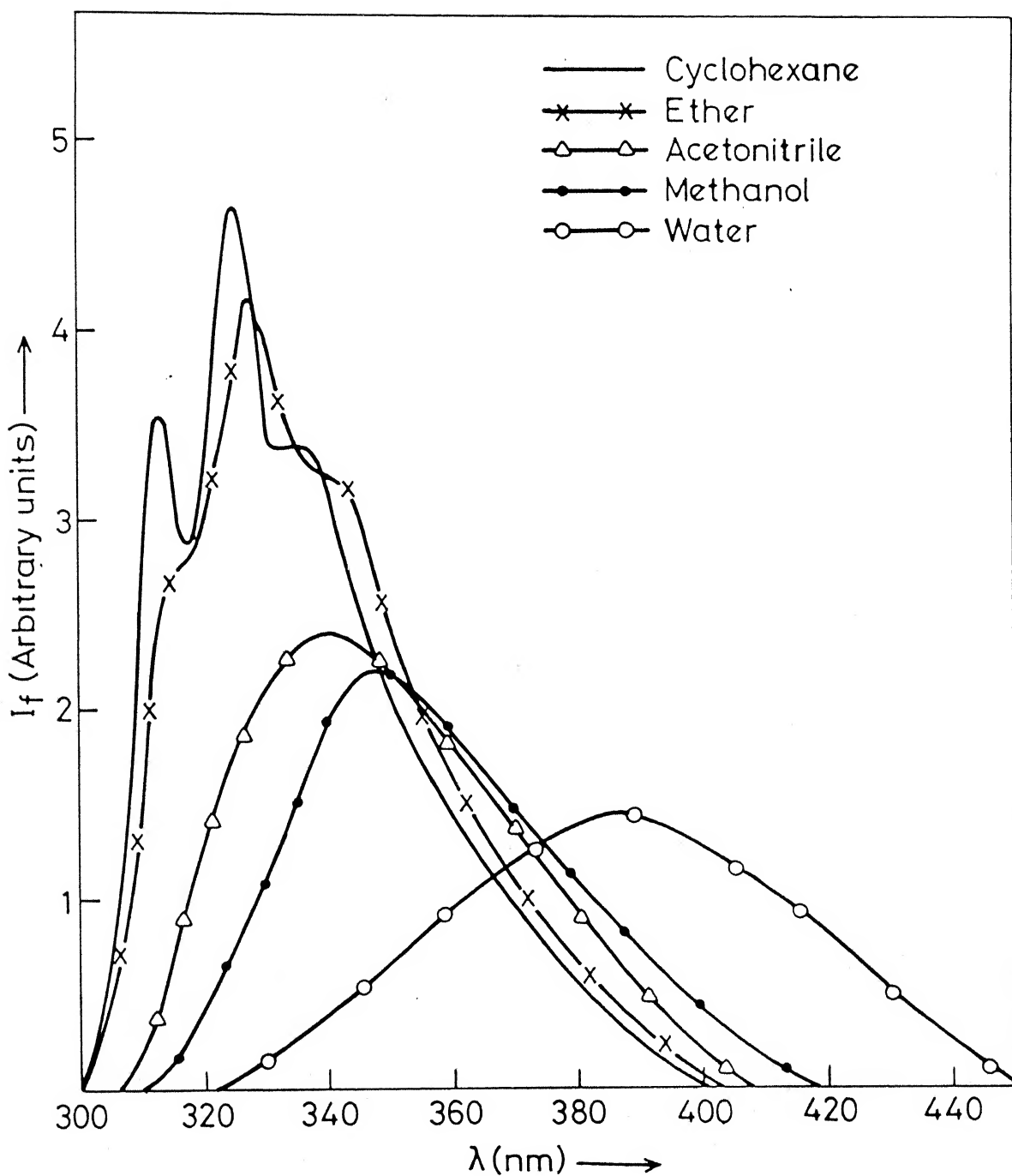


Fig.3.32 Fluorescence spectra of 5-chlorobenzimidazole-2-methylcarboxylate (CBIM) in different solvents at 298°K.

Table 3.11. Fluorescence maxima [λ_f (nm)] and quantum yield (ϕ_f) of 5-chlorobenzimidazole 2-carboxylic acid (CBIA), benzimidazole-2-carboxylic acid (BIA) and 5-chloro benzimidazole-2-methylcarboxylate (CBIM) in different solvents at 298°K.

Solvent	λ_f (nm) (ϕ_f)		
	CBIA	BIA	CBIM
Cyclohexane	405	400	335
	384 (0.01)	377 (0.09)	326 (0.10)
	366	355	318
	346	339	
Ether	405	393	343
	385 (0.01)	372 (0.13)	328 (0.11)
	366	355	316
	346	336	
Acetonitrile	-	300 (0.03)	342 (0.07)
	385 (0.02)	393	300 (0.02)
	367	372 (0.12)	288
	347	355	
Methanol	-	336	
	386 (0.003)	303(0.02)	348 (0.03)
	368	394	294 (0.11)
	349	377 (0.14)	285
Water (pH 7) ^φ	345 (0.015)	360 (0.21)	390 (0.02)
		287	

noticed in the ground state. In BIA and CBIA, the vibrational frequency noticed is $1500 \pm 50 \text{ cm}^{-1}$ in absorption and fluorescence spectra, indicating that the electronic states involved both in absorption and fluorescence spectra are the same. Besides this, the fluorescence band is not separated from and make mirror image with the absorption band. This suggests that the molecular conjugation and geometry in the excited singlet state differ very little from those in the ground state. The similar vibrational frequency is also observed in the spectral characteristics of 2-substituted benzimidazoles which make the structure rigid i.e. 2-phenyl-¹²⁸ 2-(4'-aminophenyl)-¹⁵⁶ 2-(4'-hydroxyphenyl)benzimidazole* etc. This supports our earlier conclusion based on the absorption spectral data, that the rigid structure formed due to the intramolecular hydrogen bonding, also exists in the S_1 state. Further support to this structure (i.e. formation of four ring systems) is manifested from the fluorescence spectra of condensed aromatic hydrocarbons in dilute solution i.e. vibrational frequency observed in the benzene and naphthalene fluorescence spectra is 1000 cm^{-1} , whereas that observed for polycondensed (rings equal to or more than three) ring is 1400 cm^{-1} . On the other hand, since intramolecular hydrogen bonded

* H.K. Sinha and S.K. Dogra, J. Photochem., 36, 149 (1987).

structure is not possible in CBIM, the vibrational structure is lost in more polar and proton donating solvents. It could be due to the stronger interaction of the polar solvents with CBIM. The insensitivity of the fluorescence spectra of CBIA and BIA towards the nature of the solvents further manifest the formation of rigid structure in the S_1 states. But unlike absorption spectrum, remarkable red shift in the fluorescence spectra of CBIM is observed with the change in the polarity of the solvents. The strong red shift indicate a large change in the dipole moment upon excitation. The fact that this large red shift could be due to solute solvent complex is rejected on the ground that a gradual red shift is observed on adding different percentage of water (10 to 70% v/v) to methanol solution.

Besides the structured long wavelength fluorescence band, a weak fluorescence band at ~ 300 nm in all the solvents other than cyclohexane is also observed in case of CBIA and BIA. This fluorescence band is also nearly insensitive to the polarity of the solvents. The excitation spectra recorded at 365 nm in all the solvents resembles the absorption spectra above 300 nm, however, in the former case bands below 300 nm were quite weak to extract useful informations. Whereas the excitation spectra recorded at 300 nm, shows no band system above 300 nm.

The fluorescence band structure at ~ 300 nm closely resembles that of parent BI molecule or the monocation of

benzimidazole molecule where the charge transfer transition is absent. This fluorescence band can be assigned to a species in which the carboxyl group and the BI moiety are not coplanar. Moreover, as only one fluorescence band is observed in cyclohexane, it seems that intermolecular hydrogen bonding interaction in other solvents is responsible for the creation of this species as said earlier. We give the following arguments for rejecting other possibilities:

- (i) pK_a of aromatic acids are in the range of ~ 4 , whereas the pK_a for the formation of monocation of benzimidazole is 5.5. One can speculate the formation of zwitterion with carboxylate group perpendicular to the benzimidazole, both in ground and excited states. But generally, the absorption and fluorescence band maxima of zwitterion are at longer wavelength than that of the monocation or monoanion. Though the absorption data do follow this criterion on decreasing and increasing the pH (i.e. zwitterion going to monocation or monoanion) but the blue shift observed in these cases could be due to the loss of rigid structure. The shifts observed in the fluorescence spectrum does not satisfy the above criterion. Further it has been shown latter that in case of 2-(trichloromethyl)- and 2-(trifluoromethyl)benzimidazoles [chapter 4, p.172], the presence of electron withdrawing group at the 2-position

decreases the pK_a value for the protonation reaction of tertiary nitrogen atom of BI to as low as <1 . Since carboxylic acid group is an electron withdrawing one, it is expected that the pK_a for the same reaction of BIA and CBIA should also decrease (infact the pK_a has been found to be ~ 0.5 , see later) usual spectral shifts i.e. red shift for the formation of monocation and blue shift for the formation of monoanion (deprotonation from $-COOH$ group), is observed with respect to the long wavelength fluorescence band. Thus the fluorescence band at 300 nm can not be assigned to the twisted zwitterion.

- (ii) The carboxylic acids are stronger acids in non-polar solvents as compared to that in the aqueous medium. Complete absence of 300 nm fluorescence band in cyclohexane rejects the possibility of zwitterion.

The other possibility is that, in polar solvents, there is a competition between the intra and intermolecular hydrogen bonding in BIA and CBIA, as mentioned earlier while dealing with the absorption data. This will partially decrease the amount of cyclic structure in ground and excited state. It could be possible that due to strong solvent interaction, the coplanarity of $-COOH$ group is lost and fluorescence spectrum thus observed resembles BI molecule.

In conclusion it can be said that the absorption and fluorescence spectral data combined with that of excitation spectral data suggest the existence of two conformers, in case of BIA and CBIA, in polar solvents. The long wavelength absorption and fluorescence band system represent the cyclic structure while the short wavelength absorption and fluorescence spectra confirm the species where the -COOH group and BI moiety are perpendicular to each other.

(b) BIAA and BIAE

Figures 3.33 and 3.34 depict the absorption spectra of BIAA and BIAE in different solvents. The relevant data are summarized in table 3.12.

The absorption spectrum of BIAA in different solvents are red shifted, in comparison to BI but blue shifted with respect to that of CBIA and BIA. The long wavelength band (314 nm) in case of BIAA is a broad one as compared to the structured spectra noticed for BIA and CBIA. Similar to BIA and CBIA, the long wavelength band system in BIAA has been assigned to an intramolecularly hydrogen bonded cyclic structure, as shown below. The assignment has been done based on the following observations.

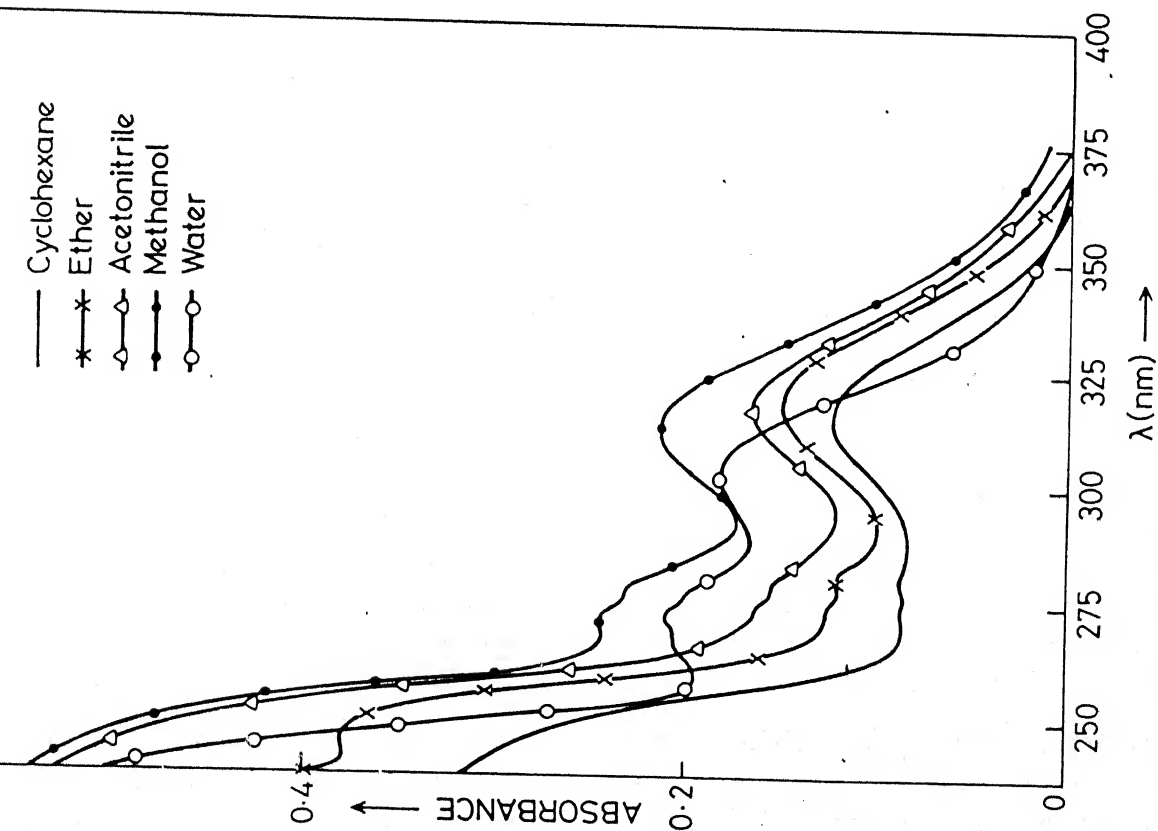


Fig.3.33 Absorption spectra of benzimidazole-2-acetic acid (BIAA) in different solvents at 298°K.

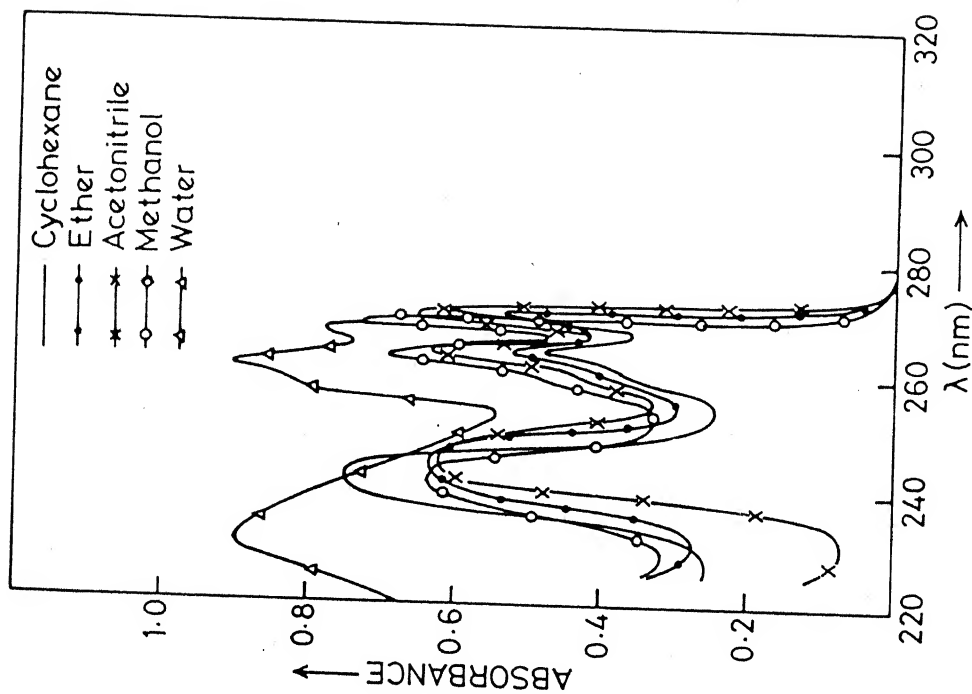
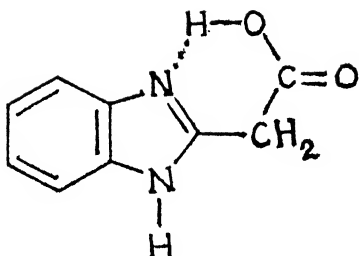


Fig.3.34 Absorption spectra of benzimidazole-2-ethylacetate (BIAE) in different solvents at 298°K.

Table 3.12. Absorption maxima [λ_a (nm)] and $\log(\epsilon_{\max})$ of benzimidazole-2-acetic acid (BIAA) and benzimidazole-2-ethylacetate (BIAE) in different solvents at 298°K.

Solvent	λ_a (nm) $\log(\epsilon_{\max})$						
	BIAA				BIAE		
Cyclohexane	314	281 275	246	219	282 275 271	243	212
Ether	319	281 275	245	225	282 275 271	245	—
Acetonitrile	317	281 275	244	219	281 275 271	245	206
Methanol	313 (3.44)	279 (3.48) 273 (3.50)	239 (3.97)	216 (4.28)	279 (3.91) 273 (3.89) 269 (3.77)	243 (3.88)	207 (4.00)
Water(pH 7) ^φ	304	277 271	—	212	277 271 267	240	206

^φ Monoanion.



- (i) The results mentioned in this thesis have shown that the presence of methylene group between two functional groups reduces their direct interactions drastically. Had it been the case here, pure BI's absorption spectrum should have been observed in BIAA. But from the data of Table 3.12 it is clear that the interaction of carboxylic acid group with the BI moiety still exists. The interaction has been recognised to be through the intramolecularly hydrogen bonded structure, as shown above. Though a six membered ring structure can be achieved, but the presence of methylene group between -COOH and BI moiety will reduce their direct conjugation, causing a blue shifted long wavelength absorption band in comparison to that of BIA and CBIA. Secondly the above structure can not be as rigid as it can be obtained in case of BIA and CBIA and this will lead to the loss of vibronic bands.

- (ii) The second set of absorption bands (below 300 nm) resembles very closely to that of pure BI moiety. Further the ratio of absorbance at 314 nm to 280 nm bands shows a gradual decrease on increasing the hydrogen bonding ability of the solvent. In more polar and protic solvents, a competition between intra and intermolecular hydrogen bonding is expected. This will destroy the cyclic structure and thereby amount of open structure will increase. According to our earlier discussion, the open structure should have an absorption spectrum very close to that of BI molecule. Similarity of the absorption spectrum (below 300 nm) of BIAA to that of BI molecule and continuous increase of the absorbance ratio ($A_{280 \text{ nm}}/A_{314 \text{ nm}}$) with increase of proton donating solvents, clearly support the above discussion. The solvent study also supports that there is an equilibrium between the cyclic structure and open structure in the polar and the protic solvents.
- (iii) The presence of cyclic structure in BIAA and the effect of solvents are further confirmed from the absorption spectrum of the ester of benzimidazole-2-acetic acid (BIAE). In this case, the absorption spectrum very closely resembles to that of BI. This is consistent with the structure of the molecule BIAE. This also favours our earlier discussion that the

presence of methylene group in between two chromophores reduces their direct interaction. The similarity of absorption spectrum of BIAE and BI further supports the presence of some amount of open structure of BIAA in all the solvents, especially in protic ones.

The fluorescence spectra of BIAA and BIAE in various solvents are shown in figures 3.35 and 3.36. The data have been compiled in Table 3.13.

It is clear from the data of Table 3.13 that the fluorescence spectra of BIAA are similar to those of BIA and CBIA, whereas that of BIAE resembles closely to BI. The fluorescence spectrum of BIAA in all the solvents is more structured, with a vibrational frequency of $\sim 1500 \pm 50 \text{ cm}^{-1}$. Similar reasons may be given here, as given in case of BIA and CBIA, to support the presence of cyclic structure in S_1 state also. Structured fluorescence spectrum and insensitivity towards solvents indicate that the intramolecular hydrogen bonding in BIAA is stronger in the S_1 state than in the S_0 state. The intramolecular hydrogen bonding is so strong that it is difficult to destroy it by allowing intermolecular hydrogen bonding in protic solvents and thus leads to the absence of fluorescence band at $\sim 300 \text{ nm}$ observed in case of BIA and CBIA.

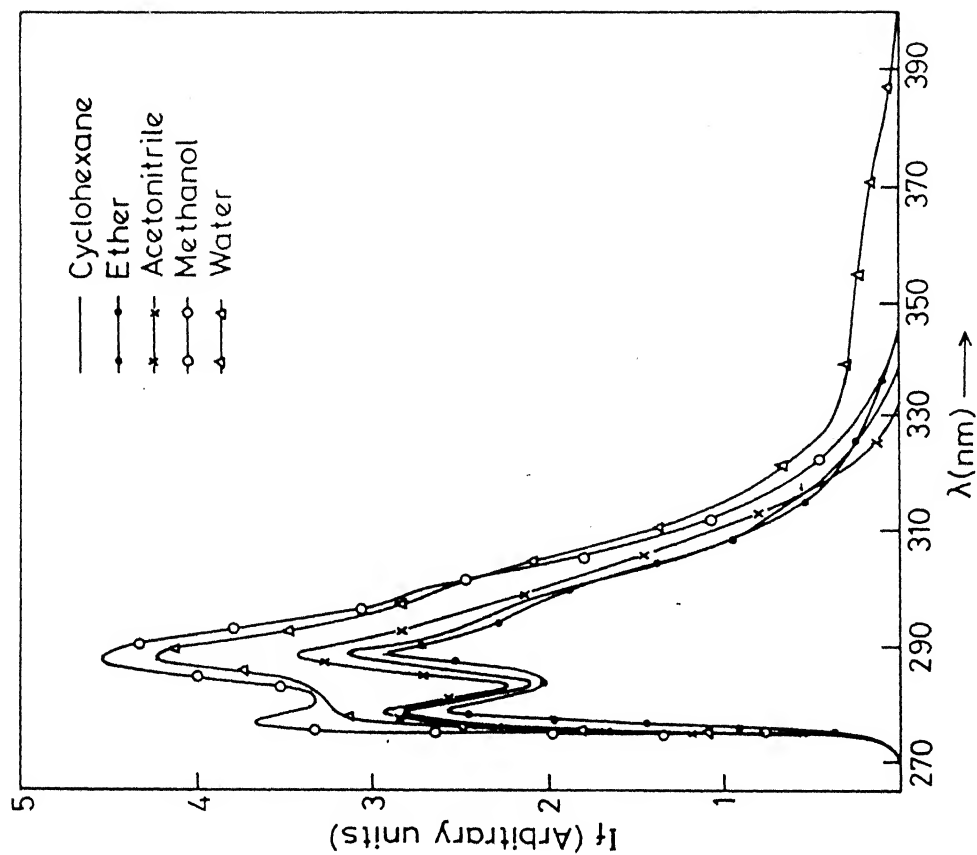


Fig.3.36 Fluorescence spectra of benzimidazole-2-ethylacetate (BIAE) in different solvents at 298°K.

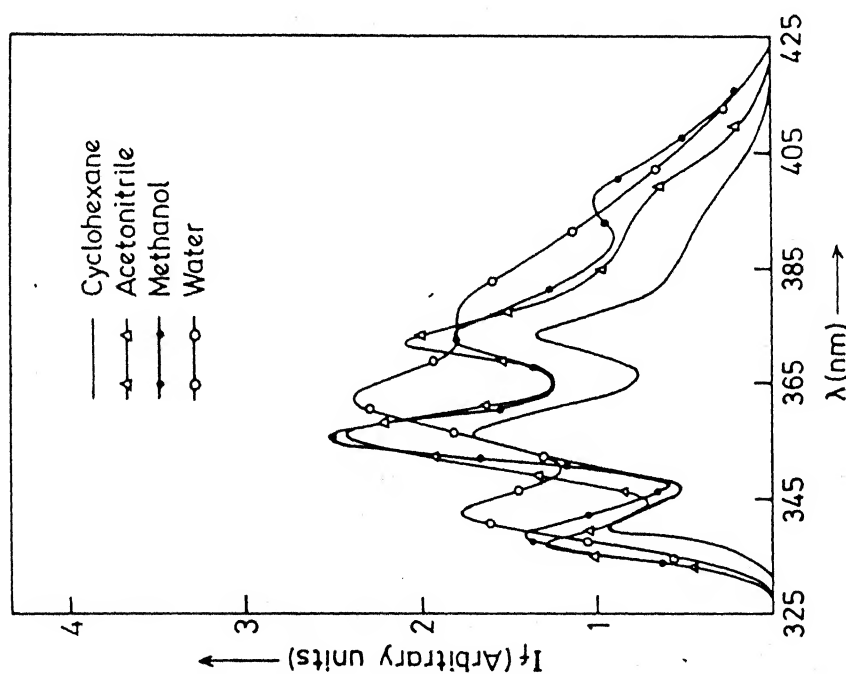


Fig.3.35 Fluorescence spectra of benzimidazole-2-acetic acid (BIAA) in different solvents at 298°K.

Table 3.13. Fluorescence maxima [λ_f (nm)] and quantum yield (ϕ_f) of benzimidazole-2-acetic acid (BIAA) and benzimidazole-2-ethylacetate (BIAE) in different solvents at 298°K.

Solvent	λ_f (nm) (ϕ_f)	
	BIAA	BIAE
Cyclohexane	—	
	373	289
	356	279(0.11)
	339	
Ether	395	289
	372	279(0.16)
	356	
	337	
Acetonitrile	395	289
	372	279(0.19)
	356	
	337	
Methanol	398	287
	374	277(0.23)
	356	
	339	
Water (pH 7) ^φ	400	287(0.11)
	378	277
	362	
	344	

^φ Monoanion.

Similarity of the fluorescence spectrum of BIAE with that of BI is due to the fact that, (i) intramolecularly hydrogen bonded cyclic structure is absent here due to the replacement of carboxylic hydrogen with ethyl group in BIAE, (ii) the presence of methylene group in between BI and $-\text{COOC}_2\text{H}_5$ groups inhibits the direct interaction between the two groups.

Similar explanation, as discussed in case of BIA and CBI, can be given here to reject the idea of the existence of zwitterionic structure in the ground and the excited states in all the solvents.

In conclusion it can be said that though the direct conjugation between $-\text{COOH}$ and BI moieties is stopped by the presence of methylene group in between, but the interaction still exists through the hydrogen bonded cyclic structure in BIAA. The existence of open structure as well as cyclic structure has been confirmed in all the solvents. All the above results are nicely substantiated from the study on BIAE in different solvents.

(c) BIPA

The absorption spectra of BIPA in different solvents are shown in figure 3.37 and the relevant spectral data are summarized in Table 3.14.

The absorption spectra of BIPA in different solvents exactly resemble to that of BI and consistent with the fact that BI and -COOH groups are behaving independently. In every respect BIPA resembles to the behaviour of parent BI (see chapter IV). So it is clear that by putting two methylene group in between -COOH and BI moiety, their mutual interaction, both hydrogen bonding as well as direct conjugation, can be arrested resulting in independent behaviour of two chromophores.

The fluorescence spectra are given in figure 3.38 and the data are compiled in Table 3.15. Similar to the absorption spectra, the fluorescence spectra of BIPA in various solvents exactly matches with that of BI, consistent with the structure of the molecule.

This behaviour of BIPA confirms that there is no interaction between -COOH and BI moiety, both in the ground as well as in the excited singlet state.

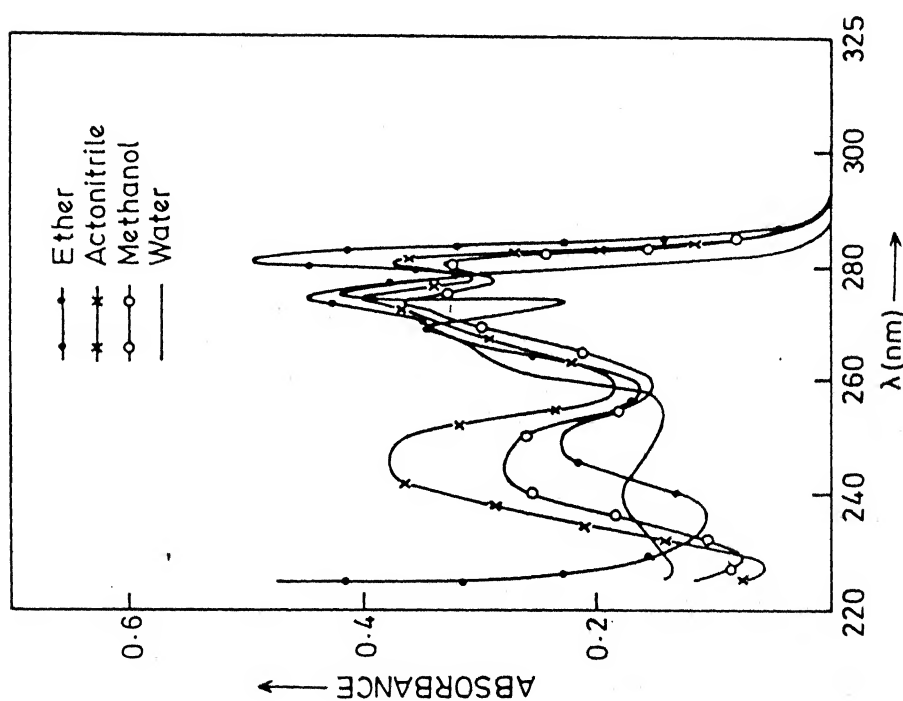


Fig.3.37 Absorption spectra of benzimidazole-2-propionic acid (BIPA) in different solvents at 298°K.

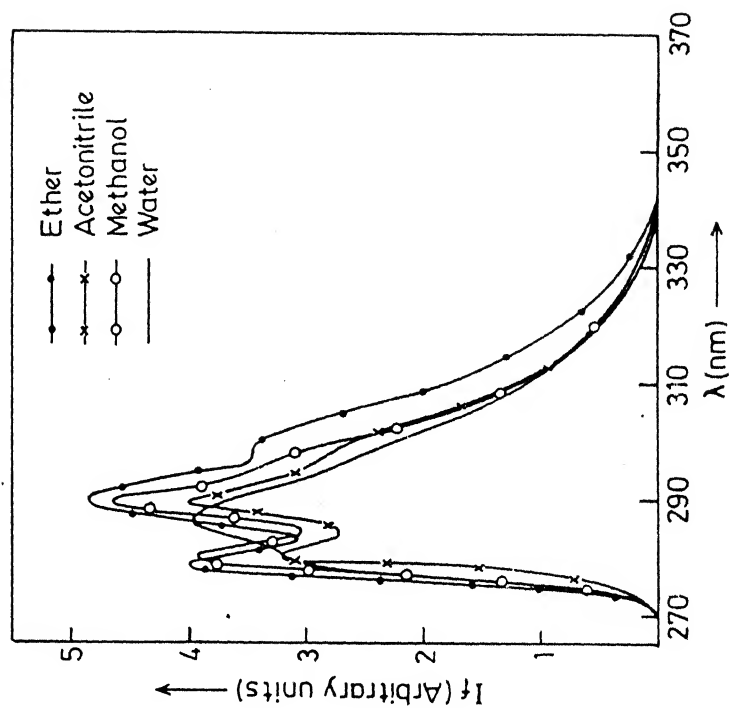


Fig.3.38 Fluorescence spectra of benzimidazole-2-propionic acid (BIPA) in different solvents at 298°K.

Table 3.14. Absorption maxima [λ_a (nm)] and $\log(\epsilon_{\max})$ of benzimidazole-2-propionic acid (BIPA) in different solvents at 298°K.

Solvent	λ_a (nm) $\log(\epsilon_{\max})$		
Cyclohexane	281	250	215
	275	244	
	268		
Ether	281	250	205
	274	244	
	268		
Acetonitrile	281	250	205
	274	244	
	268		
Methanol	281	250	205
	(3.92)	(3.77)	(4.50)
	275	244	
	(3.92)	(3.93)	
	268		
	(3.80)		
Water(pH 7) ^φ	280	249	204
	274	243	
	268		

^φ Monoanion.

Table 3.15. Fluorescence maxima [λ_f (nm)] and quantum yield (ϕ_f) of benzimidazole-2-propionic acid (BIPA) in different solvents at 298°K.

Solvent	λ_f (nm)	ϕ_f
Ether	290	0.05
	279	
Acetonitrile	289	0.40
	280	
Methanol	289	0.29
	280	
Water (pH 7) ^φ	288	—
	279	

^φ Monoanion.

CHAPTER-IV

ABSORPTION AND FLUORESCENCE SPECTRA-STUDY OF PROTOTROPISM

A thorough investigation of effect of hydrogen ion concentration on the spectral characteristics of different 2-substituted benzimidazoles has been presented in this chapter. Identification of different prototropic species, present in different $H_0/pH/H_-$ solutions and determination of pK_a values in the ground and excited singlet states, have been given prime importance here.

This chapter is divided into a number of sections (4.1-4.9), depending on the behaviour of particular BI.

4.1 2-(Aminomethyl)benzimidazole (BINH₂)^{*}

The absorption and fluorescence spectra of BINH₂ have been studied in the $H_0/pH/H_-$ range from -8 to 16. Spectral profiles are drawn in Figures 4.1 and 4.2 and the data are summarized in Table 4.1. On decreasing the pH below 10,

^{*}H.K. Sinha and S.K. Dogra, Spectrochimica Acta, 41A, 961-966 (1985).

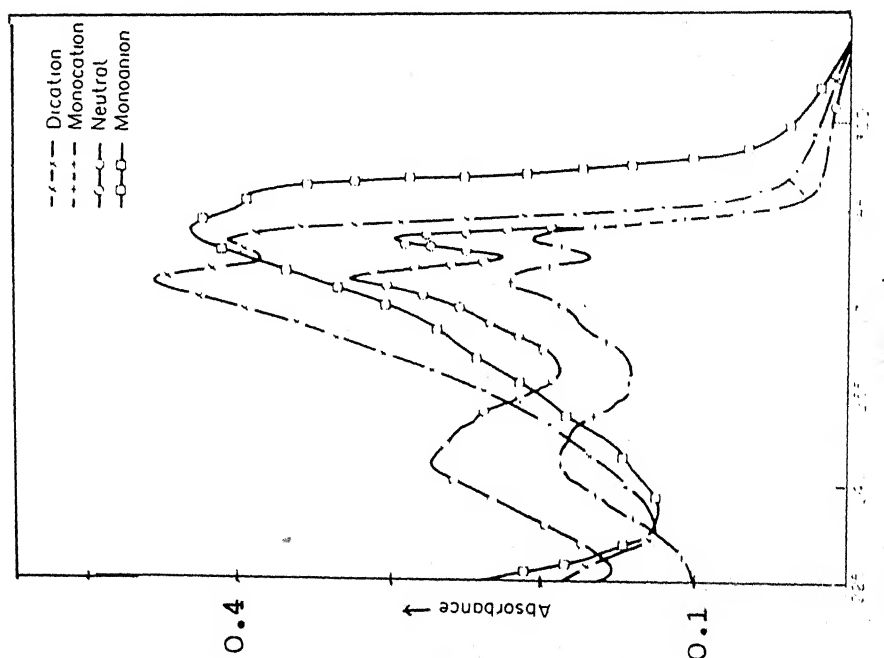


Fig. 4.1 Absorption spectra of various prototropic species of 2-(amino-methyl)benzimidazole (BINH₂) at 298°K.

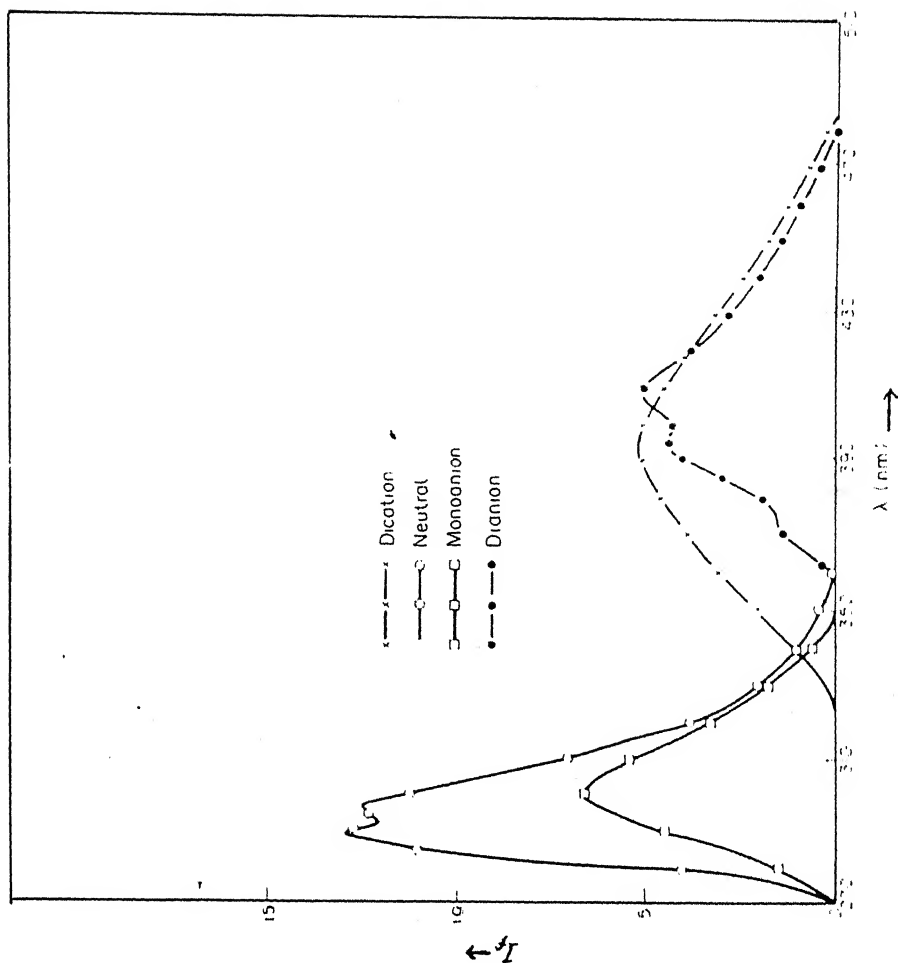


Fig. 4.2 Fluorescence spectra of various prototropic species of 2-(amino-methyl)benzimidazole (BINH₂) at 298°K.

Table 4.1. Absorption maxima [λ_a (nm)], $\log(\epsilon_{\max})$ and fluorescence maxima [λ_f (nm)] of different prototropic species of 2-(aminomethyl)benzimidazole (BINH₂) at 298°K

Species/H ₀ /pH/H ₋	λ_a (nm) $\log(\epsilon_{\max})$				λ_f (nm)
Dication (H ₀ -1)	-	-	269.5 (3.92)	277 (3.91)	400 (400) ^φ
Monocation (pH 6)	244 (3.57)	-	272.5 (3.65)	278.5 (3.62)	-
Neutral (pH 10)	243 (3.66)	244.5 (3.66)	271.5 (3.66)	277.5 (3.74)	291
Monoanion (H ₋₁₆)	-	-	280.5 (3.93)	286.5 (3.89)	302 312 (300)

^φ at 77°K.

Table 4.2. pK_a and pK_a^* of various prototropic reactions of 2-(aminomethyl)benzimidazole (BINH₂) at 298K

Equilibrium	pK_a	pK_a^*		
		Abs. ^a	Flu. ^a	FT ^b
Dication \rightleftharpoons Monocation	3.1	-	-	1.8
Monocation \rightleftharpoons Neutral	8.1	-	-	8.0
Neutral \rightleftharpoons Monoanion	12.8	10.6	8.0	12.0

^aForster cycle method.

^bFluorimetric titration method.

there is no major change in the band shape of absorption spectrum upto pH 6 and a further decrease of pH leads to a small blue shift in the long wavelength band maximum at H_0-1 . At the same time the second wavelength absorption band (244 nm) gets merged with the long wavelength absorption band system. On further increase of hydrogen ion concentration a gradual red shift in the absorption band is noticed. On increasing the pH above 10, a red shift is observed in the long wavelength band maximum with a similar effect on the second absorption band (244 nm) as observed in the acidic condition at H_0-1 . Starting with H_0-8 and decreasing the hydrogen ion concentration, the fluorescence intensity of the 400 nm broad band increases gradually, reaches a maximum at H_0-5 and is completely quenched at pH 4, without appearance of any other fluorescence band. In the pH range 6-14 there is only one fluorescence band at 292 nm and its intensity attains the maximum value at pH 10. At H_{14} , a new fluorescence band appears at 312 nm and its fluorescence intensity keeps on increasing with pH even at H_{16} . At H_{16} , besides the 312 nm band a new broad band appears at 440 nm.

$BINH_2$ can be viewed from two angles: (i) as a substituted methylamine and (ii) a compound in which the hydrogen atom of the methyl group of 2-methylbenzimidazole (BIM) is

replaced by amino group. The pK_a 's for the protonation and deprotonation reactions of methylamine¹⁶⁸ are 11.5 ± 0.5 and 16. The values of the corresponding constants for the similar reactions of BIM¹⁶⁹ are 6.19 and 14.20. Phenyl substitution at the hydrogen atom of methyl group of methylamine (benzylamine) decreases the pK_a value of protonation reaction to 9.0 ± 0.5 .¹⁷⁰ A similar substitution by electro withdrawing benzimidazolyl group in methylamine should decrease the basicity and increase the acidity of the amino group, so the pK_a values are expected to be lower than the parent molecule. However, the presence of electron donating amino group in BIM should increase the basicity at tertiary nitrogen atom, thus the pK_a should be higher. The following discussion reveals that the first protonation has occurred at the amino group and not at the tertiary nitrogen atom.

- (i) The separation of two chromophores by a saturated linkage, like methylene group, has been found to reduce their direct interactions drastically (as discussed in chapter III).

Hence $BINH_2$ behaves like benzimidazole and does not sense the presence of amino group. In other way it can be said that any prototropic reaction at amino group will not have much effect on the absorption spectral characteristics of $BINH_2$.

- (ii) The 244 nm absorption band is affected drastically on protonation (monocationic species) and deprotonation (monoanionic species) of BI or BIM as this transition is localized on the imidazole ring. But in this case it remains intact upto pH 5 and on further decreasing the pH the effect is pronounced i.e. the 244 nm band gets merged with the long wavelength absorption band.
- (iii) In amino substituted compounds it has been generally observed that proton induced fluorescence quenching of the neutral species takes place prior to the formation of monocation.⁶⁴

On taking the above points into account it is concluded that the first protonation takes place at amino group. As mentioned earlier, there is hardly any change in the absorption maxima of the neutral molecule on first protonation and so it is difficult to calculate an accurate value of pK_a by absorptiometry. The pK_a value (8.1 ± 0.5) obtained agrees well with the literature value (7.6).¹⁷¹ Since the monocation is non-fluorescent (even at 77K) and the shift in the absorption spectra is very small, the Förster cycle method can not be used to calculate the pK_a^* . The value of pK_a^* obtained from the plot of decrease of fluorescence intensities vs pH (Fig. 4.3) of $BINH_2$ is found

to be 8.0 and agrees nicely with the ground state value, thus indicating that the excited state equilibrium is not established in the S_1 state. It could be either due to low $[H^+]$ or small lifetimes of the conjugate acid base species.

In dication, formed in the pH range 6-1, the protonation occurs at the tertiary nitrogen atom of the BI moiety. The pK_a value, obtained absorptiometrically, is found to be very low (3.1) as compared to that of BI or BIM (5.5 or 6.19).¹⁶⁹ Again the Förster cycle method can not be applied to calculate pK_a^* for monocation-dication equilibrium as the monocation is nonfluorescent. The value of pK_a^* obtained from the dication formation curve (Fig. 4.3) is 1.8, lower than the ground state value. This low pK_a value indicates that in $BINH_2$ the tertiary nitrogen atom is less basic than BI, probably due to the presence of the positive charge on the amino group of monocation.

A large red shift is observed in the fluorescence spectra of dication in comparison to neutral $BINH_2$. According to the recent observation in our laboratory,¹²⁵ upon excitation the cationic species of BI, formed by the protonation at tertiary nitrogen atom, ends up in the manifold of excited states which are very close to each other (i.e. $\pi\pi^*$ and CT state). The energy of the emitting

state depends on the nature and position of the substituent as well as on the nature of the solvents. This large red shift can be attributed to the stabilization of CT state in polar solvent. Moreover the charge transfer from benzene ring to imidazole ring will be facilitated due to the presence of the positive charge on the imidazole ring, and the amino group. This will lead to the stability of the CT state.

The small red shift observed in the absorption spectrum with increase of hydrogen ion concentration ($H_0 < -1$) and quenching of the fluorescence of 400 nm band could be due to medium effect and proton induced quenching of the dication fluorescence. The quenching of fluorescence seems to be dynamic in nature rather than static as the 400 nm fluorescence band is observed at $77^\circ K$ (where the molecule is present under the ground state environment and movement of protons are restricted) and at $H_0 - 8$. Whereas the same fluorescence band is not observed under similar conditions at $300^\circ K$.

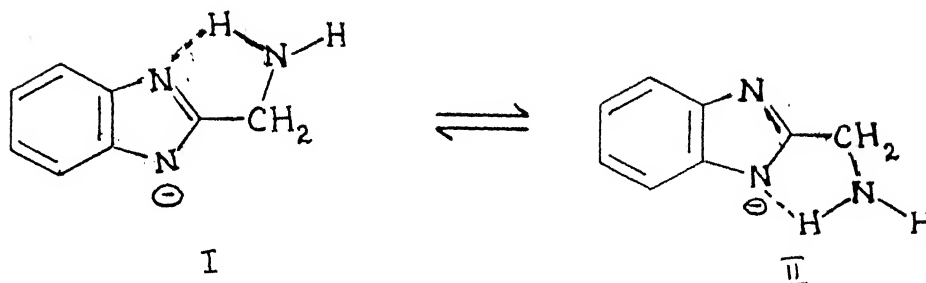
The monoanion formed above pH 10 is due to the deprotonation of imino group rather than amino group because for amino deprotonation pK_a is generally > 16 . This conclusion follows from the following results. (i) The absorption and fluorescence maxima of the monoanion match

nicely with that of BI. This is expected due to the reason mentioned earlier. (ii) The pK_a values calculated spectrophotometrically is found to be 12.8, which is very close to that of BI (13.1).

The formation curve of the 312 nm fluorescence band of monoanion can not be used to calculate pK_a^* , since its fluorescence intensity increases continuously even up to H₁₆. The pK_a^* value calculated from the plot of decrease of fluorescence intensities of BINH₂ vs pH (Fig. 4.3) is found to be 12.0. This value is consistent with the earlier results i.e. fluorimetric titration gives the ground state value in benzimidazole.

Besides the 312 nm band, a red shifted band at 440 nm is observed at 300°K and only at H₁₆. This band is structured (372, 392 and 409 nm) and blue shifted at 77°K. The vibrational frequency ($1370 \pm 50 \text{ cm}^{-1}$) observed at 77°K matches with that of the 2-phenylbenzimidazole¹²⁸ under similar condition. Similar observation has also been found in 2-(hydroxymethyl)benzimidazole (see section 4.2). This bands can not be assigned to dianion, since there is no indication of its formation in the ground state and at 77°K, where the emission characteristics are governed by the ground state environment. The structured fluorescence spectrum can be assigned to the intramolecular hydrogen bonded

structure I or II, the latter one seems to be more probable. The similar behaviour is also noticed in case of the



monoanion of 2-(hydroxymethyl)benzimidazole. This is only a speculation. Further study is necessary for the identification of this species.

The pK_a and pK_a^* values of all the prototropic reactions of $BINH_2$, are compiled in Table 4.2, whereas different prototropic species are shown in scheme, Fig. 4.4.

Conclusion: The presence of amino group have little effect on the spectral characteristics of benzimidazole due to the presence of a methylene group in between the two chromophores. Emission from CT state has been observed in case of dication, whereas in all other species the transitions are of $\pi \rightarrow \pi^*$ character.

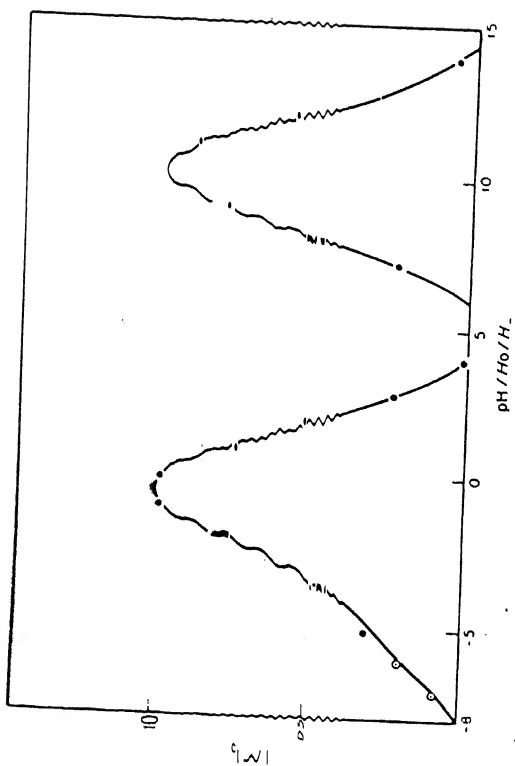


Fig.4.3 Plot of I/I_0 as a function of $H_0/pH/H_2$ of 2-(aminomethyl)benzimidazole ($BINH_2$).

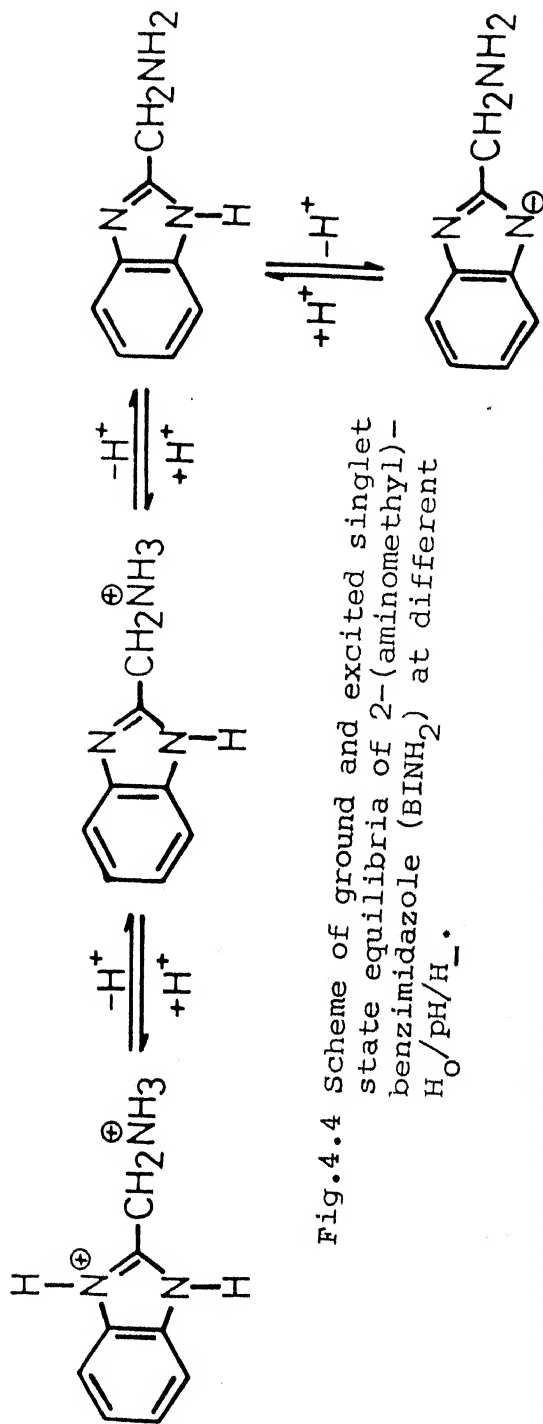


Fig.4.4 Scheme of ground and excited singlet state equilibria of 2-(aminomethyl)-benzimidazole ($BINH_2$) at different $H_0/pH/H_2$.

4.2 2-(Hydroxymethyl)- (BMOH) and N-methyl-2-(hydroxymethyl)-benzimidazoles (MBMOH)*

Figures 4.5 and 4.6 depict the absorption and fluorescence spectra of the various prototropic species of BMOH observed in the $H_0/pH/H_-$ range of -10 to 16. The relevant data are listed in Table 4.3. The same for MBMOH are included in Table 4.4. The following conclusions have been drawn on comparing the absorption and fluorescence spectra of BMOH and its various prototropic species with those of similar species of BI and BIM.

The red shift observed in the absorption and fluorescence spectra of BMOH above pH 11 is due to the formation of monoanion. No change is observed in the absorption spectrum of MBMOH upto H_-16 but the fluorescence spectral intensities of the neutral species (292 nm) start decreasing above pH 12, without appearance of any other new fluorescence band. The monoanion of BMOH can be formed by the deprotonation of either -OH group or >NH group, but in MBMOH it can only be obtained by the deprotonation of -OH group. The pK_a value for this reaction of BIM¹⁶⁹ is 14.20 and that of CH_3OH , it is 16-18.¹⁶⁸ It is also known that electron withdrawing group increases the acidity (decreases the pK_a)

*H.K. Sinha and S.K. Dogra, Indian J. Chem., 25A, 1092 (1986).

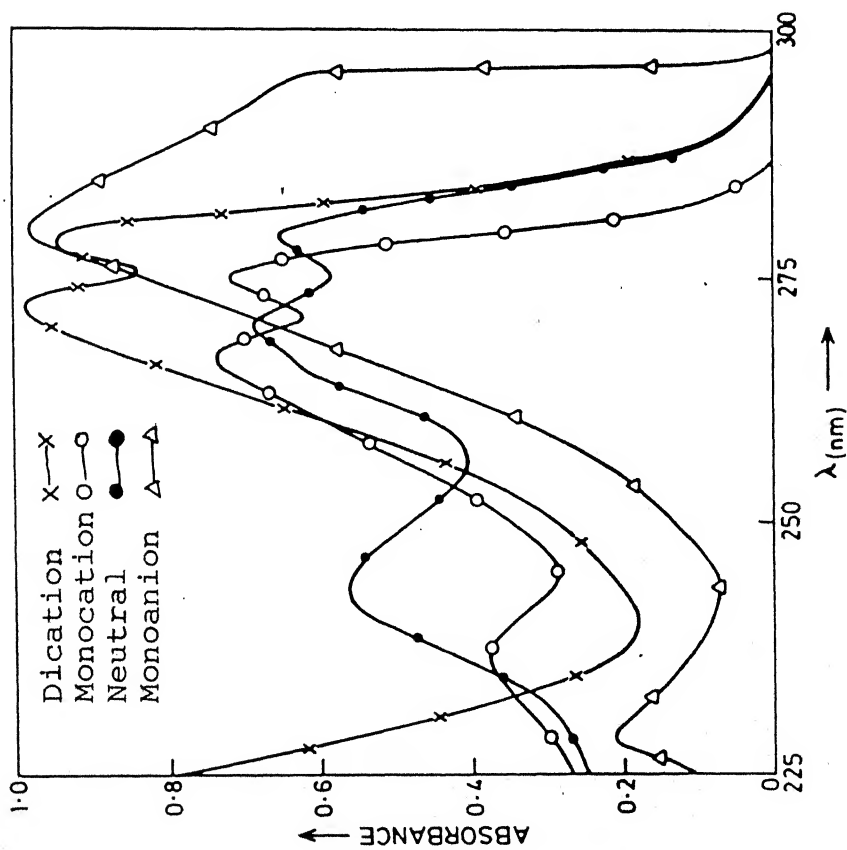


Fig.4.5 Absorption spectra of various prototropic species of 2-(hydroxymethyl)benzimidazole (BMOH) at 298°K.

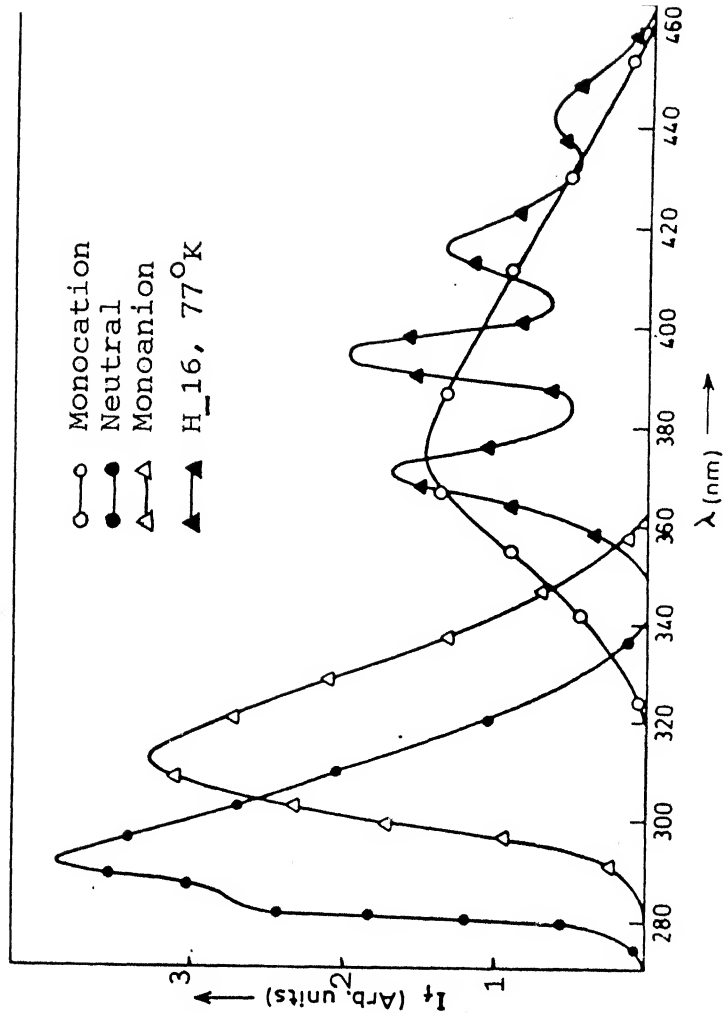


Fig.4.6 Fluorescence spectra of various prototropic species of 2-(hydroxymethyl)benzimidazole (BMOH) at 298°K.

Table 4.3. Absorption maxima [λ_a (nm)], $\log(\epsilon_{\max})$ and fluorescence maxima [λ_f (nm)] of different prototropic species of 2-(hydroxymethyl)benzimidazole (BMOH) at 298°K

Species/ H_o /pH/ H_-	λ_a (nm) $\log(\epsilon_{\max})$				λ_f (nm)
Monocation (pH 3)	237 (3.49)	268 (3.83)	275 (3.82)		372
Neutral (pH 8)	243 (3.59)	265 (3.58)	271 (3.68)	278 (3.63)	284 292
Monoanion (H_{-16})	225 (3.32)	—	280 (3.89)	295 (3.80)	312

Table 4.4. Absorption maxima [λ_a (nm)] and fluorescence maxima [λ_f (nm)] of different prototropic species of N-methyl-2-(hydroxymethyl)benzimidazole (MBMOH) at 298°K

Species/ H_o /pH/ H_-	λ_a (nm)				λ_f (nm)
Monocation (pH 3)	239	—	268	275	370
Neutral (pH 8)	254	268	277	282	286 298
— (H_{-16})	254	268	277	282	

and electron donating group decreases the acidity (increases the pK_a). The pK_a value calculated spectrophotometrically for this reaction in BMOH is 12.7 whereas for MBMOH it is greater than 16. If BMOH is considered as a substituted methanol, i.e. the hydrogen atom of methyl group in methanol is replaced by electron withdrawing benzimidazolyl group, the pK_a value of CH_3OH can not be reduced to such a low value (12.7) because of the presence of methylene group in between $-OH$ and benzimidazole moiety. The methylene group will directly inhibit the interaction between the two chromophores. Thus the agreement of absorption and fluorescence band maxima of monoanion of BMOH with those of BIM and non-formation of monoanion of MBMOH upto H_{16} clearly suggest that the monoanion in BMOH is formed by the deprotonation of the imino group, both in S_0 and S_1 states. The low pK_a (12.7) value of BMOH as compared to those of BI (13.25) and BIM (14.20) indicates that the negative inductive effect of $-OH$ group outweighs the resonance effect, thereby decreasing the charge densities at tertiary nitrogen atom and the imino group. In other words such an effect increases the acidity of the imino group and decreases the basicity of the tertiary nitrogen atom. In fact, the acidity and basicity of acidic and basic sites of benzimidazole have been seen to be modified by substituting various functional groups of different electronegativities (see later) at position 2, in particular.

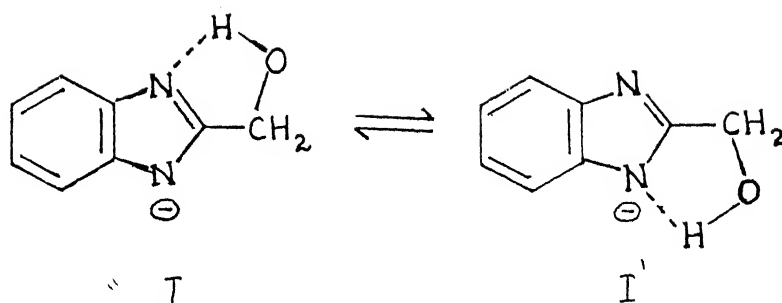
The pK_a^* value, calculated with the help of Förster cycle method and fluorimetric titration are listed in Table 4.5. Förster cycle method reveals that the imino group becomes stronger acid upon excitation. But the fluorimetric titration curves (Fig. 4.7) give a value very close to the ground state value indicating that the complete equilibrium is not established in the excited state. This result is consistent with the similar study on the deprotonation or protonation reactions of BI. Further it has been found that the fluorimetric titrations yield the ground state pK_a if these fall in the range of 3-10. This is because of the small concentration of protons (or hydroxyl ions) and thus the rate of protonation (or deprotonation) can not compete with the rate of radiative processes. It can also be due to the shorter lifetimes of the conjugate acid-base pairs and thus equilibrium is not achieved during the lifetimes of the species. The second argument seems to be more favourable because the lifetimes of the various substituted BI's are found to be less than 1 ns*.

The decrease in fluorescence intensity of MBMOH without appearance of any other band beyond pH 13, could be due to the formation of non-fluorescent monoanion. The pK_a^* value calculated from the decrease in the relative fluorescence intensity of MBMOH

* H.K. Sinha and S.K. Dogra, unpublished results.

is found to be 13.7, indicating that hydroxyl group becomes more acidic upon excitation. But this increase in acidity is less than that observed in the case of phenols,¹⁷² naphthols¹⁷³ and phenanthrols,¹⁷⁴ probably due to the presence of methylene group in between the two chromophores.

No dianion of BMOH is observed either in S_0 or S_1 state after pH 14 indicating that pK_a for deprotonation of hydroxyl group is greater than 16 and may be further increased due to the presence of negative charge on the imino nitrogen atom. But at 77°K and above pH 14 besides 312 nm band (which is slightly blue shifted) a well structured band appears after 370 nm. Similarly for MBMOH at H₁₆ and 77°K a well structured fluorescence band appears near 370 nm, though there is no ground state deprotonation and at 300°K the monoanion is non-fluorescent. This band can not be either due to dianion of BMOH or the monoanion of MBMOH as there is no indication of their formation in S_0 state and further in solid state at such a low temperature the emission characteristics are governed by the environment existing in the ground state. This could be due to the formation of species I or I' in the solid state at low temperature. Further experiment in solid state is necessary for confirming it.



The monocation is formed by the protonation of tertiary nitrogen atom below pH 6. As mentioned in section 4.1, the large red shift observed in the fluorescence spectrum of monocation as compared to the neutral species could be due to either large change in the basicity of tertiary nitrogen atom or presence of charge transfer state. A close look at the behaviour of 2-substituted benzimidazoles in acidic medium suggests that the charge transfer processes outweighs all other processes.

The pK_a value for this equilibrium reaction, calculated spectrophotometrically, is 4.2 (Table 4.5). This value is quite low as compared to the similar reaction in BI (5.3) or MBI (6.19). This can be explained with the help of negative inductive effect as suggested earlier, on the other hand, this value is quite high as compared to similar reaction of 2-hydroxybenzimidazole.¹²⁷ This is due to the introduction of the methylene group in between -OH and BI moiety, which inhibits the tautomerism or the formation of keto tautomer.

The pK_a^* data (Table 4.5) calculated with the help of Förster cycle method as well as fluorimetric titration method are consistent with those obtained in the similar compounds for protonation of tertiary nitrogen atom. Again the fluorimetric titration (Fig. 4.7) gave a ground state pK_a value, which could be due to very short lifetimes of conjugate acid-base pair, as mentioned earlier. Various prototropic reactions occurring in the ground and excited singlet states are mentioned in scheme, figure 4.8.

The fluorescence intensity of 372 nm band (monocation) starts quenching below pH 2 and is completely quenched at H_0-5 , without the appearance of any other new fluorescent species. No change in the absorption spectrum is noticed in this range of hydrogen ion concentrations. The fluorescence intensity of monocation remains the same with added amount of K_2SO_4 upto SO_4^{2-} ion concentration matching with that produced by the addition of H_2SO_4 at 300°K. This clearly suggests that the decrease in the fluorescence intensity is due to the proton induced quenching. Since the fluorescence intensity remains the same under this environment at 77°K, this reveals that the quenching of fluorescence intensity is of dynamic in nature in the S_1 state at 300°K. Plot of (I_0/I) vs proton concentration [Stern-Volmer plot] is shown in Fig. 4.9 and the plot is linear upto $[H^+] = 0.1M$. A

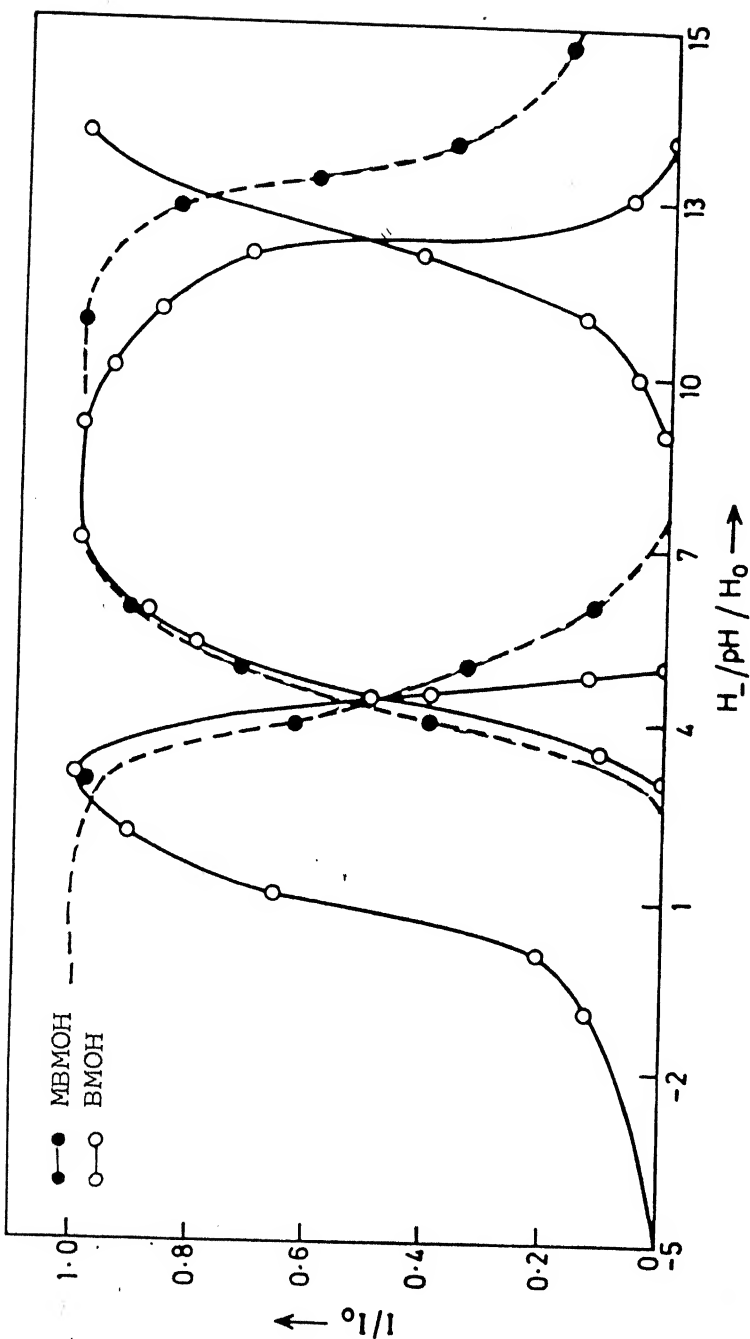


Fig. 4.7 Plot of I/I_0 as a function of $H_0/pH/H_0$ of 2-(hydroxymethyl)-2-(hydroxymethyl)benzimidazoles (BMOH) and N-methyl-2-(hydroxymethyl)benzimidazoles (MBMOH).

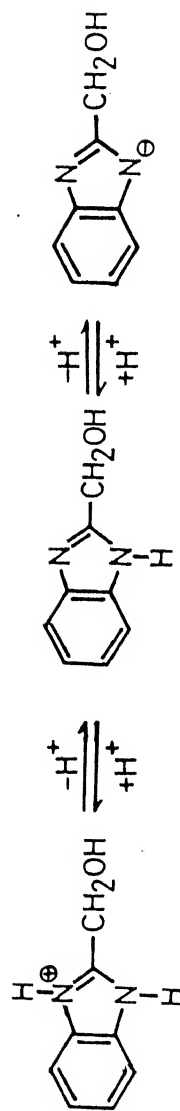


Fig. 4.8 Scheme of ground and excited singlet state equilibria of 2-(hydroxymethyl)benzimidazole (BMOH) at different $H_0/pH/H_0$.

Table 4.5. pK_a and pK_a^* of various prototropic reactions of 2-(hydroxymethyl)-(BMOH) and N-methyl-2-(hydroxymethyl)benzimidazoles (MBMOH) at 298°K

Equilibrium	pK_a	pK_a^*		
		Abs. ^a	Flu. ^a	FT ^b
<u>Reaction of BMOH</u>				
Monocation \rightleftharpoons Neutral	4.2	3.6	—	4.4
Neutral \rightleftharpoons Monoanion	12.7	10.7	8.9	12.2
<u>Reaction of MBMOH</u>				
Monocation \rightleftharpoons Neutral	4.4	2.5	—	4.3
Neutral \rightleftharpoons Monoanion	16	—	—	13.5

^aForster cycle method.

^bFluorimetric titration method.

value of $k_q\tau = 3.9 \text{ dm}^3 \text{ mol}^{-1}$ is obtained from the slope, where k_q is the proton induced quenching constant and τ is the molecular lifetime of monocation. The radiative lifetime (τ_{FM}) of the monocation is calculated using Strickler-Berg equation.¹⁷⁵ The molecular lifetime, obtained from the relation $\tau = \tau_{FM}\phi$, where ϕ is the fluorescence quantum yield, is found to be 2.2 ns. Hence $k_q = 1.7 \times 10^9 \text{ dm}^3 \text{ mol}^{-1} \text{ sec}^{-1}$. The value is of the same order of magnitude as observed in other cases.¹²⁵ The departure from linearity in the Stern-Volmer plot could be due to the non-ideal behaviour of the solution after $[H^+] = 0.1M$.

Following conclusions can be drawn from the above study.

(i) The first deprotonation reaction in BMOH takes place from the imino group rather than from the -OH group, as reported in the literature.¹⁷⁶ (ii) The molecule BMOH behaves like 2-methylbenzimidazole where the hydrogen atom of methyl group is replaced by the -OH group in one sense and like a methanol where one of the hydrogen atom of methyl group is replaced by the benzimidazole moiety. The BMOH does not behave like 2-hydroxybenzimidazole, which is reflected from the pK_a and pK_a^* values of the various prototropic reactions. (iii) The presence of methylene group between BI moiety and the -OH group stops their direct interaction.

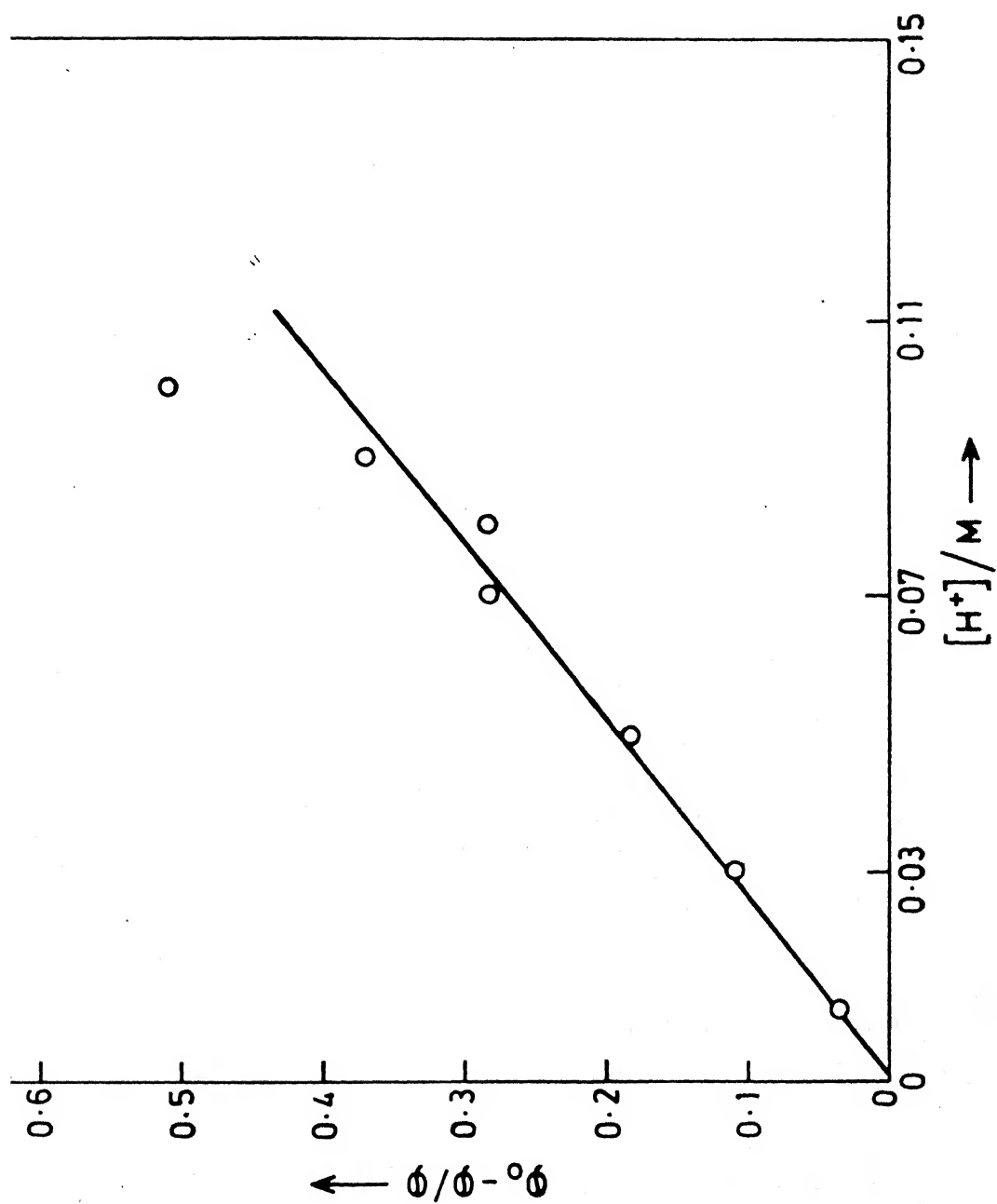


Fig.4.9 Plot of $I_0 - I / I_0$ versus $[H^+]$ at 298°K.

4.3 2-(Chloromethyl)- (CMBI), 2-(dichloromethyl)- (DMBI),
5-chloro-2-(trichloromethyl)- (TMBI), 2-(trifluoro-
methyl)- (FMBI), 2-(cyanomethyl)- (CNBI) and
2-chlorobenzimidazole (2CBI) *

Figures 4.10 and 4.11 depict the absorption and fluorescence spectra of all the BI's studied in this section. All the spectral data are summarized in Table 4.6. It is clear from Table 4.6 that the long wavelength absorption band of all the BI's are slightly blue shifted in acidic medium ($\text{pH} \leq 4$, depending on the BI's). The ~ 244 nm band under the same conditions is either merged with the long wavelength band (CMBI and FMBI) or is slightly blue shifted (DMBI, CNBI and 2CBI). The same band is slightly red shifted in TMBI. The species present under these conditions is the monocation of the respective BI, formed by the protonation of tertiary nitrogen atom. The blue shift in the long wavelength absorption band can be explained on the basis of the effect of proton donor solvents, as has been done in section 3.1, because the protonation is the extreme case of hydrogen bonding interaction. No further change is observed in the absorption spectra even upto H_0-10 , indicating that no dication or any other species is formed in the S_0 state.

* H.K. Sinha and S.K. Dogra, J. Chem. Soc. Perkin Trans. 2, in press.

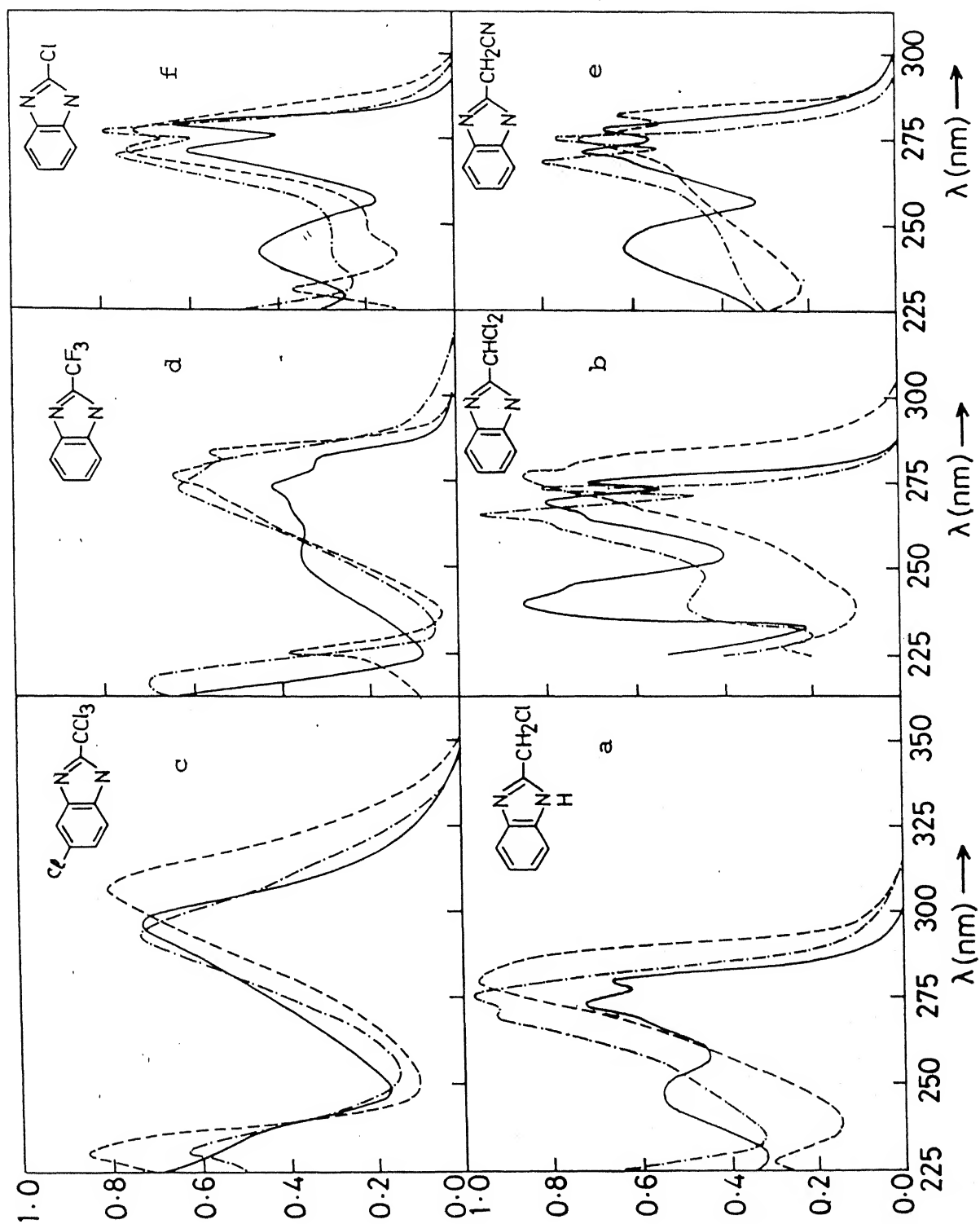


Fig.4.10 Absorption spectra of various prototropic species of (a) CMBI, (b) DMBI, (c) TMBI, (d) FMBI, (e) CNBI and (f) 2CBI at 298°K.

--- Monoanion, — Neutral, -.- Monocation

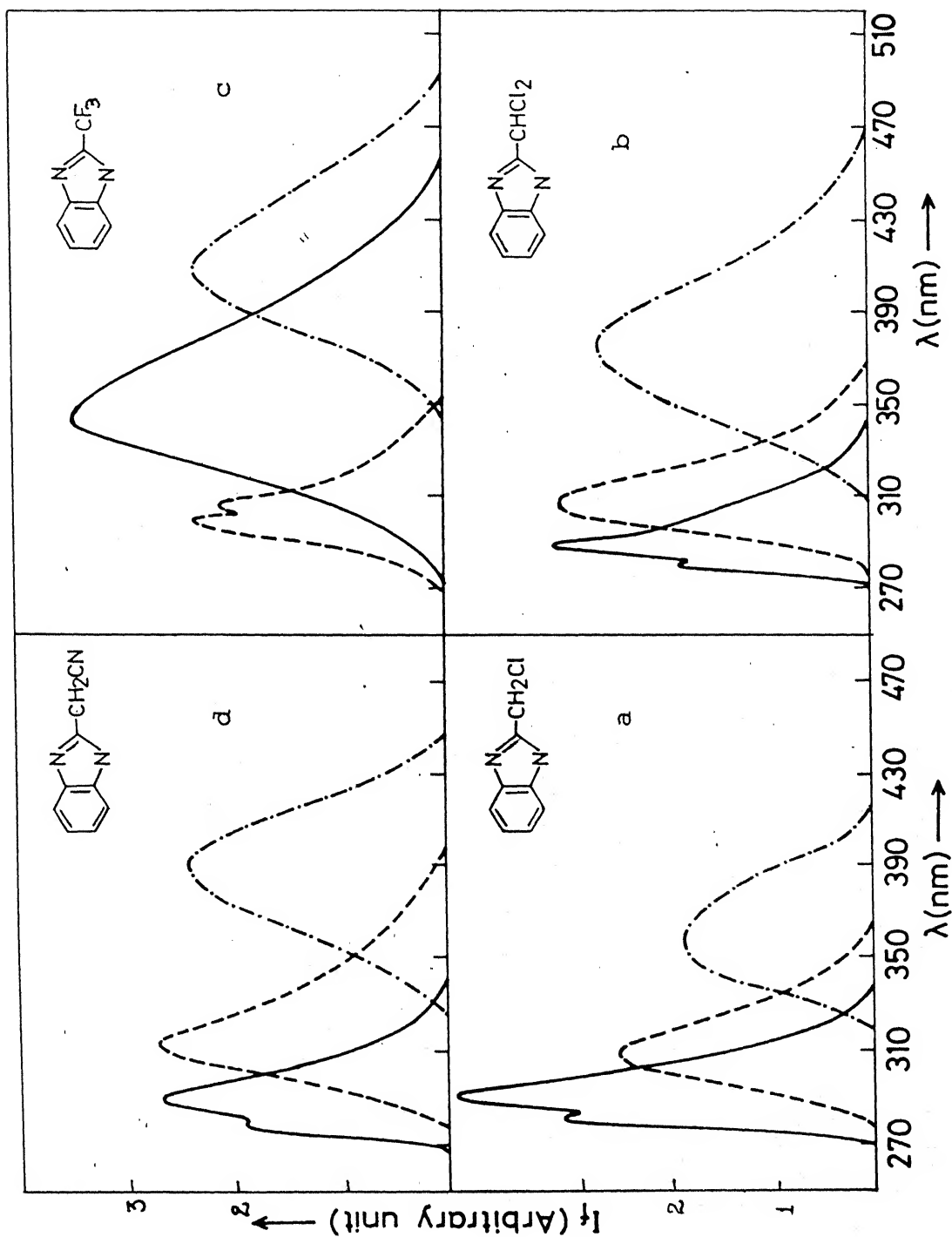


Fig.4.11 Fluorescence spectra of various prototropic species of (a) CMBI, (b) DMBI, (c) FMBI and (e) CNBI at 298°K.

--- Monocation, — Neutral, -.- Monocation

Table 4.6. Absorption maxima [λ_a (nm)], $\log(\epsilon_{\max})$ and fluorescence maxima [λ_f (nm)] of different prototropic species of 2-(chloromethyl)-(CMBI), 2-(dichloromethyl)-(DMBI), 5-chloro-2-(trichloromethyl)-(TMBI), 2-(trifluoromethyl)-(FMBI), 2-(cyanomethyl)-(CNBI) and 2-chlorobenzimidazole (2CBI) at 298°K

Compound	Neutral		Monocation		Monoanion	
	λ_a (nm) $\log(\epsilon_{\max})$	λ_f (nm)	λ_a (nm) $\log(\epsilon_{\max})$	λ_f (nm)	λ_a (nm) $\log(\epsilon_{\max})$	λ_f (nm)
CMBI	277	304	275(3.95)	358	286(3.93)	308
	271	293	270(3.87)		280(4.00)	
	244	283	—		—	
	203		220(4.31)		227(3.54)	
DMBI	278(3.81)	297	274(3.98)	375	281(3.68)	308
	271(3.84)	289	267(4.00)		277(3.73)	
	265(3.74)	280	261(3.88)		225(3.12)	
	249(3.83)		240(3.78)			
	244(3.86)		203(3.91)			
TMBI	205(4.21)					
	292	354	300(3.65)	—	306(3.78)	—
	230		235(3.54)		220(3.88)	
FMBI	198		—		—	
	281(3.50)	340	280(3.70)	410	284(3.75)	310
	274(3.62)		273(3.78)		277(3.82)	
	268(3.58)		216(3.60)		225(3.59)	
	255(3.54)					
2CBI	279(3.81)	304	277(3.90)	—	284(3.83)	—
	272(3.79)		270(3.89)		278(3.84)	
	263(3.71)		241(3.47)		258(3.59)	
	245(3.65)				249(3.59)	
CNBI	278(3.86)	290	275(3.92)	390	281(3.86)	313
	271(3.86)	278	269(3.93)		275(3.84)	
	243(3.78)		239(3.62)		219(3.75)	

The absorption spectrum is red shifted at $\text{pH} \geq 10$, depends on the particular BI. The absorption spectrum in each case is assigned to monoanion, formed by deprotonation of the imino group. The spectral changes observed are consistent with the deprotonation reaction of the imino group of BI. But in the basic solution TMBI behaves quite differently, which will be discussed at the end of this section.

Fluorescence spectra of all the BI's are largely red shifted in the acidic medium ($\text{pH} \leq 3$ depending on particular BI), with the exception of 2CBI and TMBI, which are non-fluorescent. The species formed is a monocation in the excited state, similar to that formed in the ground state prototropic reaction. The unusual red shift is due to the stabilization of charge transfer state in polar solvents. Thus unlike neutral BI's where lowest energy excited state is a $\pi\pi^*$ state, with the exception of TMBI and FMBI, the lowest energy excited state in the monocations of BI's is the CT state. Further, unlike methyl substituted benzimidazoles¹²⁵, no other fluorescence band of monocation of BI's, blue shifted as compared to the neutral ones, are observed. This suggests that either fluorescence quantum yield of the $\pi \leftarrow \pi$ transition of these cations are very low or CT state is the only pathway for deactivation of the monocations from the manifold of excited states.

On the other hand, the red shift observed in the fluorescence spectrum of monoanions is very small, with the exception that monoanion of 2CBI is non-fluorescent and a blue shift is noticed in case of FMBI. The fluorescence maxima in all these cases closely match with those observed in all other BI's studied. Thus the emitting state in case of monoanions is of $\pi\pi^*$ character.

As mentioned in section 3.1, the lowest excited singlet state of TMBI and FMBI is of CT character and the assignment is based on the effect of solvents of various polarities on the fluorescence spectra. This has been explained on the basis that the presence of the strong electron-withdrawing group in the imidazole ring at 2-position acts as a driving force for the charge migration from benzene to imidazole ring. The possible reason for the fluorescing state to be of $\pi\pi^*$ character in case of monoanion of all the BI's is the presence of negative charge on the imino group of the imidazole ring. This will inhibit the charge migration from benzene to imidazole ring. The blue shift observed in case of FMBI is consistent with the above explanation, because the negative charge present on the imino group of imidazole ring, is absent in the neutral molecule. This is further confirmed from the results of FMBI in cyclohexane containing 1% piperidine (v/v), where 310 nm fluorescence band is

observed due to the formation of monoanion. Here the proton attached to the imino group of the imidazole ring has been extracted by piperidine as the pK_a value for the protonation of piperidine is more than the pK_a value for the deprotonation reaction of FMBI, (see later in this section).. The behaviour of TMBI in similar basic condition either in aqueous media or non-polar media containing piperidine is quite different and this is discussed in the following paragraph.

The absorption spectrum of TMBI is red shifted on increasing the pH upto 13, indicating the formation of monoanion, by deprotonation of $>NH$ group, as this is generally observed in all BI's. But further increase of basic strength of the solution results in a blue shift in the absorption spectrum (from 310 nm to 300 nm). This blue shifted absorption spectrum matches with the dianion, obtained by deprotonating the $-COOH$ and $>NH$ groups of 5-chlorobenzimidazole-2-carboxylic acid (see section 4.7). On the other hand the intensity of fluorescence spectrum (350 nm) of the neutral TMBI under these condition remains constant upto pH 12 and a sudden enhancement is observed at pH 13, without appearance of any other new fluorescence band. The intensity of this fluorescence band increases very slowly after H₁₄. This behaviour also resembles to that observed in case of above mentioned acid in the basic conditions. All these reactions are irreversible in the sense that on slow acidification the absorption

and fluorescence spectra of various species obtained do not agree with those of TMBI but agree nicely with those of the acid. This clearly suggests that at high pH, hydrolysis of TMBI occurs to give respective 2-substituted carboxylic acid, as reported in the literature.¹⁴⁴ The absorption and fluorescence spectra of TMBI in cyclohexane containing piperidine were recorded. Unlike FMBI, this reaction seems to be more complicated than the simple removal of proton from $>NH$ group to form monoanion. This could be due to the reaction of $-CCl_3$ group with the base, where the chlorine atoms can be replaced by a base if present in excess.¹⁷⁷

pK_a values: The pK_a values for the monocation-neutral and neutral-monoanion for all the BI's are calculated spectrophotometrically and are listed in Table 4.7. The pK_a values for the protonation and deprotonation reactions of parent BI are 5.48 and 13.25 respectively. Further it has been seen that the presence of electron donating group in the parent molecule increases the pK_a and the presence of electron-withdrawing group decreases the pK_a of the respective equilibrium. Here as all the groups are of electron-withdrawing in nature, the results are consistent with the above observations i.e. pK_a values are lower than that observed in case of parent BI.

Comparison of the pK_a values of the monocation-neutral and neutral-monoanion equilibria of 2CBI and CMBI indicate that

the pK_a values of the former are lower than those observed in the latter compound. This again reflects that the presence of methylene group in between benzimidazolyl and chloro group inhibits their direct interactions. This also indicates that the inductive effect of chloro group is more predominant than the resonance effect. Further, cyano group is a better electron-withdrawing group than the chloro, but it can be visualized by comparing the results of CMBI and CNBI that the presence of methylene group has really decreased their direct interactions, whereas in 2CBI, chlorine atom is directly attached to the ring and can interact more effectively.

pK_a^* values for both the equilibria have been calculated with the help of fluorimetric titration (Fig. 4.12, 4.13 and 4.14) and Förster cycle method using absorption and fluorescence data wherever applicable. For example, the latter method can not be applied to calculate the pK_a^* of monocation-neutral equilibrium in all the cases except FMBI, because $\pi \leftarrow \pi^*$ is the nature of transition in the neutral molecule, whereas CT is the lowest energy transition in case of monocations. Similarly the latter method can not be used to calculate the pK_a^* of the neutral-monoanion equilibrium of FMBI. But wherever this method is applicable the trend observed in pK_a^* is consistent with the behaviour of all the BI's studied. The results obtained from fluorimetric titration are agreeing with the earlier findings that either ground state

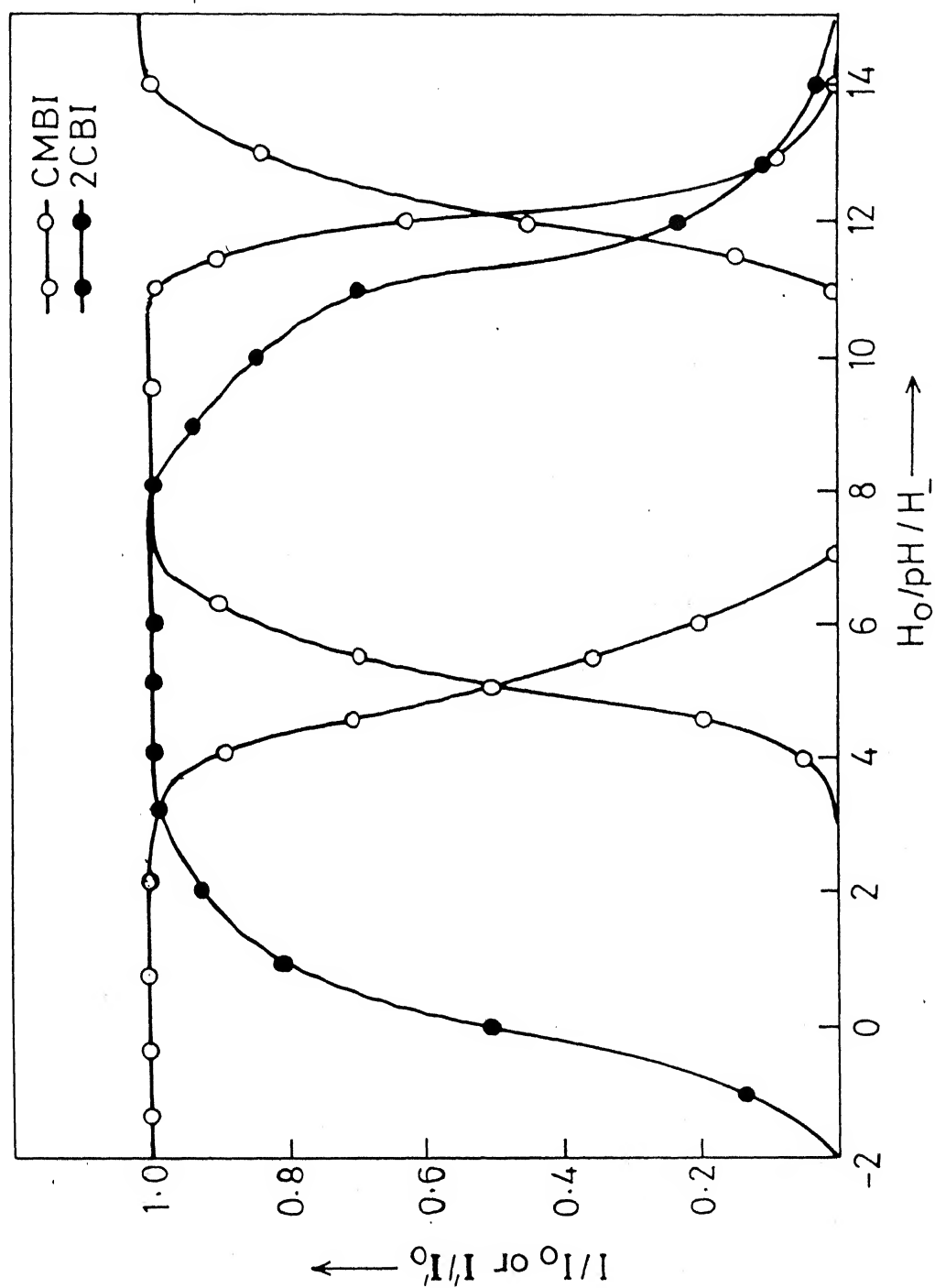


Fig.4.12 Plot of I/I_0 as a function of $H_0/pH/H^-$ of 2-(chloromethyl)- (CMBI) and 2-Chlorobenzimidazoles (2CBI).

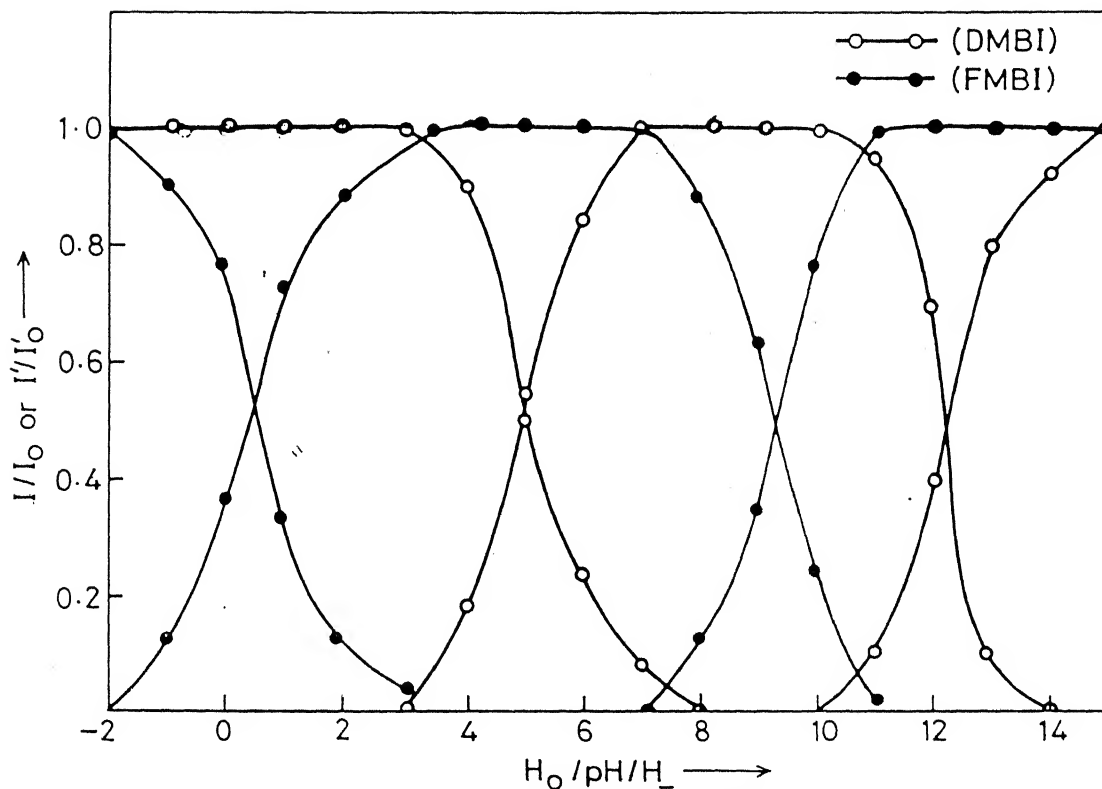


Fig.4.13 Plot of I/I_0 as a function of $H_0/pH/H_-$ of 2-(dichloromethyl)- (DMBI) and 2-(trifluoromethyl)benzimidazoles (FMBI).

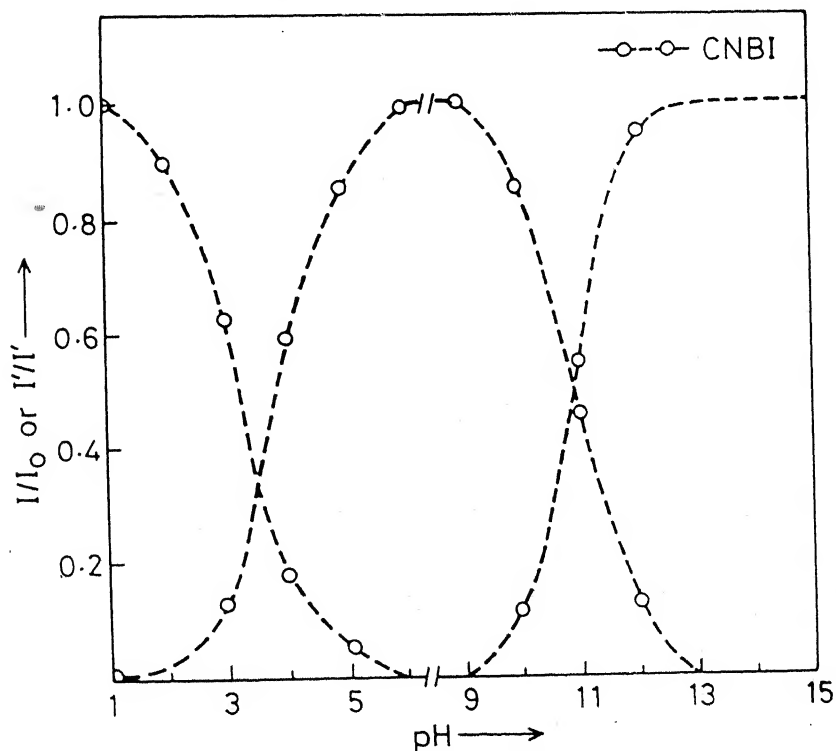


Fig.4.14 Plot of I/I_0 as a function of $H_0/pH/H_-$ of 2-(cyanomethyl)benzimidazole (CNBI).

Table 4.7. pK_a and pK_a^* of various prototropic reactions of 2-(chloromethyl)-(CMBI), 2-(dichloromethyl)-(DMBI), 5-chloro-2-(trichloromethyl)-(TMBI), 2-(trifluoromethyl)-(FMBI), 2-(cyanomethyl)-(CNBI) and 2-chlorobenzimidazoles at 298°K

Compound	pK _a	pK _a [*]		
		Abs. ^a	Flu. ^a	FT ^b
Monocation \rightleftharpoons Neutral				
CMBI	4.0	3.4	—	5.0
DMBI	4.1	3.0	—	5.0
TMBI	0.3	2.2	—	—
FMBI	0.6	0.3	—	0.4
CNBI	3.5	2.7	—	3.5
2CBI	2.1	1.6	—	0.0
Neutral \rightleftharpoons Monoanion				
CMBI	12.7	10.3	11.8	12.2
DMBI	12.9	12.1	10.4	12.2
TMBI	10.3	7.0	—	—
FMBI	10.1	9.3	—	9.3
CNBI	12.0	11.2	6.7	11.0
2CBI	9.4	8.1	—	11.3

^aFörster cycle method.

^bFluorimetric titration method.

pK_a values are observed from fluorimetric titration because of the short lifetimes of the conjugate acid-base pair or the tertiary nitrogen atom becomes stronger base and imino group becomes stronger acid upon excitation. The pK_a values for the neutral-monoanion equilibrium of TMBI can not be calculated from fluorimetric titration because of the reasons mentioned earlier.

In case of 2CBI the pK_a^* values for these equilibria are different from the rest of the BI's mentioned in this section i.e. tertiary nitrogen atom becomes less basic and $>NH$ group becomes more basic upon excitation, an exactly opposite trend. Since monocation and monoanion of 2CBI are non-fluorescent, nothing can be inferred conclusively but it seems that (i) At low pH conditions, the inductive effect of chloro group is more predominant and thereby reducing the charge density at the tertiary nitrogen atom and (ii) at high pH condition, the resonance effect of chloro group is more predominant and thereby increasing the charge density at the imino group. Similar kind of behaviour of chloro and bromo groups have been observed in other cases also.¹⁷⁸

Conclusion: The substitution of strong electron-withdrawing group at 2 position of the imidazole ring has been found to enhance the charge transfer character of the emitting state.

Insertion of a methylene group in between two functional groups reduces their direct interaction drastically.

4.4 2-(2'-Hydroxyphenyl)-(OHBI) and 2-(2'-Methoxyphenyl)-benzimidazoles (OMBI)*

The absorption spectra of various prototropic species of OHBI and OMBI were recorded in different hydrogen ion concentrations and the relevant data are summarized in Tables 4.8 and 4.9 respectively. The absorption spectra of the various prototropic species of OHBI and OMBI are given in Figures 4.15 and 4.16 respectively.

At the highest $H_0(-10)$ value the species present in the ground state are the dications of OHBI and OMBI formed by the protonation of tertiary nitrogen atom and the ring carbon atom. This conclusion is drawn from the absorption spectral study as the red shift in the absorption spectrum of the monocation is observed when the dication is formed on further protonation. This is consistent with the results obtained by others for similar protonation reaction of aromatic hydrocarbons.³⁸ Had the protonation occurred at the hydroxy or methoxy group, there would have

* H.K. Sinha and S.K. Dogra, Chem. Phys., 102, 337-347 (1986).

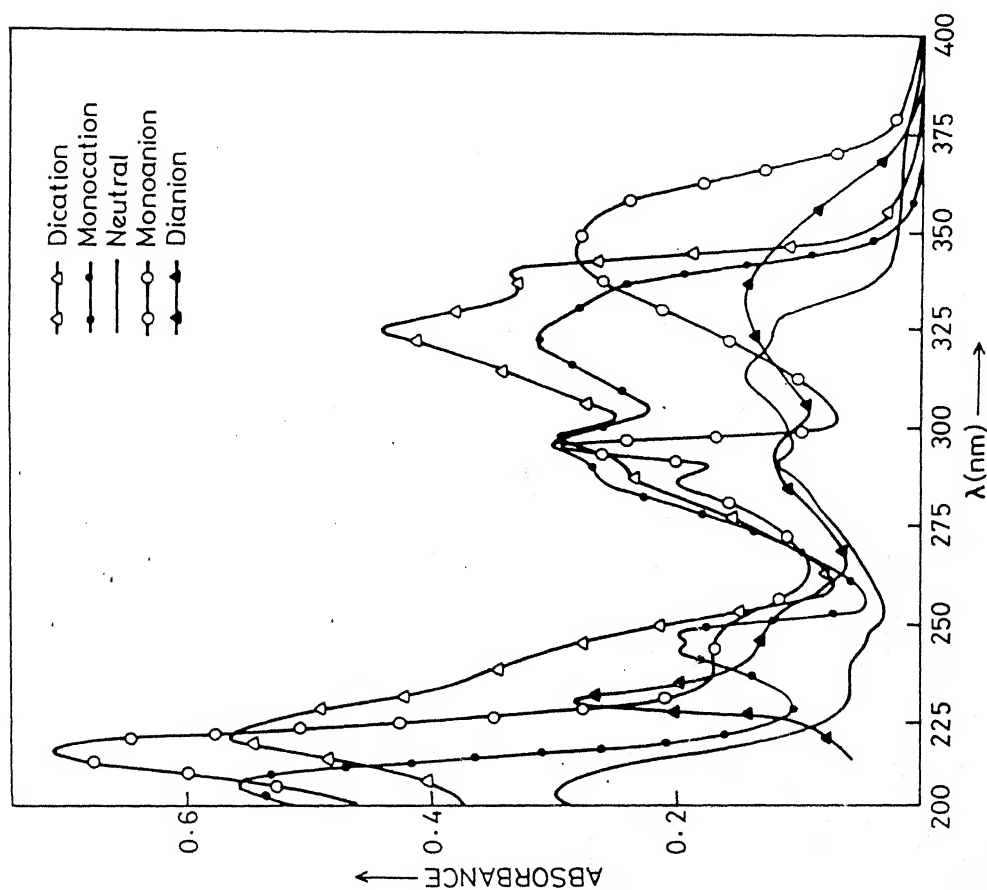


Fig.4.15 Absorption spectra of various prototropic species of 2-(2'-hydroxyphenyl)benzimidazole (OHBI) at 298°K.

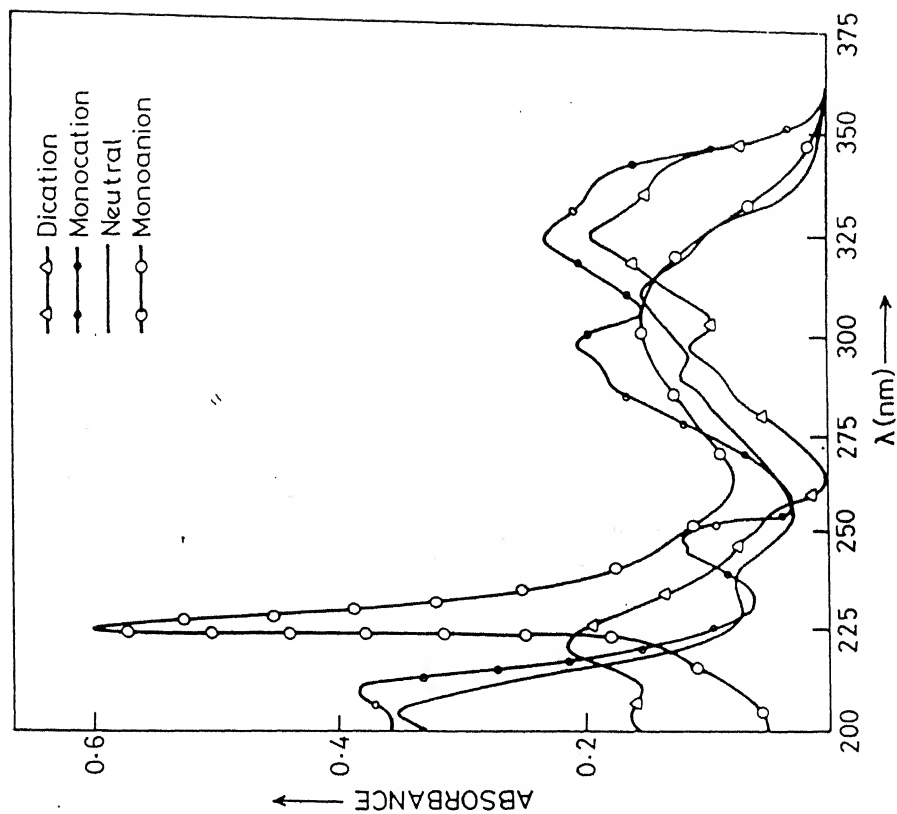
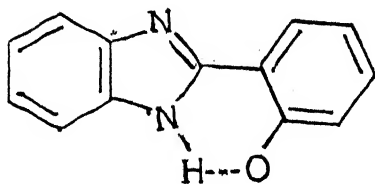


Fig.4.16 Absorption spectra of various prototropic species of 2-(2'-methoxyphenyl)benzimidazole at 298°K.

been a blue shift in the absorption spectra of the monocation, as noticed in other similar compounds.¹²⁷ The blue shift observed in all the absorption bands, with the decrease of hydrogen ion concentration (H_0 -5 to pH 3) suggests the formation of monocations, formed by the protonation of tertiary nitrogen atom. In the pH range 5-8, the species present are neutral. A red shift in the band maxima of OHBI indicates that the monoanion is formed, in the pH/ H_- range 9 to 15, by the deprotonation of hydroxyl group. The deprotonation of aromatic hydroxyl group generally falls in this pK_a range. The large red shift (22 nm) in the long wavelength absorption band of OHBI and unchanged absorption spectrum until H_-15 , does suggest that some other process is taking place besides this deprotonation of phenolic group. The pK_a for the deprotonation of $>NH$ group of benzimidazole is 13.25, which is not observed in the above case. Only at H_-16 , a large blue shift is observed, suggesting that the dianion is formed by deprotonating the $>NH$ group. But the spectral shift observed in the last step is opposite to what is normally observed in the deprotonation of an imino groups.^{97,148,179-180} A similar kind of observation is also found in the deprotonation reaction of the $>NH$ group of OMBI, but the monoanion is formed at a lower pH (~ 13). The pK_a value for the deprotonation reaction of imino group of OMBI (13.3) is

consistent with the similar reaction of other benzimidazoles. But the blue shift observed in the absorption spectrum could be due to the loss of coplanarity of the phenyl ring. The broad absorption spectrum without any vibrational structure also indicates this."

The large red shift observed in the absorption spectrum of neutral species of OHBI due to the formation of monoanion, could be due to the formation of a rigid structure as depicted below. The driving force behind this structure is the formation o



intramolecular hydrogen bond between the phenolate ion and the imino proton, leading to the formation of a six membered ring structure. Further support to the existence of this structure can be obtained from the following arguments: (i) The pK_a value of $>NH$ deprotonation reaction is >16 , higher than the pK_a value for similar reaction in OMBI and BI's. (ii) The blue shift observed in the absorption maximum of dianion also agrees to the above description that the imino proton is tightly bound to the phenolate ion and its deprotonation will lead to loss of intramolecular hydrogen bonding as well as co-planarity of the phenyl group as noticed in case of OMBI.

The fluorescence spectra of various prototropic forms of OHBI and OMBI are shown in figures 4.17 and 4.18 respectively. The relevant spectral data are summarized in Tables 4.8 and 4.9. The fluorescence spectral data clearly indicate that the prototropic species of OMBI formed in the excited singlet state are same as those in the ground state, with the exception at highest H_0 value, where the blue shift observed in the fluorescence spectrum at H_0-10 is due to the dication formed by the protonation of tertiary nitrogen atom and methoxy group. Similar results have also been observed in case of 2-hydroxy- and 2-methoxy-carbazole¹⁸¹ and 2-hydroxybenzimidazole.¹²⁷ At low hydrogen ion concentration, the red shift observed in the fluorescence spectrum is due to the monocation of OMBI, protonated at the tertiary nitrogen atom. The blue shift followed by a red shift in the fluorescence spectrum in the pH range 3 to 14, indicate the formation of neutral species first and then the monoanion, formed by deprotonation of $>NH$ group. The above results are consistent with earlier findings that the red shift is observed in fluorescence spectra when protonation takes place at the tertiary nitrogen atom or when the deprotonation of the imino group occurs if $\pi \leftarrow \pi^*$ is the lowest energy transition. Unlike the absorption spectral shift, the red shift observed in the fluorescence spectrum of monoanion on its formation from neutral species shows that the molecule acquires planarity in the excited singlet state.

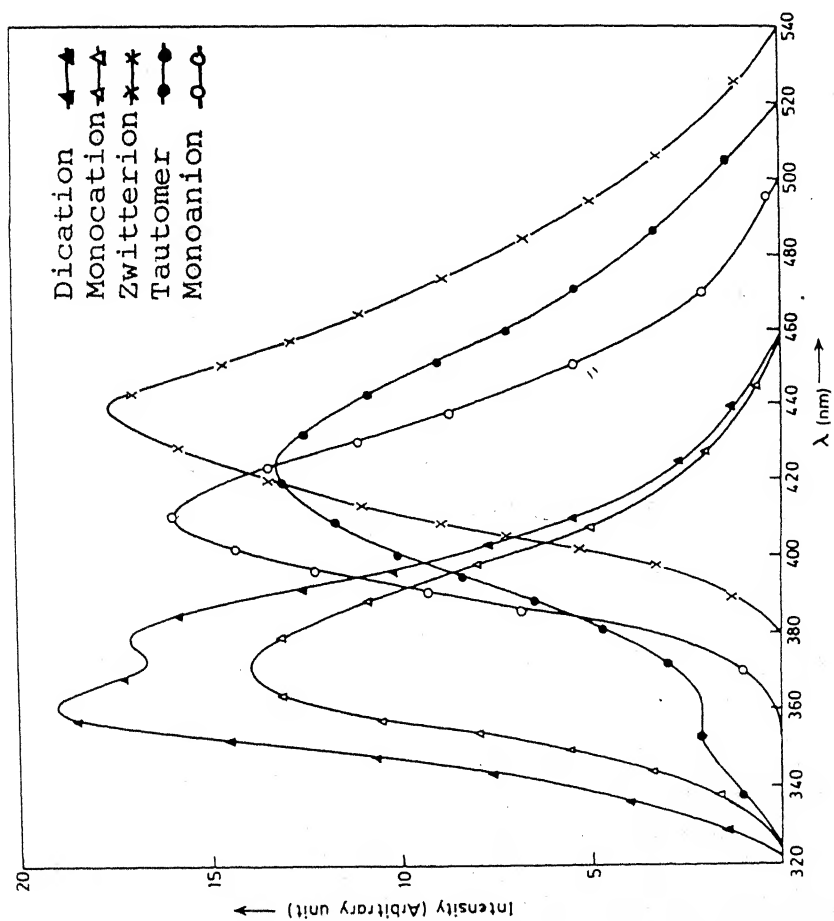


Fig.4.17 Fluorescence spectra of various prototropic species of 2-(2'-hydroxyphenyl)-benzimidazole (OHBI) at 298°K.

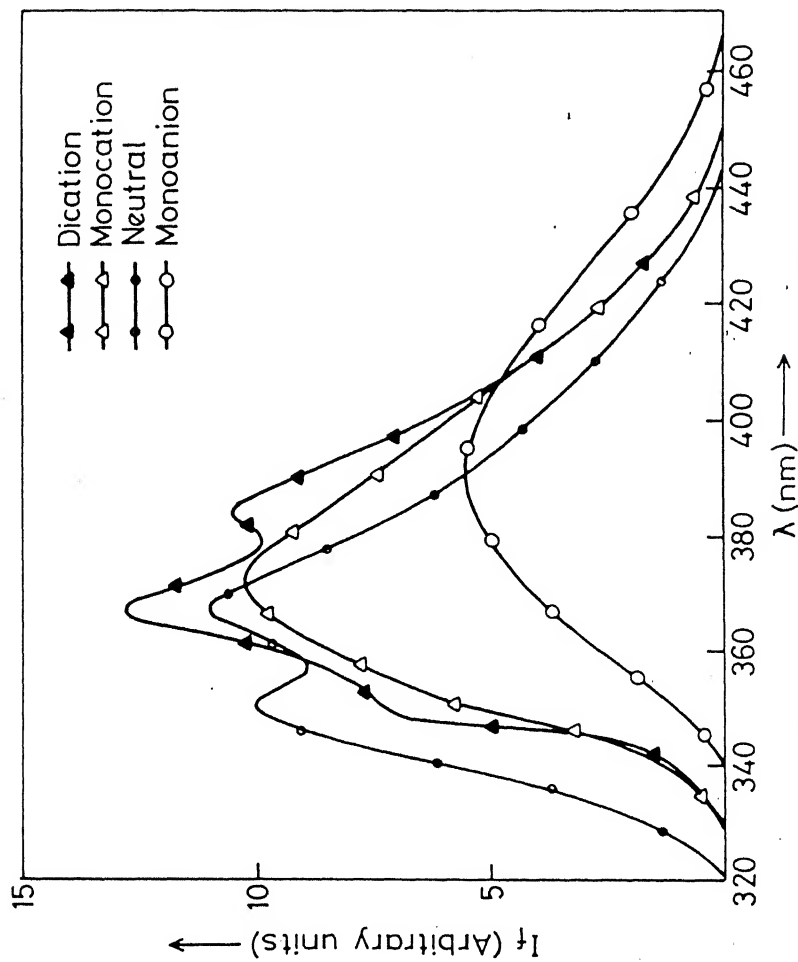


Fig.4.18 Fluorescence spectra of various prototropic species of 2-(2'-methoxyphenyl)-benzimidazole (OMBI) at 298°K.

Table 4.8. Absorption maxima [λ_a (nm)], $\log(\epsilon_{\max})$ and fluorescence maxima [λ_f (nm)] of different prototropic species of 2-(2'-hydroxyphenyl)benzimidazole (OHBI) at 298°K.

Species/ $H_0/pH/H_-$	λ_a (nm) $\log(\epsilon_{\max})$					λ_f (nm)	
Dication (H_0-10)	220 (4.46)	288 (4.06)	295 (4.18)	324 (4.34)	337 (4.22)	344	360 376
Monocation (H_0-5)	207.5 (4.45)	247 (3.95)	285 (4.12)	295 (4.17)	320 (4.19)	330 (4.04)	386
Zwitterion* (pH 4)	-	-	-	-	-	-	440
Neutral (pH 7)	241.5	248.5	-	290	312.5	325	350 430 ^a
Monoanion (pH 12)	221 (4.55)	244 (3.93)	285 (4.00)	295 (4.19)	347.5 (4.17)	-	410
Dianion (H_-16)	231 (4.15)	250 (3.81)	-	294 (3.77)	331 (3.86)	-	-

* Zwitterion is formed only in the excited singlet state, whereas the same monocation of OHBI is present in the ground state.

^a Emission maxima of tautomeric species.

Table 4.9. Absorption maxima [λ_a (nm)], $\log(\epsilon_{\max})$ and fluorescence maxima [λ_f (nm)] of different prototropic species of 2-(2'-methoxyphenyl)benzimidazole (OMBI) at 298°K.

Species/ $H_o/pH/H_-$	λ_a (nm) $\log(\epsilon_{\max})$				λ_f (nm)		
Dication (H_o-10)	220	-	285	299	326	341.5	350 366 384
Monocation (pH 2)	207.5 (4.56)	249 (4.61)	286 (4.11)	296 (4.13)	320 (4.13)	336 (3.97)	372
Neutral (pH 7)	206 (4.56)	248 (3.89)	291.5 (4.09)	-	312.5 (4.19)	326.5 (3.99)	350 368
Monocation (H_-16)	227.5 (4.27)	-	-	-	304 (4.22)	-	394

The fluorescence results of OHBI (Table 4.8) indicate that the prototropic reactions observed in the excited singlet state are different from those in the ground state. The fluorescence band maximum and intensity of the 410 nm band (monoanion) remain constant in the pH/H₊ range 10 to 16, indicating that no dianion of OHBI is formed in the excited singlet state. This is unlike the ground state reaction of OHBI, as said earlier. This suggests that the intramolecular hydrogen bond formed between the imino proton and the phenolate ion is much stronger in the excited singlet state than in the ground state. The existence of a cyclic structure (see page 178) is further confirmed from the fact that the quantum yield of the monoanion is very large as compared to any other prototropic species of OHBI. The 410 nm band is thus assigned to the monoanion formed by the deprotonation of the hydroxyl group. In the pH range 9 to 6 the fluorescence band systems observed resemble to those observed in near neutral aqueous solution i.e. 430 nm fluorescence band is assigned to tautomer (species IV, Fig. 4.19) and 350 nm band to the open structure (species III, Fig. 4.19) formed in the excited singlet state, as said earlier in the previous chapter (page 98). The protonation at the phenolate ion without any structural reorganisation or intramolecular proton transfer would have lead to a blue shift in the fluorescence spectrum of the anion, because the protonation of the latter system i.e. phenolate,^{43,182} naphtholate³⁸ and 9-phenanthrolate¹⁷⁴ have given rise to blue shift in the

absorption and fluorescence spectra. But on increasing the acid concentration, a gradual red shift in the 430 nm band upto 440 nm, with the disappearance of normal Stokes shifted band (350 nm), is observed. This new band is assigned to the formation of zwitterion (species V, Fig. 4.19) due to the electronic reorganisation. The assignment of 440 nm band to zwitterion can be made on two grounds: (i) band maxima observed for various species are in the order of $\lambda_{\text{zwitterion}} > \lambda_{\text{anion}} > \lambda_{\text{cation}} > \lambda_{\text{neutral}}$ ⁸¹ and thus agrees with our observation and (ii) increase in the acidity and basicity of hydroxyl group and tertiary nitrogen atom in excited singlet state is such that the order of the prototropic reactions changes upon excitation with respect to the ground state. Similar observations have been observed in case of molecules containing both electron donating and electron withdrawing functional groups.^{97,183} Below H_0-4 , a large blue shift (from 410 nm to 386 nm) is observed in the fluorescence spectrum. With the above arguments in mind and the resemblance of this fluorescence spectrum with the monocation of OMBI, we conclude that this band is due to the monocation of OHBI, formed by protonating the tertiary nitrogen atom (species VI, Fig. 4.19). Lastly at H_0-10 , a blue shifted structured fluorescence band (λ_{max} 344, 360, 376 nm), similar to that observed for OMBI is noticed. This species is identified as dication (species VIII,

Fig. 4.19), formed by further, protonating the hydroxyl group of monocation. Figures 4.19 and 4.20 depict the scheme of the various prototropic reactions of OMBI and OHBI both in the ground and excited singlet states, respectively.

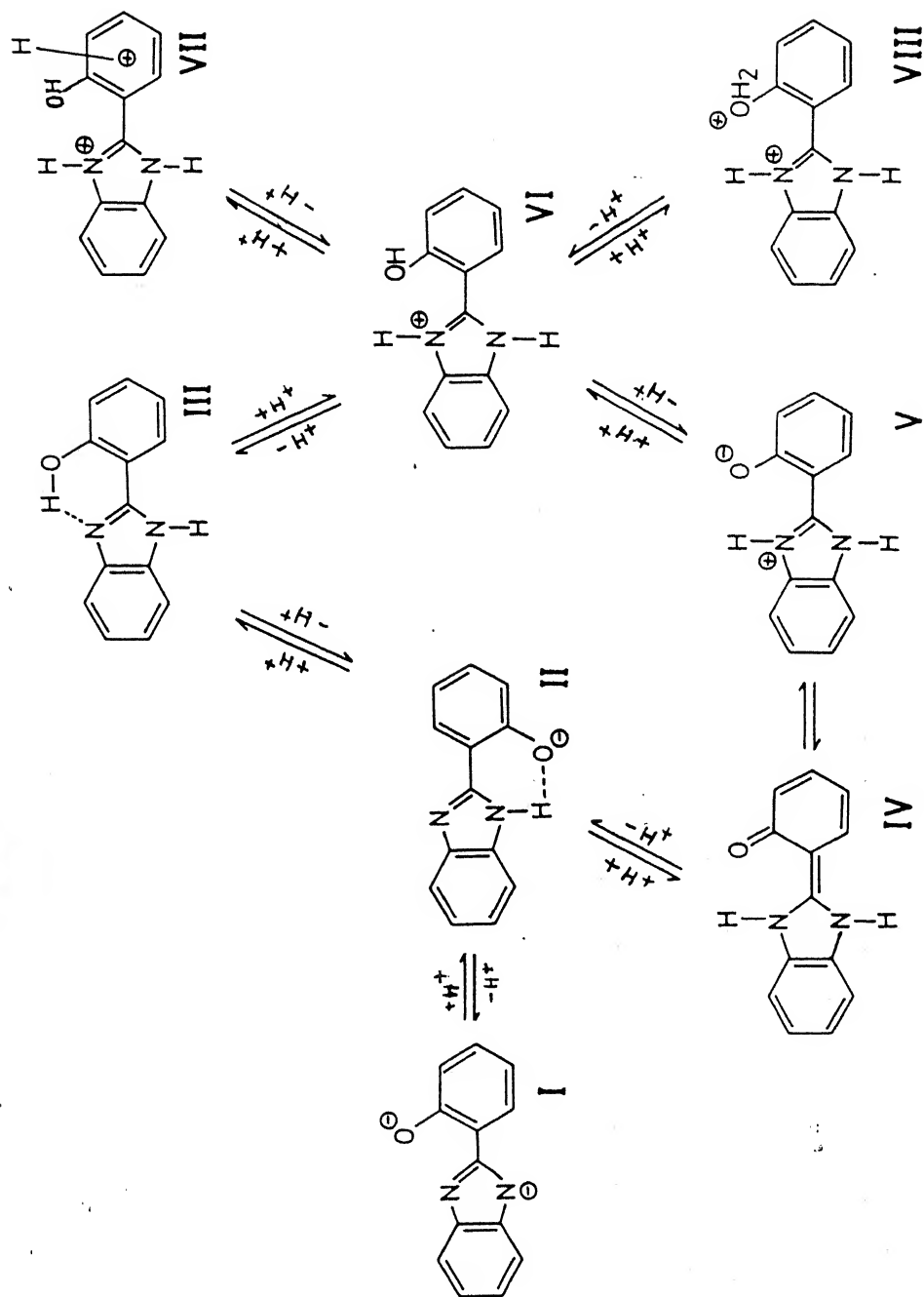
pK_a values

pK_a and pK_a^{*} values of various prototropic reaction of OHBI and OMBI were determined by absorptiometric and fluorimetric titration. The fluorimetric titration curves are shown in figure 4.21. The pK_a^{*} values for various equilibria were also determined by Förster cycle method, using absorption and fluorescence data wherever applicable. All the data are summarized in Table 4.10.

The Förster cycle method can not be used to calculate the pK_a^{*} values in case of OHBI as the various equilibria involved are different in the ground and the excited singlet states. The pK_a^{*} value for the dication-monocation equilibrium of OHBI and OMBI could not be evaluated by fluorimetric titrations as the formation of the former species are not complete even at the highest acid concentration used in this experiment. Again the Förster cycle method can not be used for this equilibrium also because the prototropic reaction involved in the ground state is different from that in the excited singlet state.

The pK_a^{*} values for the monocation-neutral and neutral-monoanion equilibria of OMBI are consistent with the earlier

GROUND STATE PROTOTROPISM



EXCITED STATE PROTOTROPISM

Fig.4.19 Scheme of ground and excited state equilibria of 2-(2'-hydroxyphenyl)benzimidazole (OHBI) at different $H_0/pH/H_-$.

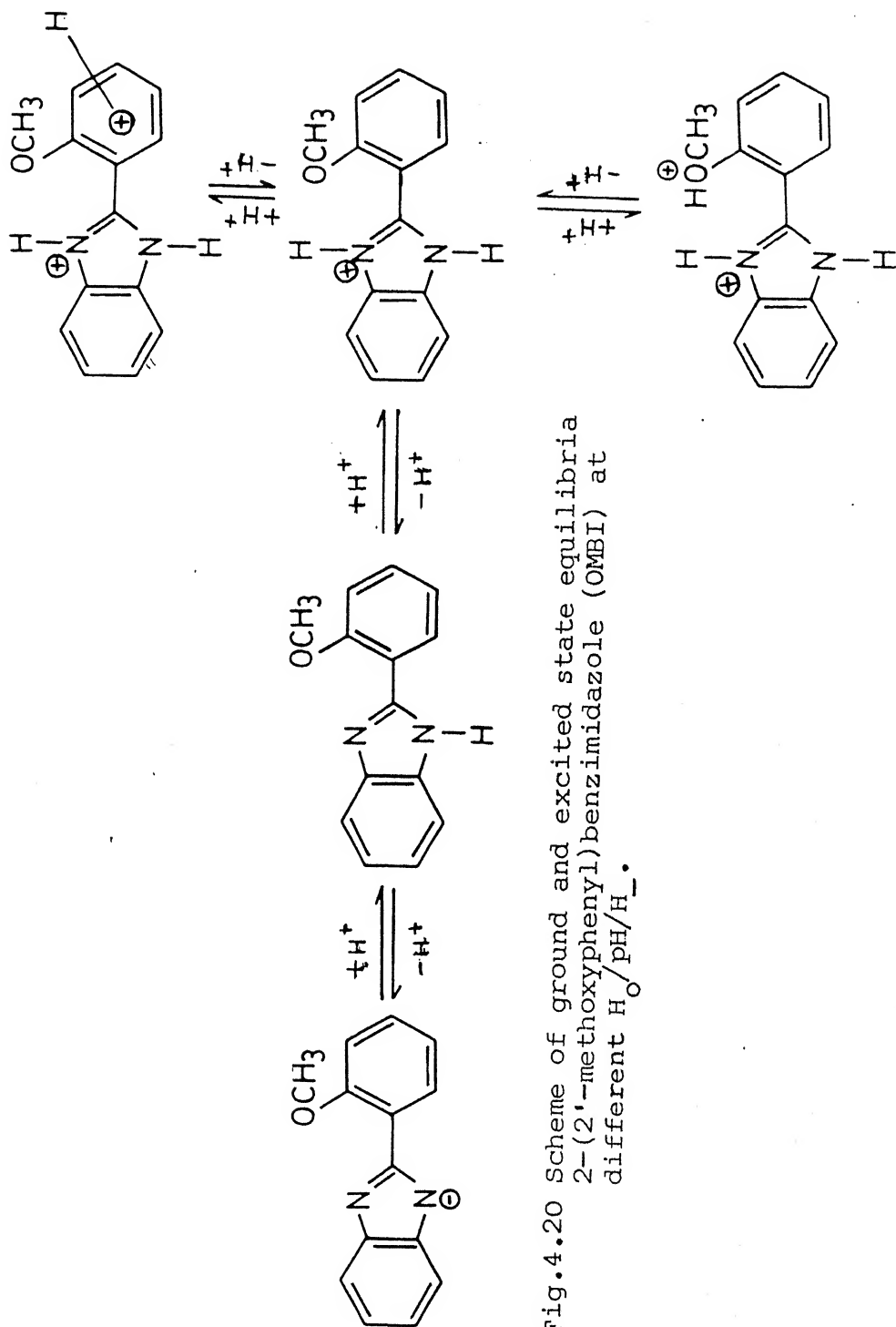


Fig.4.20 Scheme of ground and excited state equilibria 2-(2'-methoxyphenyl)benzimidazole (OMBI) at different $H_0/pH/H_-$.

findings that the fluorimetric titrations give the ground state values for the protonation and deprotonation reactions of tertiary nitrogen atom and imino group respectively. Since the pK_a^* values calculated for different prototropic reactions of OMBI, using Förster cycle method, indicate that the tertiary nitrogen atom becomes more basic and an imino group becomes more acidic upon excitation to the singlet state, it can be inferred that the radiative lifetimes of the neutral, monocation and monoanion species must be short for proton exchange to occur appreciably within the lifetimes of these species at these pH values in the excited singlet states. The small difference observed using absorption and fluorescence data could be due to the use of band maxima rather than using o-o transitions and the different solvent relaxations for the conjugate acid-base species involved in the particular equilibrium in different electronic states. The increase in the basicity of the tertiary nitrogen atom OMBI upon excitation is quite small as compared to that in pyrazoles^{38,179,180} and imidazoles.¹⁸⁴ This is because the charge migrated from the benzene ring to the imidazole ring is not only concentrated on imidazole ring but also distributed over the phenyl ring substituted at 2-position. Similar results are observed in the similar system of benzimidazoles. As the difference in the fluorescence intensities of tautomeric species

OHBI
OMBI

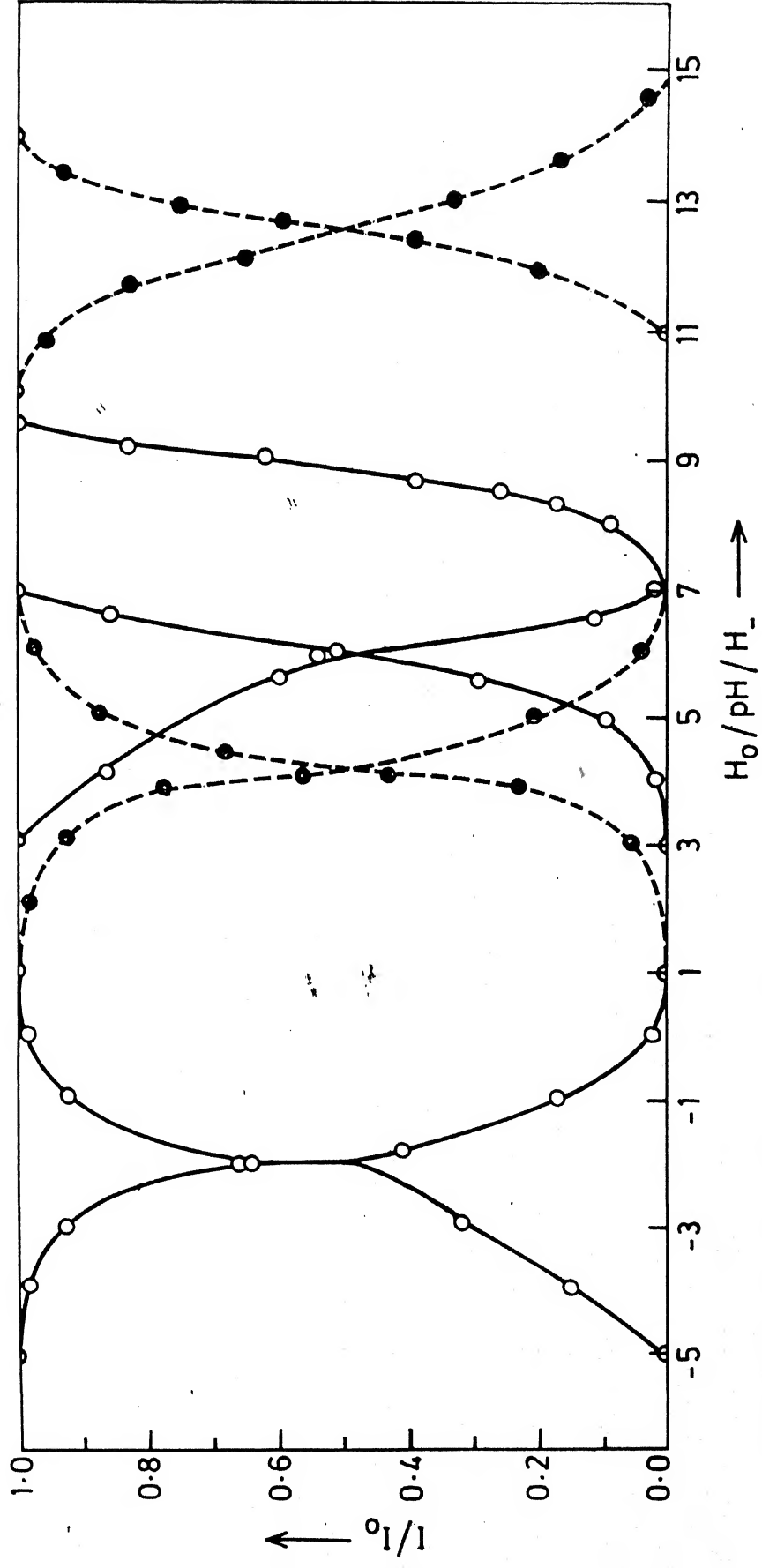


Fig.4.21 Plot of I/I_0 as a function of $H_0/pH/H_-$ of 2-(2'-hydroxyphenyl)-(OHBI) and 2-(2'-methoxyphenyl)benzimidazole (OMBI).

Table 4.10. pK_a and pK_a^* of various prototropic reactions of 2-(2'-hydroxyphenyl)-(OHBI) and 2-(2'-methoxyphenyl)benzimidazoles (OMBI) at 298°K.

Equilibrium	pK _a	pK _a [*]		
		Abs. ^a	Flu. ^a	F.T. ^b
Reactions of OHBI				
Monocation \rightleftharpoons Neutral	4.7	-	-	-
Monocation \rightleftharpoons Zwitterion	-	-	-	-2.0
Neutral \rightleftharpoons Monoanion	9.0	-	-	-
Tautomer \rightleftharpoons Monoanion	-	-	-	9.0
Monoanion \rightleftharpoons Dianion	16	-	-	16
Reactions of OMBI				
Monocation \rightleftharpoons Neutral	3.5	4.98	4.01	4.1
Neutral \rightleftharpoons Monoanion	13.3	-	9.59	12.6

^aFörster cycle method.

^bFluorimetric titration method.

and anionic species are quite large, the pK_a^* value for this equilibrium is calculated at $I/I_0 = 0.5$ for the anionic species (see Fig. 4.21)

Following conclusions can be drawn from the above study:

- (i) Intramolecular proton transfer is very fast in the excited singlet state. Competition between the intra and intermolecular proton transfer in protic solvents leads to the establishments of the equilibrium between the open (where intramolecular hydrogen bond is absent) structure and phototautomer.
- (ii) Excitation spectra recorded at two fluorescence band maxima showed that the ground state species is the same for two fluorescent species, indicating that the phototautomer is formed in the excited singlet state.
- (iii) The Stokes shift observed in the phototautomer is very large.
- (iv) Prototropic species formed in the excited states are different from those formed in the ground state i.e.
 - (i) Phototautomer and the zwitterion are formed only in the excited state
 - (ii) Dianion of OHBI is not formed in the S_1 state
 - (iii) The dication of OHBI in S_0 and S_1 states are different.

4.5 2-(4'-Hydroxyphenyl)-(PHBI) and 2-(4'-Methoxyphenyl)-benzimidazoles (PMBI)*

Figures 4.22, 4.23, 4.24 and 4.25 show the absorption and fluorescence spectral profiles of PHBI and PMBI studied in the $H_0/pH/H_-$ range of -10 to 16. The relevant data are compiled in Tables 4.11 and 4.12.

In the highly basic condition i.e. H_-16 , formation of the dianion of PHBI (312.5 nm) is indicated, this being obtained by deprotonation of the hydroxyl and imino groups. With a decrease in pH a blue shift (307.5 nm) is observed in the absorption spectrum and this reflects the formation of monoanion. The monoanion can be formed by the protonation of either imino group nitrogen atom or the phenolate ion. Since the phenolate ion is more acidic than the imino group, the proton will be added to the imino group at $pH > 11$. This is further confirmed by a pK_a values of 13.9 for this reaction calculated spectrophotometrically and it is in agreement with the value for the deprotonation reaction of the imino group of benzimidazoles. A similar pK_a value (12.10) is observed in case of its methoxy derivative, where there is no dissociable hydroxyl proton. With increase in hydrogen ion concentration a further blue shift (289 nm) is noted in the absorpti-

*H.K. Sinha and S.K. Dogra, J. Photochem., 36, 149 (1987).

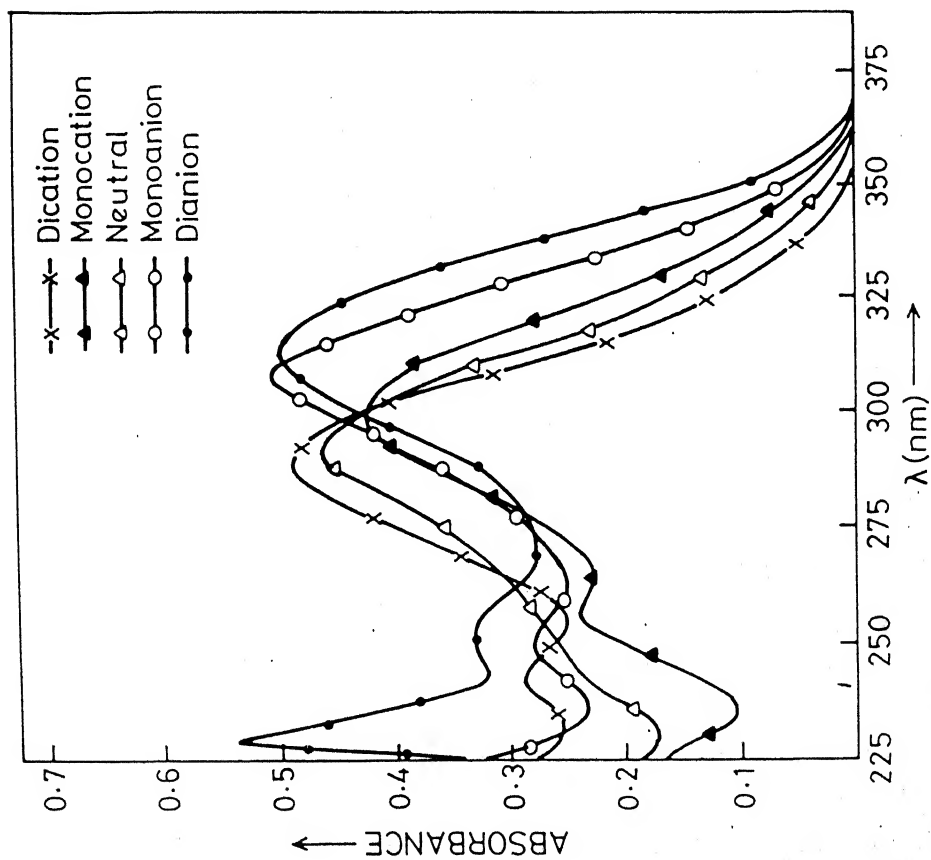


Fig.4.22 Absorption spectra of different prototropic species of 2-(4'-hydroxyphenyl)benzimidazole (PHBI) at 298°K.

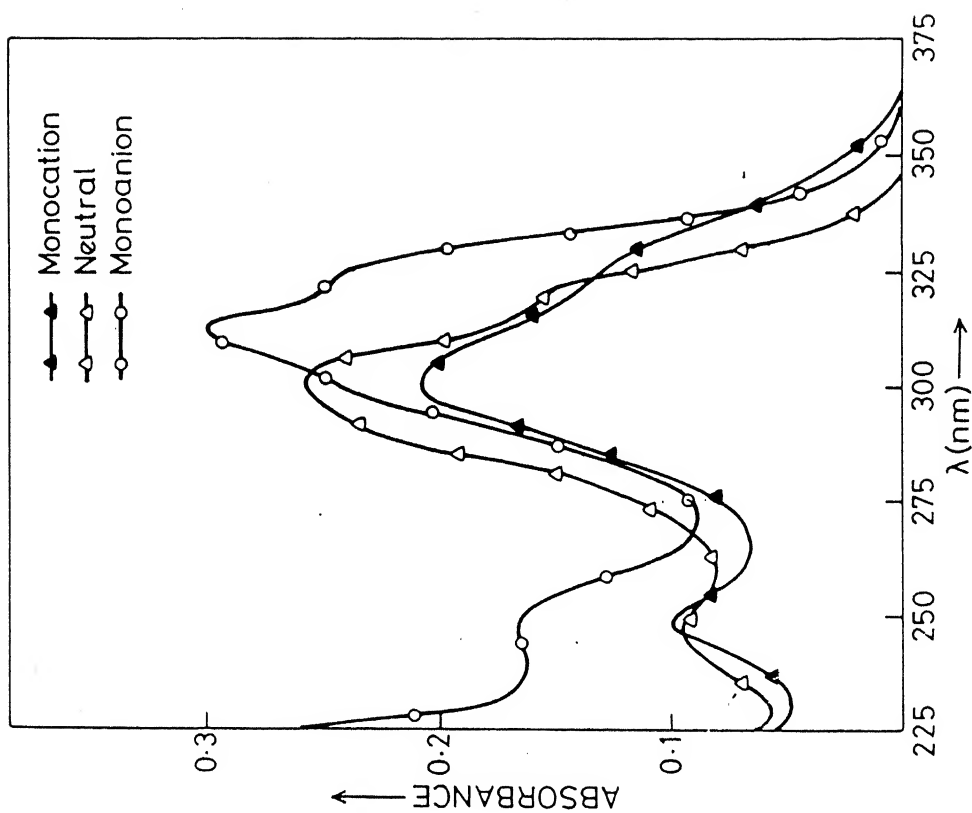


Fig.4.23 Absorption spectra of different prototropic species of 2-(4'-methoxyphenyl)benzimidazole (PMBI) at 298°K.

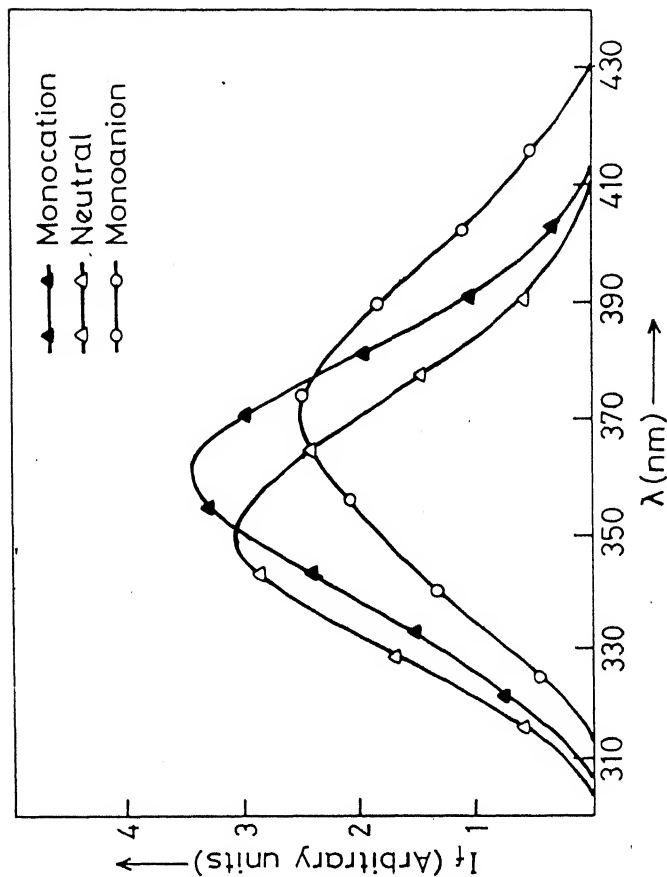


Fig.4.25 Fluorescence spectra of various prototropic species of 2-(4'-methoxyphenyl)benzimidazole.

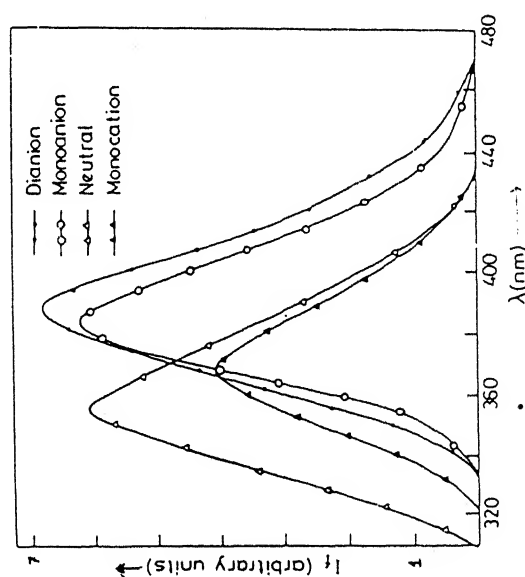


Fig.4.24 Fluorescence spectra of different prototropic species of 2-(4'-hydroxyphenyl)benzimidazole.

Table 4.11. Absorption maxima [λ_a (nm)], $\log(\epsilon_{\max})$ and fluorescence maxima [λ_f (nm)] of different prototropic species of 2-(4'-hydroxyphenyl)benzimidazole (PHBI) at 298°K.

Species/ H_O /pH/ H_-	λ_a (nm) $\log(\epsilon_{\max})$			λ_f (nm)		
Dication (H_O-10)	—	242.5 (3.89)	288 (4.28)	—		
Monocation (pH 2)	—	255 (3.99)	297 (4.17)	366		
Neutral (pH 7)	—	245 (3.97)	289 (4.10)	326	344	356
Monoanion (pH 11)	202.5 (4.90)	250 (3.96)	307.5 (4.23)	386		
Dianion (H_-16)	227.5 (4.60)	252 (4.09)	312.5 (4.27)	390		

Table 4.12. Absorption maxima [λ_a (nm)], $\log(\epsilon_{\max})$ and fluorescence maxima [λ_f (nm)] of 2-(4'-methoxyphenyl)benzimidazole (PMBI) at 298°K.

Species/ H_O /pH/ H_-	λ_a (nm) $\log(\epsilon_{\max})$			λ_f (nm)		
Monocation (pH 2)	242 (4.03)	294 (4.27)	325 (3.84)	375		
Neutral (pH 7)	239 (4.03)	294 (4.27)	316 (4.03)	357		
Monoanion (H_-16)	250 (4.08)	311 (4.28)	330 (4.05)	370		

spectrum, where as such a change is not observed in case of the PMBI. This indicates that the neutral species has formed by protonating the phenolate ion. The pK_a value for the neutral species-monoanion equilibrium (9.4) falls in the region where phenolic -OH dissociates. With further increase in hydrogen ion concentration, a red shift is observed both in PHBI (297 nm) and PMBI (325 nm), indicating the formation of respective monocations by the protonation of tertiary nitrogen atom. These pK_a values also lie in the same region where the monocation of the benzimidazoles are formed. Lastly, at H_0-10 , a small blue shift in the absorption band reflects the formation of dication by the protonation of hydroxyl and methoxy groups of monocations of PHBI and PMBI respectively.

The changes observed in the fluorescence spectra are similar in nature to the absorption spectra over the complete range of $H_0/pH/H_-$. At H_{-16} dianion is present (390 nm), which is followed by the formation of monoanion (386 nm) like absorption spectrum with the increase in hydrogen ion concentration at pH 11. Neutral species is present at pH 7 (356 nm) and the monocation at pH 2 (366 nm). The similar shifts in the fluorescence spectrum are observed in case of its methoxy derivatives (PMBI).

The red shift observed in the fluorescence spectrum of monocation of PHBI is quite small as compared to that of the

similar species of alkyl derivatives of benzimidazole¹²⁵, but this small red shift resembles the shift observed for the cation of benzimidazoles when substituted by the phenyl¹²⁸ or the 4-thiazolyl¹⁵⁷ groups at the 2-position. This is because the positive charge over the tertiary nitrogen atom in the monocation is delocalized over the complete π system of the phenyl group, instead of being concentrated on the tertiary nitrogen atom. This behaviour is different from that of the methyl substituted derivatives of the benzimidazole, where a large red shift is observed in the formation of monocation, when compared with that of the neutral species. Thus it can be concluded that the stabilisation of charge transfer (CT) state in case of PHBI and PMBI does not occur to such an extent so as to make its energy lower than that of the 1L_b state. Therefore, the emitting state of the monocations of PHBI and PMBI is the same as that observed in the absorption spectrum, i.e. 1L_b . In contrast to the absorption spectrum, no further change is noticed in the fluorescence spectrum even upto H₁₀. This indicates that the dication formed in the ground state is unstable in the excited singlet state. This could be due to the distribution of the positive charge of the monocation over the phenyl ring, making the -OH group more acidic in the S_1 state than in the S_0 state. Different prototropic species formed in the ground and excited states are shown in the scheme, Fig. 4.26.

pK_a values

The ground state pK_a values for the various prototropic reactions were calculated spectrophotometrically and are listed in Table 4.13. The pK_a^{*} values were calculated by Förster cycle method, using absorption and fluorescence data and the average of absorption and fluorescence maxima. This method is valid in these cases, since it has been established that the electronic transition involved in the respective species are the same in the S₀ and S₁ states. The pK_a^{*} so obtained are listed in Table 4.13. The fluorimetric titrations (Fig. 4.27) gave the ground state values indicating that the lifetimes of the respective species are quite short and the equilibrium is not established in the excited singlet state. The Förster cycle method has clearly indicated that -OH and >NH groups become more acidic on excitation, whereas the tertiary nitrogen atom becomes more basic. The values of pK_a^{*} obtained by different methods are very close to each other. This agrees with the earlier discussion that especially in PHBI and its methoxy derivative the polarity of the molecules in the S₀ and S₁ states are nearly same and thus the solvent relaxation for different species is nearly the same in the two states. The small difference can be attributed to the use of band maxima rather than o-o transition.

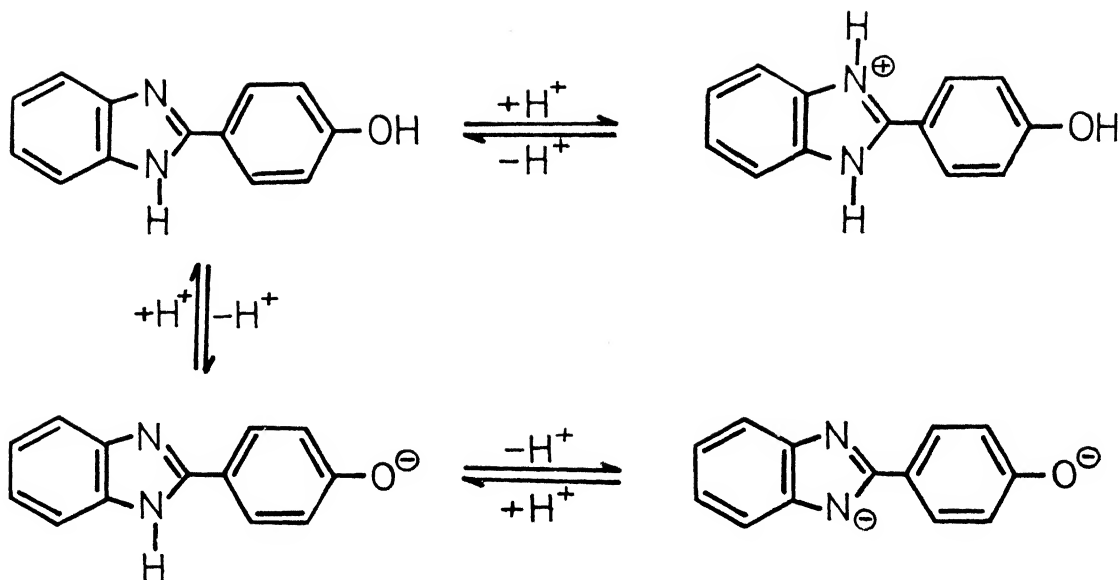


Fig.4.26 Scheme of ground and excited state equilibria of 2-(4'-hydroxyphenyl)benzimidazole at 298°K.

Table 4.13. pK_a and pK_a^* of various prototropic reactions of 2-(4'-hydroxyphenyl)-(PHBI) and 2-(4'-methoxyphenyl)-benzimidazoles (PMBI) at 298°K.

Equilibrium		pK _a	pK _a [*]		
			Abs. ^a	Flu. ^a	F.T. ^b
<u>Reactions of PHBI</u>					
Monocation	⇌ Neutral	4.4	6.5	5.9	5.0
Neutral	⇌ Monoanion	9.4	5.0	5.0	9.1
Monoanion	⇌ Dianion	13.9	12.9	13.4	13.9
<u>Reactions of PMBI</u>					
Monocation	⇌ Neutral	4.5	5.7	7.3	4.6
Neutral	⇌ Anion	12.1	10.9	8.9	12.2

^aFörster cycle method

^bFluorimetric titration method.

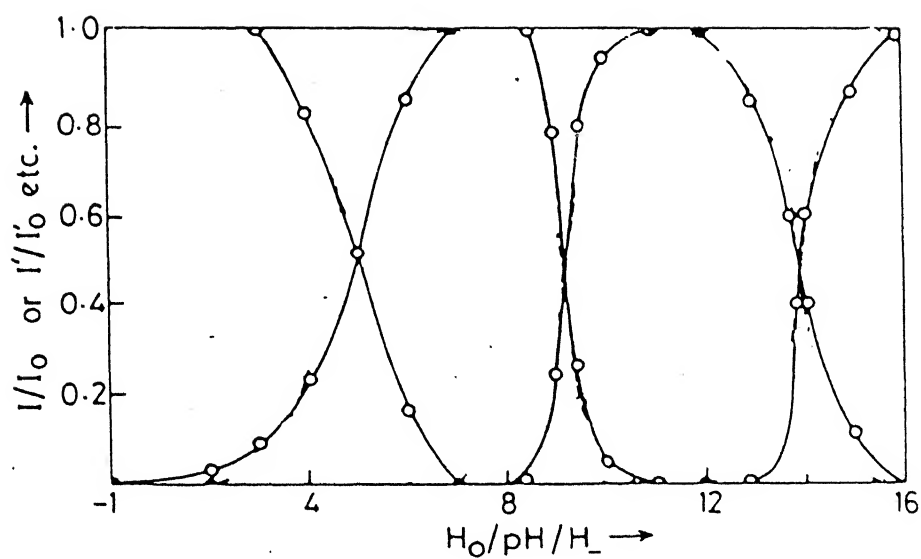


Fig.4.27 Plot of I/I_0 as a function of $H_0/pH/H_-$ of 2-(4'-hydroxyphenyl)-benzimidazole at 298°K.

In conclusion it can be summarised that the proton transfer reactions of PHBI and PMBI are same in the ground and excited singlet states except at the highest H_0 value. As the molecule is planar, both in the S_0 and S_1 states, all the prototropic species show normal shift in the absorption and fluorescence spectra with respect to each other. This behaviour is quite different from its ortho- and meta- isomers. This could be again due to the para-position of the hydroxyl group, which is a favourable position in extending the conjugation over the whole molecule.

4.6 2-(3'-Hydroxyphenyl)- (MHBI) and 2-(3'-Methoxyphenyl)-benzimidazoles (MMBI)*

The absorption and fluorescence spectral profiles of MHBI and MMBI, in the $H_0/pH/H_-$ range of -10 to 16, are shown in figures 4.28, 4.29, 4.30 and 4.31. The relevant data are compiled in Tables 4.14 and 4.15. The various prototropic reactions occurring in the ground and excited singlet states are given scheme, Fig. 4.32). The changes in the absorption spectra of MHBI and MMBI and the fluorescence spectra of MMBI follow the same trend as that observed in the corresponding reactions of PHBI. Since we have already discussed

* H.K. Sinha and S.K. Dogra, J. Photochem., 36, 149 (1987).

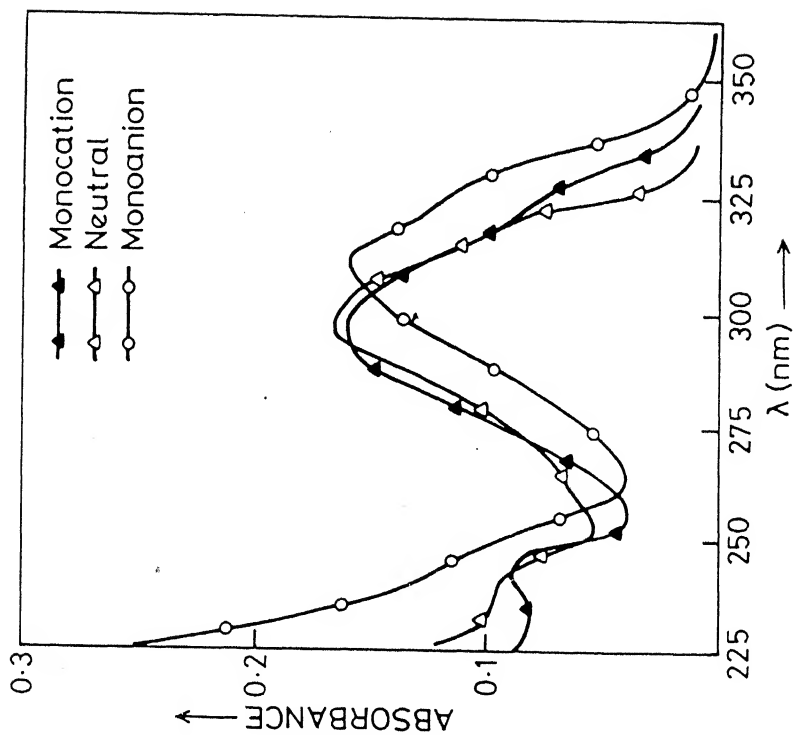


Fig.4.29 Absorption spectra of different prototropic species of 2-(3'-methoxyphenyl)benzimidazole at 298°K.

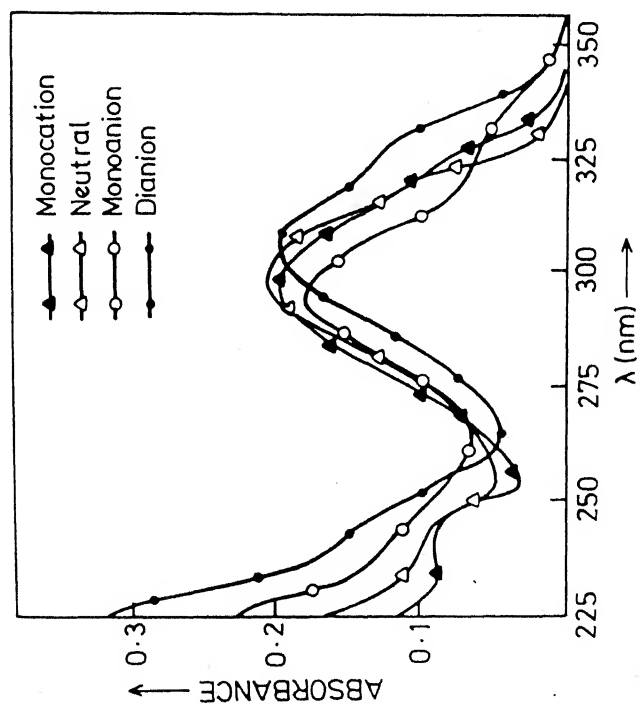


Fig.4.28 Absorption spectra of different prototropic species of 2-(3'-hydroxyphenyl)benzimidazole at 298°K.

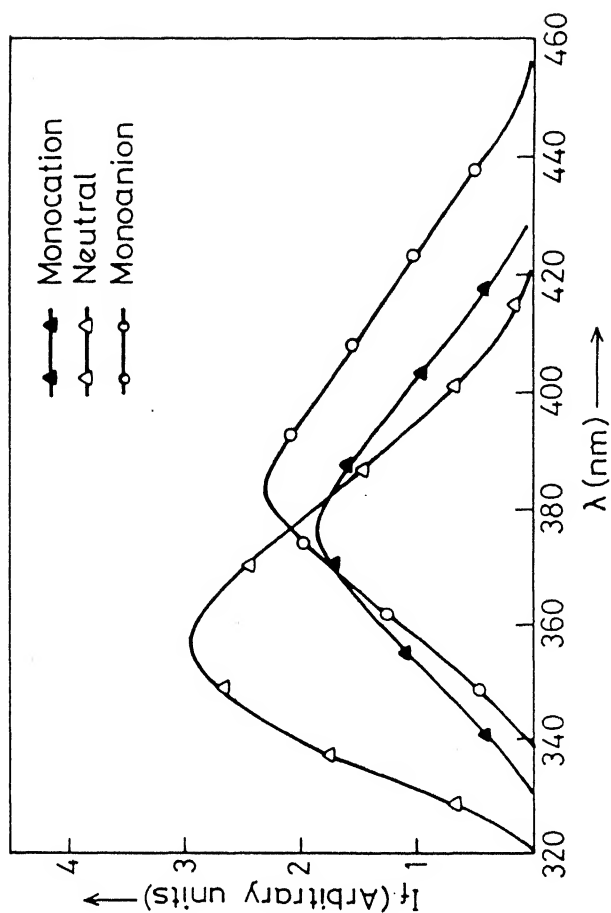


Fig.4.31 Fluorescence spectra of different prototropic species of 2-(3'-methoxyphenyl)benzimidazole at 298 K.

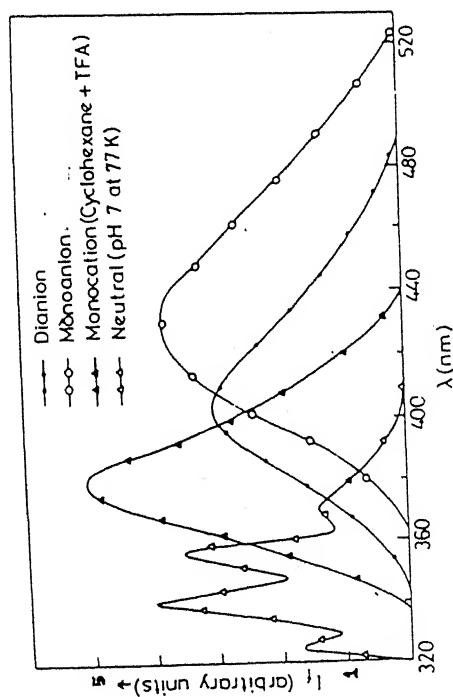


Fig.4.30 Fluorescence spectra of different prototropic species of 2-(3'-hydroxyphenyl)benzimidazole at 298 K.

Table 4.14. Absorption maxima [λ_a (nm)], $\log(\epsilon_{\max})$ and fluorescence maxima λ_f (nm) of different prototropic species 2-(3'-hydroxyphenyl)benzimidazole (MHBI) at 298°K.

Species/ H_o /pH/ H_-	λ_a (nm) $\log(\epsilon_{\max})$					λ_f (nm)
Dication (H_o-10)	205 (4.45)	243 (4.01)	-	300 (4.26)	-	-
Monocation (pH 2)	209 (4.50)	244 (4.00)	-	294 (4.32)	325 (3.95)	384 [*] 380 ^a , 390 ^b
Neutral (pH 7)	207 (4.65)	240 (4.04)	-	300 (4.31)	317 (4.16)	330 352 <u>324, 340, 357, 370[*]</u>
Monoanion (pH 11)	200 (4.45)	246 (4.13)	296 (4.30)	306 (4.22)	325 (3.89)	430
Dianion (H_{-16})	230 (4.62)	250 (4.28)	-	311 (4.37)	333 (4.18)	402

* at 77°K.

^aIn cyclohexane with 2% TFA

^bIn methanol with 2% H_2SO_4

Table 4.15. Absorption maxima [λ_a (nm)], $\log(\epsilon_{\max})$ and fluorescence maxima [λ_f (nm)] of different prototropic species of 2-(3'-methoxyphenyl)benzimidazole (MMBI) at 298°K.

Species/ H_o /pH/ H_-	λ_a (nm) $\log(\epsilon_{\max})$			λ_f (nm)
Monocation (pH 2)	248 (3.89)	300 (4.27)	325 (3.94)	362
Neutral (pH 7)	246 (3.83)	302 (4.22)	319 (4.00)	350
Monoanion (H_{-16})	250 (4.09)	312 (4.31)	325 (4.22)	370

the results of PHBI in the previous section, this section will only highlight the changes observed in the fluorescence spectrum of MHBI which are quite different from the results of other similar molecules studied in this thesis.

At the highest basic condition i.e. H₁₆ the fluorescence spectrum (402 nm) is assigned to the dianion of MHBI, formed by the deprotonation of -OH and >NH groups. Unlike the behaviour of PHBI mentioned in the previous section, there is a large red shift in the fluorescence spectrum (430 nm), when the pH is lowered. Under these conditions, the protonation can only take place either at imino nitrogen atom or at phenolate ion, both these reactions generally lead to a blue shift in the absorption and fluorescence spectra, as observed in many other similar reactions.^{38,179,180} This anomalous behaviour can be explained as follows. Unlike the dianion of PHBI or the ground state behaviour of MHBI, the negative charges on imino group and phenolate ion are localised on their respective rings, because of the meta- position of the hydroxyl group in the 2-substituted phenyl ring. Due to this, an electrostatic repulsion may occur between the two rings. This will lead to the removal of coplanarity of the two rings and thus a blue shift results on the formation of dianion by the deprotonation of the >NH group. Since the methoxy derivative does not possess a dissociable proton, the normal phenomenon is observed. Therefore, based on

the above results, the 430 nm fluorescence band is assigned to monoanion formed by the protonation of the imino group of the dianion. This is further confirmed as the pK_a value falls in the same region where the deprotonation reaction of benzimidazoles occur.

The fluorescence intensity of the neutral MHBI is quenched at pH 1 and a new band appears at H_0-1 (384 nm). No further change in fluorescence maxima is observed even at H_0-10 , once the maximum intensity is attained. Similar behaviour is also noticed when methanol is used as solvent and the hydrogen ion concentration is increased. The fluorescence spectrum of MHBI in cyclohexane containing 1-2% v/v trifluoroacetic acid (TFA) matches with the above band (380 nm). Fluorescence spectra were also recorded at 77°K and pH/ H_0 2,0 and -2. These are the hydrogen ion concentration where the monocation of MHBI is present in the S_0 state, but the fluorescence spectrum of the monocation is only observed at H_0-2 and 298°K. At 77°K, the fluorescence spectra observed at these hydrogen ion concentrations (pH/ H_0 2,0 and -2) are the same and match with that observed at 298°K. The 384 nm fluorescence band is thus assigned to the monocation. This is formed by the protonation of tertiary nitrogen atom. This assignment is based on the following grounds (a) Based on the structure of the molecule, no other cationic species can be formed in such acid condition. A non-fluorescent zwitterion can be formed in

the excited singlet state from the neutral molecule with the assumption that the acidity of the -OH group and the basicity of the tertiary nitrogen atom increase upon excitation to match the rate of deprotonation of the -OH group and rate of protonation of the tertiary nitrogen atom, but this species can not be formed from the excitation of monocation, which is present in the S_0 state. (b) Proton induced fluorescence quenching of monocations of methyl substituted benzimidazoles have been observed¹²⁵ but not of neutral benzimidazole derivatives. Even if we assume that fluorescence quenching of neutral MHBI occurs, the pK_a^* value of monocation-neutral species equilibrium can be calculated only from the relative increase in fluorescence intensity of the monocation and not from the relative decrease in the fluorescence intensity of neutral MHBI. The pK_a^* obtained from the formation curve of monocation is 0.5, indicating that tertiary nitrogen atom becomes less basic upon excitation, whereas it was always been observed that tertiary nitrogen becomes more basic.³⁸ (c) The fluorescence quantum yield of most of the monocations of benzimidazole derivatives are very small as compared to that of the neutral species and this originates either from radiationless process or from solute-solvent interactions leading to quenching. Results at low temperature and in non-polar media confirm the above observation, i.e. fluorescence from monocation at 77°K is observed in the pH regions where it was absent in aqueous media

and at 298°K. The monocation of 2-(3'-aminophenyl)benzimidazole¹⁸⁵ is also found to be non-fluorescent. Thus it can be concluded that the monocation of MHBI is formed below 3, as the fluorescence intensity of the neutral molecule starts decreasing. This species is only observed at high acid concentration may be due to the reason mentioned above. Formation of dication is not observed even at H_0 -10 and hence similar explanation is given as in PHBI. The various proton transfer reactions of MHBI are shown in scheme, Figure 4.32.

pK_a values

The ground state pK_a values for the various prototropic reactions were calculated spectrophotometrically and are summarised in Table 4.16. The pK_a values are in the same range as those observed in the PHBI. Thus similar arguments can be offered.

The pK_a^{*} values for various proton transfer reaction were calculated with the help of fluorimetric titration (Fig. 4.33) and the Förster cycle method, using absorption and fluorescence data and the average of absorption and fluorescence maxima. The pK_a^{*} value for the equilibrium between anion dianion species of MHBI can not be calculated by Förster cycle method using fluorescence data because it was established that in the latter species the phenyl ring is not coplanar with the benzimidazole moiety in

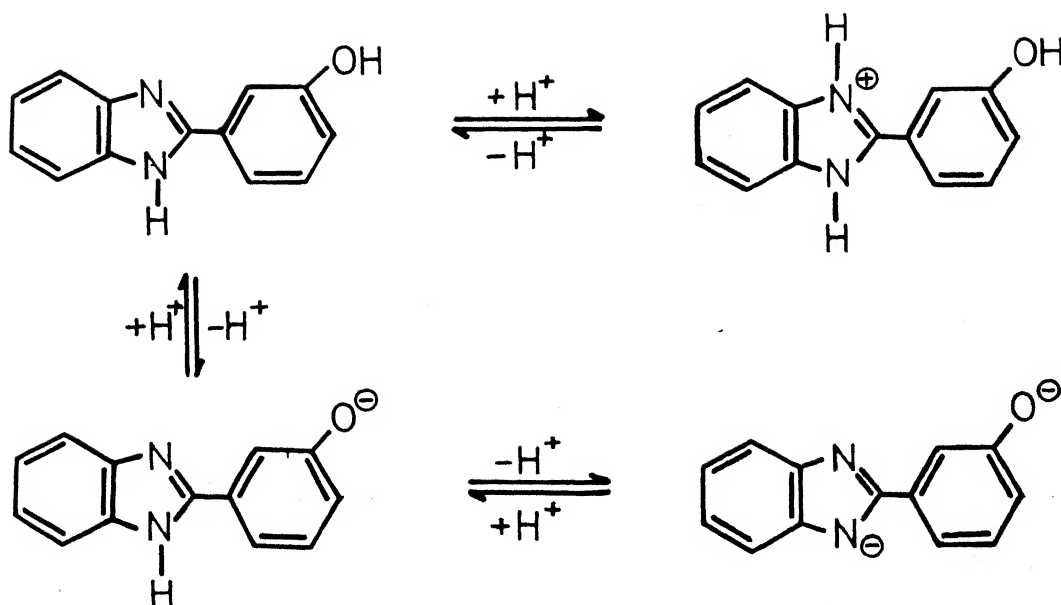


Fig.4.32 Scheme of ground and excited state equilibria of 2-(3'-hydroxyphenyl)benzimidazole at 298°K.

Table 4.16. pK_a and pK_a^* of various prototropic reactions of 2-(3'-hydroxyphenyl)-(MHBI) and 2-(3'-methoxyphenyl)-benzimidazoles (MMBI) at 298°K.

Equilibrium		P <i>K</i> _a	p <i>K</i> _a [*]		
			Abs. ^a	Flu. ^a	F.T. ^b
<u>Reactions of MHBI</u>					
Monocation	⇌ Neutral	4.5	6.0	9.5	4.5
Neutral	⇌ Monoanion	9.0	7.5	1.8	9.1
Monoanion	⇌ Dianion	13.4	11.9	—	13.5
<u>Reactions of MMBI</u>					
Monocation	⇌ Neutral	4.2	6.0	7.1	4.5
Neutral	⇌ Monoanion	12.9	10.1	9.1	12.5

^aFörster cycle method

^bFluorimetric titration method.

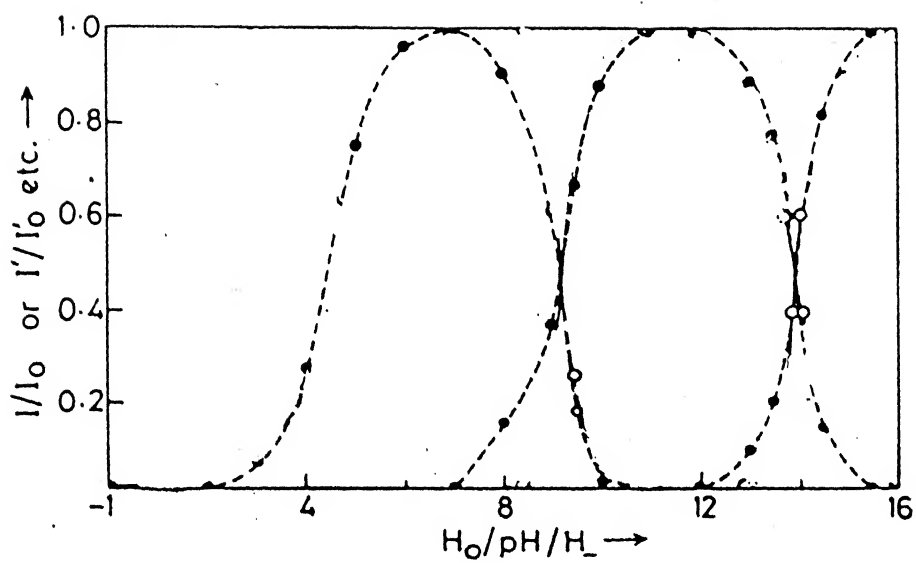


Fig.4.33 Plot of I/I_0 as a function of $H_0/pH/H_-$ of 2-(3'-hydroxyphenyl)benzimidazole at 298°K.

the S_1 state. Fluorimetric titrations produced the ground state value, may be because of the reason mentioned earlier. The Förster cycle method has clearly indicated that $-OH$ and $>NH$ groups become more acidic on excitation, whereas the tertiary nitrogen atom become more basic. The results of Table 4.16 indicate that the pK_a^* values obtained by different methods for MHBI are quite different as compared to PHBI. As pointed out earlier, it could be due to the more polar nature of the ions of MHBI in the excited state than in ground state.

Like PHBI it can be concluded that in case of MHBI, the ground and excited state prototropic reactions are the same. Further, the fluorescence quantum yield of monocation of MHBI is very low as compared to those of monocation of PHBI.

4.7 5-Chlorobenzimidazole-2-carboxylic acid (CBIA), Benzimidazole-2-carboxylic acid (BIA) and 5-Chlorobenzimidazole-2-methyl-carboxylate (CBIM)*

The absorption spectra of all the compounds were recorded in the $H_0/pH/H_-$ range of -10 to 16. The spectral profiles of CBIA, BIA and CBIM are shown in Figures 4.34, 4.35 and 4.36 respectively and the relevant data are compiled in Table 4.17. In the ground state, at the extreme basic

* H.K. Sinha and S.K. Dogra, communicated.

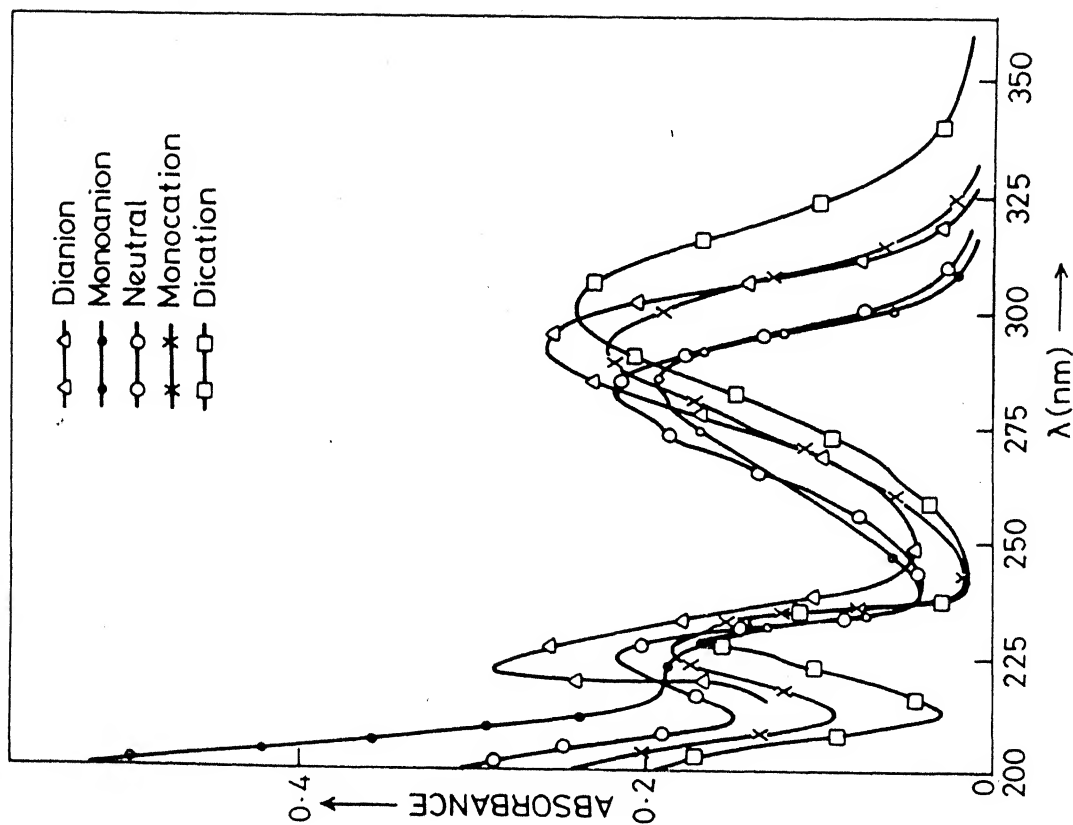


Fig.4.35 Absorption spectra of different prototropic species of benzimidazole-2-carboxylic acid at 298°K.

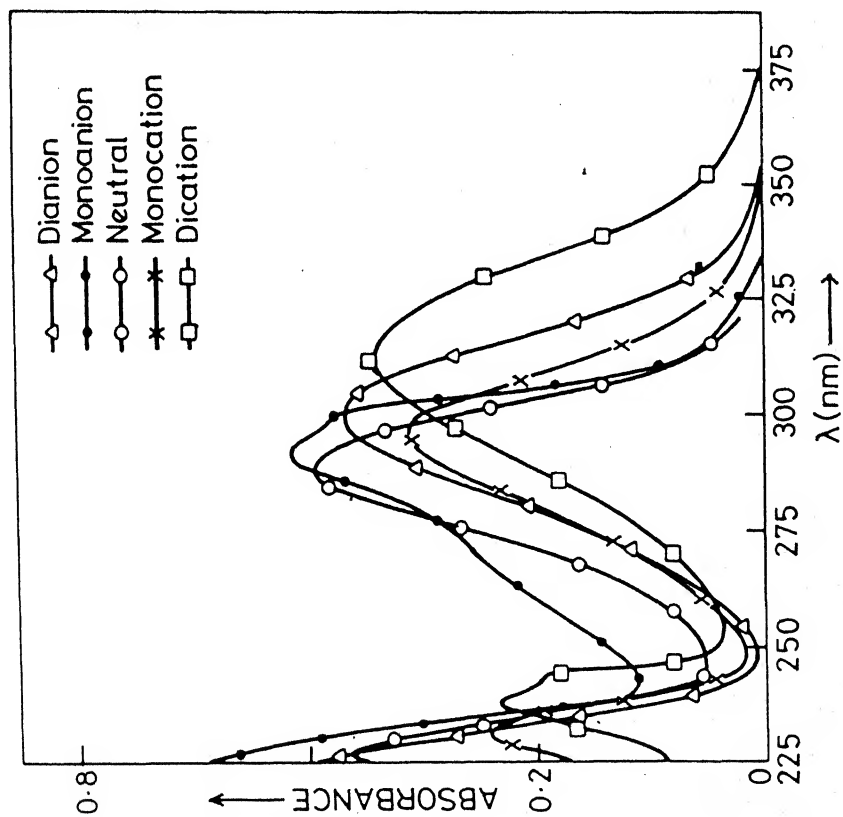


Fig.4.34 Absorption spectra of different prototropic species of 5-chlorobenzimidazole-2-carboxylic acid at 298°K.

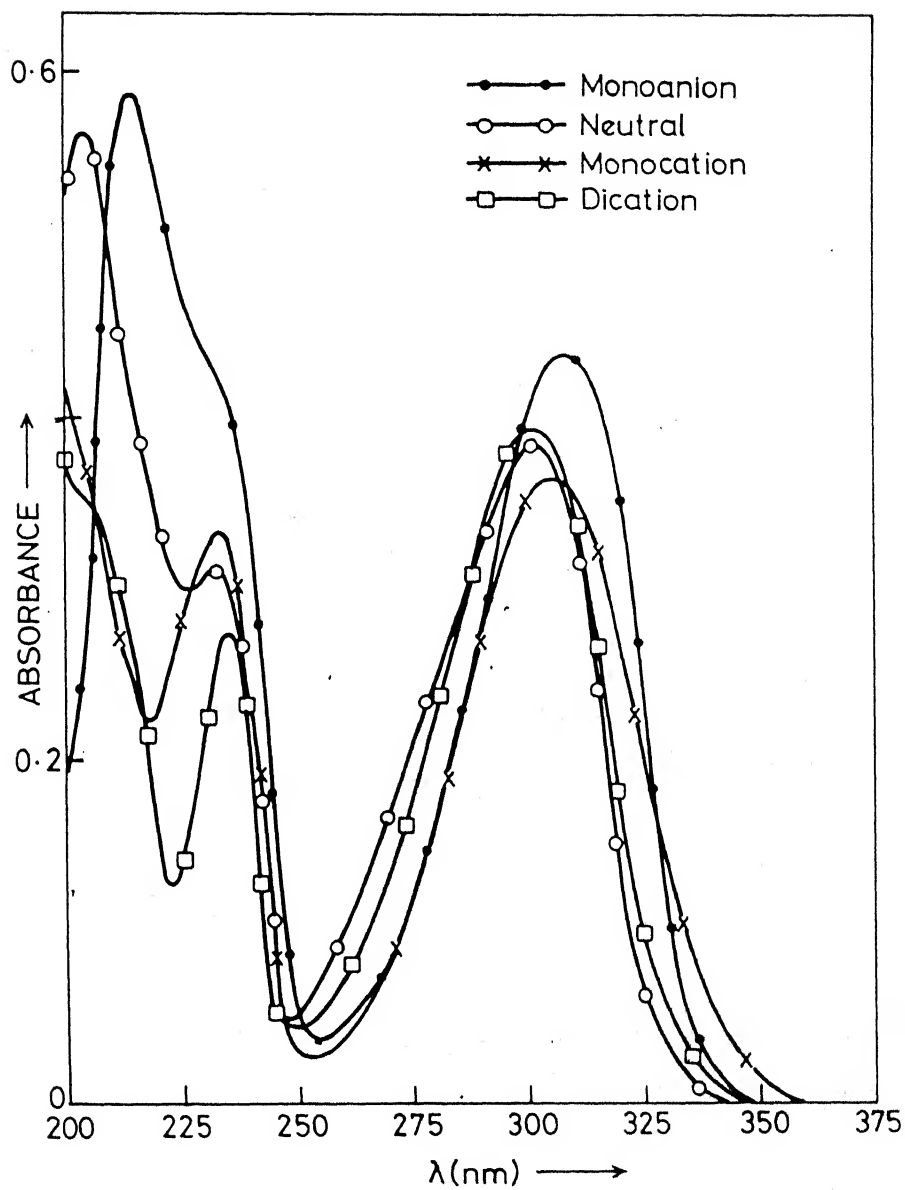


Fig.4.36 Absorption spectra of different prototropic species of 5-chlorobenzimidazole-2-methylcarboxylate at 298 K.

Table 4.17. Absorption maxima [λ_a (nm)], $\log(\epsilon_{\max})$ and fluorescence maxima [λ_f (nm)] of various prototropic species of 5-chlorobenzimidazole-2-carboxylic acid (CBIA), benzimidazole-2-carboxylic acid (BIA) and 5-chlorobenzimidazole-2-methylcarboxylate (CBIM) at 298°K.

Species/ $H_0/pH/H_-$	λ_a (nm) $\log(\epsilon_{max})$		λ_f	λ_a (nm) $\log(\epsilon_{max})$		λ_f	λ_a (nm) $\log(\epsilon_{max})$		λ_f
	CBIA			BIA			CBIM		
Dication (H_{O-8})	<u>311</u> (3.55)		-	<u>304</u> (3.60)		-	<u>307</u> (3.69)		-
	237.5 (3.38)			235 (3.52)			237 (3.55)		
	207.5 (3.44)			230 (3.55)			207.5 (3.64)		
Monocation (H_{O-1})	<u>297</u> (3.52)		410	<u>293</u> (3.71)		410	<u>302</u> (3.71)		410
	232.5 (3.40)			275 (3.55)			235 (3.62)		
				232 (3.70)			207 (3.62)		
				229 (3.51)					
Neutral (pH 2)	<u>289</u> (3.61)		380	<u>281</u> (3.70)		392	<u>300</u> (3.71)		390
	227.5 (3.60)			273 (3.52)			232.5 (3.64)		
				222 (3.69)					
Monoanion (pH 8)	999 (3.61)		345	<u>285</u> (3.65)		360	<u>308</u> (3.77)		360
	<u>291</u> (3.69)			278 (3.62)			212 (3.84)		
	260 (3.41)			271 (3.59)					
	202 (3.78)			222 (3.55)					
Dianion (H_{16})	<u>299</u> (3.69)		350	305 (3.75)		365	-		-
	226 (3.89)			224 (3.80)					

Underlined are the absorption maxima.

condition (H₁₆) the species present in case of CBIA and BIA are the dianion (formed by the deprotonation of -COOH and >NH groups and monoanion in case of CBIM (formed by the deprotonation of only >NH group as it does not possess the dissociable proton at -COOH group). The absorption spectrum shows only two bands, one at ~299 nm and the other at 226 nm. The band at 250 nm (present in neutral BI) is absent. This resembles with the behaviour of monoanion of BI. Because of the reason that the ~250 nm band is polarised along the shorter axis of the molecule (¹L_a) and >NH group is present along the shorter axis, the deprotonation of >NH group will affect the 250 nm band system more as compared to long axis polarised ~299 nm band (¹L_b). Decrease of pH has little affect on the ~299 nm band system but the band system at ~250 nm starts appearing and a blue shift is noticed in ~226 nm band. This is consistent with the earlier observations on protonation at the imino group. After protonation, the species thus formed is a monoanion in case of CBIA and BIA and a neutral species in case of CBIM. At pH 3, the absorption spectra of CBIA, CBIM and BIA resemble with those observed in non-polar and polar solvents (both aprotic and protic solvents). This indicates that the species formed are the neutral species of the respective molecule. The long wavelength (~300 nm) structured absorption band of the neutral species, as reported in the solvent study (section 3.3) is present as a tail in the pH solution, probably

because of polar nature of the solvents and low concentration used for the pH study. At this hydrogen ion concentration, the protonation can also occur at the tertiary nitrogen atom as the pK_a for this protonation reaction in pure benzimidazole is 5.5. Moreover, on comparing the pK_a of the formic acid (3.77) it can be inferred that the first protonation should have taken place at the tertiary nitrogen atom. Had this been the case in BIA and CBIA, the species formed in case of CBIM in this pH would have been the monocation and hence corresponding spectral changes should have been observed around pH 5. But the absorption spectrum of CBIM remains unchanged until pH 2, proving our earlier conclusion that the protonation takes place at the $-COO^-$ group, leading to the neutral species in case of CBIA and BIA. On further increase of hydrogen ion concentration ($H_0 \leq 0.0$), the spectral changes observed are similar to those observed for the formation of monocation of BI molecule. In all these compounds, the pK_a values for the monocation-neutral equilibria are nearly equal. A further increase of hydrogen ion concentration leads to a large red shift in all the absorption band systems. This change is attributed to the formation of dication species by the protonation of carboxyl group and the behaviour resembles to that observed for the similar reaction of carboxylic acids.¹⁶⁶

The fluorescence spectra of CBIA, BIA and CBIM studied in the $H_0/pH/H_-$ range of -10 to 16 are shown in figure 4.38, 4.39 and 4.40 respectively. All the spectral data are compiled in

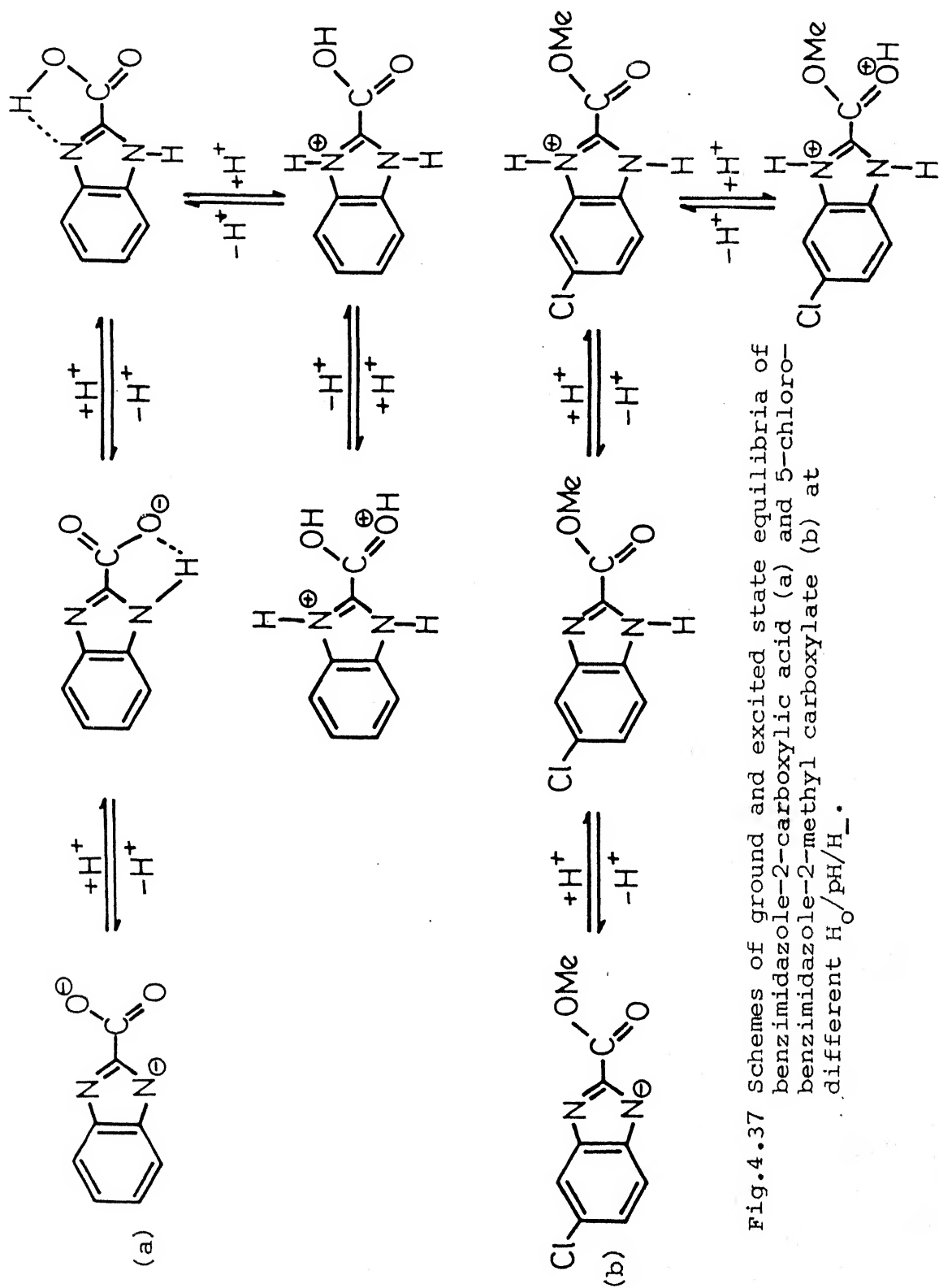


Fig.4.37 Schemes of ground and excited state equilibria of benzimidazole-2-carboxylic acid (a) and 5-chloro-benzimidazole-2-methyl carboxylate (b) at different $H_0/pH/H_-$.

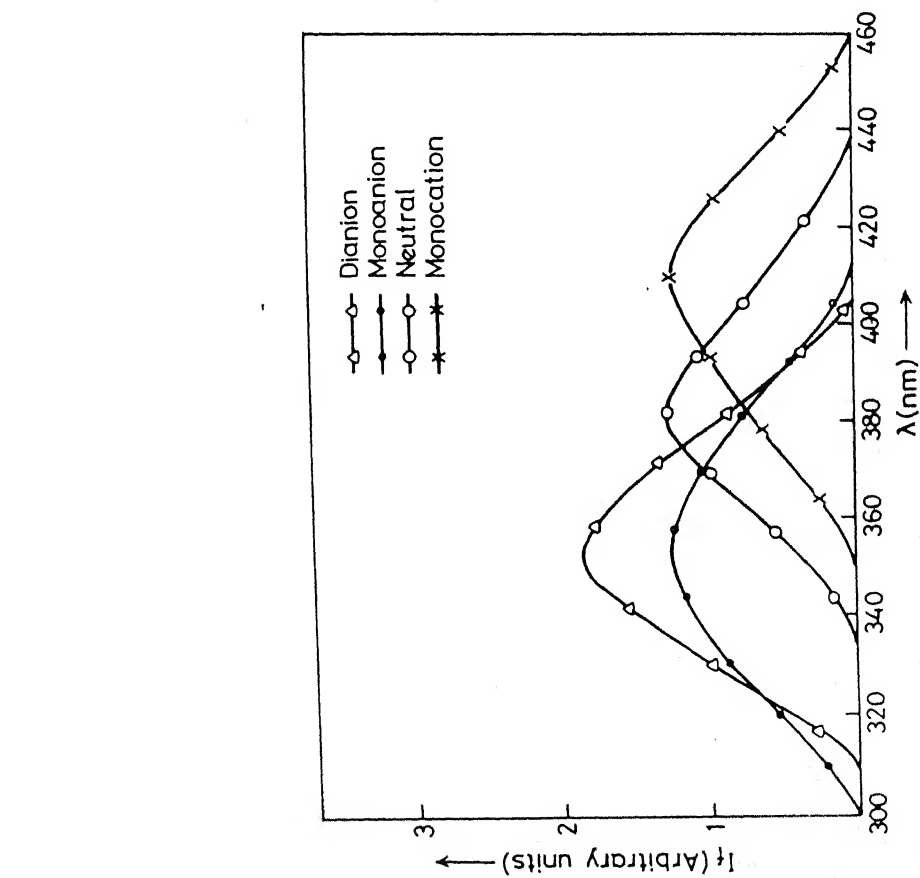


Fig.4.38 Fluorescence spectra of different prototropic species of 5-chloro-benzimidazole-2-carboxylic acid at 298°K.

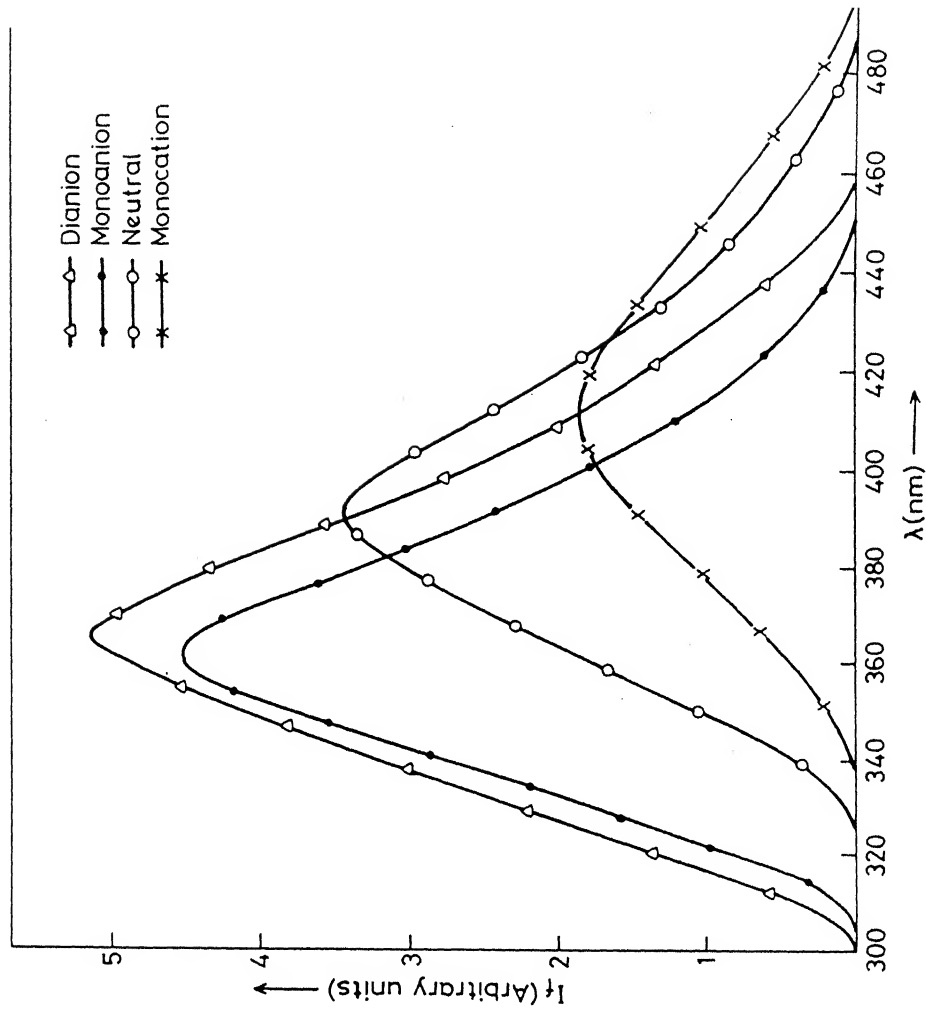


Fig.4.39 Fluorescence spectra of different prototropic species of benzimidazole-2-carboxylic acid at 298°K.

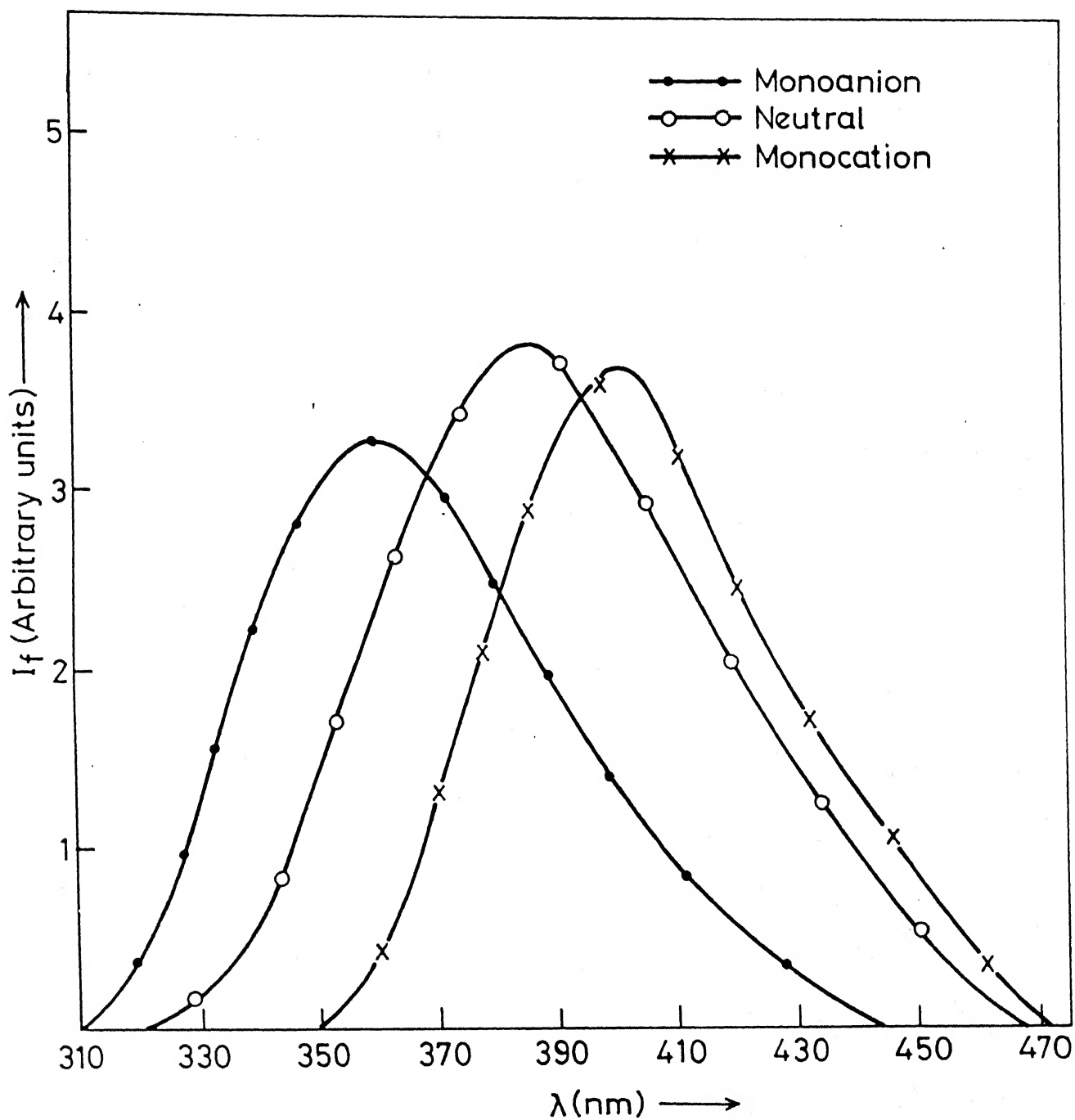
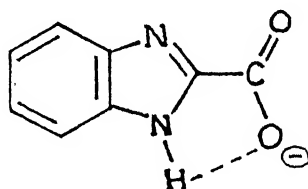


Fig.4.40 Fluorescence spectra of different prototropic species of benzimidazole-2-methylcarboxylate at 298°K.

Table 4.17. A close look at the data of Table 4.17 shows that the prototropic reactions in the excited state are similar to those observed in the ground state i.e. dianion (monoanion in case of CBIM) is present in case of CBIA and BIA at H_{-15} . The formation of dianion in case of BIA and CBIA is consistent because the fluorescence band maxima in these cases are similar to that of monoanion of CBIM, indicating that the positions of $-COO^-$ and $-COOMe$ groups in space, with respect to BI moiety are the same. The monoanion of CBIA and BIA is formed at $pH \sim 6$ and the neutral species at $pH \sim 3$. The confirmation of the latter species is done from the resemblance of the fluorescence spectra of CBIA and BIA with CBIM. Monocations are formed at $H_0 \sim 0.0$. Again the monocations of all three compounds resemble each other with respect to its fluorescence maxima, reflecting their structural similarity in space. The dications are non-fluorescent for all the molecules.

The pK_a values for various prototropic reactions have been determined spectrophotometrically and are compiled in Table 4.18. The pK_a for the monoanion-dianion equilibrium is very low for CBIM as compared to that calculated for CBIA and BIA, as well as for BI molecule. The carboxyl group, being an electron withdrawing group, will decrease the charge densities at the tertiary nitrogen atom and imino group, leading to decrease in the pK_a values for the protonation reaction of the former and deprotonation reaction of the latter. This effect has been clearly manifested in case of 2-(trifluoromethyl)- and 2-(trichloromethyl)benzimidazoles (section 4.3). The higher value of pK_a for CBIA (12.7)

and BIA (13.1) in comparison to CBIM (9.6) for the deprotonation reaction of imino group can be explained on the following lines. A strong intramolecular hydrogen bonding between imino proton and the negatively charged oxygen of carboxylate ion is present in monoanionic species of BIA and CBIA as shown below, which makes the deprotonation reaction difficult. The reason for low pK_a



value of CBIM is that a similar structure can not be achieved in CBIM. This also reflects that the hydrogen bonding interaction between imino proton and the lone pair of the carbonyl group is either very weak or absent in CBIM. The stability of this type of intramolecular hydrogen bonded structure has been found to be very large, when it leads to the formation of a six membered ring instead of a five membered one as in the present case. For example, the deprotonation of $>NH$ group is not observed even at H_{15} in case of benzimidazole-2-acetic acid (section 4.8) and 2-(2'-hydroxyphenyl)benzimidazole (section 4.4). The pK_a values for the neutral-monoanion equilibria for CBIA and BIA are consistent with the similar results of other carboxylic acids.¹⁶⁶ The pK_a values for the monocation-neutral equilibria for all three

compounds are very low as compared to that for BI and can be explained on the same line as has been done earlier. Lastly, the pK_a values for the dication-monocation equilibria are higher than that reported for the similar reaction of the carboxyl groups. It could be due to the flow of charge from the heterocyclic ring to the carboxylic group and hence making it more basic. Various prototropic reactions observed as well as molecular conformations at different pH in these molecules are presented in schemes, Fig. 4.37.

pK_a^* values have been calculated with the help of fluorimetric titrations and Förster cycle method using absorption and fluorescence spectral data wherever applicable. All the pK_a^* values are compiled in Table 4.18. The fluorimetric titration curves (figures 4.41) in all these cases generate the ground state value, which can be explained on the same line as has been done earlier i.e. prototropic equilibrium is not established in the excited singlet state due to very short lifetimes of the conjugate acid-base pair. The Förster cycle method wherever applicable clearly indicates that carboxyl group and tertiary nitrogen atom become more basic and imino group become more acidic upon excitation.

The following conclusions can be made from the study of absorption and fluorescence spectra of above mentioned compounds.

(i) In BIA, CBIA and CBIM, the carboxyl group and BI moiety are

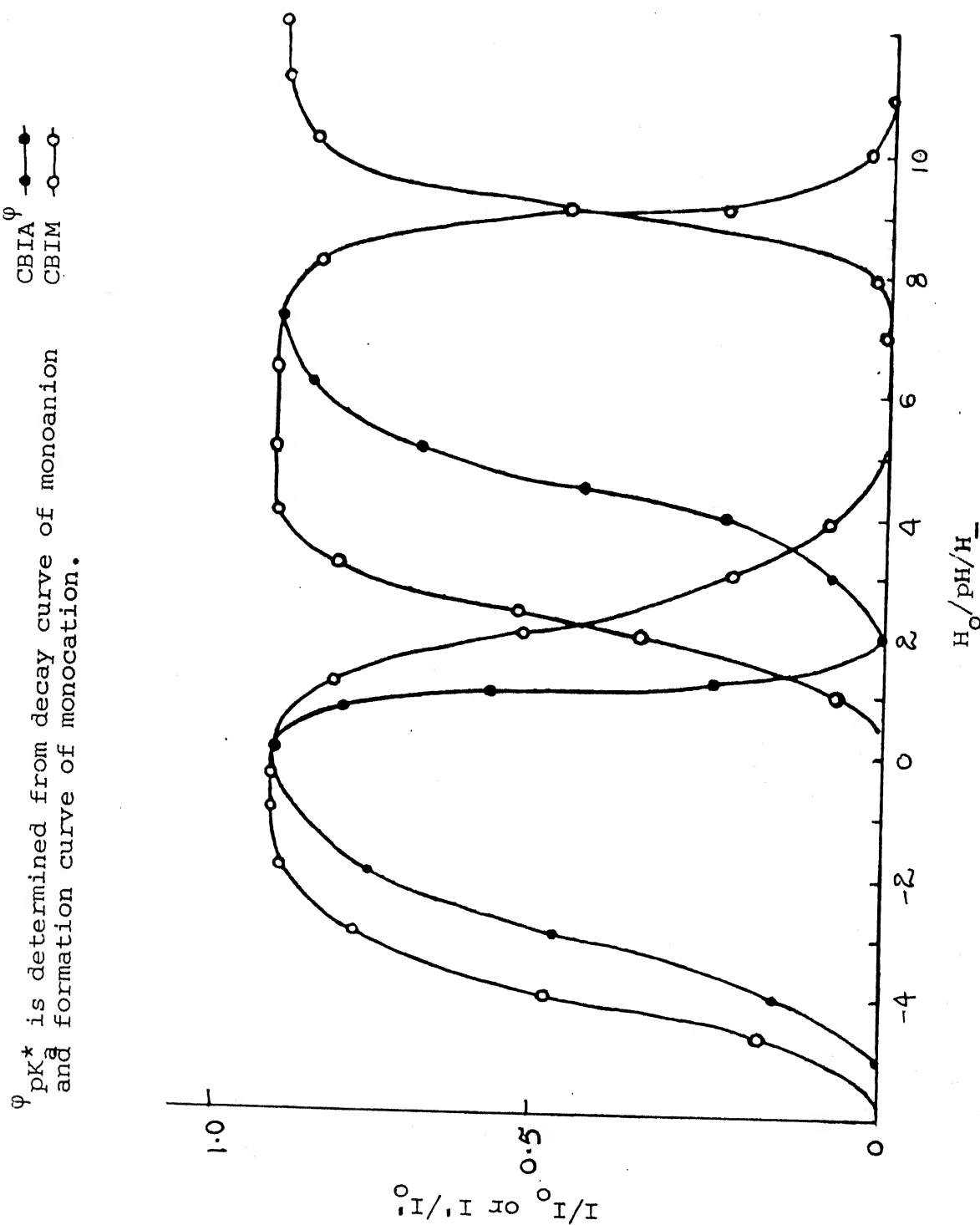


Fig.4.41 Plot of I/I_0 as a function of $H_0/pH/H_-$ of 5-chlorobenzimidazole-2-carboxylic acid (CBIA) and 5-chlorobenzimidazole-2-methylcarboxylate (CBIM).

Table 4.18. pK_a and pK_a^* of various prototropic reactions of 5-chlorobenzimidazole-2-carboxylic acid (CBIA), benzimidazole-2-carboxylic acid (BIA) and 5-chlorobenzimidazole-2-methylcarboxylate (CBIM) at 298°K.

Equilibrium	pK _a	pK _a [*]		
		Abs. ^a	Flu. ^a	F.T. ^b
Reactions of CBIA and BIA ^ψ				
Dication ⇌ Monocation	-4.9(-5.0)	-1.71(-2.40)	-	-3.0(-4.5)
Monocation ⇌ Neutral	0.0(0.4)	1.9 (3.4)	4.0(2.8)	1.0(0.9)
Neutral ⇌ Monoanion	4.3(4.8)	-	-	4.4(4.8)
Monoanion ⇌ Dianion	12.7(13.1)	-	-	-
Reactions of CBIM				
Dication ⇌ Monocation	-4.4	-3.2	-	-4.1
Monocation ⇌ Neutral	0.3	-0.7	-2.6	2.1
Neutral ⇌ Monoanion	9.6	7.8	-	9.0

^aFörster cycle method

^bFluorimetric titration method

^φMentioned in the parenthesis

coplanar to each other and the molecule is held together in a rigid frame by intramolecular hydrogen bonding.

- (ii) Due to the presence of electron withdrawing group at 2-position the electron densities decrease at tertiary nitrogen atom and imino group, which is reflected from its pK_a values. The pK_a values for the deprotonation of the imino group of CBIA and BIA are higher than that of CBIM because of the existence of intramolecular hydrogen bonded structure in case of former, which restricts the removal of imino proton.

4.8 Benzimidazole-2-acetic acid (BIAA) and Benzimidazole-2-ethylacetate (BIAE)*

The absorption spectra of various prototropic forms of BIAA and BIAE, formed in the $H_0/pH/H_-$ range of -10 to 16, are shown in figures 4.42 and 4.43. The corresponding spectral data are summarized in Tables 4.19 and 4.20.

Unlike BIA and CBIA (see section 4.7) the dianion of BIAA is not formed even at H_-16 , the highly basic condition used in the experiment. This could be due to the existence of an intramolecularly hydrogen bonded structure as shown below in case of monoanion of BIAA, which will restrict the removal

*H.K. Sinha and S.K. Dogra, communicated.

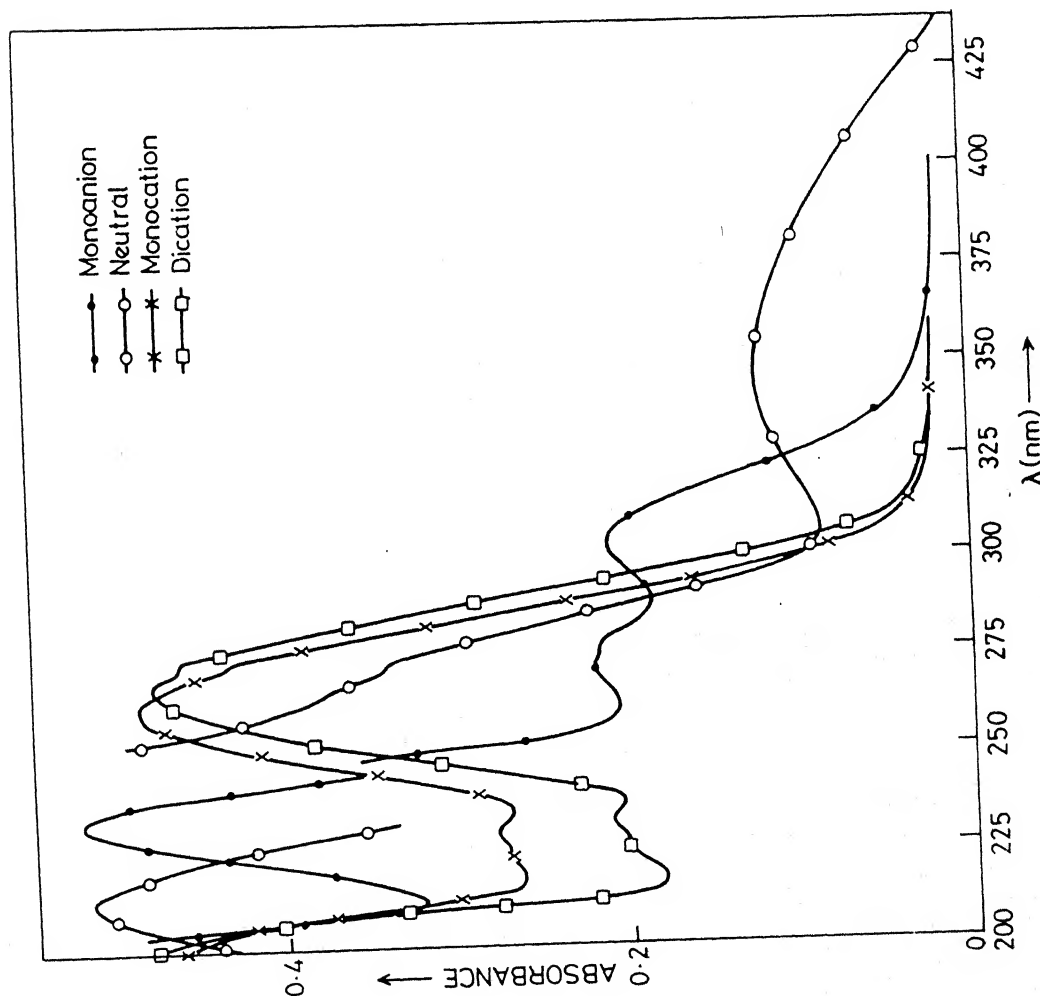


Fig.4.42 Absorption spectra of various prototropic species of benzimidazole-2-acetic acid (BIAA) at 298°K.

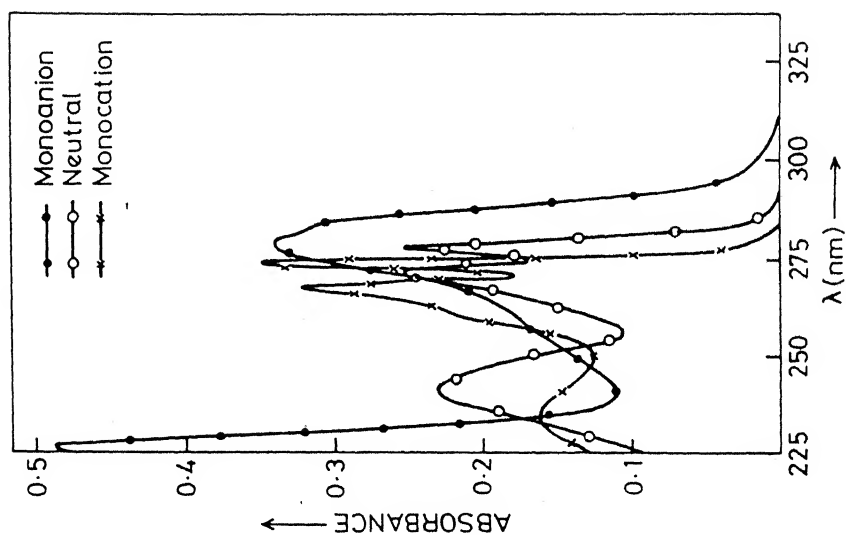


Fig.4.43 Absorption spectra of various prototropic species of benzimidazole-2-ethylacetate at 298°K.

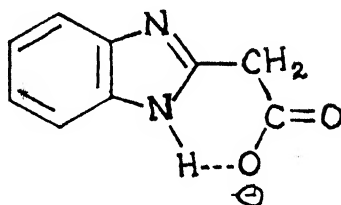
Table 4.19. Absorption maxima [λ_a (nm)], $\log(\epsilon_{\max})$ and fluorescence maxima [λ_f (nm)] of various prototropic species of benzimidazole-2-acetic acid (BIAA) at 298°K.

Species/ H_o /pH/ H_-	λ_a (nm) $\log(\epsilon_{\max})$			λ_f (nm)
Dication (H_o-8)	-	274(3.99) 268(4.00)	233(3.64) 225(3.60)	390 410 430
Monocation (H_o-2)	-	274(3.96) 263(4.01)	230(3.76) 224(3.74)	383 402 426
Zwitterion (pH 3)	345(3.39)	274(3.85) 268(3.89)	237(4.36)	390
Monoanion (pH 9)	304(3.63)	277(3.67) 271(3.66)	212(4.45)	344 363 378 400

Table 4.20. Absorption maxima [λ_a (nm)], $\log(\epsilon_{\max})$ and fluorescence maxima [λ_f (nm)] of various prototropic species of benzimidazole-2-ethylacetate (BIAE) at 298°K.

Species/ H_o /pH/ H_-	λ_a (nm) $\log(\epsilon_{\max})$			λ_f (nm)	
Dication (H_o-8)	274(4.26) 268(4.20)	235(3.90)	-	-	-
Monocation (pH 3)	274(4.24) 268(4.20)	237(3.95)	-	282 271	363
Neutral (pH 7)	278(4.10) 273(4.21)	241(4.08)	-	287 277	-
Monoanion (H_-16)	285(4.22) 280(4.25)	-	225(4.60)	307	-

of imino proton. Similar behaviour has also been observed in case of 2-(2'-hydroxyphenyl)benzimidazole (section 4.4) i.e. only



monoanion, formed by deprotonation of hydroxyl group, exists in high basic conditions in the excited singlet state. Further in case of BIAA, the intramolecularly hydrogen bonded structure will be more stable than that observed in case of CBIA and BIA (section 4.7) because a six membered cyclic structure is achieved in the former case whereas a five membered one is possible in the latter. The study on BIAE gives further support to the above mentioned structure, as the pK_a value obtained for the deprotonation reaction of imino group is found to be 13.6 which is very close to that of BIM. This also indicates that the carbonyl group ($C=O$) is not involved in the hydrogen bonding with the imino proton or this interaction may be very weak.

No other spectral changes were observed in the range H₁₆ to pH 6 in case of BIAA. With further decrease in pH, a largely red shifted and broad absorption band is observed. In this pH

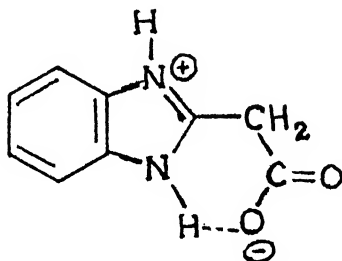
region, protonation can occur either at tertiary nitrogen atom to form a zwitterion or at carboxylate group to form a neutral species. The formation of the former species is suggested, based on the following reasons:

- (i) The absorption spectrum of the neutral species formed by the protonation of carboxylate group should be comparable to that in the protic solvents like methanol where the presence of neutral species is confirmed (section 3.3) But the large red shift from 313 nm to 345 nm shows that the species present in this pH region is different from the simple neutral one.
- (ii) The pK_a for the deprotonation of acetic acid is 4.76 and that of phenyl acetic acid is 4.31, whereas the pK_a for the protonation BI is 5.5 and that for BIM 6.19. It can be assumed that the pK_a for the dissociation of $-CH_2-COOH$ group of BIAA should be nearly equal to that of the phenyl acetic acid and that for protonation of tertiary nitrogen atom should be similar to or little less than that of BIM. This assumption suggests that the protonation take place at tertiary nitrogen atom.
- (iii) The pK_a for the protonation reaction of BIAE is found to be 5.7, close to that of BI or BIM, indicating that the methylene group inhibits the direct interaction between BI moiety and

ester group. This result also supports above assumption.

- (iv) The spectral shift observed in the formation of monocation of BIAE is similar to that observed in case of BI or BIM.

Based on the above experimental results the presence of a zwitterionic species, as shown below, is suggested in the pH region of 5 to 2.



With further increase of hydrogen ion concentration, the long wavelength absorption band (345 nm) completely disappeared and the absorption spectrum of BIAA resembles with that of monocation of BIAE or BI. This indicates that the species formed is a monocation having a open structure like that of BIAE. No further change is observed in the absorption spectrum of monocation of BIAA and BIAE on increasing the acid concentration. This is consistent with the fact that if the open structure is present, the

protonation reaction at $-\text{COOH}$ or $-\text{COOCH}_3$ group will have little effect on the absorption spectrum of BI moiety. This is due to the presence of methylene group in between the two functional groups, which acts as an insulator. Similar observation has also been found in 2-(aminomethyl)benzimidazole (section 4.1).

Fluorescence spectra of all the prototropic species of BIAA and BIAE are shown in figures 4.44 and 4.45 respectively. The data are compiled in Table 4.19 and 4.20. Like prototropic reactions of BIAA in the ground state, dianion is not formed in S_1 state because no change in the fluorescence spectrum is observed even at H_{16} . Same arguments can be given as mentioned earlier. In the pH/H_{16} range 6 to 16 structured fluorescence is observed which suggests the existence of a rigid structure due to strong intramolecular hydrogen bonding in the S_1 state. Above pH 12 the fluorescence spectrum of BIAE resembles to that of monoanion of BIM, suggesting the presence of monoanion. Similar to the absorption spectrum of BIAA a large red shift (362 to 390 nm) in the fluorescence spectrum is observed on decreasing the pH to 3. On the basis of similar arguments given earlier, it can be concluded that the species present is a zwitterion. A further decrease in pH (H_0 0.0) leads to the formation of monocation, similar to the ground state. The red shift observed in the fluorescence

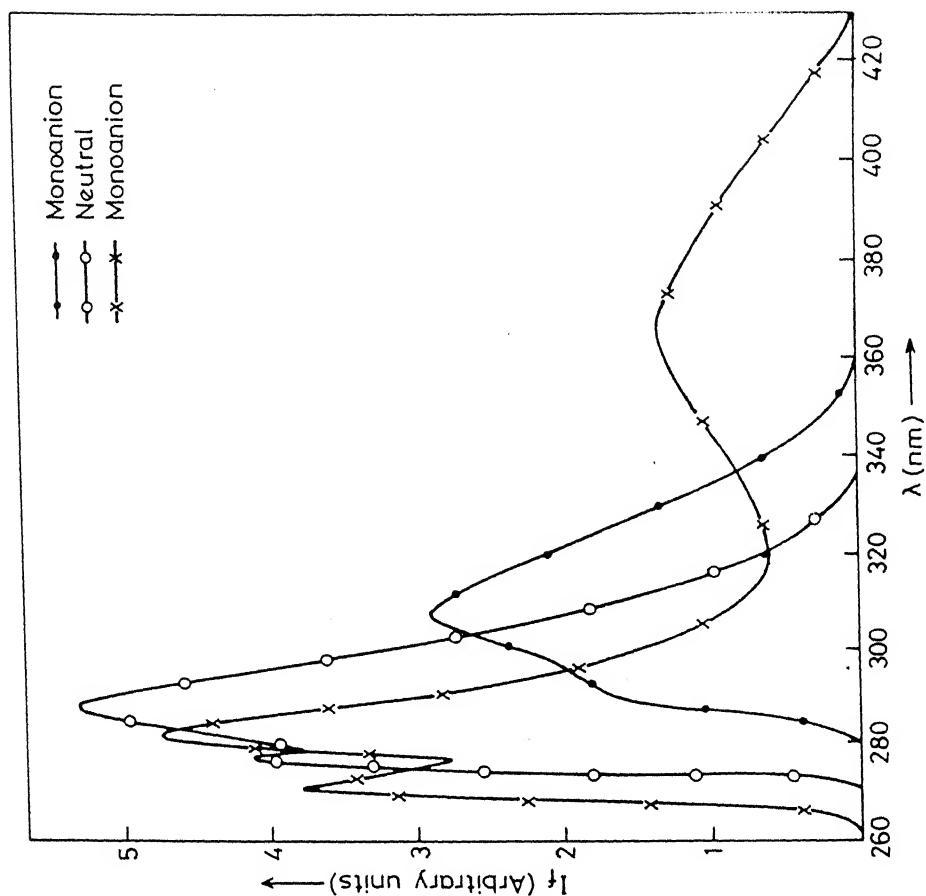


Fig.4.45 Fluorescence spectra of various prototropic species of benzimidazole-2-ethylacetate (BIAE) at 298 K.

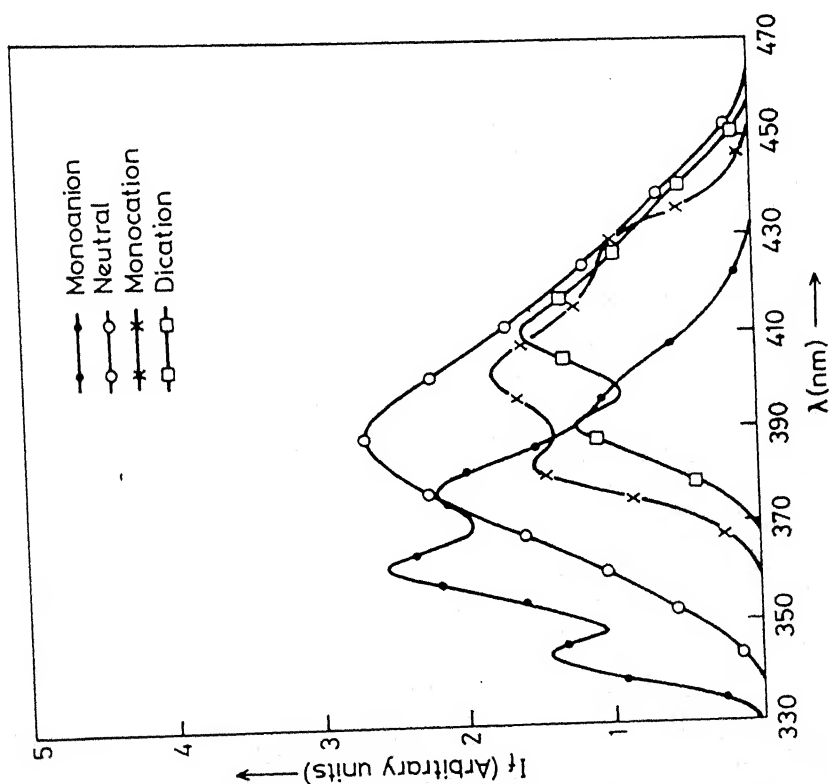


Fig.4.44 Fluorescence spectra of various prototropic species of benzimidazole-2-acetic acid (BIAA) at 298 K.

spectrum of monocation in comparison to zwitterion could be due to the stabilization of charge transfer state, because the monocation behaves like BIM. The charge transfer state has been seen to be the emitting state for the monocationic species of BIM.¹²⁵ This is further clear, on examining the fluorescence spectrum of monocation of BIAE, where the spectral characteristics exactly match with that of BIM. Similar to BIM, the fluorescence from both π^* and CT, state is observed in case of BIAE. The former transition is slightly blue shifted and the latter one is largely red shifted with respect to the fluorescence spectrum of the neutral species. At $H_0 - 5$, a further red shift in the fluorescence spectrum of the monocation of BIAA suggests the presence of dication formed by protonating the carbonyl group. Similar species is found to be non-fluorescent in case of BIAE.

The pK_a values for the various prototropic reactions of BIAA and BIAE have been calculated spectrophotometrically and are compiled in Table 4.21. The pK_a value for the monoanion-dianion equilibrium of BIAA can not be calculated due to the reason mentioned earlier. The pK_a values for the different proton transfer reactions of BIAE reflect the insulating character of the methylene group present in between BI moiety and $-COOMe$ group.

The pK_a^* values for all the equilibria of BIAA and BIAE have been calculated by fluorimetric titration and Förster cycle

method (Table 4.21). Absorption and fluorescence spectral data, wherever applicable are used in the latter method for the evaluation of pK_a^* . Fluorimetric titration curves (Fig. 4.46) gave the ground state value, indicating that equilibrium is not established in the excited singlet state due to the short lifetimes of the conjugate acid-base pair. This is consistent with the results obtained in other benzimidazole derivatives studied in this thesis. The different prototropic species of BIAA and BIAE present in the complete $H_0/pH/H_-$ range of -10 to 16 are shown in scheme, Fig. 4.47.

In conclusion it can be mentioned that BIAA behaves quite differently than CBIA or BIA (section 4.7) due to the presence of methylene group in between $-COOH$ group and BI moiety. Unlike other compounds mentioned earlier, the absorption and fluorescence spectral characteristics of BIAA reflect that one methylene group is not enough to stop the direct interactions between the two functional groups. Carefully designed experiments have shown that in BIAA, the interaction is through a intramolecular hydrogen bond. The presence of zwitterionic species of BIAA became possible on arresting the change in the charge density at tertiary nitrogen atom by putting an insulating methylene group in between $-COOH$ group and BI moiety.

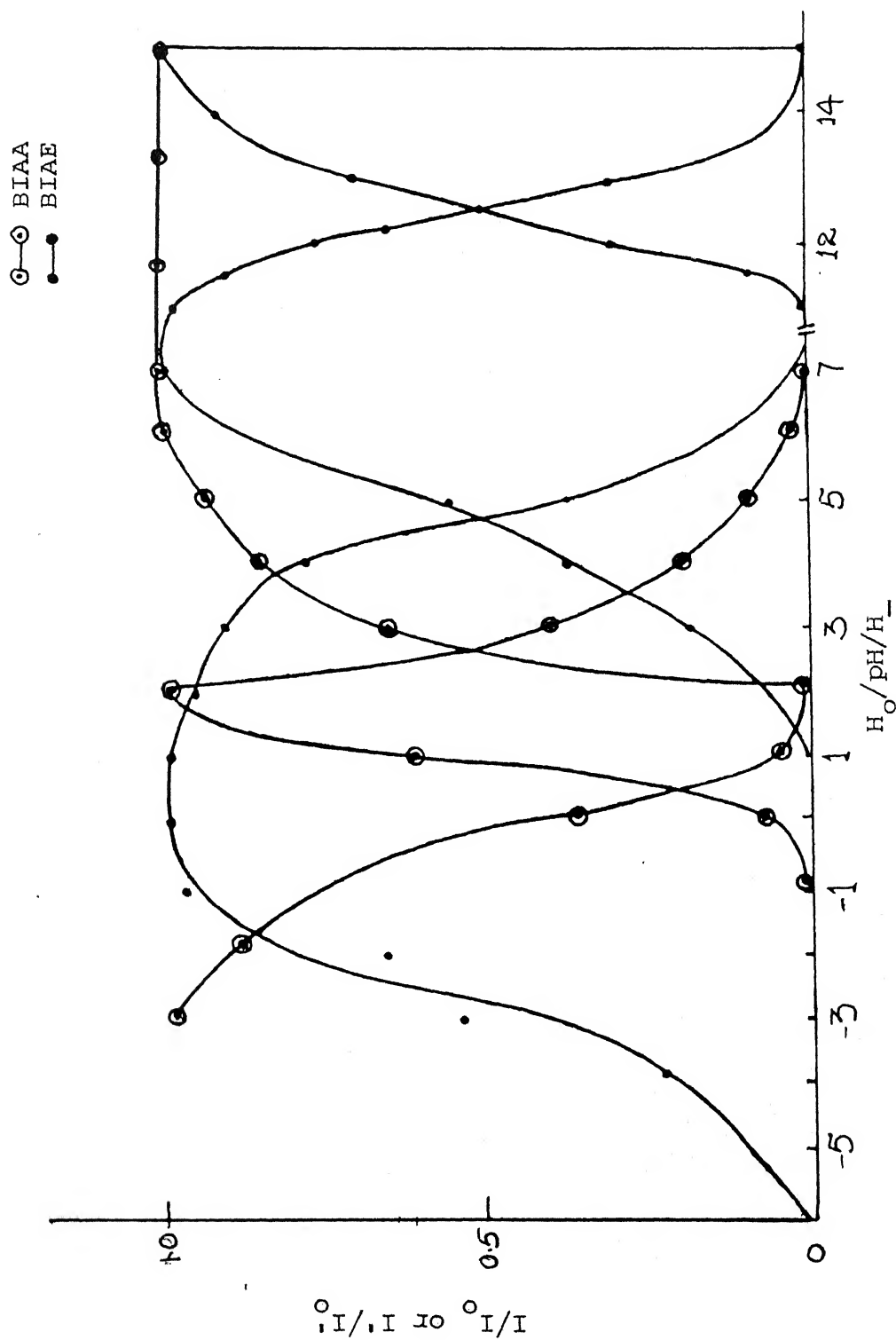


Fig.4.46 Plot of I/I_0 as a function of $H_0/pH/H_-$ of benzimidazole-2-acetic acid⁰(BIAA) and benzimidazole-2-ethylacetate (BIAE).

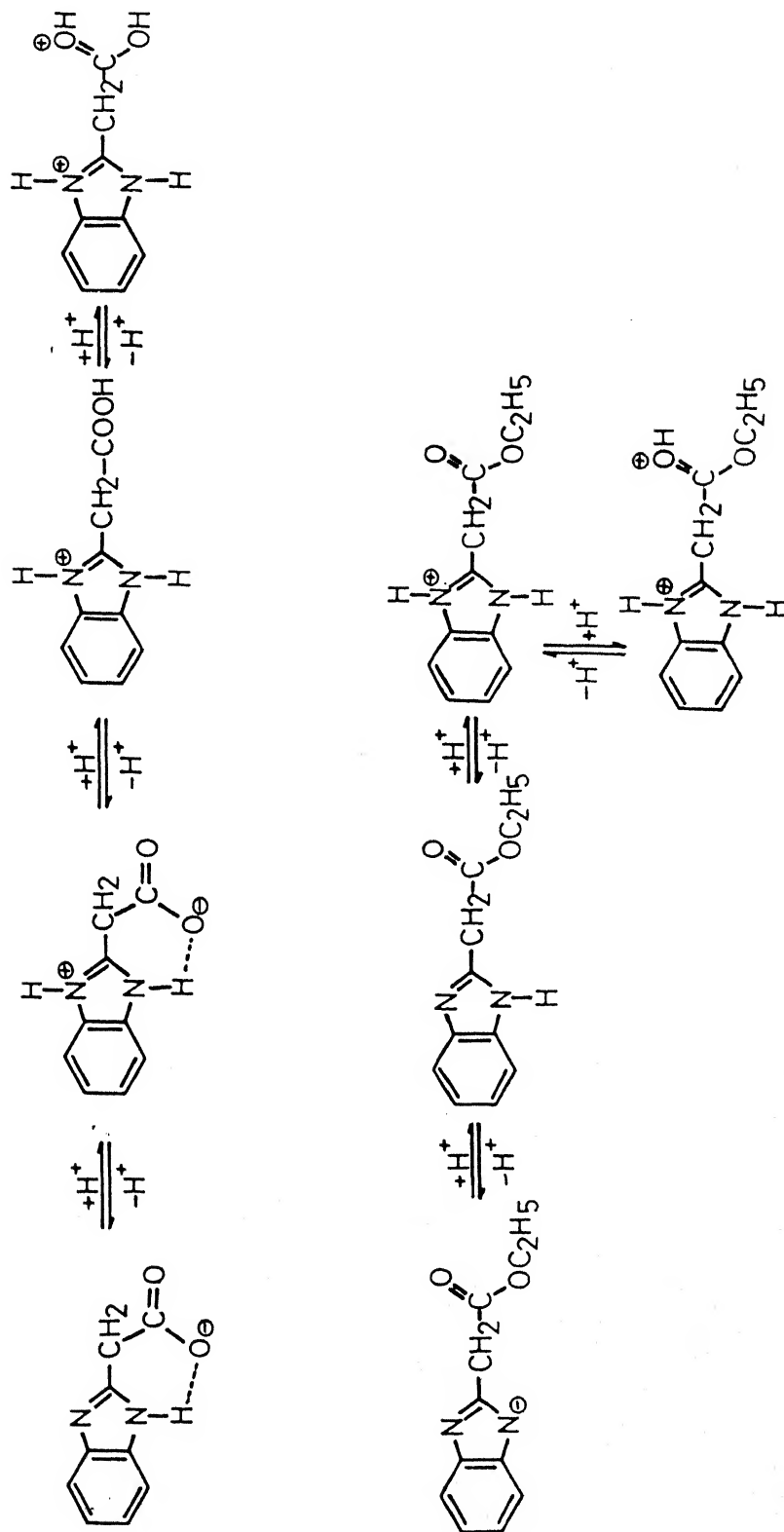


Fig.4.47 Schemes of ground and excited state equilibria of benzimidazole-2-acetic acid of benzimidazole-2-ethylacetate at different $H_0/pH/H_-$.

Table 4.21. pK_a and pK_a^* of various prototropic reactions of benzimidazole-2-acetic acid (BIAA) and benzimidazole-2-ethylacetate (BIAM) at 298°K.

Equilibrium	pK _a	pK _a [*]		
		Abs. ^a	Flu. ^a	F.T. ^b
<u>Reactions of BIAA</u>				
Dication \rightleftharpoons Monocation	-4.7	-	-4.2	-4.5
Monocation \rightleftharpoons Zwitterion	0.2	-	-	0.4
Zwitterion \rightleftharpoons Monoanion	4.1	-	-	2.6
<u>Reactions of BIAE</u>				
Dication \rightleftharpoons Monocation	-	-	-	-3.8
Monocation \rightleftharpoons Neutral	5.7	4.6	-	4.7
Neutral \rightleftharpoons Monoanion	13.1	11.2	8.3	12.6

^aFörster cycle method

^bFluorimetric titration method

4.9 Benzimidazole-2-propionic acid (BIPA)*

The absorption and fluorescence spectra of different prototropic species of BIPA, shown in figures 4.48 and 4.49, are exactly similar to that of BI or MBI (Table 4.22). Due to the presence of two methylene groups in between -COOH group and BI moiety, no spectral changes are observed in the absorption and fluorescence spectra of BIPA, when the prototropic reactions occur at -COOH group. The prototropic reactions occurring at the BI moiety, bring about changes in the spectral characteristics which are similar to that observed for 2-ethyl- and 2-methylbenzimidazoles.¹²⁵

The pK_a and pK_a^* calculated by the methods mentioned earlier are shown in Table 4.23. Fluorimetric titration curves are shown in Fig. 4.50. In this regard the behaviour of BIPA is quite different from other acids studied in this thesis. Due to the presence of two methylene groups in between -COOH group and imidazole moiety, the direct interaction between these two is completely absent. Therefore, the molecule behaves like parent BI and changes occurring in the -COOH group are not reflected in the spectrum of benzimidazole. For example, at H₁₆, the BIPA is supposed

*H.K. Sinha and S.K. Dogra, communicated.

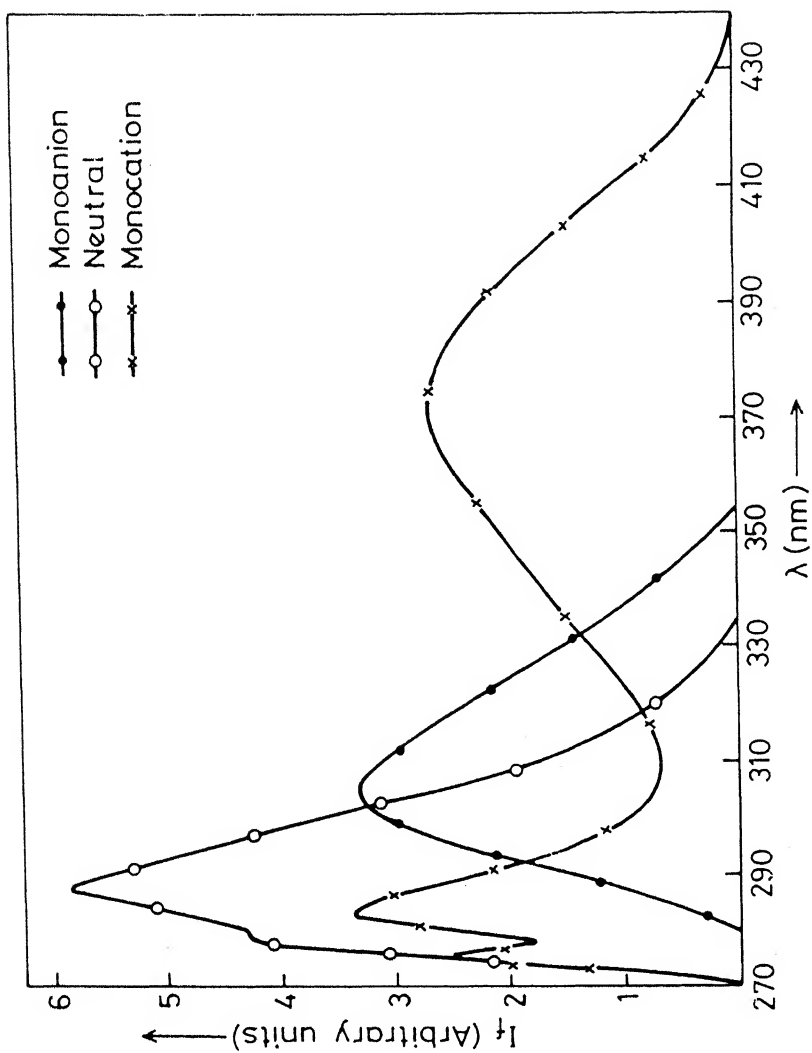


Fig.4.49 Fluorescence spectra of various prototropic species of benzimidazole-2-propionic acid at 298°K.

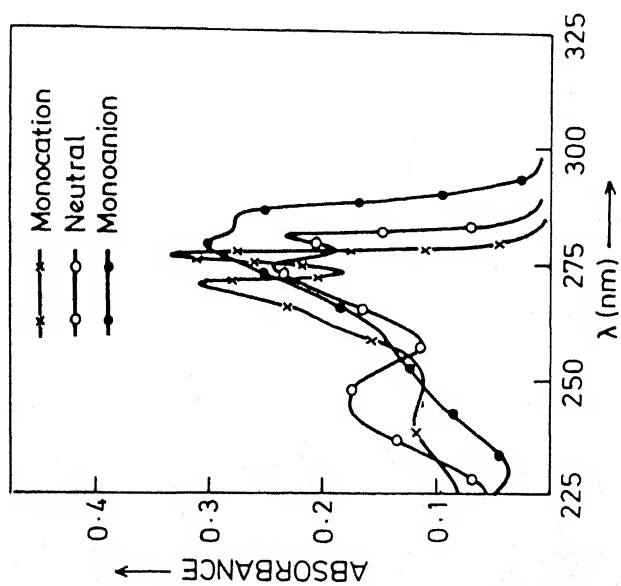


Fig.4.48 Absorption spectra of various prototropic species of benzimidazole-2-propionic acid at 298°K.

Table 4.22. Absorption maxima [λ_a (nm)], $\log(\epsilon_{\max})$, fluorescence maxima [λ_f (nm)] of various prototropic species of benzimidazole-2-propionic acid (BIPA) at 298°K.

Species/ H_o /pH/ H_-	λ_a (nm) $\log(\epsilon_{\max})$			λ_f (nm)	
Dication (H_o-6)	276(4.10)	-	214(4.11)	-	
	269(4.11)				
	262(3.98)				
Monocation (pH 2)	274(4.05)	-	214(4.30)	284	370
	266(4.02)			275	
	262(3.83)				
Zwitterion (pH 4)	274(4.05)	-	-	284	370
	266(4.02)			275	
	262(3.83)				
Monoanion (pH 7)	280(3.94)	249(3.80)	204(4.34)	288	-
	274(3.93)	243(3.81)		279	
	268(3.80)				
Dianion (H_-14)	286(3.97)	250(3.57)	205(3.05)	306	-
	279(4.02)				

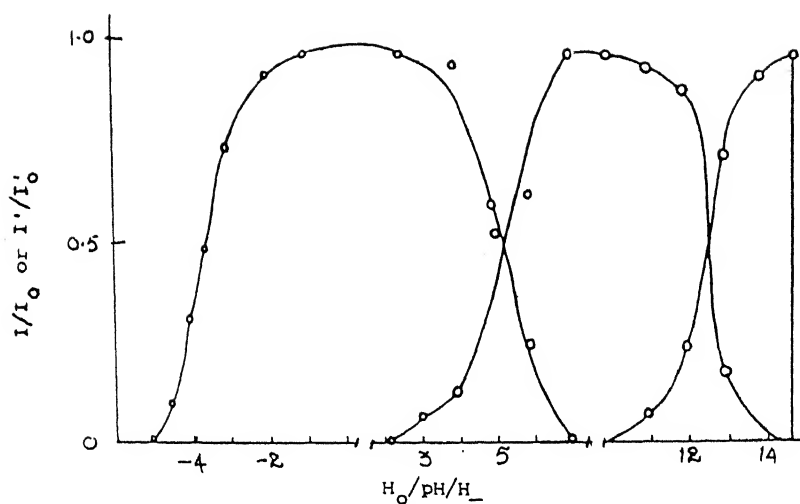


Fig.4.50 Plot of I/I_0 of the prototropic species of benzimidazole-2-propionic acid versus $H_0/pH/H_-$.

Table 4.23. pK_a and pK_a^* of various prototropic reactions of benzimidazole-2-propionic acid (BIPA) at 298°K.

Equilibrium	pK_a	pK_a^*		
		Abs. ^a	Flu. ^a	F.T. ^b
Dication \rightleftharpoons Monocation	—	—	—	-3.6
Monocation \rightleftharpoons Zwitterion	5.7	—	—	5.3
Zwitterion \rightleftharpoons Monoanion	—	—	—	—
Monoanion \rightleftharpoons Dianion	13.1	11.5	8.8	12.6

^aFörster cycle method

^bFluorimetric titration method

to be a dianionic species, hence absorption and fluorescence spectra should have resembled to other similar species, had there been any interaction between BI moiety and -COOH group, but the absorption and fluorescence maxima resemble the monoanion of BIM. At pH 6, the absorption and fluorescence spectral shift also resemble to those of BIM. The pK_a for the protonation reaction of tertiary nitrogen atom of BIM is 6. This data clearly suggest that the first protonation should occur at tertiary nitrogen atom of BIPA, rather than at carboxylate anion, because the pK_a for similar reaction of propionic acid is 4.0. This shows a zwitterion of BIPA is formed at this pH. But the absorption and fluorescence maxima of zwitterion resemble to those of monocation of BIM. This is due to the presence of two methylene groups, which does not allow the BI moiety to sense the presence of carboxyl group. This is further clear from the fact that the formation of monocation and dicationic species by protonation of carboxylate and carboxylic groups respectively, does not bring about any changes in the absorption and fluorescence characteristics of the zwitterionic species. All the prototropic species are shown in Fig. 4.51.

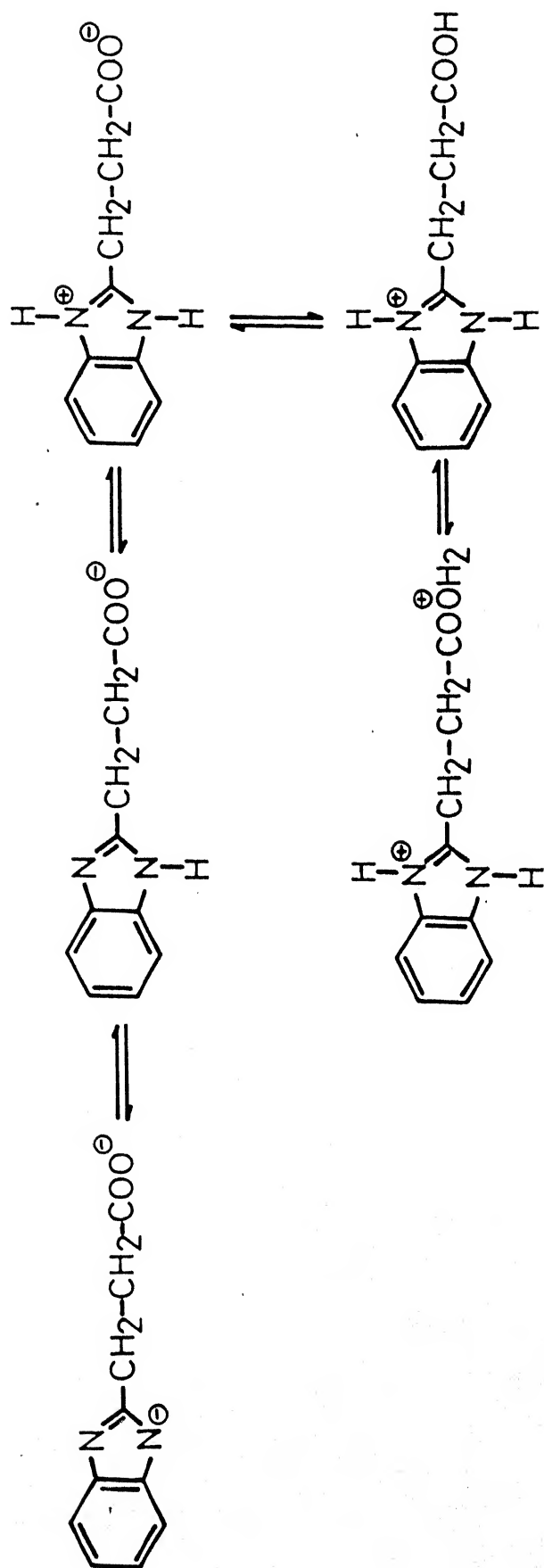


Fig.4.51 Scheme of prototropic equilibria of benzimidazole-2-propionic acid (BIPA) at different $\text{H}_0/\text{pH}/\text{H}_-$.

CONCLUSIONS

Absorption and emission characteristics of a series of 2-substituted benzimidazoles in different solvents and at different pH values have been investigated and results are summarised in the earlier chapters. The conclusions drawn are listed below:

- (i) Introduction of a methylene group in between the interacting chromophores reduces their direct interaction. The electronic absorption and fluorescence profiles, therefore, will not be affected much from that of the parent molecule.
- (ii) Effect of substituents at position-2 of the benzimidazole moiety have indicated that the luminescent character of the emitting state depends on the nature of the substituent. With strongly electron withdrawing groups like $-\text{CCl}_3$, $-\text{CF}_3$ etc, the lowest energy emitting state is of charge-transfer character, whereas with other weak electron withdrawing or electron donating groups the emitting state is of $\pi\pi^*$ character.
- (iii) Protonation of the tertiary nitrogen atom of benzimidazole leads to the formation of a monocation and the latter too possesses two emitting states, the charge-transfer state being the lower energy state and the $\pi\pi^*$ state is of

higher energy one. The driving force for the charge-transfer from the carbocyclic ring to the heterocyclic ring is the presence of positive charge on the tertiary nitrogen atom.

- (iv) Deprotonation of the $>NH$ group leads to the formation of a monoanion in all the substituted benzimidazoles.

Irrespective of the substituents present at position-2, the emitting state of the monoanion is found to be only $\pi\pi^*$. The negative charge, present on the imino nitrogen atom of the anion may prevent the charge migration from the carbocyclic to the heterocyclic ring.

- (v) Presence of electron withdrawing substituents like $-CF_3$, $-CCl_3$, $-COOH$ and $-COOCH_3$ at position-2 is found to alter the charge density on the acidic and basic centres at position-1 and position-3, respectively. The removal of the imino proton can be prevented if intramolecular hydrogen bond is formed between the imino proton and the negative centres present on the substituent at position-2. This is also evident from the results of the pK_a values of the deprotonation of the $>NH$ group.

- (vi) The imino group becomes more acidic than that of the $-OH$ group in 2-(hydroxymethyl)benzimidazole. This might be due to the fact that the $-OH$ group is not attached to the aromatic

ring directly but separated by a methylene group and the whole substituent can be considered as methanol.

- (vii) Monoprotonic phototautomerism observed in case of 2-(2'-hydroxyphenyl)benzimidazole is due to the possible interaction of the substituent with the benzimidazole moiety being in the same plane and also due to the possible proton transfer reactions with the -OH group of the substituent. The same is true as it could not be obtained with meta and para hydroxyphenyl substituents.
- (viii) The rigidity and the electronic spectral shifts with a change in solvent polarity of benzimidazole-2-carboxylic acid and 5-chlorobenzimidazole-2-carboxylic acid are due to the intramolecular hydrogen bonding between the benzimidazole moiety and the carboxylic acid group.
- (ix) In benzimidazole-2-acetic acid, though the insulating methylene group separates the interacting benzimidazole moiety and the carboxylic acid, the spectral shifts can be explained by the interaction through a intramolecular hydrogen bond. In benzimidazole-2-propionic acid the interaction between the benzimidazole moiety and the carboxylic acid is completely restricted because of the presence of two methylene groups between the interacting groups.

SCOPE OF FURTHER WORK

Although the present work provides an insight into the nature of transitions, prototropic reactions and the geometry of the 2-substituted benzimidazoles, a better understanding will be achieved by studying other substituted benzimidazoles where the substituents are restricted to the benzene ring only. Proton transfer reactions can also be carried out in biomimetic systems like micelles. The scope is widened if it is looked at in the light of quantitative aspects like rate of radiative and non-radiative transfers. Since the lifetime of benzimidazole molecules in the S_1 state is in the order of 10^{-10} sec, picosecond time resolved fluorescence spectroscopy will be much helpful in establishing the proton transfer kinetics.

REFERENCES

1. G.J. Brearly and M. Khasa, J. Am. Chem. Soc., 77, 4462 (1955).
2. N.S. Bayliss and E.G. McRae, J. Phys. Chem., 58, 1002 (1954).
3. G.C. Pimental and A.L. McClellan, ''The Hydrogen Bond'', W.H. Freeman and Co., N.Y. (1960).
4. E. Lippert, Z. Elektrochem., 61, 962 (1957).
5. E.G. McRae, J. Phys. Chem., 61, 562 (1957).
6. P. Suppan and C. Tsiamis, Spectrochim. Acta, 36A, 971 (1950).
7. N. Mataga, Y. Kaefu and M. Koizumi, Bull. Chem. Soc. Jpn., 29, 465 (1956).
8. H.H. Jaffe and M. Orchin, ''Theory and Application of Ultraviolet Spectroscopy'', John Wiley, N.Y. (1962).
9. H. Suzuki, ''Electronic Absorption Spectra and Geometry of Organic Molecules'', Academic Press, N.Y. (1967).
10. N. Mataga and H. Kutoba, ''Molecular Interaction and Electronic Spectra'', Marcel Dekker Inc, N.Y. (1970).
11. J.R. Lakwicz, ''Principle of Fluorescence Spectroscopy'', Plenum Press, N.Y. (1986).
12. P. Pringsheim, ''Fluorescence and Phophorescences'', Interscience Publishers, Inc., N.Y. (1949).
13. Th. Forster, ''Fluorescenz Organisher Verbindungen'', Vanderhoeck and Ruprecht, Gottingen (1951).
14. B.L. Van Durren, Chem. Rev., 63, 325 (1963).
15. G.C. Pimental, J. Am. Chem. Soc., 79, 3323 (1957).
16. N. Mataga and S. Tsuno, Bull. Chem. Soc. Jpn., 30, 368 (1957).

17. N. Mataga and Y. Kaifu, *Mol. Phys.*, 7, 137 (1964).
18. N. Mataga, *Bull. Chem. Soc. Jpn.*, 31, 487 (1958).
19. A. Weller, "'Progress in Reaction Kinetics'", Vol. I, Pergamon Press, London, 1961.
20. N.J. Turro, "'Modern Molecular Photochemistry'", The Benjamin/Cummings Publishing Co. Inc. (1978).
21. S.B. Costa, A.L. Maccanita and M.J. Prieto, *J. Photochem.*, 11, 109 (1979).
22. P. Suppan, *Chem. Phys. Lett.*, 94, 272 (1983).
23. P. Suppan, *Spectrochim. Acta*, 41A, 1353 (1985).
24. H. Inoue, M. Hida, N. Nakashima and K. Yoshihara, *J. Phys. Chem.*, 86, 3184 (1982).
25. B.F. Barbara, L.E. Brus and P.M. Rentzepis, *J. Am. Chem. Soc.*, 102, 2786 (1980).
26. S.R. Flom and P.F. Barabara, *J. Phys. Chem.*, 89, 4489 (1985).
27. P.F. Barbara, S.D. Rand and P.M. Rentzepis, *J. Am. Chem. Soc.*, 103, 2156 (1981).
28. S.P. Velsko and G.R. Flemming, *J. Chem. Phys.*, 76, 3553 (1982).
29. S.Y. Hou, W.M. Hetherington, G.M. Kovenowski and B.K. Eienthal, *Chem. Phys. Lett.*, 68, 282 (1982).
30. P.F. Barbara, L.E. Brus and P.M. Rentzepis, *Chem. Phys. Lett.*, 69, 447 (1980).
31. K. Brederck, Th. Forster and H.G. Oesterlin, "'Luminescence of Organic and Inorganic Materials'", H.P. Kallman and G.M. Spruch (eds.), John Wiley, N.Y. (1962).
32. R. Livingston, *J. Am. Chem. Soc.*, 71, 1542 (1949).
33. N. Mataga, *Bull. Chem. Soc. Jpn.*, 29, 353 (1956).

34. D. Saperstein and E. Levin, J. Chem. Phys., 62, 3560 (1975).
35. M.V. Encinas, M.A. Rubio and E.A. Lissi, J. Photochem., 18, 137 (1982).
36. K.C. Ingham and M.A. El-Bayovmi, J. Am. Chem. Soc., 96, 1674 (1974).
37. J. Walvk, S.J. Komorowski and H. Jerbich, J. Phys. Chem., 90, 3868 (1986).
38. J.F. Ireland and P.A.H. Wyatt, 'Advances in Physical Organic Chemistry' V. Gold and D. Bethel (eds), Academic Press, N.Y., Page (1976).
39. Th. Forster, Z. Elektrochem., 54, 42 (1950).
40. Th. Forster, Z. Elektrochem., 54, 531 (1950).
41. C.F. Mason, J. Phillip and B.F. Smith, J. Chem. Soc., 3051 (1968).
42. H.H. Joffe and H. Loydjones, J. Org. Chem., 30, 964 (1964).
43. E.L. Wehry and L.B. Rogers, J. Am. Chem. Soc., 87, 4235 (1965).
44. H.H. Jaffe, D.L. Beveridge and H.L. Jones, J. Am. Chem. Soc., 86, 2962 (1964).
45. W. Bartok, P.J. Lucchesi and N.S. Sndder, J. Am. Chem. Soc., 84, 1842 (1962).
46. S.G. Schulman, P.T. Tidwell, J.J. Aason and J.D. Winefordner, J. Am. Chem. Soc., 93, 3179 (1971).
47. S.G. Schulman and A.C. Capomacchia, J. Phys. Chem., 79, 1337 (1975).
48. A. Weller, Z. Elektrochem., 56, 662 (1952).
49. J. Haylock, S.F. Mason and B.F. Smith, J. Chem. Soc., 4897 (1963).

50. K. Tsutsumi and H. Shizuka, Chem. Phys. Lett., 52, 485 (1977).
51. K. Tsutsumi and H. Shizuka, Z. Phys. Chem. N.F., 111, 1297 (1978).
52. H. Shizuka, K. Tsutsumi, H. Takeuchi and I. Tanka, Chem. Phys. Lett., 62, 408 (1979).
53. H. Shizuka and K. Tsutsumi, J. Photochem., 9, 334 (1978).
54. K. Tsutsumi and H. Shizuka, Z. Phys. Chem. N.F., 122, 129 (1980).
55. H. Hofner, J. Worner, W. Steiner and M. Houser, Chem. Phys. Lett., 72, 139 (1980).
56. C.M. Harris and B.K. Sellinger, J. Phys. Chem., 84, 891, 1366 (1980).
57. K. Tsutsumi, S. Sekiguchi and H. Shizuka, J. Chem. Soc. Faraday Trans. I, 78, 1087 (1982).
58. Z.R. Grabowski and A. Grabowska, Z. Phys. Chem. N.F., 101, 197 (1976).
59. S. Tobita and H. Shizuka, Chem. Phys. Lett., 75, 140 (1980).
60. M. Swaminathan and S.K. Dogra, Can. J. Chem., 61, 1064 (1983).
61. Th. Forster, Chem. Phys. Lett., 17, 309 (1972).
62. S.G. Shulman and R.J. Sturgeon, J. Am. Chem. Soc., 99, 7209 (1977).
63. H. Shizuka and S. Tobita, Chem. Phys. Lett., 104, 6919 (1982).
64. H. Shizuka, Acc. Chem. Res., 18, 141 (1985).
65. B.S. Vogt and S.G. Shulman, Chem. Phys. Lett., 99, 157 (1983).
66. S.G. Shulman, B.S. Vogt and M.W. Lovell, Chem. Phys. Lett., 75, 224 (1980).
67. D.D. Rosenbrock and W.W. Brandt, J. Phys. Chem., 70, 3851 (1966).

68. K. Abate, A.C. Capomacchia, D. Jackmar, P.J. Kovi and S.G. Shulman, *Anal. Chim. Acta.*, 65, 59 (1973).
69. H. Shizuka, K. Tsutsumi, K. Aoki and T. Morita, *Bull. Chem. Soc. Jpn.*, 44, 3245 (1971).
70. E. Vander Donckt, ''Progress in Reaction Kinetics'', G. Porter (Ed), Vol.5, Pergamon Press, N.Y., 273 (1970).
71. S.G. Shulman, *Rev. Anal. Chem.*, 1, 85 (1971).
72. S.G. Shulman, ''Physical Methods in Heterocyclic Chemistry'', A.R. Katritzky (Ed), Vol. VI, Academic Press, N.Y., 147 (1974).
73. J. Jortner, R.P. Levine and S.A. Rice, ''Advances in Chemical Physics'' Part 2, John Wiley, N.Y. (1981).
74. S.G. Shulman, R.M. Threatte, A.C. Capomacchia and W.L. Paul, *J. Pharm. Sci.*, 63, 876 (1974).
75. S.G. Shulman, D.V. Naik, A.C. Capomacchia and T. Roy, *J. Pharm. Sci.*, 64, 982 (1975).
76. A.C. Capomacchia and S.G. Shulman, *J. Pharm. Sci.*, 64, 1256 (1975).
77. P.J. Kovi and S.G. Shulman, *Anal. Chim. Acta*, 63, 39 (1973).
78. S.G. Shulman, ''Modern Fluorescence Spectroscopy'', Vol.2, E.L. Wehry (Ed), Plenum Press, N.Y. 239 (1976).
79. S.G. Shulman, ''Fluorescence and Phosphorescence Spectroscopy: Physicochemical Principles and Practice'', Pergamon Press, N.Y. (1977).
80. L.S. Rosenberg, J. Simons and S.G. Shulman, *Talanta*, 26, 862 (1979).
81. S.G. Shulman, A.C. Capomacchia and B. Tussey, *Photochem. Photobiol.* 14, 733 (1971).
82. P.J. Zarata, M.D. Radcliffe and S.G. Shulman, *Talanta*, 32, 285 (1985).

83. J. Elguero and C. Marzine, "The Tautomerism of Heterocycles", A.R. Katritzky and A.J. Boutton (Ed), Academic Press, N.Y. (19).
84. A. Weller, Z. Elektrochem., 60, 1144 (1956).
85. A.L. Huston, C.D. Merrit, W.G. Scott and A. Gupta, in "Picosecond Phenomena", R.M. Horchstrasser, W. Kaiser and C.V. Shank (Eds), Springer Verlag, West Berlin, 232 (1980).
86. J. Scaiano, Chem. Phys. Lett., 92, 97 (1982).
87. S.R. Flom and P.F. Barbara, Chem. Phys. Lett., 94, 448 (1983).
88. A.K. Mishra and S.K. Dogra, J. Photochem., 31, 333 (1985).
89. G.J. Woolfe, M. Melzig, S. Sehneider and F. Dorr, Chem. Phys., 77, 213 (1983).
90. M. Krishnamurthy and S.K. Dogra, J. Photochem., 32, 235 (1986).
91. B.F. Barbara, L.E. Brus and R.M. Rentzepis, J. Am. Chem. Soc., 102, 5631 (1980).
92. D. Ford, P.J. Thistlethwaite and G.J. Woolfe, Chem. Phys. Lett., 69, 246 (1980).
93. K.C. Ingham and M.A. El-Bayoumi, J. Am. Chem. Soc., 96, 1674 (1974).
94. M.A. El-Bayoumi, P. Avouris and W.R. Ware, J. Chem. Phys., 62, 2499 (1975).
95. C. Chang, N. Shabestary and M.A. El-Bayoumi, Chem. Phys. Lett., 75, 107 (1980).
96. G.J. Yakatan, R.J. Juneau and S.G. Shulman, Anal. Chem., 44, 1044 (1972).
97. M. Swaminathan and S.K. Dogra, J. Am. Chem. Soc., 105, 6223 (1983).
98. C.D. Gutsche and B.A.M. Oude-Alink, J. Am. Chem. Soc., 90, 5855 (1968).

99. C.D. Gutsche, B.A.M. Oude-Alink and A.W.K. Chan, J. Org. Chem., 38, 1993 (1973).
100. T.S. Godfrey, G. Porter and P. Suppan, Disc. Faraday. Soc., 39, 194 (1965).
101. G. Batroeci, T. Bartolus and V. Mazzcato, J. Phys. Chem., 77, 605 (1973).
102. K.E. Hine and R.F. Childs, J. Am. Chem. Soc., 95, 6116 (1973).
103. V. Rehak, A. Novak and G. Israel, Chem. Phys. Lett., 114, 154 (1985).
104. H.J. Heller, Eur. Polym. J. Suppl., 105 (1969).
105. H.J. Heller and H.R. Blattman, Pure, Appl. Chem., 30, 145 (1972).
106. H.J. Heller and H.R. Blattman, Pure. Appl. Chem., 36, 141 (1974).
107. D.L. Williams and A. Heller, J. Phys. Chem., 74, 4473 (1970).
108. J.E.A. Otterstedt, J. Phys. Chem., 58, 5716 (1973).
109. W.K. Klopfler, in "'Adv. in Photochemistry'", J.N. Pitts. Jr, G.S. Hammond and K. Gollnick (Eds), Vol. 10, John Wiley, N.Y. 311-358 (1977).
110. O. Kysel, Kinet. Mech. Polyreactions. Int. Symp. Macromol. Chem. Prepr., 5, 263 (1969).
111. W.J. McCarthy and J.D. Winefordner, in "'Fluorescence, Theory, Instrumentation and Practice, G.G. Guilbault (Ed), Arnold, London (1967).
112. R. Argauer and E.C. White, "'Fluorescence Analysis'", Dekker, N.Y. (1970).
113. S.C. Shulman and J.D. Wineforlner, Talanta, 17, 607 (1970).
114. B.B. Brodie, S. Udenfriend, W. Dill and G. Downing, J. Biol. Chem., 168, 311 (1947).

115. R.A. Mortan, J.A. Hopkins, and H.H. Selinger, *Biochemistry*, 8, 1598 (1969).
116. M.R. Loken, J.W. Hayes, J.R. Gohlke and L. Brand, *Biochemistry*, 11, 4779 (1972).
117. J.A. Mayer, I. Itzkaw and E. Kierstead, *Nature*, 225, 544 (1970).
118. A.U. Acuna and J. Katalan, *J. Phys. Chem.*, 90, 2807 (1986).
119. P. Chou, D. McMorro, T. Aartsma and M. Kasha, *J. Phys. Chem.*, 88, 4596 (1984).
120. P. Chou and T. Aartsma, *J. Phys. Chem.*, 90, 721 (1986).
121. R. Bonnett, *Chem. Rev.*, 63, 573 (1963).
122. P.N. Preston, in *'The Chemistry of Heterocyclic Compounds'*, Vol. 40, Part I, Wiley Interscience, 65 (1981).
123. H.C. Barrensen, *Acta. Chem. Scand.*, 17, 921 (1963).
124. M. Kondo and H. Kuwano, *Bull. Chem. Soc. Jpn.*, 42, 1433 (1969).
125. M. Krishnamurthy, P. Phaniraj and S.K. Dogra, *J. Chem. Soc. Perkin Trans.2*, 1917, 1986.
126. A.K. Mishra and S.K. Dogra, *Indian J. Chem.*, 24A, 815 (1985).
127. A.K. Mishra and S.K. Dogra, *J. Photochem.*, 29, 435 (1985).
128. A.K. Mishra and S.K. Dogra, *Spectrochim. Acta*, 39A, 609 (1983).
129. R. Argauer and C.F. White, *'Fluorescence Analysis'*, Dekker, N.Y. (1970).
130. C.E. White, M. Ho and E.Q. Weimer, *Anal. Chem.*, 32, 438 (1960).
131. C.A. Parker and W.T. Rees, *Analyst.*, 85, 587 (1960).
132. W.H. Melhuish, *J. Opt. Soc. Amer.*, 52, 1256 (1960).

133. R.F. Chen, Anal. Biochem., 20, 339 (1967).
134. C.A. Parker, 'Photoluminescence of Solutions', Elsevier Publications, N.Y. (1968).
135. R.A.B. Copeland and A.R. Day, J. Am. Chem. Soc., 65, 1072 (1943).
136. A. Bloom and A.R. Day, J. Org. Chem., 4, 14 (1939).
137. W.T. Smith and E.C. Steinle, J. Am. Chem. Soc., 75, 1292 (1953).
138. H. Lawniczak, Pr. Inst. Przem. Org., 21 (1971).
139. C.M. Orlando, J.G. Smith and D.R. Health, J. Org. Chem., 35, 3147 (1970).
140. J. Sawlewicz and Z. Sznigir, Acta. Pol. Pharm., 18, 1 (1961).
141. B.S. Furniss, A.J. Hannaford, V. Rogers, P.W.G. Smith and A.R. Tatchell, Vogel's Text Book of Practical Organic Chemistry, 4th edn, p.755, ELBS London (1978).
142. D. Harrison, J.T. Ralph and A.C.B. Smith, J. Chem. Soc., 2930 (1963).
143. B. Piliarski, Liebigs Ann. Chem., 1078 (1983).
144. B.C. Ennis, G. Holan and E.L. Samuel, J. Chem. Soc., C, 30 (1967).
145. B.C. Ennis, G. Holan and E.L. Samuel, J. Chem. Soc., C, 20 (1967).
146. M.V. Betrabet and G.C. Chakrabarti, J. Indian. Chem. Soc., 7, 191 (1930).
147. J.A. Riddick and W.B. Bunger, in 'Organic Solvents', Wiley Interscience, London, 592, 644, 695 (1970).
148. A.K. Mishra, M. Swaminathan and S.K. Dogra, J. Photochem., 26, 49 (1984).

149. L.P. Hammett and A.J. Deyrup, J. Am. Chem. Soc., 85, 878 (1963).
150. M.J. Jorgenson and D.R. Harter, J. Am. Chem. Soc., 85, 878 (1963).
151. G. Yagil, J. Phys. Chem., 71, 1034 (1967).
152. G.G. Guilbault, 'Practical Fluorescence', Marcel Dekker Inc., N.Y., p.12 (1973).
153. Ref. (152), p.14.
154. A.K. Mishra and S.K. Dogra, J. Photochem., 31, 333 (1985).
155. A.K. Mishra and S.K. Dogra, Indian J. Phys., 58B, 480 (1984).
156. A.K. Mishra and S.K. Dogra, Bull. Chem. Soc. Jpn., 58, 3587 (1985).
157. P.C. Tway and C.J. Cline love, J. Phys. Chem., 86, 5223, 5227 (1982).
158. R.V. Subba Rao, M. Krishnamurthy and S.K. Dogra, J. Photochem., 34, 55 (1986).
159. R.V. Subba Rao, M. Krishnamurthy and S.K. Dogra, Indian J. Chem., 25A, 517 (1986).
160. P. Phaniraj, M. Krishnamurthy and S.K. Dogra, Indian J. Chem., 25A, 513 (1986).
161. P. Phaniraj, A.K. Mishra and S.K. Dogra, Indian J. Chem., 24A, 913' (1985).
162. M. Krishnamurthy, A.K. Mishra and S.K. Dogra, Photochem. Photobiol., 45, 359 (1987).
163. M. Krishnamurthy, H.K. Sinha and S.K. Dogra, J. Lumin., 35, 343 (1986).
164. P.J. Kovi, C.L. Muller and S.G. Schulman, Anal. Chim. Acta., 62, 59 (1972).

165. T.C. Werner and D.M. Hercules, J. Phys. Chem., 73, 2005 (1969), 77, 1611 (1973), 74, 1030 (1970).
166. R. Monoharan and S.K. Dogra, Spectrochim. Acta., 43A, 91 (1987).
167. J.C. Baum and D.S. McClure, J. Am. Chem. Soc., 102, 720 (1980).
168. D.D. Perrin, in "Dissociation Constants of Organic Bases in Aqueous Solution, Butterworths, London, p.13 (1965).
169. Ref. (122), p.80.
170. Ref. (169), p.785.
171. H. Irring and O.A. Weber, J. Chem. Soc., 2560 (1959).
172. E.L. Wehry, J. Am. Chem. Soc., 89, 41 (1967).
173. A. Weller, Z. Phys. Chem. N.F., 15, 438 (1958).
174. M. Swaminathan and S.K. Dogra, J. Chem. Soc. Perkin Trans.2, 947 (1984).
175. S.J. Strickler and R.A. Berg., J. Chem. Phys., 37, 814 (1962).
176. T.T. Lane and K.P. Quinian, J. Am. Chem. Soc., 82, 2994 (1960).
177. Ref. (122), p.118
178. J.J. Aarron, P. Thiao, C. Parkanyi, A.J. Jeffries III and B.L. Kalsotra, Photochem. Photobiol., 29, 339 (1979).
179. M. Swamihathan and S.K. Dogra, Indian J. Chem., 22A, 853 (1983).
180. M. Swaminathan and S.K. Dogra, J. Photochem., 21, 245 (1983).
181. M. Krishnamurthy and S.K. Dogra, Spectrochim. Acta., 42A, 793 (1986).
182. J.D. Winefordner, S.G. Schulman and L.B. Sanders, Photochem. Photobiol., 13, 381 (1971).

183. P.J. Kovi, C.J. Muller and S.C. Schulman, Anal. Chim. Acta., 61, 7 (1972).
184. M. Swaminathan and S.K. Dogra, Indian J. Chem., 22A, 278 (1983).
185. A.K. Mishra and S.K. Dogra, Indian J. Chem., 24A, 364 (1985).

VITAE

Born on July 7, 1960 at Bhubaneswar (Orissa), the author had his early education at Capital High School, Bhubaneswar. He obtained his B.Sc. and M.Sc. degree from Ravenshaw College, Cuttack in 1980 and 1983 respectively.

LIST OF PUBLICATIONS

- * 1. H.K. Sinha and S.K. Dogra,
Absorption and fluorescence of 2-(aminomethyl)benzimidazole
solvent and pH dependence.
Spectrochim. Acta, 41A, 961 (1985).
- * 2. H.K. Sinha and S.K. Dogra,
Ground and excited state prototropism in 2-(2'-hydroxyphenyl)-
benzimidazole.
Chem. Phys., 102, 337 (1986).
- 3. M. Krishnamurthy, H.K. Sinha and S.K. Dogra,
On the proton transfer reactions of indolecarboxylic acids
in the excited singlet state.
J. Lumin., 35, 343 (1986).
- 4. P. Phaniraj, H.K. Sinha and S.K. Dogra,
Ionisation equilibria and electronic spectroscopy of
5-hydroxyindole-2-carboxylic acid.
J. Photochem., 34, 209 (1986).
- * 5. H.K. Sinha and S.K. Dogra,
Acidity Constants of 2-(hydroxymethyl)benzimidazole.
Indian J. Chem., 25A, 1092 (1986).
- * 6. H.K. Sinha and S.K. Dogra,
Effect of solvents and pH on the spectral characteristics
of 2-(3'-hydroxyphenyl)benzimidazole and 2-(4'-hydroxyphenyl)-
benzimidazole and their methoxy derivatives.
J. Photochem., 36, 149 (1987).
- * 7. H.K. Sinha and S.K. Dogra,
Absorptiometric and fluorimetric study of solvent dependence
and prototropism of 2-substituted benzimidazole homologues.
J. Chem. Soc. Perkin Trans. 2, XXX (1987).

8. H.K. Sinha, S.K. Dogra and M. Krishnamurthy,
Excited state and ground state proton transfer reactions
in 5-aminoindole.
Bull. Chem. Soc. Jpn., 60, XXXX (1987).
 9. M. Krishnamurthy, H.K. Sinha and S.K. Dogra,
Luminescence characteristics of 5-hydroxyindole and
5-hydroxyindole-3-acetic acid. Solvent dependence and
prototropism in the lowest excited state.
Communicated.
 - * 10. H.K. Sinha and S.K. Dogra,
Absorptiometric and fluorimetric study of solvent
dependence and prototropism in 2-substituted
carboxylic acids of benzimidazole.
Communicated.
 11. A. Kumar, H.K. Sinha and S.K. Dogra,
Electronic spectroscopy of bis-benzimidazole homologues.
Medium effects on structural aspects.
Communicated.
-

* Included in the thesis.